UNIVERSITAT POLITÈCNICA DE CATALUNYA
BARCELONATECH
Departament d'Enginyeria Tèxtil i Paperera

UNIVERSITAT POLITÈCNICA DE CATALUNYA
BARCELONATECH
Institut d'Investigació Tèxtil
i Cooperació Industrial de Terrassa

Preparación de soportes biomateriales con estructuras fibrilares obtenidas mediante electro-hilatura

Memoria presentada por

Marisa Erencia Millan

Para optar al grado de Doctora

Por la Universitat Politècnica de Catalunya

Departamento de Ingeniería Textil y Papelera

Universitat Politècnica de Catalunya

Terrassa, 2016

AGRADECIMIENTOS

El trabajo experimental de esta tesis se ha llevado a cabo principalmente en los laboratorios de Tecnología Textil Química y de Sistemas, del Instituto de Investigación Textil de Terrassa, de la Universitat Politècnica de Catalunya. Al centro y a las personas responsables, muchas gracias por permitirme estar aquí, por su apoyo y compañerismo.

Agradecer a la Universitat Politècnica de Catalunya el apoyo económico por la concesión de una beca dentro de su programa de Formación de Personal Investigador (FPI-UPC) para la realización de esta tesis doctoral.

Deseo expresar mi agradecimiento a todas las personas que han contribuido a que esta tesis doctoral se haya llevado a cabo.

En primer lugar, agradezco a mi director de tesis el Prof. Fernando Carrillo la orientación y el apoyo recibidos a lo largo de todos estos años y al Prof. Jorge Macanás por su inestimable contribución para alcanzar los objetivos propuestos, así como la motivación y el ánimo recibido durante el proceso.

Gracias al Prof. Josep Valledeperas, al Prof. Manel Lis y a los demás compañeros del Laboratorio de Tecnología Textil Química, Paulina Ferrer y Remedios Prieto, por acompañarme todo este tiempo y hacer agradable el ambiente de trabajo. Y un agradecimiento especial para mi compañera (y ya “más mejor amiga”) Aïda Duran, por su valiosa ayuda en la parte experimental y edición de esta tesis, pero especialmente por aguantarme en los malos ratos. Solo por conocerte ha valido la pena.

Agradezco también a José Antonio Tornero, Francesc Cano y a todo el personal del laboratorio de Sistemas por poner a mi disposición el conocimiento y el equipo necesario para la realización del trabajo experimental. Sin su inestimable ayuda no habría podido desarrollarse esta tesis.

A Montse Raspall y Valentina Buscio les agradezco el tiempo compartido y su compañía en los momentos de bajón.

También quiero agradecer a las personas que me permitieron utilizar sus instalaciones:

A la Prof. Mónica Ardanuy y Francisco Jimbel por su ayuda y permitirme utilizar su equipo de microscopia óptica.

A la Prof. Diana Cayuela, Carmen Escamilla y Montse García por prestarme los viscosímetros y el equipo de calorimetría.
Al Prof. Tzanko Tzanov y al personal del laboratorio del Grupo de Biotecnología Molecular e Industrial (UPC), en especial a Margarida Fernandez, por su disposición y amabilidad a la hora de realizar los ensayos.
A la Prof. Sunita P- Ho, de la Division of Biomaterials and Bioengineering, School of Dentistry de la University of California San Francisco (UCSF) de USA, por su colaboración y suministro de muestras utilizadas.

No puedo dejar de agradecer a mis padres y a mi hermano su apoyo a lo largo de mi vida y su insistencia en este proyecto. Por fin dejaré de escuchar la frase “¿Cuándo vas a presentar la tesis?”.

Y por último, pero no por eso menos importante, a Dersu, Kai, Ina y Leela por acompañarme en todo momento y hacerme ver lo que es realmente importante en la vida.

“Cada día sabemos mas

y entendemos menos”

Albert Einstein

RESUMEN

La creación de soportes capaces de imitar las propiedades estructurales y funcionales de las matrices extracelulares, y actuar como andamios para el crecimiento y multiplicación celular en líneas in vitro, es uno de los puntos de estudio más importantes dentro del campo de la ingeniería de tejidos. En este sentido se han desarrollado diversas técnicas para la fabricación de soportes tisulares con capacidad de soportar las células durante la reconstrucción de los tejidos biológicos, así como permitir la difusión de nutrientes. Entre estas técnicas, los métodos basados en nanotecnología, tales como la electro-hilatura, han demostrado jugar un papel relevante a la hora de obtener soportes capaces de imitar las propiedades fibrilares de las proteínas que forman matriz extracelular.

Teniendo en cuenta las premisas mencionadas, el objetivo principal de la presente tesis se basa en la fabricación de nanofibras de base proteica (ej. gelatina y colágeno) para la obtención de soportes fibrilares mediante la técnica de la electrohilatura. De forma resumida, el método de electro-hilatura consiste en la aplicación de un campo electrostático de alto voltaje que opera entre el capilar metálico de una jeringa, conteniendo una solución del polímero a hilar, y un colector conectado a tierra sobre el que se depositarán las fibras. Dado que la matriz extracelular está formada principalmente por proteínas estructurales, se utilizó gelatina y colágeno para la creación de los soportes tisulares, con el principal objetivo de garantizar la elevada compatibilidad celular, similar a la presentada por la estructura nativa.

En primer lugar el trabajo se centró en estudiar el **efecto de los distintos parámetros operacionales y químicos que gobiernan el proceso de electrospinning** sobre la morfología y tamaño de las fibras obtenidas. Como resultado, se establecieron los parámetros óptimos de proceso para obtener nanofibras de propiedades predefinidas. Los resultados mostraron que los parámetros operacionales tales como voltaje, caudal y distancia entre la aguja y el colector no tenían una influencia significativa en las propiedades de las nanofibras electro-hiladas siempre que se trabajara dentro de los rangos en los que el haz de fibras era estable. Por el contrario se demostró que los parámetros de la solución tales como tipo de polímero (gelatinas o colágeno), su concentración y el tipo de solvente, así como la conductividad del colector tenían un efecto significativo en el proceso de electro-hilado, determinando las propiedades finales de las nanofibras.

En segundo lugar, dado que las proteínas presentan ciertas dificultades frente a los polímeros sintéticos a la hora de hilar, debido a su capacidad de desnaturalización y degradación, se estudió en profundidad la elección de un solvente adecuado para la preparación de la solución a hilar. En este sentido, el estudio se centró en la búsqueda de **solventes alternativos con capacidad de mantener la integridad de las proteínas impidiendo su desnaturalización y degradación.** Con este objetivo, se llevó a cabo una amplia investigación sobre la fabricación de nanofibras electro-hiladas a temperatura ambiente a partir de mezclas de sistemas benignos de gelatina/ácido acético/agua. Además, se establecieron los límites de electrohilabilidad de este sistema y se modelaron los resultados a partir de un completo análisis reológico de las propiedades del sistema, con el objetivo de predecir las propiedades finales de las fibras en base a la composición de la solución. Alternativamente, se propuso un nuevo sistema benigno basado en una mezcla ternaria de PBS/Agua/Etanol para la electro-hilatura de tres tipos diferentes de gelatinas. En este caso, se evaluó el efecto del tipo de gelatina en la electrohilabilidad y morfología de las nanofibras obtenidas en base a su distinto origen y proceso de extracción.

En tercer lugar, se abordó el estudio de la estabilidad de las nanofibras electrohiladas teniendo en cuenta la importancia de su estabilidad en sistemas acuosos a la hora de actuar como potenciales soportes tisulares. Se utilizó vapor de glutaraldehído como agente reticulante dada sus numerosas ventajas respecto a otros productos (bajo coste, alta eficiencia y mínima toxicidad a baja concentración). Diversos métodos de aplicación del glutarladheido como reticulante fueron analizados, así como su influencia en la morfología y el tamaño de las fibras obtenidas. Asimismo, se propuso un método directo de estabilización por incorporación de pequeñas cantidades de glutaraldehído en la solución de hilatura, ofreciendo la posibilidad de obtener nanofibras estables directamente sin necesidad de realizar un tratamiento posterior.

Finalmente, con el objetivo de incrementar las propiedades mecánicas de los soportes de nanofibras se realizó un estudio de creación de biomateriales compuestos basados en la deposición de una nanocapa de fibras proteicas sobre la superficie de un biomaterial sintético. Para ello, las nanofibars de colágeno fueron fabricadas por electro-hilatura y depositadas sobre diferentes poliuretanos con distintas modificaciones superficiales. Los resultados permitieron evaluar la morfología y la distribución de las nanofibras teniendo en cuenta la química superficial del biomaterial, así como el efecto de la nanocapa de fibras en las propiedades finales de los poliuretanos.

ABSTRACT

The fabrication of scaffolds materials with the ability to mimic the structural and functional properties of extracellular matrix for promoting cell growing and multiplication in vitro lines is one of the most important points of interest into the tissue engineering field. Hence, several techniques have been developed to fabricate scaffolds with capacity to attach the cells and to allow the nutrient diffusion during the reconstruction of biological tissues. Among these techniques, nanotechnology based methods such as electrospinning have demonstrated to play a relevant role in mimicking the properties of proteins fibers of the extracellular matrices.

Taking on board the aforementioned premises, the aim of this Thesis is focused on the fabrication of protein based nanofibers (i.e. gelatin and collagen) to prepare artificial scaffolds using the electrospinning technique. Briefly, electrospinning method is based on the application of an electrostatic high voltage field between the metallic capillary of a syringe, containing the polymer solution to spin, and a ground connected collector where the nanofibers are deposited. Since the extracellular matrix is mainly constituted by structural proteins, gelatin and collagen materials were used for the creation of the tissue scaffolds, with the main objective to guarantee the high cell compatibility, similar to the native structure.

Firstly, the work was concentrated on the study of the **effect of the operational and chemical parameters controlling the electrospinning process** on the morphology and size of the obtained nanofibers. As a result, the optimal process parameters to obtain nanofibers of predefined properties were established. The results show that operational parameters such as voltage, flow rate and distance between needle and collector have not significant influence on the properties of electrospun nanofibers whenever you work into the range where the jet of nanofibers is stable. By contrast, it was demonstrate that the solution parameters such as type of polymer (gelatins or collagen), polymer concentration and type of solvent, as well as the collector conductivity have a significant effect on the electrospinning process determining the final properties of the nanofibers.

Secondly, since proteins such as gelatin and collagen are natural biopolymers with limited capacity for electrospinning, due to the easy of denaturation and degradation in contrast to synthethic polymers, the choice of an appropriate solvent for the preparation of the spinning dope was extensively studied. In this way, the study was concentrated in the search of **alternative solvents able to keep the integrity of the proteins, that**

is, avoiding the denaturation and degradation of the polymer chains. With this objective, a comprehensive research about the fabrication of electrospun nanofibers at room temperature from mixtures of **gelatin/acetic acid/water benign system** was carried out. The results confirmed the viability to obtain electrospun gelatin scaffolds using low acid concentrations (25%) with a high biocompatibility (cell viability upper than 90%). Also, the electrospinnability limits of this system were established and the results were modeled from a complete analysis of the rheological system properties, in order to allow the **prediction of the final fiber properties** based on the solution composition. Alternatively, a ternary mixture of **PBS/Water/Ethanol was proposed as a new benign solvent for the electrospinning of three different gelatin materials.** In this case, the effect of the type of gelatin on the electrospinninability and morphology of the nanofibers has also been studied based on their different origin and extraction process.

Thirstly, the stability of the electrospun nanofibers was addressed taking into account its importance regarding a potential application in tissue engineering as a scaffold. In this sense, nanofibers should be stable to wet treatments avoiding their solubility. In order to achieved this goal, glutaraldehyde vapor was used as crosslinking agent due to its numerous advantages, such as low price, high efficiency and lower cytotoxicity when is used in low concentrations. In this work, **several application methods of glutaraldehyde as crosslinker** were analyzed along as their influence on the morphology and size of electrospun fibers. In addition, a direct method of stabilization has been proposed based on the incorporation of low amounts of glutaraldehyde in the spinning solution offering the possibility to obtain stable nanofibers directly without the need of a post-spinning treatment.

Finally, with the purpose of increasing the mechanical properties of the nanofibers scaffolds, composite biomaterials were designed based on the deposition of proteins nanofibers over the surface of a synthetic biomaterial such as polyurethane. In this case, collagen nanofibers were fabricated by electrospinning and deposited onto different end-group-modified polyurethanes. The morphology and distribution of the nanofibers was studied taking into account the chemistry of the biomaterial. Also the effect of the nanolayer of fibers on the final properties of the polyurethanes was analyzed.

Índice

Índice de figuras

Índice de tablas

CAPÍTULO 1:

Introducción general

Introducción General

1.1. Ingeniería de tejidos

La ingeniería de tejidos constituye una tecnología biomédica emergente basada en la reparación y regeneración de tejidos deficientes o heridos, cuyo desarrollo aplica conocimientos de diversas áreas, siendo por tanto, una tecnología multidisciplinar (**Figura 1.1**).

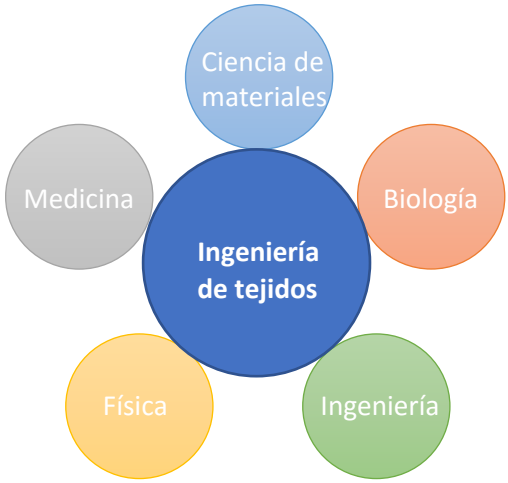

***Figura 1.1**: Áreas de conocimiento relacionadas con el desarrollo de la ingeniería tisular*

Los gastos sanitarios derivados del trasplante de tejidos y órganos constituyen una parte importante del presupuesto destinado a sanidad [1.1]. La ingeniería de tejidos se ofrece como una alternativa importante a la hora de mejorar la atención médica así como en la reducción significativa de los costes sanitarios [1.2]. El incremento significativo en la publicación de artículos originales referentes a la ingeniería tisular [1.3] en los últimos años proporciona una idea de la importancia reciente de este campo de estudio (**Figura 1.2**).

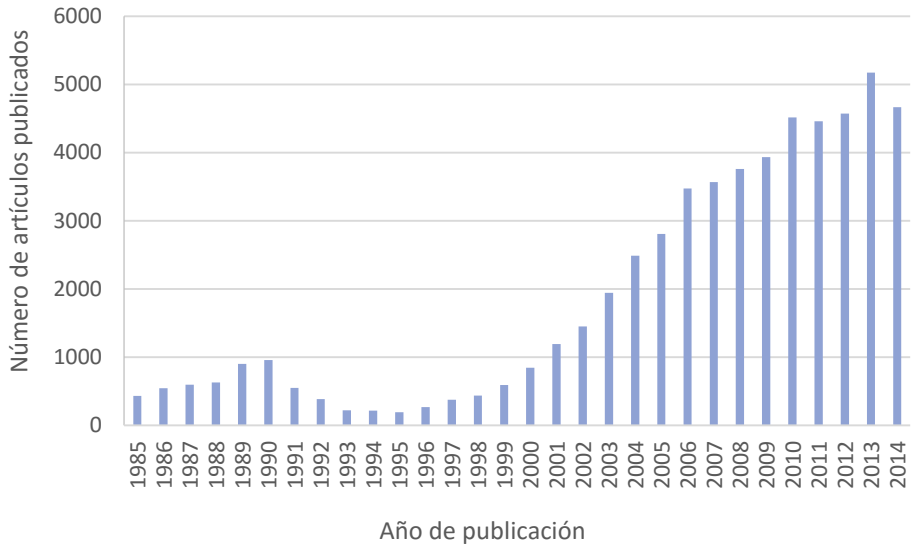

Figura 1.2: *Evolución del número de artículos publicados referentes a la ingeniería de tejidos (Resultados obtenidos vía Scopus® usando la palabra clave "Tissue Engineering")*

Los objetivos principales de la ingeniería de tejidos son restaurar, mantener o mejorar funciones de tejidos que se muestran defectuosos o se han perdido debido a diferentes patologías, tanto por la vía de desarrollar substitutos biológicos como por la reconstrucción de los tejidos activos.

Las estrategias que adopta la ingeniería de tejidos se dividen en tres grupos generales [1.4]:

- Implantación de células aisladas o células substitutas en el organismo.
- Incorporación de substancias en el tejido, tales como factores de crecimiento.
- Colocación las células encima o en el interior de diferentes matrices, (también llamadas andamios).

Dentro de éstas, la estrategia mayormente asociada al concepto de ingeniería tisular es la mostrada en la **Figura 1.3**, basada en el uso de células vivas sembradas sobre un sustrato extracelular natural o sintético con el objetivo de crear piezas implantables en el organismo.

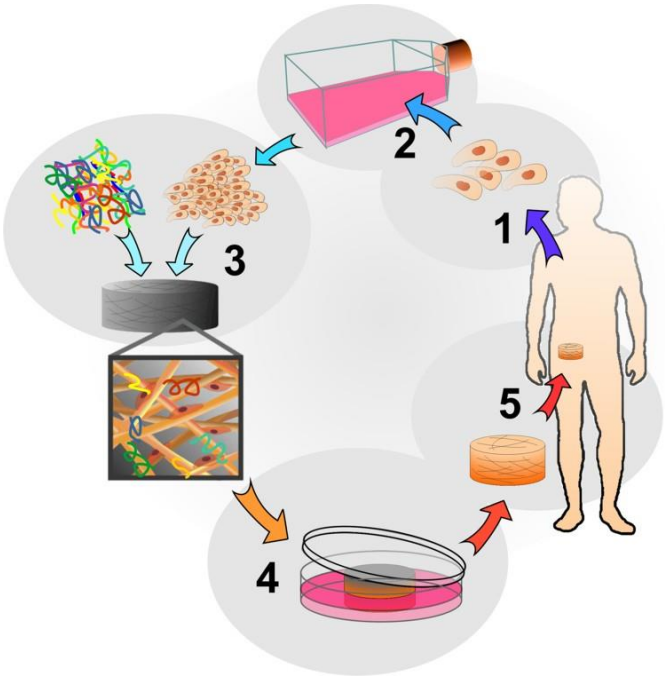

***Figura 1.3**: Ciclo de la ingeniera tisular. 1: Las células son extraídas del cuerpo. 2: Se realiza la proliferación celular in vitro. 3: Se siembran las células en andamios porosos. 4: Los andamios con las células se incuban para promover el crecimiento celular. 5: El tejido regenerado se implanta en el cuerpo para integrarse con el tejido natural* [1.5]

1.2. Andamios para ingeniería de tejidos

Una de las partes más importantes dentro de la ingeniería de tejidos es la obtención del andamio adecuado [1.6]. El andamio es una construcción tridimensional que sirve como soporte temporal para células aisladas que crecen en un nuevo tejido antes de su trasplante al tejido de origen. El diseño del soporte determina la funcionalidad de la construcción en un alto porcentaje. Aunque los requerimientos finales del material dependen del propósito específico del andamio, existen diversas características comunes a todos los diseños [1.7]:

- **Biocompatibilidad**: las células deben ser capaces de adherirse al andamio, crecer y diferenciarse. El andamio, además, debe provocar una respuesta biológica apropiada en cuerpo y prevenir cualquier respuesta adversa a los alrededores del tejido.

- **Biodegradabilidad**: El objetivo de la ingeniería de tejidos es permitir que las propias células del cuerpo puedan reemplazar el andamio implantado. De esta manera el andamio debe ser biodegradable, permitiendo así la formación de su propia matriz extracelular por parte de las células. A medida que se produce la

regeneración tisular el andamio debe degradarse sin interferir con los alrededores del tejido.

- **Propiedades mecánicas**: El andamio debe tener propiedades mecánicas consistentes con el tejido huésped en el que vaya a ser implantado, así como ser lo suficientemente fuerte para permitir su manipulación durante la implantación.

- **Arquitectura**: La porosidad es el factor clave en la estructura de los andamios. La porosidad debe ser suficientemente alta para asegurar la penetración celular, así como permitir la difusión adecuada de nutrientes a las células. Estudios recientes basan su investigación en la capacidad para controlar la formación de los poros en los andamios celulares [1.8-1.10].

En conclusión, el desarrollo de un andamio con capacidad de imitar las propiedades estructurales y funcionales de la matriz extracelular en el cual las células puedan adherirse y proliferar constituye un papel fundamental en la ingeniería tisular.

1.2.1. Materiales

Entre los materiales más utilizados para aplicaciones biomédicas se encuentran los metales y sus aleaciones [1.11], los materiales cerámicos [1.12] y los materiales poliméricos [1.13]. En función de las características mecánicas y físicas necesarias para su uso se utilizará un tipo de material u otro.

Así, para la ingeniería tisular fuerte (substitución de huesos, implantes, etc.), se utiliza generalmente polímeros rígidos de materiales cerámicos y metales, mientras que para aplicaciones de ingeniería de tejido suaves (cartílago, válvulas de corazón y arterias, páncreas, nervios, corneas, etc.), se aplica una gran variedad de materiales poliméricos [1.14].

La **Tabla 1.1** muestra un resumen de los distintos biomateriales utilizados en ingeniería tisular, así como sus propiedades y aplicaciones más comunes.

***Tabla 1.1**: Tipos de materiales usados en ingeniería de tejidos* [1.15]

Material soporte	Ventajas	Desventajas	Aplicaciones	Ejemplos	Figuras ejemplo
Metales y aleaciones	Muy fuerte, duro, dúctil	Denso, se puede corroer, dificultad para fabricarlo	Implantes óseos, restauración dental, etc.	Aleaciones de titanio [1.16]	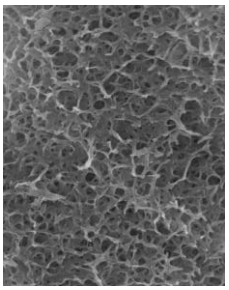
Cerámicos	Bioinerte Bioactivo Bioreabsorbible Alta resistencia al desgaste, resistencia a la corrosión	Frágil, baja tenacidad, no resiliente	Implantes óseos de bajo peso molecular, ingeniería de tejidos, liberación de fármacos,etc.	Alúmina, Hidroxiapatita (HA) [1.17] Fosfato de calcio.	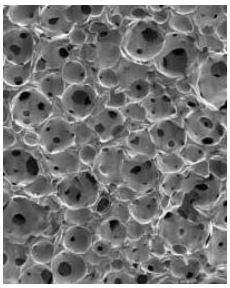
Polímeros	Flexible, baja densidad, resiliente, superficie modificable, grupos químicos funcionales	Baja rigidez, se puede degradar	Ingeniería de tejidos, liberación de fármacos, suturas, aumento de la piel, válvulas de corazón, etc.	Colágeno[1.18] Gelatina, PLLA, PGA.	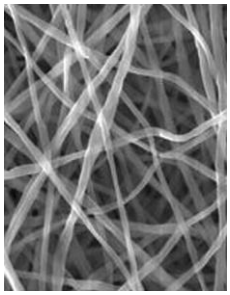
Composites	Fuerte, flexible, mayor fiabilidad mecánica respecto los monolíticos.	Propiedades variables según método de fabricación.	Ingeniería de tejidos, liberación de fármacos, restauración dental, cirugía espinal, etc.	HA-colágeno, HA-PLLA. Colágeno-PLGA-HA[1.19]	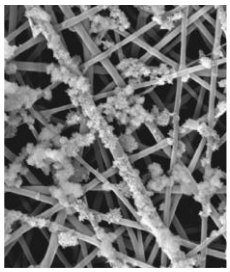

Polímeros como el poliestireno, ácido poliláctico (PLLA) [1.20] y ácido poliglicólico (PGA) [1.21] han sido ampliamente utilizados en la ingeniería de tejidos debido a sus propiedades únicas como la alta relación de superficie y volumen, su elevada porosidad con tamaño de poro muy pequeño, su capacidad de biodegradación y sus propiedades mecánicas. Los materiales poliméricos pueden ofrecer además ventajas de biocompatiblidad, versatilidad química y propiedades biológicas que lo convierten en material clave para la ingeniería tisular y la substitución de órganos [1.14].

Dentro de los materiales poliméricos se puede distinguir entre polímeros naturales y sintéticos. En la **Tabla 1.2** se muestran los polímeros más utilizados en la ingeniería de tejidos suave [1.22-1.23]:

***Tabla 1.2**: Biomateriales poliméricos frecuentemente aplicados en aplicaciones de ingeniería de tejidos suave*

Origen	Polímero (familia)
Natural	Colágeno (componente de la matriz extracelular- ECM) Fibroina Gelatina Polihidroxibutirato Polisacáridos (ácido hialurónico, chitosan, almidón, alginatos)
Sintético	Poliésteres (ácido poliláctico (PLA), ácido poliglicólico (PGA)) Poly (e-caprolactanos) Poli(propileno fumaratos) Poli(anhídridos) Poli(ortoesteres)

1.2.2. Diseños y técnicas de obtención

Las características del andamio utilizado dependen de su aplicación, de manera que se debe seleccionar cuidadosamente tanto los polímeros que compondrán el andamio como la técnica de fabricación.

Los diseños típicos de los andamios incluyen mallas, fibras, esponjas y espumas entre otros. Del diseño del andamio dependerá la adecuada distribución y crecimiento de células así como la difusión de nutrientes [1.4, 1.24].

La **Tabla 1.3** muestra algunas de las principales técnicas de fabricación de andamios tisulares porosos:

***Tabla 1.3**: Principales técnicas de fabricación de andamios tisulares porosos*

Diseño	Fundamento	Ejemplo
Liofilización [1.25]	Liofilización de una emulsión polímero-agua.	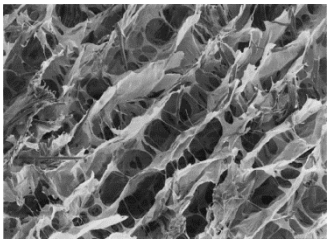
Formación de espumas [1.26]	Uso de un gas inerte como agente de soplado a través del polímero.	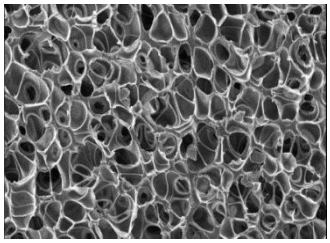
Sinterización [1.27]	Tratamiento térmico de un polvo para hacer que las partículas se adhieran entre sí.	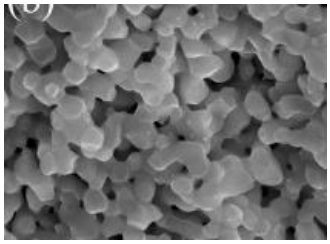
Lixiviación de partículas [1.28]	Creación de poros en el polímero mediante partículas llamadas porógenos.	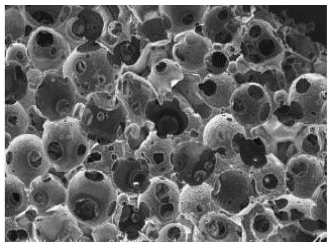
Malla de fibras [1.29]	Formación de un andamio no-tejido mediante técnicas textiles.	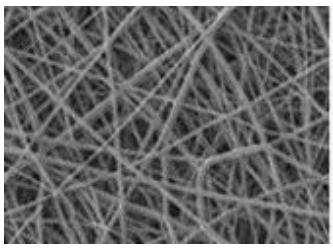

Los avances en nanotecnología, especialmente dentro del área de la fabricación de nanofibras, resultan una prometedora opción para el desarrollo y formación de andamios clínicos.

La fabricación de nanofibras poliméricas se puede realizar mediante distintas técnicas de obtención tales como:

- **“Drawing”**: Consiste en fabricar nanofibras a partir de una micropipeta con un diámetro de pocos micrómetros, la cual se sumerge en una gota del polímero a hilar, cerca del punto de contacto. A continuación la micropipeta se retira a una velocidad de aproximadamente 10^{-4} m/s, formando la nanofibra.

- **Síntesis por molde**: Implica el uso de una plantilla o molde para obtener la estructura deseada. La plantilla consiste en una membrana de un óxido de metal con poros de diámetros a escala nanométrica. La presión ejercida por el agua permite la extrusión de la solución de polímero, que pasará a un medio de solidificación donde quedaran fijadas con el diámetro a escala nanometrica.

- **Separación de fases**: En primer lugar el polímero se mezcla con un disolvente para posteriormente someterse a gelificación. El principal mecanismo en este proceso es la separación de fases debido a su incompatibilidad física. Tras la gelificación una fase se separa del resto. Los pasos a seguir son: a) disolución del polímero b) gelificación c) congelación d) secado.

- **Auto-ensamblaje**: Consiste en la acumulación de fibras a escala nanométrica con moléculas más pequeñas que ejercen como bloque de construcción básico. El principal mecanismo para el auto ensamblaje son las fuerzas intermoleculares, que unen las unidades más pequeñas, junto con la forma de éstas, que determinará la forma de las nanofibras macromoleculares.

- **Electrospinning**: proceso patentado por Formhals en 1934 [1.30] basado en la producción de nanofibras poliméricas a partir del uso de fuerzas electrostáticas actuando entre el cabezal de la aguja de una jeringa, cargada con una solución del polímero a hilar, y el colector sobre el que se recogerán las fibras.

La **Tabla 1.4** muestra los esquemas de las principales técnicas de obtención de nanofibras descritos con sus principales ventajas e inconvenientes [1.31-1.32]:

***Tabla 1.4**: Técnicas de fabricación de nanofibras con sus principales ventajas e inconvenientes*

"DRAWING"[1.33]	**SÍNTESIS POR MOLDE**[1.34]	**SEPARACIÓN DE FASES**[1.35]	**AUTOENSAMBLAJE** [1.36]	**ELECTROSPINNING**[1.37]
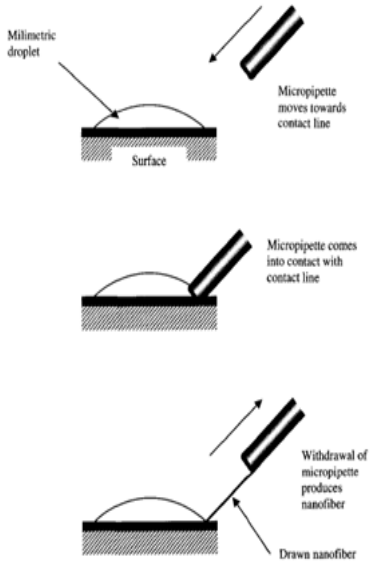	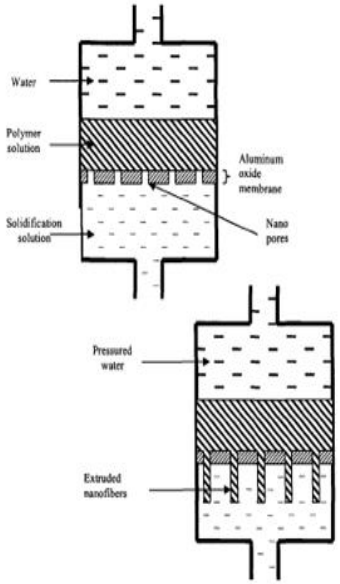	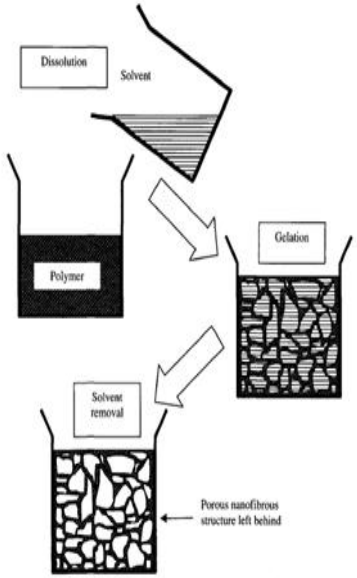		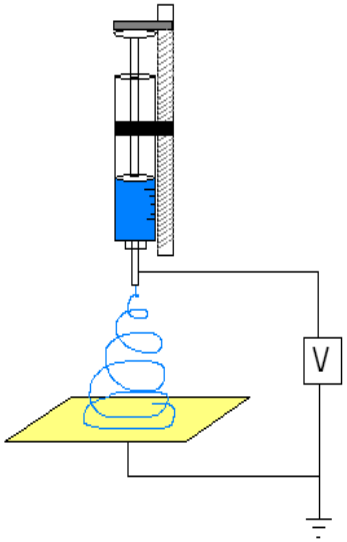
Mínimo equipo ✓	Varios diámetros ✓	Matriz directa ✓	Diámetro pequeño ✓	Versátil y sencillo ✓
Discontinuo ×	Complejo ×	Polímeros específicos ×	Complejo ×	Control del haz ×

1.3. Electrohilatura o "Electrospinning"

Comparado con las técnicas de autoensamblaje y separación de fases, el electrospinning constituye una técnica con mayor simplicidad de uso a la vez que presenta una mayor eficiencia para la producción de andamios con estructura porosa interconectada, así como diámetros de fibra por debajo de la micra. Es por esto que el incremento en el número de publicaciones recientes relacionadas con la fabricación de nanofibras mediante electrospinning ha sido considerable (**Figura 1.4**).

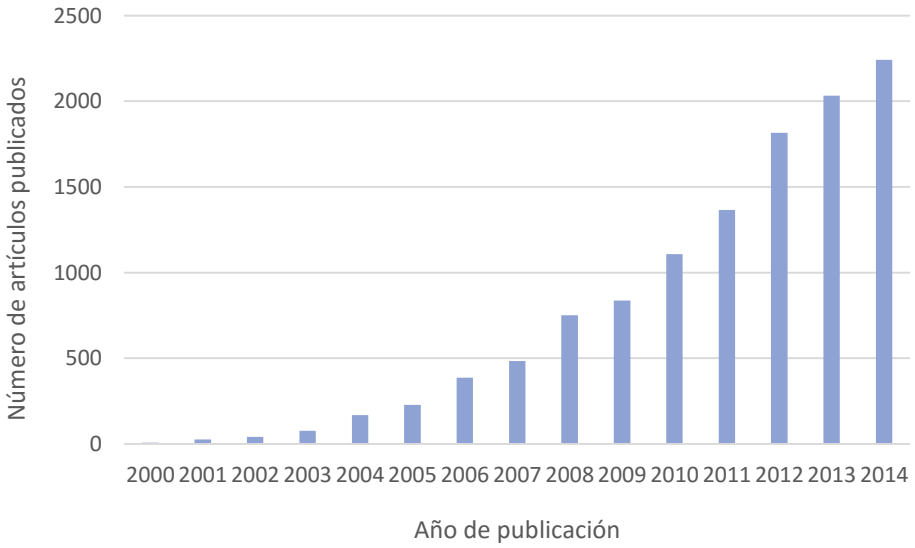

***Figura 1.4**: Evolución del número de artículos publicados referentes a la técnica de electrospinning. (Resultados obtenidos vía Scopus® usando la palabra clave "Electrospinning")*

Aunque la técnica de electrospinning ha sido utilizada comercialmente desde principios del siglo 20 dentro de los procesos textiles, el descubrimiento reciente de la capacidad para electrohilar polímetros naturales ha revitalizado el proceso, ampliando sus aplicaciones potenciales [1.37].

Las nanofibras obtenidas por electrospinning se han aplicado ya con éxito en diversos ámbitos tales como: nanocatálisis, ingeniería de tejidos, ropa de protección, filtración, ingeniería ambiental, etc. [1.38-1.39].

En la **Figura 1.5** [1.39] se muestra un diagrama esquemático del proceso de electrospinning, en el que pueden diferenciarse esencialmente tres partes: una alimentación de alta tensión, una jeringa controlada por una bomba y un colector a tierra.

El equipo produce fibras aprovechando la fuerza electrostática que genera una fuente de alimentación de corriente continua de alto voltaje. Esta fuerza actúa sobre la gota de solución de polímero impulsada por una bomba y que queda suspendida en la punta de una aguja. Cuando la fuerza de repulsión electrostática supera la fuerza de tensión superficial de la solución de polímero, el líquido acumulado se desprende de la punta de la aguja y forma un filamento continuo extremadamente fino. La deformación sufrida por la gota en la punta de la jeringa a medida que se aplica la diferencia de potencial fue estudiada por Taylor en 1964 [1.40], dando lugar al denominado cono de Taylor (**Figura 1.6**), un fenómeno característico asociado al proceso de electrospinning.

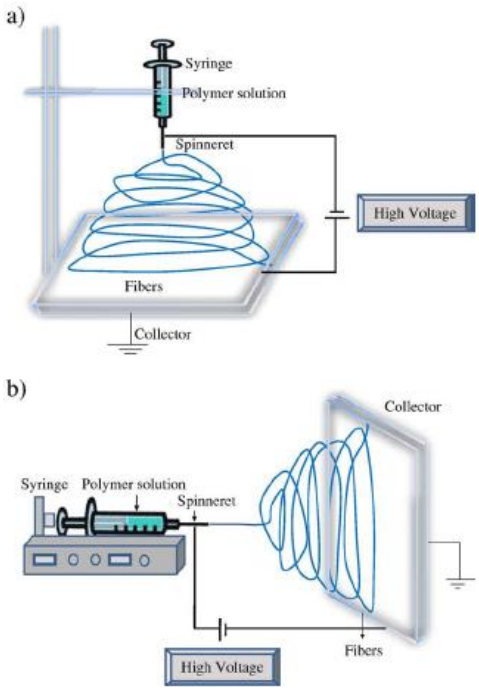

***Figura 1.5**: Esquemas del proceso de electrospinning. a) Vertical b) Horizontal [1.39]*

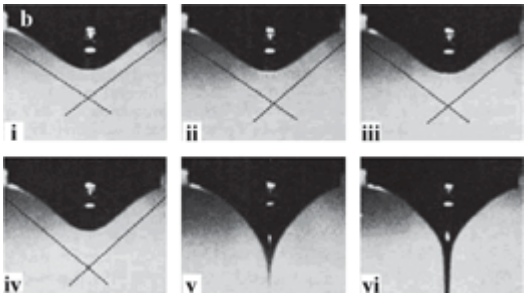

***Figura 1.6**: Evolución de una gota de solución hacia el cono de Taylor a partir del que se expulsa un flujo cargado dando lugar a las nanofibras* [1.41]

Los filamentos que se producen se recogen en un colector, que puede ser tanto rotativo como estacionario, con un electrodo con carga opuesta a la del cabezal de hilado, donde se acumulan y se unen las nanofibras.

El proceso de electrospinning está gobernado por varios parámetros clasificados en parámetros de la solución, de proceso y ambientales [1.39, 1.42]. En la **Tabla 1.5** se puede observar la influencia de cada parámetro del electrospinning sobre la morfología de las fibras obtenidas según estudios precedentes realizados por diversos autores.

Tabla 1.5: *Efecto de los diferentes parámetros que influyen en el proceso de electrospinning*

		Efecto sobre las fibras	Estudios realizados
SOLUCIÓN	Viscosidad	Baja: mala continuidad de las fibras. Alta: Aumento del diámetro.	Seda [1.43], Dextran [1.44], PLGA [1.45-1.46], PEO [1.47-1.49], PVA [1.50-1.52], PLLA [1.53], PP [1.54]
	Concentración	A mayor concentración, mayor diámetro de fibra.	Seda [1.43], Dextran [1.44], PCL [1.55], PAN[1.56], PVA [1.51,1.57], PEO [1.48], Nylon 6 [1.58], PA-6 [1.59-1.60]
	Tensión superficial	Baja: fibras sin gotas. Alta: Inestabilidad de chorro. Spraying.	PVA [1.51-1.52, 1.61], PA-6 [1.59], Nylon 6 [1.58]
	Peso molecular	A mayor peso molecular mejor continuidad de fibras.	PVA [1.51-1.52, 1.61], Poliestireno [1.62], Nylon 6 [1.63-1.64], PA-6 [1.59]
	Conductividad	Alta: menor diámetro. Fibras continuas. Baja: mayor diámetro.	PEO[1.47, 1.65], PVA [1.50], PP [1.54], Nylon 6 [1.66]
PROCESO	Voltaje	A mayor voltaje menor diámetro de fibra.	Seda [1.43], Dextran [1.44], PLGA [1.46], PEO [1.48, 1.65, 1.67], PVA [1.52], PLLA [1.53], PA-6 [1.59] Nylon 6 [1.68], PAN [1.69]
	Distancia al colector	Demasiado corta o demasiado larga produce fibras discontinuas.	Seda [1.43], Dextran [1.44], PLGA [1.46], PVA [1.51] PA-6 [1.60], PAN [1.69]
	Caudal	Menor caudal: fibras finas. Caudal demasiado alto: fibras discontinuas.	PEO[1.47], PVA [1.50], PCL [1.55], Nylon 6 [1.70]
AMBIENTE	Humedad	Alta humedad produce poros circulares en las fibras.	PLLA [1.53], Poliestireno [1.62]
	Temperatura	Mayor temperatura da fibras de menor diámetro.	PA-6 [1.59], Nylon 6 [1.66]

Además de estos parámetros, los disolventes empleados para preparar la solución de polímero también tienen una influencia significativa en la capacidad de hilar. La disolución en un solvente adecuado es el primer paso a tener en cuenta en el proceso de electrospinning [1.37, 1.71].

Los disolventes deben presentar unas propiedades óptimas de volatilidad, presión de vapor y punto de ebullición.

En la **Tabla 1.6** se muestran las propiedades principales de algunos de los disolventes más utilizados para la electrohilatura de polímeros:

***Tabla 1.6**: Características de los disolventes más utilizados en electrospinning* [1.39]

Disolvente	Tensión superficial (mN/m)	Constante dieléctrica	Punto Ebullición (ºC)	Densidad (g/ml)
Cloroformo	26,5	4,8	61,6	1,498
Dimetilformamida (DMF)	37,1	38,3	153	0,994
Hexafluoropropanol (HIPF)	16,1	16,70	58,2	1,596
2,2,2-Trifluoroetanol (TFE)	21,1	27	78	1,393
Acetona	25,2	21	56,1	0,786
Metanol	22,3	33	64,6	0,791
Ácido acético	26,9	6,2	118,1	1,049
Ácido fórmico	37	58	100	1,21
Diclorometano	27,2	9,1	40	1,326
Etanol	21,9	24	78,3	0,789
Agua	72,8	80	100	1,000

1.4. Electrohilatura de biopolímeros

Desde la comercialización de la técnica de electrohilatura a principios del siglo XX numerosos polímeros han demostrado su capacidad de formar nanofibras para su uso en diferentes aplicaciones, tales como la ingeniería tisular [1.4].

Se ha reportado la obtención de nanofibras electrohiladas a partir de polímeros sintéticos (PLA [1.72], PCL [1.73], Acetato de célulosa [1.74], etc.), naturales, así como mezclas de ambos, incluyendo proteínas, ácidos nucleicos (DNA [1.75]) y polisacáridos (chitosan [1.76], ácido hialurónico [1.77], dextran [1.78], etc.).

Mientras que los soportes fabricados a partir de polímeros sintéticos pueden imitar la matriz extracelular nativa, la hilatura de polímeros naturales presenta ciertas ventajas frente a los primeros ya que proporciona a las células una plataforma reconocible y fisiológicamente apropiada para su proliferación y diferenciación. Esta capacidad inherente para unirse a las células de los polímeros naturales es uno de los principales motivos que ha impulsado su uso en aplicaciones biomédicas.

Dentro de los polímeros naturales es destacable el creciente uso de proteínas como el colágeno [1.18, 1.79] y la gelatina [1.80] para la fabricación de soportes tisulares mediante electrohilatura. En estos casos, deben sopesarse algunos inconvenientes relacionados con la degradación y desnaturalización de dichos soportes.

1.4.1. Colágeno

El colágeno se encuentra entre las más abundantes proteínas fibrosas y cumple una variedad de funciones mecánicas, particularmente en los mamíferos.

Constituye la mayor parte de los tendones y ligamentos, forma parte de la matriz orgánica del hueso y la dentina, está presente en la piel, arterias, cartílago y en la mayor parte de la matriz extracelular en general (**Figura 1.7**).

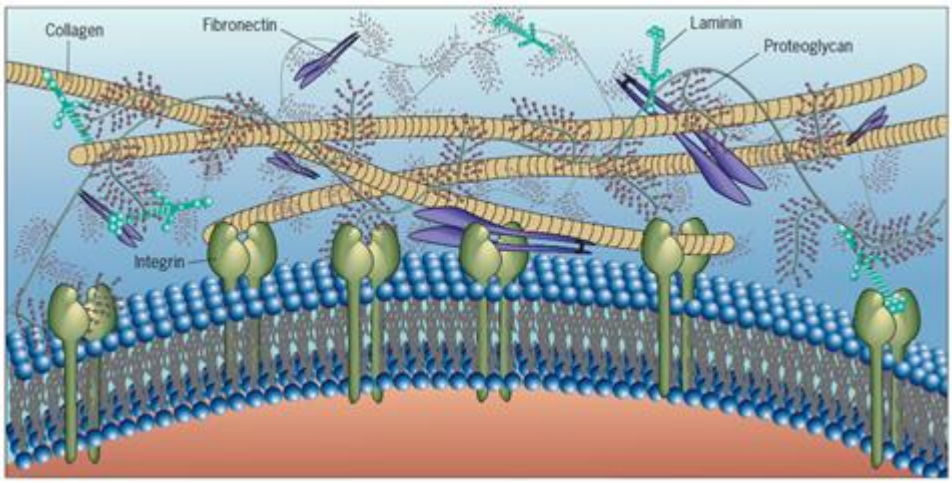

***Figura 1.7**: Visión general de la organización molecular de la matriz extracelular* [1.81]

Hasta el momento se han identificado hasta 26 tipos de colágeno genéticamente distintos, siendo el colágeno tipo I y tipo III los más presentes en los elementos de la matriz extracelular.

El nombre de colágeno es usado como un término genérico para cubrir una amplia gama de moléculas de proteínas que forman estructuras matriciales supramoleculares, compartiendo una textura básica de tres cadenas alfa (α) individuales que forman una triple hélice (estructura terciaria) con un peso molecular de aproximadamente 300.000 g/ml, una longitud de aproximadamente 300 nm y un diámetro de 1.5 mm (**Figura 1.8**). Cada cadena α está constituida por un polipéptido, formado por una repetición en tándem de tres aminoácidos ricos en prolina (Pro) o hidroxiprolina (Hyp) y glicina (Gly), los cuales son fundamentales en la formación y estabilización de la superhélice por su implicación en la formación de puentes de hidrógeno [1.82]

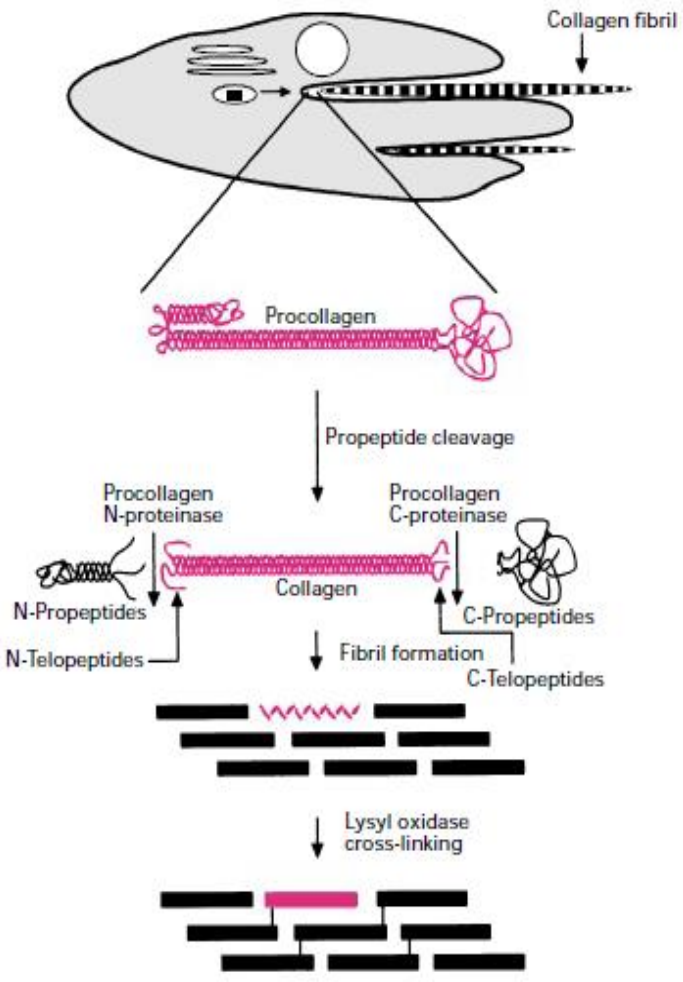

***Figura 1.8**: Síntesis de fibrillas de colágeno* [1.82]

Las fibrillas de colágeno se caracterizan por poseer un alto grado de alineamiento axial y exhibir las bandas características D, resultado del empaquetamiento de sus moléculas. Estas bandas D aparecen con una periodicidad de 67 nanómetros en el colágeno nativo y son observables mediante distintas técnicas tales como TEM y AFM [1.82] (**Figure 1.9**).

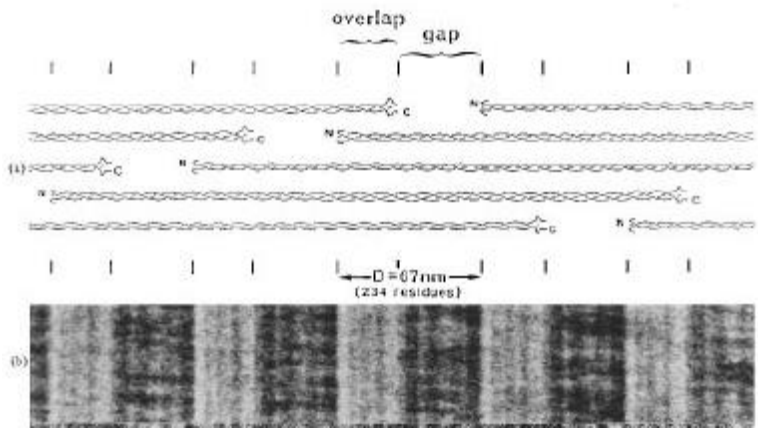

***Figure 1.9**: Representación esquemática del empaquetamiento axial de la triple hélice de colágeno con sus bandas características* [1.82]

Debido a que la función principal del colágeno en el organismo es aportar una estructura de soporte para los tejidos, se ha considerado éste como un material “ideal” a la hora de diseñar andamios para la ingeniería de tejidos.

El punto principal a tener en cuenta a la hora de obtener nanofibras de colágeno vía electrospinning es la identificación del solvente adecuado capaz de disolver el colágeno a una concentración suficiente que permita el electrohilado, así como proporcionar la volatilidad necesaria para su rápida evaporación y obtención de nanofibras secas en el colector.

La mayor parte de los estudios realizados hasta el momento sobre electrospinning de colágeno trabajan con fluoroalcoholes de alta volatilidad como disolventes, siendo los más utilizados el 1,1,1,3,3,3- hexafluoro-2-propanol (HFP) [1.18, 1.80, 1.83-1.89] así como el 2,2,2-trifluoroetanol (TFE) [1.89-1.90].

Pero la naturaleza del colágeno electrohilado es objeto de conflicto en la comunidad científica. Varios estudios han demostrado el efecto negativo de los fluoroalcoholes sobre las estructuras nativas de las proteínas, así como la disminución de su temperatura de desnaturalización [1.91-1.92]. Además se ha demostrado mediante la técnica de dicroísmo circular que el propio proceso de electrospinning hace perder un

45% de la estructura nativa del colágeno [1.93]. Estos datos apuntan a la idea que el colágeno obtenido una vez electrohilado no es más que colágeno desnaturalizado, o en otras palabras, gelatina [1.94], la cual, aun teniendo propiedades distintas al colágeno nativo, no debe ser descartada como material para la ingeniería de tejidos [1.88].

1.4.2. Gelatina

La gelatina es un polímero natural derivado de la hidrólisis controlada del colágeno, usada comúnmente para aplicaciones médicas y farmacéuticas debido a su alta biodegradabilidad y biocompatiblidad en ambientes fisiológicos. Resulta una alternativa económica al uso del colágeno.

1.4.2.1. Composición

Se trata de un polipéptido de alto peso molecular derivado de la desnaturalización térmica y la degradación física y química del colágeno, cuyo peso molecular oscila habitualmente entre 20.000 y 250.000 g/ml.

La estructura química de la proteína se describe como una secuencia lineal de amino ácidos, siendo la glicina, prolina e hidroxiprolina los predominantes, tales como ocurre en su proteína precursora, el colágeno. La **Figura 1.10** muestra una representación esquemática de la composición de aminoácidos en la gelatina, mientras que en la **Tabla 1.7** aparecen todos los aminoácidos constituyentes de la gelatina con sus abreviaciones y estructuras lineales.

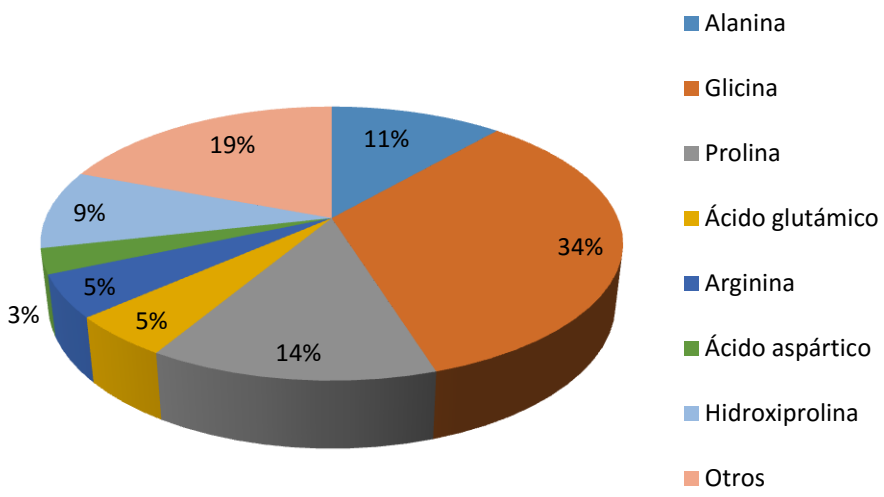

***Figura 1.10**: Composición de aminoácidos de la gelatina* [1.95]

***Tabla 1.7**: Nombres, abreviaturas y estructuras lineales de los aminoácidos presentes en la gelatina* [1.96]

Nombre	Abreviatura	Estructura lineal
Alanina	**Ala A**	CH_3-CH(NH_2)-COOH
Arginina	**Arg R**	HN=C(NH_2)-NH-(CH_2)$_3$-CH(NH_2)-COOH
Asparagina	**Asn N**	H_2N-CO-CH_2-CH(NH_2)-COOH
Ácido aspártico	**Asp D**	HOOC-CH_2-CH(NH_2)-COOH
Cisteína	**Cys C**	HS- CH_2-CH(NH_2)-COOH
Ácido glutámico	**Glu E**	HOOC-(CH_2)$_2$-CH(NH_2)-COOH
Glutamina	**Gln Q**	H_2N-CO-(CH_2)$_2$-CH(NH_2)-COOH
Glicina	**Gly G**	H-CH(NH_2)-COOH
Histidina	**His H**	NH-CH=N-CH=C-CH_2-CH(NH_2)-COOH
Isoluecina	**Ile I**	CH_3-CH_2-CH(CH_3)-CH(NH_2)-COOH
Leucina	**Leu L**	(CH_3)$_2$-CH-CH_2-CH(NH_2)-COOH
Lisina	**Lys K**	H_2N-(CH_2)$_4$-CH(NH_2)-COOH
Metionina	**Met M**	CH_3-S-(CH_2)$_2$-CH(NH_2)-COOH
Fenilalanina	**Phe F**	Ph-CH_2-CH(NH_2)-COOH
Prolina	**Pro P**	NH-(CH_2)$_3$-CH-COOH
Serina	**Ser S**	HO-CH_2-CH(NH_2)-COOH
Treonina	**Thr T**	CH_3-CH(OH)-CH(NH_2)-COOH
Triptofano	**Trp W**	Ph-NH-CH=C-CH_2-CH(NH_2)-COOH
Tirosina	**Tyr Y**	HO-Ph-CH_2-CH(NH_2)-COOH
Valina	**Val V**	(CH_3)$_2$-CH-CH(NH_2)-COOH

1.4.2.2. Estructura

La estructura de la gelatina se clasifica, al igual que el resto de proteínas, en cuatro grupos (**Figura 1.12**):

- **Estructura primaria**

  Viene determinada por la secuencia de aminoácidos en la cadena proteica, estructurada principalmente en tripletes Glicina-X-Y, donde X e Y corresponden usualmente a prolina e hidroxiprolina, respectivamente (**Figura 1.11**). Los aminoácidos se mantienen unidos entre sí mediante enlaces peptídicos, de tipo covalente.

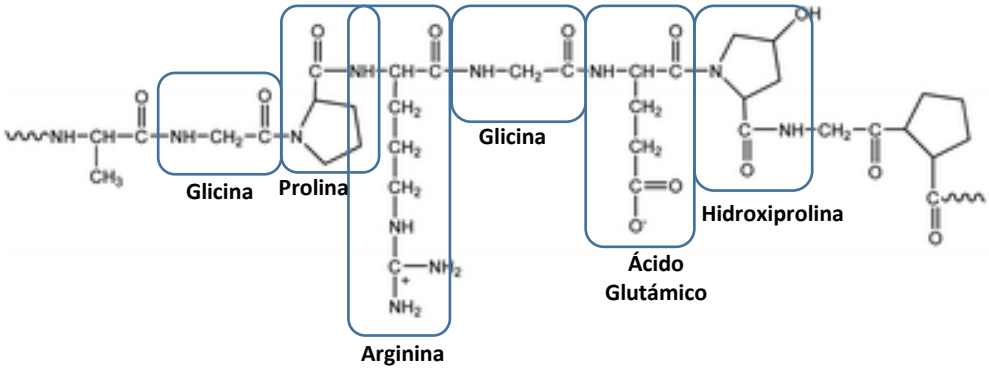

***Figura 1.11**: Estructura química de la gelatina* [1.97]

- **Estructura secundaria**

  Consiste en el plegamiento regular local entre residuos aminoacídicos cercanos de la cadena polipeptídica mediante la formación de puentes de hidrógeno entre los átomos que forman el enlace peptídico, sin tener en cuenta la conformación de su cadena lateral o su interrelación con otros segmentos. En las proteínas existen tres tipos de estructuras secundarias: hélices alfa, hojas beta y giros beta, siendo las dos primeras las conformaciones más comunes y termodinámicamente estables de la estructura secundaria de los polipéptidos.

- **Estructura terciaria**

  Es la disposición tridimensional de todos los átomos que componen la proteína y se forma a partir de interacciones entre cadenas de aminoácidos a largas distancias.

- **Estructura cuaternaria:**
  Se refiere a las relaciones espaciales entre cadenas individuales de polipéptidos en una proteína multicadena.

1.4.2.3. Fabricación

Existen dos tipos de gelatina en función de su proceso de obtención: gelatina tipo A (extraída por proceso en medio ácido) y gelatina tipo B (obtenida por proceso en medio básico).

El proceso ácido consiste en el uso de una solución diluida de ácido clorhídrico (aproximadamente al 4%) para la acidificación, desnaturización y solubilización del colágeno. Se usa principalmente para la extracción en pieles porcinas y de pescado y la gelatina resultante de este proceso (Tipo A) presenta un punto isoeléctrico de pH=7-9 en función de la severidad y duración del tratamiento.

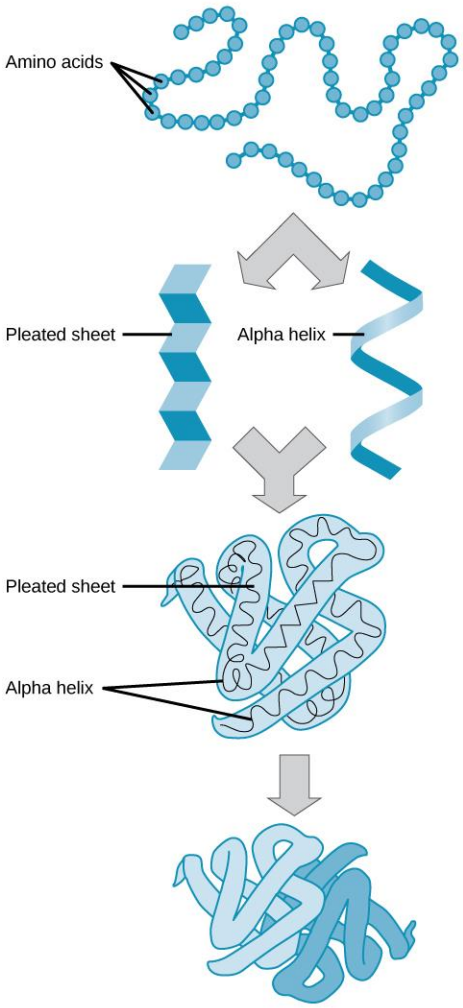

***Figura 1.12**: Representación esquemática de la estructura primaria, secundaria, terciaria y cuaternaria de la proteína (Fuente: www.boundless.com)*

El proceso básico se aplica para la extracción de gelatina de pieles y huesos. En este caso el colágeno se pone en contacto con una solución alcalina (carbonato de sodio o potasio) para su extracción. A diferencia de la gelatina Tipo A, la gelatina obtenida por extracción alcalina presenta un punto isoeléctrico menor, de pH=4.8-5.2, el cual puede aumentar hasta pH=6 si el tratamiento básico es de corta duración.

La **Figura 1.13** muestra un diagrama de flujo con las distintas etapas del proceso de extracción de gelatina en función de la materia prima utilizada.

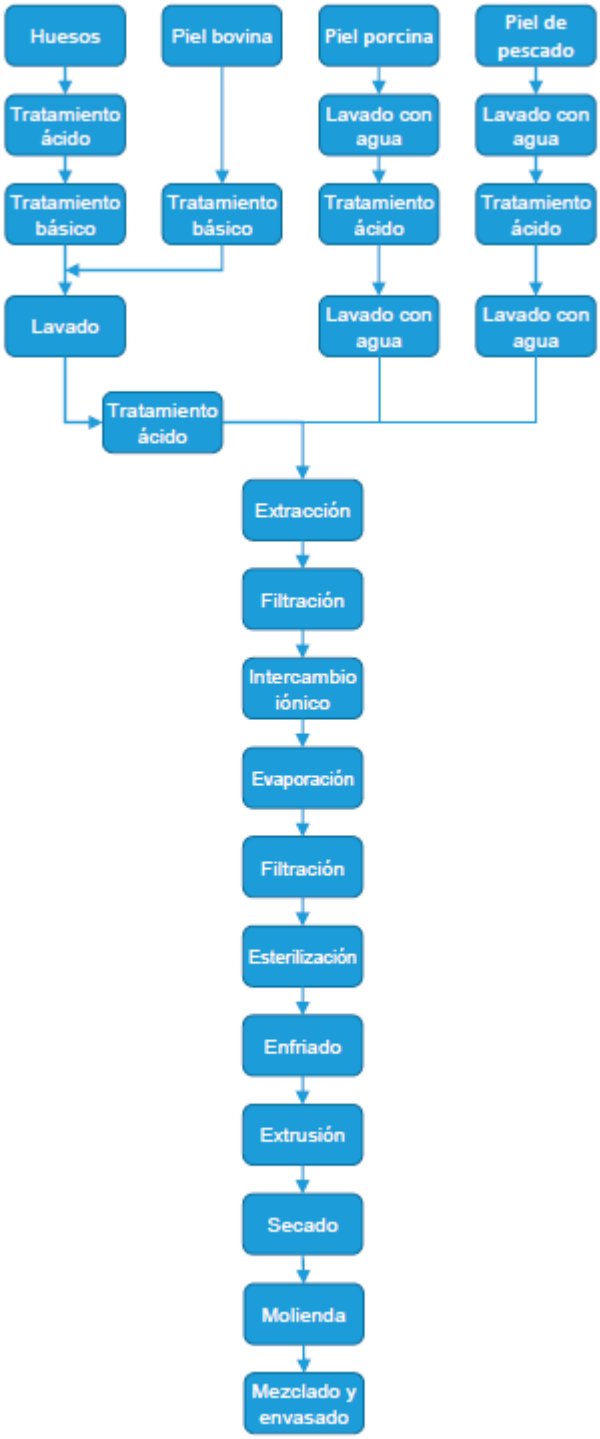

***Figura 1.13**: Proceso de la producción de gelatina (Adaptado de: www.vyse.com)*

1.4.2.4. Propiedades físicas y químicas

- Solubilidad

En la mayoría de usos comerciales la gelatina se utiliza en forma de solución. La gelatina es prácticamente insoluble en alcohol absoluto, acetona, tetracloruro de carbono, éter, benceno, y la mayoría de solventes orgánicos no polares. Por el contrario es soluble en agua, ácido acético y en soluciones acuosas de alcoholes polihídricos tales como glicerol o polipropilen glicol.

La gelatina en polvo absorbe el agua exotérmicamente, siendo la velocidad y el grado de hinchamiento una característica particular de cada tipo de gelatina. Al sumergirse en agua fría las partículas de gelatina se hidratan y es al aumentar la temperatura (por encima de 35ºC) cuando los gránulos empiezan a disolverse rápidamente dando lugar a una solución uniforme. Además de la temperatura, otros parámetros deben ser considerados a la hora de controlar el comportamiento de la gelatina en disolución, tales como el pH, el método de fabricación, la concentración usada, etc.

- Punto isoeléctrico

La gelatina en disolución presenta un carácter anfótero, con capacidad de actuar como ácido y como base, debido a los grupos funcionales de los aminoácidos y los grupos terminales amino y carboxilo creados durante la hidrólisis del colágeno.

En soluciones ácidas la gelatina se encuentra cargada positivamente, mientras que en soluciones básicas presenta carga negativa. El pH en el cual la solución de gelatina tiene carga neutra es conocido como punto isoeléctrico, y depende directamente del proceso de fabricación utilizado para la obtención de la gelatina (ácido o básico), y por tanto del tipo de gelatina (A o B).

Para la gelatina tipo A el punto isoeléctrico se encuentra entre pH 7 y 9, mientras que para la gelatina tipo B se encuentra en pH=4.8-5.2, dependiendo de la duración del tratamiento de extracción. La **Figura 1.14** muestra el patrón de distribución de cargas en las soluciones de gelatina tipo A y B.

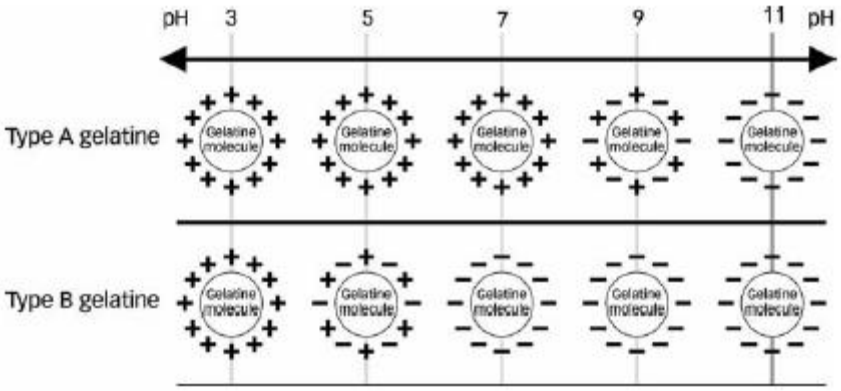

***Figura 1.14**: Distribución de carga en soluciones de gelatina tipo A y B en función del pH* [1.95]

- Fuerza de gel

La formación de geles termorreversibles en agua es una de las propiedades más importantes de la gelatina.

Cuando una solución acuosa de gelatina con una concentración superior aproximadamente al 0.5% se enfría por debajo de 35ºC empieza incrementando su viscosidad para finalmente formar un gel, cuya rigidez o fuerza depende de varios factores tales como la concentración de gelatina, pH, temperatura, la presencia o no de aditivos y la fuerza intrínseca del gel, función esta última propiedad de su estructura y masa molecular.

El proceso de gelificación se puede dividir en tres etapas diferenciadas termorreversibles [1.98-1.99] (**Figura 1.15**):

1- Reorganización de las cadenas moleculares individuales debido a la renaturalización de la gelatina en hélices tipo colágenas.
2- Asociación de varios segmentos ordenados creando una estructura cristalina.
3- Estabilización de la estructura por puentes de hidrógeno entre cadenas laterales dentro de las regiones helicoidales.

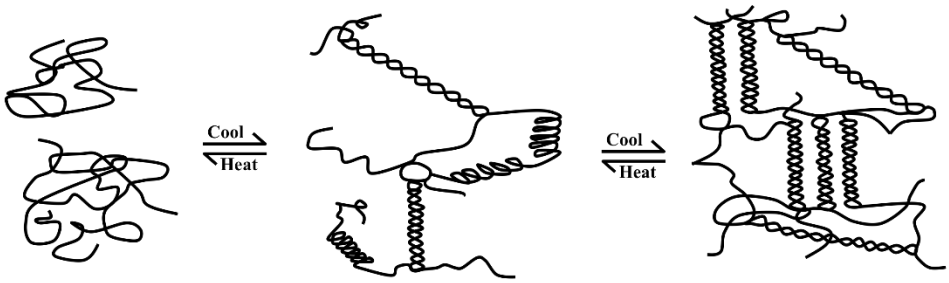

***Figura 1.15**: Etapas del proceso de gelificación* [1.100]

La calidad en la formación del gel es un parámetro físico cualitativo importante a tener en cuenta en función de la aplicación de la gelatina. La medida analítica de la fuerza de gel es el llamado valor de Bloom, consistente en la masa (en gramos) requerida para deprimir un cilindro de 12.5 mm de diámetro en la superficie de un gel de gelatina elaborado enfriando una solución de 6,67% a 10ºC durante 17 horas. Dicho protocolo, así como el equipo para llevarlo a cabo fue patentado por el científico Oscar T.Bloom en 1925 [1.101], dando nombre al valor obtenido.

Para las gelatinas comerciales el Bloom se encuentra en un rango entre 50 y 325 g.

- Viscosidad

La viscosidad es la propiedad más importante de las disoluciones de gelatina. Como polímero, la naturaleza macromolecular de la gelatina produce una viscosidad en disolución con propiedades reológicas de carácter newtoniano en la mayoría de temperaturas y concentraciones utilizadas para la preparación de las muestras.

Las propiedades de viscosidad de la gelatina están principalmente relacionadas con la distribución de pesos moleculares, y consecuentemente con la fuerza de gel. Se entiende como viscosidad característica de una gelatina aquella obtenida mediante un método estandarizado que indica el tiempo de flujo de 100 ml de solución acuosa de gelatina al 6.67% a 60ºC a través de una pipeta estándar. Este valor de viscosidad permite estimar el peso molecular medio de la gelatina.

1.4.2.5. Nanofibras de gelatina

La obtención de microfibras de gelatina por el método convencional de hilatura húmedo/seco es complicada debido a la naturaleza polielectrolítica de la gelatina que, junto con la presencia de fuertes enlaces de puentes de hidrógeno de sus soluciones, dificulta la capacidad de la formación de fibras [1.39].

A los inconvenientes mencionados anteriormente se suman la dificultad para obtener soluciones de gelatina a temperaturas superiores a 37ºC en agua, así como la aparición del fenómeno de gelificación a temperaturas inferiores a los 37 ºC. Este comportamiento ha hecho que la gelatina no haya sido comúnmente considerada como un material candidato para la ingeniería de tejidos. Sin embargo, la posibilidad de obtener fibras de tamaño micrométrico por electrohilatura de soluciones de gelatina ha motivado la investigación y la búsqueda de alternativas a dichos problemas con el objetivo de obtener soluciones de hilatura electrohilables para la fabricación de soportes para ingeniería de tejidos.

La **Tabla 1.8** muestra un resumen de las condiciones de electrohilatura que han propuesto estudios precedentes dedicados a la preparación de fibras de gelatina mediante la técnica de electrohilatura.

***Tabla 1.8**: Resumen de los estudios realizados sobre electrospinning de gelatina*

	Disolvente	[Gelatina]	[Disolvente]	Temp (ºC)	Voltaje (kV)	Distancia (cm)	Caudal (ml/h)
2004[1.102]	2,2,2-Trifluoroetanol	2,5 – 15 % w/v	Puro	Ambiente	10-16	12	0,8
2005[1.103]	Ácido Fórmico	7-12 % w/v	98%	Ambiente	6-25	7,5 – 25	Ajustado
2007[1.104]	Ácido Acético (AA) +(TFE/DMSO/EG/F)	15-29% w/v	AA:40-90 TFE: 10-60 AA: 91-97 DMSO: 3-9 AA: 91-97 EG: 3-9 AA: 91-97 F: 3-9	Ambiente	7,5	7,5	-
2007[1.105]	Acético glacial/ Etil acetato	10%	AA 9-81% / EA 0-35%	37ºC	12	8	0,06
2008[1.106]	Etanol +Ácido fórmico	10-20 wt%	Etanol: 20 wt% Fórmico: 2 wt%	35ºC	15-25	10	1
2008[1.107]	Acético/Fórmico	5-29 wt%	Ácido : 10-100%	40ºC	-	15	-
2009[1.108]	Ácido acético	6-12% w/v	50-90%	Ambiente	10-16	8-15	-
2009[1.109]	Acético /Alginato sodio/agua	11-18 w/v%	Alginato: 0,1-1wt% Acético : 80 wt%	45ºC	8-15	12	-
2010[1.110]	Agua destilada	30-40 wt%	Puro	40ºC	22	12	-
2011[1.112]	Acético / Agua bidestilada	30 w/v%	Acético: 60% Agua bidest: 40%	50ªC	15	15	0,005
2012[1.112]	20xPBS/Etanol	90-140 mg/ml	PBS: 5X-20X PBS/Etanol: 3:2/1:1/2:3	-	12	12	0,25

De igual forma que sucede con el colágeno, la elección del disolvente adecuado es un punto clave para la electrohilatura de gelatina.

La gelatina es prácticamente insoluble en alcohol absoluto, acetona, tetracloruro de carbono, éter, benceno, así como en la mayoría de solventes orgánicos no polares, mientras que presenta solubilidad en agua, ácido acético y soluciones acuosas de alcoholes polihídricos, como son el glicerol y el propilenglicol [1.113].

Inicialmente se utilizó el 2, 2, 2-Trifluoroetanol (TFE) como disolvente, basándose en los buenos resultados obtenidos para el colágeno. El TFE permite disolver la gelatina a temperatura ambiente a una concentración suficientemente elevada para hilar sin que ocurra la gelificación [1.102]. Posteriormente se substituyó el uso de los alcoholes fluorados por los ácidos orgánicos, especialmente el ácido fórmico y acético [1.103-1.109, 1.110].

Sin embargo, tanto los alcoholes fluorados como los ácidos orgánicos a las elevadas concentraciones necesarias para conseguir electrohilar nanofibras de gelatina [1.105, 1.107-1.108, 1.111] presentan una elevada toxicidad. Con el objetivo de disminuir la toxicidad del solvente y teniendo en cuenta la dificultad de disolver la gelatina en sistemas acuosos debido a su gelificación, diferentes estudios han considerado el uso de co-solventes (p.e. etil acetato [1.105], etano [1.106]), así como la mezcla con otros polímeros (p.e. PLA [1.108], alginato de sodio [1.109], PVA [1.110]). Además se observa como la mayoría de los estudios realizados, independientemente del solvente utilizado, proponen trabajar a alta temperatura, añadiendo dificultad al proceso.

Recientemente se han realizado estudios basados en el uso de etanol y un tampón salino de fosfato (PBS) como solvente con resultados prometedores [1.112]. Sin embargo esta es una vía de estudio nueva que requiere una mayor investigación.

1.5. Reticulación de las nanofibras

Las nanofibras de gelatina obtenidas por electrospinning presentan una elevada solubilidad en agua. Consecuentemente será necesario la aplicación de un tratamiento de reticulación posterior a la hilatura que estabilice las fibras obtenidas habilitando así su uso para aplicaciones en ingeniería de tejidos. De esta forma el proceso de reticulación para obtener nanofibras insolubles se convierte en el segundo punto más importante después de la obtención del solvente adecuado.

Los materiales derivados del colágeno pueden ser reticulados usando una gran variedad de métodos, tanto físicos, incluyendo tratamientos dehidrotermales [1.114] y

radiaciones gamma y ultravioleta [1.115], como químicos, siendo estos últimos los de mayor eficiencia.

La reticulación química se basa en el uso de moléculas reactivas que modifican la gelatina por reacción con sus grupos amino, carboxilos o hidroxilos. Entre la amplia variedad de reactivos químicos utilizados para este fin, tales como carbodiimidas [1.116-1.118], glyoxal, genipin [1.119-1.122] y transglutaminasa [1.123-1.124], es el glutaraldehído (GA) el más comúnmente utilizado.

La reticulación con vapor de glutaraldehído es un método simple, de bajo coste y efectivo para la estabilización de materiales de base protéica que ha sido aplicado para la reticulación de nanofibras electrohiladas [1.120, 1.125-1.126].

La reacción de reticulación ocurre entre los grupos carboxilos del glutaraldehído y los grupos amina de la proteína, tal y como muestra la **Figura 1.16**:

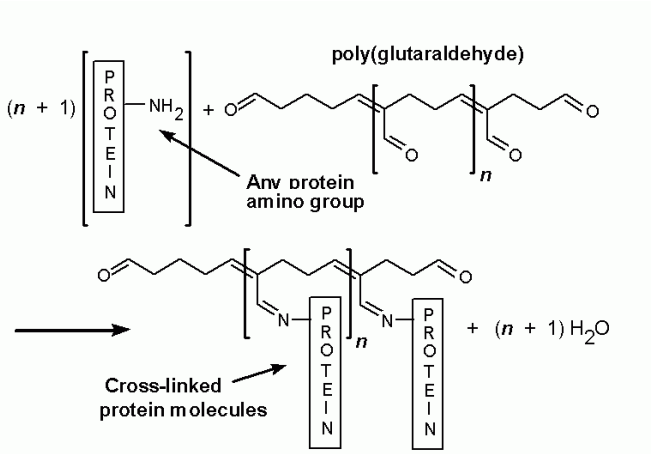

***Figura 1.16**: Mecanismo de reacción entre el glutaraldehído y las proteínas* [1.127]

La **Tabla 1.9** muestra un resumen de los estudios realizados en los que aparece reticulación de gelatina mediante glutaraldehído con diferentes métodos: vapor (contacto de la gelatina hilada con vapor de una solución de GA), Inmersión (inmersión directa de la gelatina hilada en una solución de GA) y reticulación in –situ (introducción de GA directamente en la solución a hilar para obtener fibras ya reticuladas).

***Tabla 1.9**: Resumen de los estudios realizados sobre reticulación de gelatina con glutaraldehído*

Ref.	Polímero	Método	[GA]	Disolvente	Tiempo	Tratamiento posterior	Medida de Estabilidad
[1.128]	Gelatina	Vapor	0.5% w/w	-	19 h	-	DMEM 37ºC 2 semanas
[1.112]	Gelatina	Vapor	1.5 % w/v	Etanol	48 h	Secado aire 100ºC 2h	Lavado con agua
[1.106]	Gelatina	Inmersión	2.5%	-	72h	Secado a vacío.	Cultivo celular
[1.129]	Gelatina	In situ	0.05% w/v	PBS	-	-	PBS 0.5, 2, 12 y 24 h
[1.110]	PVA/Gel	Inmersión	Sin	Metanol	24h	Secado 25ºC	Cultivo celular
[1.30]	Gelatina	Inmersión	-	t-BuOH	1 h a 30ºC	Lavado con t-BuOH y congelación	Cultivo celular
[1.125]	Gelatina	Vapor	-	Agua	-	Secado aire 100ºC 1h	Agua 37ºC 6h-4d
[1.131]	Chitosan	Vapor	-	-	24h	-	NaOH, Acético, Agua 15 min y 72h
[1.132]	Gelatina /PVA	Vapor	50% wt	Agua	2 h a 25ºC	-	PBS 37ºC 10-300 min
[1.133]	Gelatina /PVA	Vapor	50% wt	Agua	0,15,45, 90,360 min	-	-
[1.134]	PVA	Vapor	0.5, 1, 2, 2.56 M	Agua	6,12,24,48 h	-	-
[1.135]	Gelatina	Inmersión	2%wt	Etanol	2 y 4h	Lavado con glicina 0.2M.	-
[1.136]	Gelatina	Vapor	50%	Agua	2- 48 h	-	-
[1.137]	Gelatina	Inmersión	0.125-2.5% w/w	PBS	24 h	Lavado y secado con aire.	-

El principal problema del uso de glutaraldehído para la reticulación de gelatina es su elevada citotoxicidad a partir de determinadas concentraciones, debida a la incorporación del compuesto en el material reticulado [1.116, 1.138]. Sin embargo, aunque tanto el método de las carbodimidas como el de la genipina presentan una alternativa no tóxica a la reticulación de las nanofibras de gelatina, los estudios han demostrado la mayor estabilidad en agua de las muestras reticuladas con GA en comparación con las obtenidas por estos métodos alternativos [1.139].

Con la reticulación de las nanofibras se garantiza su estabilidad estructural así como su insolubilidad en medios acuosos pero no por ello se satisfacen las propiedades mecánicas necesarias para actuar como soporte dentro de la ingeniería de tejidos [1.140]. En este sentido, con el objetivo de conseguir un andamio tisular con unas propiedades mecánicas óptimas así como una elevada compatibilidad celular, diversos estudios han propuesto el uso de mezclas de polímeros biodegradables sintéticos (PCL, PVA, PLGA , Poliuretano, Poliéster, etc) o naturales (alginato, etc) con proteínas naturales (colágeno, gelatina, elastina, etc) [1.127, 1.132, 1.140-1.146]. La obtención de estos copolímeros se obtiene por electrospinning de una solución compuesta por la mezcla de los dos polímeros en la proporción deseada.

1.6. Referencias

[1.1] R. Langer, Tissue engineering., Mol. Ther. 1 (2000) 12–5.

[1.2] B. Hüsing, B. Bührlen, S. Gaisser, Human Tissue Engineered Products – Today ' s Markets and Future Prospects, Karlsruhe, Germany, 2003.

[1.3] M.B. Fisher, R.L. Mauck, Tissue engineering and regenerative medicine: recent innovations and the transition to translation., Tissue Eng. Part B. 19 (2013) 1–13.

[1.4] B. Dhandayuthapani, Y. Yoshida, T. Maekawa, D.S. Kumar, Polymeric Scaffolds in Tissue Engineering Application: A Review, Int. J. Polym. Sci. 2011 (2011) 1–19.

[1.5] J.H.S. George, Engineering of Fibrous Scaffolds for use in Regenerative Medicine Department of Materials, Imperial College, London, 2009.

[1.6] B.P. Chan, K.W. Leong, Scaffolding in tissue engineering: general approaches and tissue-specific considerations., Eur. Spine J. 17 (2008) 467–79.

[1.7] F.J. O'Brien, Biomaterials & scaffolds for tissue engineering, Mater. Today. 14 (2011) 88–95.

[1.8] S. V Madihally, H.W.T. Matthew, Porous chitosan scaffolds for tissue engineering., Biomaterials. 20 (1999) 1133–1142.

[1.9] H. Tai, M.L. Mather, D. Howard, W. Wang, L.J. White, J.A. Crowe, et al., Control of pore size and structure of tissue engineering scaffolds produced by supercritical fluid processing., Eur Cell Mater. 17 (2007) 64–77.

[1.10] K. Scoffin, Scaling the Scaffolds : Control of Pore Size in Tissue Engineering Scaffolds, Am. Lab. (2011) 5.

[1.11] H. Hermawan, D. Ramdan, J.R.P. Djuansjah, Metals for Biomedical Applications, in: R. Frazel (Ed.), Biomed. Eng. From Theory to Appl., InTech, 2009: pp. 411–430.

[1.12] T. V Thamaraiselvi, S. Rajeswari, Biological Evaluation of Bioceramic Materials - A Review, Trends Biomater. Artif. Organs. 18 (2004) 9–17.

[1.13] B.D. Ulery, L.S. Nair, C.T. Laurencin, Biomedical Applications of Biodegradable Polymers., J. Polym. Sci. B. Polym. Phys. 49 (2011) 832–864.

[1.14] S. Kara, ed., A roadmap of biomedical engineers and milestones., InTech, 2012.

[1.15] C. Flor, A study of the formation of collagen nanofibers using electrospinning, Universitat Politecnica de Catalunya, 2008.

[1.16] W. Xue, X. Liu, X. Zheng, C. Ding, In vivo evaluation of plasma-sprayed titanium coating after alkali modification., Biomaterials. 26 (2005) 3029–37.

[1.17] H. Yoshikawa, N. Tamai, T. Murase, A. Myoui, Interconnected porous hydroxyapatite ceramics for bone tissue engineering., J. R. Soc. Interface. 6 (2009) 341–348.

[1.18] J.A. Matthews, G.E. Wnek, D.G. Simpson, G.L. Bowlin, Electrospinning of collagen nanofibers, Biomacromolecules. 3 (2002) 232–238.

[1.19] M. Ngiam, S. Liao, A.J. Patil, Z. Cheng, C.K. Chan, S. Ramakrishna, The fabrication of nano-hydroxyapatite on PLGA and PLGA/collagen nanofibrous composite scaffolds and their effects in osteoblastic behavior for bone tissue engineering, Bone. 45 (2009) 4–16.

[1.20] F. Carfì, S. Rigogliuso, V. La, G. Anotnio, G. Ghersi, V. Brucato, Poly Lactic Acid Based Scaffolds for Vascular Tissue Engineering, Chem. Eng. Trans. 27 (2012) 409–414.

[1.21] H. Hajiali, S. Shahgasempour, M.R. Naimi-Jamal, H. Peirovi, Electrospun PGA/gelatin nanofibrous scaffolds and their potential application in vascular tissue engineering., Int. J. Nanomedicine. 6 (2011) 2133–2141.

[1.22] Y. Tabata, Biomaterial technology for tissue engineering applications., J. R. Soc. Interface. 6 (2009) 311–324.

[1.23] B.J. Papenburg, Design strategies for tissue engineering scaffolds, University of Twente, 1981.

[1.24] E. Sachlos, J.T. Czemuszka, Making tissue engineering scaffolds work. Review on the application of solid freeform fabrication technology to the production of tissue engineering scaffolds., Eur Cell Mater. 30 (2003) 29–39.

[1.25] P. Buijtenhuijs, L. Buttafoco, A.A. Poot, W.F. Daamen, T.H. Van Kuppevelt, P.J. Dijkstra, et al., Tissue engineering of blood vessels : characterization of smooth-muscle cells for culturing on collagen-and-elastin- based scaffolds., Biotechnol Appl Biochem. 149 (2004) 141–149.

[1.26] L.Y. Lee, S.H. Ranganath, Y. Fu, J.L. Zheng, H.S. Lee, C.-H. Wang, et al., Paclitaxel release from micro-porous PLGA disks., Chem. Eng. Sci. 64 (2009) 4341–4349.

[1.27] Q. Wu, X. Zhang, B. Wu, W. Huang, Effects of microwave sintering on the properties of porous hydroxyapatite scaffolds., Ceram. Int. 39 (2013) 2389–2395.

[1.28] J. Zhang, L. Wu, D. Jing, J. Ding, A comparative study of porous scaffolds with cubic and spherical macropores., Polymer (Guildf). 46 (2005) 4979–4985.

[1.29] W.-J. Li, J. a Cooper, R.L. Mauck, R.S. Tuan, Fabrication and characterization of six electrospun poly(alpha-hydroxy ester)-based fibrous scaffolds for tissue engineering applications., Acta Biomater. 2 (2006) 377–85.

[1.30] A. Formhals, Process and apparatus for preparing artificial threads., US Patent No. 1,975,504, 1934.

[1.31] S. Ramakrishna, K. Fujihara, W.-E. Teo, T.-C. Lim, Z. Ma, An introduction to electrospinning and nanofibers., 2005.

[1.32] C.E. Ayres, B.S. Jha, S.A. Sell, G.L. Bowlin, D.G. Simpson, Nanotechnology in the design of soft tissue scaffolds: innovations in structure and function, Wiley Interdiscip Rev Nanomed Nanobiotechnol. 2 (2010) 20–34.

[1.33] A.S. Nain, J.C. Wong, C.H. Amon, M. Sitti, Drawing suspended polymer micro-/nanofibers using glass micropipettes., Appl. Phys. Lett. 89 (2006).

[1.34] S.L. Tao, T.A. Desai, Aligned Arrays of Biodegradable Poly(ε-caprolactone) Nanowires and Nanofibers by Template Synthesis., Nano Lett. 7 (2007) 1463–1468.

[1.35] J. Zhao, W. Han, H. Chen, M. Tu, R. Zeng, Y. Shi, et al., Preparation, structure and crystallinity of chitosan nano-fibers by a solid–liquid phase separation technique, Carbohydr. Polym. 83 (2011) 1541–1546.

[1.36] M. Rolandi, R. Rolandi, Self-assembled chitin nanofibers and applications., Adv. Colloid Interface Sci. 207 (2014) 216–22.

[1.37] S. a. Sell, P.S. Wolfe, K. Garg, J.M. McCool, I. a. Rodriguez, G.L. Bowlin, The Use of Natural Polymers in Tissue Engineering: A Focus on Electrospun Extracellular Matrix Analogues, Polymers (Basel). 2 (2010) 522–553.

[1.38] A. Greiner, J.H. Wendorff, Electrospinning: a fascinating method for the preparation of ultrathin fibers, Angew. Chem. Int. Ed. Engl. 46 (2007) 5670–703.

[1.39] N. Bhardwaj, S.C. Kundu, Electrospinning: a fascinating fiber fabrication technique., Biotechnol. Adv. 28 (2010) 325–47.

[1.40] G. Taylor, Disintegration of Water Drops in an Electric Field, Proc. R. Soc. A Math. Phys. Eng. Sci. 280 (1964) 383–397.

[1.41] J. Di, Y. Zhao, J. Yu, Fabrication of molecular sieve fibers by electrospinning, J. Mater. Chem. 21 (2011) 8511.

[1.42] Q.P. Pham, U. Sharma, A.G. Mikos, Electrospinning of polymeric nanofibers for tissue engineering applications: a review, Tissue Eng. 12 (2006) 1197–211.

[1.43] S. Sukigara, M. Gandhi, J. Ayutsede, M. Micklus, F. Ko, Regeneration of Bombyx mori silk by electrospinning—part 1: processing parameters and geometric properties., Polymer (Guildf). 44 (2003) 5721–5727.

[1.44] H. Jiang, D. Fang, B.S. Hsiao, B. Chu, W. Chen, Optimization and characterization of dextran membranes prepared by electrospinning., Biomacromolecules. 5 (2004) 326–33.

[1.45] H.S. Kim, K. Kim, H.J. Jin, I.-J. Chin, Morphological Characterization of Electrospun Nano-Fibrous Membranes of Biodegradable Poly(L-lactide) and Poly(lactide-co-glycolide)., Macromol. Symp. 224 (2005) 145–154.

[1.46] H. Zhang, Effects of electrospinning parameters on morphology and diameter of electrospun PLGA/MWNTs fibers and cytocompatibility in vitro., J. Bioact. Compat. Polym. 26 (2011) 590–606.

[1.47] L. Huang, K. Nagapudi, R.P. Apkarian, E.L. Chaikof, Engineered collagen–PEO nanoŽ bers and fabrics, J Biomater Sci Polym Ed. 12 (2001) 979–993.

[1.48] J.. Deitzel, J. Kleinmeyer, D. Harris, N.. Beck Tan, The effect of processing variables on the morphology of electrospun nanofibers and textiles, Polymer (Guildf). 42 (2001) 261–272.

[1.49] W.K. Son, J.H. Youk, T.S. Lee, W.H. Park, The effects of solution properties and polyelectrolyte on electrospinning of ultrafine poly(ethylene oxide) fibers, Polymer (Guildf). 45 (2004) 2959–2966.

[1.50] C. Zhang, X. Yuan, L. Wu, Y. Han, J. Sheng, Study on morphology of electrospun poly(vinyl alcohol) mats, Eur. Polym. J. 41 (2005) 423–432.

[1.51] F. Cengiz, T.A. Dao, O. Jirsak, Influence of solution properties on the roller electrospinning of poly(vinyl alcohol), Polym. Eng. Sci. 50 (2010) 936–943.

[1.52] S.-P. Rwei, C.-C. Huang, Electrospinning PVA solution-rheology and morphology analyses, Fibers Polym. 13 (2012) 44–50.

[1.53] J. Jeun, Y. Kim, Y. Lim, J. Choi, C. Jung, P. Kang, Electrospinning of Poly (L-lactide- co -D , L-lactide), J. Ind. Eng. Chem. 13 (2007) 592–596.

[1.54] R. Nayak, R. Padhye, I.L. Kyratzis, Y.B. Truong, L. Arnold, Effect of viscosity and electrical conductivity on the morphology and fiber diameter in melt electrospinning of polypropylene., Text. Res. J. 83 (2012) 606–617.

[1.55] V. Beachley, X. Wen, Effect of electrospinning parameters on the nanofiber diameter and length, Mater Sci Eng C Mater Biol Appl. 29 (2009) 663–668.

[1.56] J. He, Y.-Q. Wan, J.-Y. Yu, Effect of Concentration on Electrospun Polyacrylonitrile (PAN) Nanofibers., Fibers Polym. 9 (2008) 140–142.

[1.57] J. Lin, X. Qin, Effect of solution concentration on jet stretching of electrospinning PVA nanofiber., Int. J. Fluid Mech. Res. 38 (2011) 479–488.

[1.58] M. Chowdhury, G. Stylios, Effect of Experimental Parameters on the Morphology of Electrospun Nylon 6 fibres, Int. J. Basic Appl. Sci. 10 (2010) 70–78.

[1.59] P. Supaphol, C. Mit-Uppatham, M. Nithitanakul, Ultrafine electrospun polyamide-6 fibers: Effect of emitting electrode polarity on morphology and average fiber diameter, J. Polym. Sci. Part B Polym. Phys. 43 (2005) 3699–3712.

[1.60] a. H. Hekmati, A. Rashidi, R. Ghazisaeidi, J.-Y. Drean, Effect of needle length, electrospinning distance, and solution concentration on morphological properties of polyamide-6 electrospun nanowebs, Text. Res. J. 83 (2013) 1452–1466.

[1.61] A. Koski, K. Yim, S. Shivkumar, Effect of molecular weight on fibrous PVA produced by electrospinning, Mater. Lett. 58 (2004) 493–497.

[1.62] C.L. Casper, J.S. Stephens, N.G. Tassi, D.B. Chase, J.F. Rabolt, Controlling surface morphology of electrospun polystyrene fibers: Effect of humidity and molecular weight in the electrospinning process., Macromolecules. 37 (2004) 573–578.

[1.63] S.S. Ojha, M. Afshari, R. Kotek, R.E. Gorga, Morphology of electrospun nylon-6 nanofibers as a function of molecular weight and processing parameters., J. Appl. Polym. Sci. 108 (2008) 308–319.

[1.64] H.R. Pant, K.-T. Nam, H.-J. Oh, G. Panthi, H.-D. Kim, B. Kim, et al., Effect of polymer molecular weight on the fiber morphology of electrospun mats., J. Colloid Interface Sci. 364 (2011) 107–11.

[1.65] C.J. Angammana, S. Member, S.H. Jayaram, Analysis of the Effects of Solution Conductivity on Electrospinning Process and Fiber Morphology., IEEE Trans. Ind. Appl. 47 (2011) 1109–1117.

[1.66] R.B. K.C., K.W. Kim, S.R. Bhattarai, H.Y. Kim, D.R. Lee, Effect of collector temperature and conductivity on the chain conformation of nylon 6 electrospun nanofibers., Fibers Polym. 8 (2007) 186–191.

[1.67] Y. Yang, Z. Jia, J. Liu, Q. Li, L. Hou, L. Wang, et al., Effect of electric field distribution uniformity on electrospinning., J. Appl. Phys. 103 (2008) 104307.

[1.68] A. Sohrabi, P.M. Shaibani, T. Thundat, The effect of applied electric field on the diameter and size distribution of electrospun Nylon6 nanofibers., Scanning. 35 (2013) 183–8.

[1.69] R. Jalili, S.A. Hosseini, M. Morshed, The Effects of Operating Parameters on the morphology of electrospun polyacrilonitrile nanofibres., Iran. Polym. J. 14 (2005) 1074–1081.

[1.70] S. Zargham, S. Bazgir, A. Tavakoli, A.S. Rashidi, R. Damerchely, The Effect of Flow Rate on Morphology and Deposition Area of Electrospun Nylon 6 Nanofiber., J. Eng. Fiber. Fabr. 7 (2012) 42–49.

[1.71] T. Subbiah, G.S. Bhat, R.W. Tock, S. Parameswaran, S.S. Ramkumar, Electrospinning of nanofibers, J. Appl. Polym. Sci. 96 (2005) 557–569.

[1.72] X.D.Z. Xian Tao Wen, Hong Song Fan, Yan Fei Tan, H.D. Cao, H. Li, B. Cai, Preparation of electrospun PLA nanofiber scaffold and the evaluation in vitro., Key Eng. Mater. 288-289 (2005) 139–142.

[1.73] A. Cipitria, A. Skelton, T.R. Dargaville, P.D. Dalton, D.W. Hutmacher, Design, fabrication and characterization of PCL electrospun scaffolds-a review, J. Mater. Chem. 21 (2011) 9419–9453.

[1.74] J.H.C. Hui Wang, Xiao Hong Qin, Study on Structures of electrospinning cellulose acetate nanofibers., Adv. Mat. Res. 175-176 (2011) 242–246.

[1.75] X. Fang, D.H. Reneker, DNA fibers by electrospinning, J. Macromol. Sci. Part B. 36 (1997) 169–173.

[1.76] H. Homayoni, S.A.H. Ravandi, M. Valizadeh, Electrospinning of chitosan nanofibers: Processing optimization., Carbohydr. Polym. 77 (2009) 656–661.

[1.77] E.K. Brenner, J.D. Schiffman, E.A. Thompson, L.J. Toth, C.L. Schauer, Electrospinning of hyaluronic acid nanofibers from aqueous ammonium solutions., Carbohydr. Polym. 87 (2012) 926–929.

[1.78] W. Ritcharoen, Y. Thaiying, Y. Saejeng, I. Jangchud, R. Rangkupan, C. Meechaisue, et al., Electrospun dextran fibrous membranes., Cellulose. 15 (2008) 435–444.

[1.79] S.A. Sell, M.J. McClure, K. Garg, P.S. Wolfe, G.L. Bowlin, Electrospinning of collagen/biopolymers for regenerative medicine and cardiovascular tissue engineering., Adv. Drug Deliv. Rev. 61 (2009) 1007–19.

[1.80] M. Li, M.J. Mondrinos, M.R. Gandhi, F.K. Ko, A.S. Weiss, P.I. Lelkes, Electrospun protein fibers as matrices for tissue engineering., Biomaterials. 26 (2005) 5999–6008.

[1.81] G. Karp, Cell and Molecular Biology: Concepts and Experiments, Wiley, 2009.

[1.82] K.E. Kadler, D.F. Holmes, J.A. Trotter, J.A. Chapman, Collagen fibril formation., Biochem J. 11 (1996) 1–11.

[1.83] K.S. Rho, L. Jeong, G. Lee, B.-M. Seo, Y.J. Park, S.-D. Hong, et al., Electrospinning of collagen nanofibers: effects on the behavior of normal human keratinocytes and early-stage wound healing., Biomaterials. 27 (2006) 1452–61.

[1.84] Y.-R. V Shih, C.-N. Chen, S.-W. Tsai, Y.J. Wang, O.K. Lee, Growth of mesenchymal stem cells on electrospun type I collagen nanofibers., Stem Cells. 24 (2006) 2391–7.

[1.85] T.A. Telemeco, C. Ayres, G.L. Bowlin, G.E. Wnek, E.D. Boland, N. Cohen, et al., Regulation of cellular infiltration into tissue engineering scaffolds composed of submicron diameter fibrils produced by electrospinning., Acta Biomater. 1 (2005) 377–85.

[1.86] S. Zhong, W.E. Teo, X. Zhu, R.W. Beuerman, S. Ramakrishna, L. Yue, et al., An aligned nanofibrous collagen scaffold by electrospinning and its effects on in vitro fibroblast culture., J. Biomed. Mater. Res. Part A. 79A (2006) 456–463.

[1.87] W.-J. Chen, D.-J. Ying, Design and Preparation of an Electrospun Biomaterial Surgical Patch, J. Bioact. Compat. Polym. 24 (2009) 158–168.

[1.88] B.S. Jha, C.E. Ayres, J.R. Bowman, T. a. Telemeco, S. a. Sell, G.L. Bowlin, et al., Electrospun Collagen: A Tissue Engineering Scaffold with Unique Functional Properties in a Wide Variety of Applications, J. Nanomater. 2011 (2011) 1–15.

[1.89] Y.Z. Zhang, J. Venugopal, Z.-M. Huang, C.T. Lim, S. Ramakrishna, Characterization of the surface biocompatibility of the electrospun PCL-collagen nanofibers using fibroblasts., Biomacromolecules. 6 (2005) 2583–9.

[1.90] S. Zhong, W.E. Teo, X. Zhu, R. Beuerman, S. Ramakrishna, L. Yue, et al., Formation of Collagen - Glycosaminoglycan Blended Nanofibrous Scaffolds and Their Biological Properties., Biomacromolecules. 6 (2005) 2998–3004.

[1.91] D. Hong, M. Hoshino, R. Kuboi, Y. Goto, Clustering of Fluorine-Substituted Alcohols as a Factor Responsible for Their Marked Effects on Proteins and Peptides., J. Am. Chem. Soc. 121 (1999) 8427–8433.

[1.92] A. Kundu, N. Kishore, 1,1,1,3,3,3- Hexafluoroisopropanol Induced Thermal Unfolding and Molten Globule State of Bovine □-Lactalbumin- Calorimetric and Spectroscopic Studies., Biopolymers. 73 (2004) 405–20.

[1.93] L. Yang, C.F.C. Fitié, K.O. van der Werf, M.L. Bennink, P.J. Dijkstra, J. Feijen, Mechanical properties of single electrospun collagen type I fibers., Biomaterials. 29 (2008) 955–62.

[1.94] D.I. Zeugolis, S.T. Khew, E.S.Y. Yew, A.K. Ekaputra, Y.W. Tong, L.-Y.L. Yung, et al., Electro-spinning of pure collagen nano-fibres - just an expensive way to make gelatin?, Biomaterials. 29 (2008) 2293–305.

[1.95] R. Schrieber, H. Gareis, Gelatin handbook- Theory and Insutrial Practice, Wiley, 2007.

[1.96] M. Zandi, Studies on the gelation of gelatin solutions and on the use of resulting gels for medical scaffolds., Universitat Duisburg-Essen, 2008.

[1.97] Y. Ge, J. Wang, Z. Shi, J. Yin, Gelatin-assisted fabrication of water-dispersible graphene and its inorganic analogues., J. Mater. Chem. 22 (2012) 17619.

[1.98] M. Djabourov, J. Leblond, P. Papon, Gelation of aqueous gelatin solutions. I. Structural Investigation., J. Phys. Fr. 49 (1988) 319–332.

[1.99] GMIA, Gelatin Handbook, (2012) 26.

[1.100] P. Wu, M. Imai, Novel Biopolymer Composite Membrane Involved with Selective Mass Transfer and Excellent Water Permeability., in: R. Y.Ning (Ed.), Adv. Desalin., 2012.

[1.101] O.T. Bloom, Machine for testing jelly strength of glues, gelatines and the like., 1540979, 1925.

[1.102] Z.-M. Huang, Y.. Zhang, S. Ramakrishna, C.. Lim, Electrospinning and mechanical characterization of gelatin nanofibers, Polymer (Guildf). 45 (2004) 5361–5368.

[1.103] C.S. Ki, D.H. Baek, K.D. Gang, K.H. Lee, I.C. Um, Y.H. Park, Characterization of gelatin nanofiber prepared from gelatin–formic acid solution., Polymer (Guildf). 46 (2005) 5094–5102.

[1.104] N. Choktaweesap, K. Arayanarakul, D. Aht-ong, C. Meechaisue, P. Supaphol, Electrospun Gelatin Fibers: Effect of Solvent System on Morphology and Fiber Diameters., Polym. J. 39 (2007) 622–631.

[1.105] J.-H. Song, H.-E. Kim, H.-W. Kim, Production of electrospun gelatin nanofiber by water-based co-solvent approach., J. Mater. Sci. Mater. Med. 19 (2008) 95–102.

[1.106] H.-C. Chen, W.-C. Jao, M.-C. Yang, Characterization of gelatin nanofibers electrospun using ethanol/formic acid/water as a solvent., Polym. Adv. Technol. 20 (2009) 98–103.

[1.107] P. Songchotikunpan, J. Tattiyakul, P. Supaphol, Extraction and electrospinning of gelatin from fish skin., Int. J. Biol. Macromol. 42 (2008) 247–255.

[1.108] S.-Y. Gu, Z.-M. Wang, J. Ren, C.-Y. Zhang, Electrospinning of gelatin and gelatin/poly(l-lactide) blend and its characteristics for wound dressing., Mater. Sci. Eng. C. 29 (2009) 1822–1828.

[1.109] S. Moon, R.J. Farris, Electrospinning of Heated Gelatin-Sodium Alginate-Water Solutions, Polym. Eng. Sci. 49 (2009) 1616–1620.

[1.110] N.T.B. Linh, B.-T. Lee, Electrospinning of polyvinyl alcohol/gelatin nanofiber composites and cross-linking for bone tissue engineering application, J. Biomater. Appl. 27 (2012) 255–266.

[1.111] S. Panzavolta, M. Gioffrè, M.L. Focarete, C. Gualandi, L. Foroni, A. Bigi, Electrospun gelatin nanofibers: optimization of genipin cross-linking to preserve fiber morphology after exposure to water, Acta Biomater. 7 (2011) 1702–9.

[1.112] Z. Zha, W. Teng, V. Markle, Z. Dai, X. Wu, Fabrication of gelatin nanofibrous scaffolds using ethanol/phosphate buffer saline as a benign solvent., Biopolymers. 97 (2012) 1026–1036.

[1.113] T.R. Keenan, Gelatin, in: Kirk-Othmer Encycl. Chem. Technol., 2003.

[1.114] M.G. Haugh, M.J. Jaasma, F.J. O'Brien, The effect of dehydrothermal treatment on the mechanical and structural properties of collagen-GAG scaffolds., J. Biomed. Mater. Res. A. 89 (2009) 363–9.

[1.115] D. Lew, P.H. Liu, D.P. Orgill, Optimization of UV Cross-Linking Density for

Durable and Nontoxic Collagen GAG Dermal Substitute., J Biomed Mater Res B Appl Biomater. 82 (2007) 51–56.

[1.116] R. Zeeman, Cross-linking of collagen-based materials, University of Twente, 1970.

[1.117] L. Meng, O. Arnoult, M. Smith, G.E. Wnek, Electrospinning of in situ crosslinked collagen nanofibers., J. Mater. Chem. 22 (2012) 19412.

[1.118] J. Bart, R. Tiggelaar, M. Yang, S. Schlautmann, H. Zuilhof, H. Gardeniers, Room-temperature intermediate layer bonding for microfluidic devices., Lab Chip. 9 (2009) 3481–8.

[1.119] A. Bigi, G. Cojazzi, S. Panzavolta, N. Roveri, K. Rubini, Stabilization of gelatin films by crosslinking with genipin., Biomaterials. 23 (2002) 4827–4832.

[1.120] I. Rault, V. Frei, D. Herbage, N. Abdul-Malak, A. Huc, Evaluation of different chemical methods for cross-linking collagen gel, films and sponges., J. Mater. Sci. Mater. Med. 7 (1996) 215–221.

[1.121] H. Sung, I. Liang, C. Chen, R. Huang, H. Liang, Stability of a biological tissue fixed with a naturally occurring crosslinking agent (genipin), J Biomed Mater Res. 55 (2001) 538–546.

[1.122] L. Solorio, C. Zwolinski, A.W. Lund, M.J. Farrell, J.P. Stegemann, Gelatin microspheres crosslinked with genipin for local delivery of growth factors., J. Tissue Eng. Regen. Med. 4 (2010) 514–23.

[1.123] S. Torres-Giner, J. V Gimeno-Alcañiz, M.J. Ocio, J.M. Lagaron, Comparative performance of electrospun collagen nanofibers cross-linked by means of different methods., ACS Appl. Mater. Interfaces. 1 (2009) 218–23.

[1.124] R.. de Carvalho, C.R.. Grosso, Characterization of gelatin based films modified with transglutaminase, glyoxal and formaldehyde., Food Hydrocoll. 18 (2004) 717–726.

[1.125] Y.Z. Zhang, J. Venugopal, Z.-M. Huang, C.T. Lim, S. Ramakrishna, Crosslinking of the electrospun gelatin nanofibers., Polymer (Guildf). 47 (2006) 2911–2917.

[1.126] Y.-F. Qian, K.-H. Zhang, F. Chen, Q.-F. Ke, X.-M. Mo, Cross-linking of gelatin

and chitosan complex nanofibers for tissue-engineering scaffolds., J. Biomater. Sci. Polym. Ed. 22 (2011) 1099–1113.

[1.127] J.A. Kierman, Formaldehyde, formalin, paraformaldehyde and glutaraldehyde: what they are and what they do., Micros. Today. 00-1 (2000) 8–12.

[1.128] K. Sisson, C. Zhang, M.C. Farach-Carson, D.B. Chase, J.F. Rabolt, Evaluation of cross-linking methods for electrospun gelatin on cell growth and viability., Biomacromolecules. 10 (2009) 1675–80.

[1.129] T.-H. Nguyen, Fabrication and characterization of cross-linked gelatin electro-spun nano-fibers., J. Biomed. Sci. Eng. 03 (2010) 1117–1124.

[1.130] M. Skotak, S. Noriega, G. Larsen, A. Subramanian, Electrospun cross-linked gelatin fibers with controlled diameter: the effect of matrix stiffness on proliferative and biosynthetic activity of chondrocytes cultured in vitro., J. Biomed. Mater. Res. A. 95 (2010) 828–36.

[1.131] J.D. Schiffman, C.L. Schauer, Cross-linking chitosan nanofibers, Biomacromolecules. 8 (2007) 594–601.

[1.132] D. Yang, Y. Li, J. Nie, Preparation of gelatin/PVA nanofibers and their potential application in controlled release of drugs., Carbohydr. Polym. 69 (2007) 538–543.

[1.133] S.-C. Wu, W.-H. Chang, G.-C. Dong, K.-Y. Chen, Y.-S. Chen, C.-H. Yao, Cell adhesion and proliferation enhancement by gelatin nanofiber scaffolds., J. Bioact. Compat. Polym. 26 (2011) 565–577.

[1.134] A.G. Destaye, C.K. Lin, C.K. Lee, Glutaraldehyde vapor cross-linked nanofibrous PVA mat with in situ formed silver nanoparticles., ACS Appl. Mater. Interfaces. 5 (2013) 4745–4752.

[1.135] M.A. Oraby, A.I. Waley, A.I. El-dewany, E.A. Saad, M.A. El-hady, Electrospun Gelatin Nanofibers : Effect of Gelatin Concentration on Morphology and Fiber Diameters., Polym. J. 9 (2013) 534.

[1.136] D.M. Correia, J. Padrão, L.R. Rodrigues, F. Dourado, S. Lanceros-Méndez, V. Sencadas, Thermal and hydrolytic degradation of electrospun fish gelatin membranes., Polym. Test. 32 (2013) 995–1000.

[1.137] A. Bigi, G. Cojazzi, S. Panzavolta, K. Rubini, N. Roveri, Mechanical and thermal properties of gelatin films at different degrees of glutaraldehyde crosslinking., Biomaterials. 22 (2001) 3–8.

[1.138] L.H.H.O. Damink, P.J. Dijkstra, M.J.A. Van Luyn, P.B. Van Wachem, P. Nieuwenhuis, J. Feijen, Glutaraldehyde as a crosslinking agent for collagen-based biomaterials, J. Mater. Sci. Mater. Med. 6 (1995) 460–472.

[1.139] C.P. Barnes, C.W. Pemble, D.D. Brand, D.G. Simpson, G.L. Bowlin, Cross-linking electrospun type II collagen tissue engineering scaffolds with carbodiimide in ethanol., Tissue Eng. 13 (2007) 1593–605.

[1.140] C. Yang, X. Wu, Y. Zhao, L. Xu, S. Wei, Nanofibrous scaffold prepared by electrospinning of poly(vinyl alcohol)/gelatin aqueous solutions., J. Appl. Polym. Sci. 121 (2011) 3047–3055.

[1.141] Y. Zhang, H. Ouyang, C.T. Lim, S. Ramakrishna, Z.-M. Huang, Electrospinning of gelatin fibers and gelatin/PCL composite fibrous scaffolds., J. Biomed. Mater. Res. B. Appl. Biomater. 72 (2005) 156–65.

[1.142] J. Han, P. Lazarovici, C. Pomerantz, X. Chen, Y. Wei, P.I. Lelkes, Co-electrospun blends of PLGA, gelatin, and elastin as potential nonthrombogenic scaffolds for vascular tissue engineering., Biomacromolecules. 12 (2011) 399–408.

[1.143] S.E. Kim, D.N. Heo, J.B. Lee, J.R. Kim, S.H. Park, S.H. Jeon, et al., Electrospun gelatin/polyurethane blended nanofibers for wound healing., Biomed. Mater. 4 (2009) 044106.

[1.144] H.M. Powell, S.T. Boyce, Engineered human skin fabricated using electrospun collagen-PCL blends: morphogenesis and mechanical properties., Tissue Eng. Part A. 15 (2009) 2177–2187.

[1.145] D. Klumpp, M. Rudisle, R.I. Kühnle, A. Hess, A. Arkudas, O. Bleiziffer, et al., Three-dimensional vascularization of electrospun PCL/collagen-blend nanofibrous scaffolds in vivo., J Biomed Mater Res A. 100 (2012) 2302–2311.

[1.146] Z.-C. Xing, S.-J. Han, Y.-S. Shin, I.-K. Kang, Fabrication of Biodegradable Polyester Nanocomposites by Electrospinning for Tissue Engineering., J. Nanomater. 2011 (2011) 1–18.

CAPÍTULO 2:

Enfoque de la investigación

2.1. Objetivos

En base al estado actual de la investigación en el campo de estudio, el objetivo general de la presente tesis doctoral es obtener soportes de nanofibras de base polimérica por electrohilatura de soluciones preparadas con disolventes alternativos más benignos para su futuro uso en aplicaciones de ingeniería de tejidos.

A partir del objetivo general se plantearon los siguientes objetivos específicos:

- Optimización de los distintos parámetros operacionales que controlan el proceso de electrohilatura (caudal, voltaje y distancia entre la aguja y el colector) en función del tipo de proteína y solvente utilizado. Análisis de la posible influencia de dichos parámetros sobre la formación de las nanofibras.

- Determinación de la influencia del diseño y tipo de colector sobre las propiedades (morfología, tamaño y distribución) de las nanofibras obtenidas.

- Estudio de disolventes de hilatura más benignos, alternativos a los propuestos actualmente (ej. alcoholes fluorados), para la disolución e hilado de gelatina a temperatura ambiente.

- Análisis del efecto de la viscosidad de las soluciones de hilatura en la capacidad de electrohilar nanofibras de gelatina, evaluando la incidencia sobre las propiedades de las nanofibras obtenidas.

- Estudio de la influencia del tipo de gelatina (3 tipos) en la capacidad de electrohilar las soluciones de hilatura obtenidas y en las propiedades de las nanofibras obtenidas.

- Control del proceso de estabilización de las nanofibras mediante tratamientos basados en el uso de glutaraldehído (GA): vapor, inmersión en solución de GA y adición de GA en la solución de hilatura.

- Desarrollo de tratamientos superficiales mediante deposición de las nanofibras sobre biomateriales poliméricos con distinta funcionalización superficial.

2.2. Estructura experimental y justificación

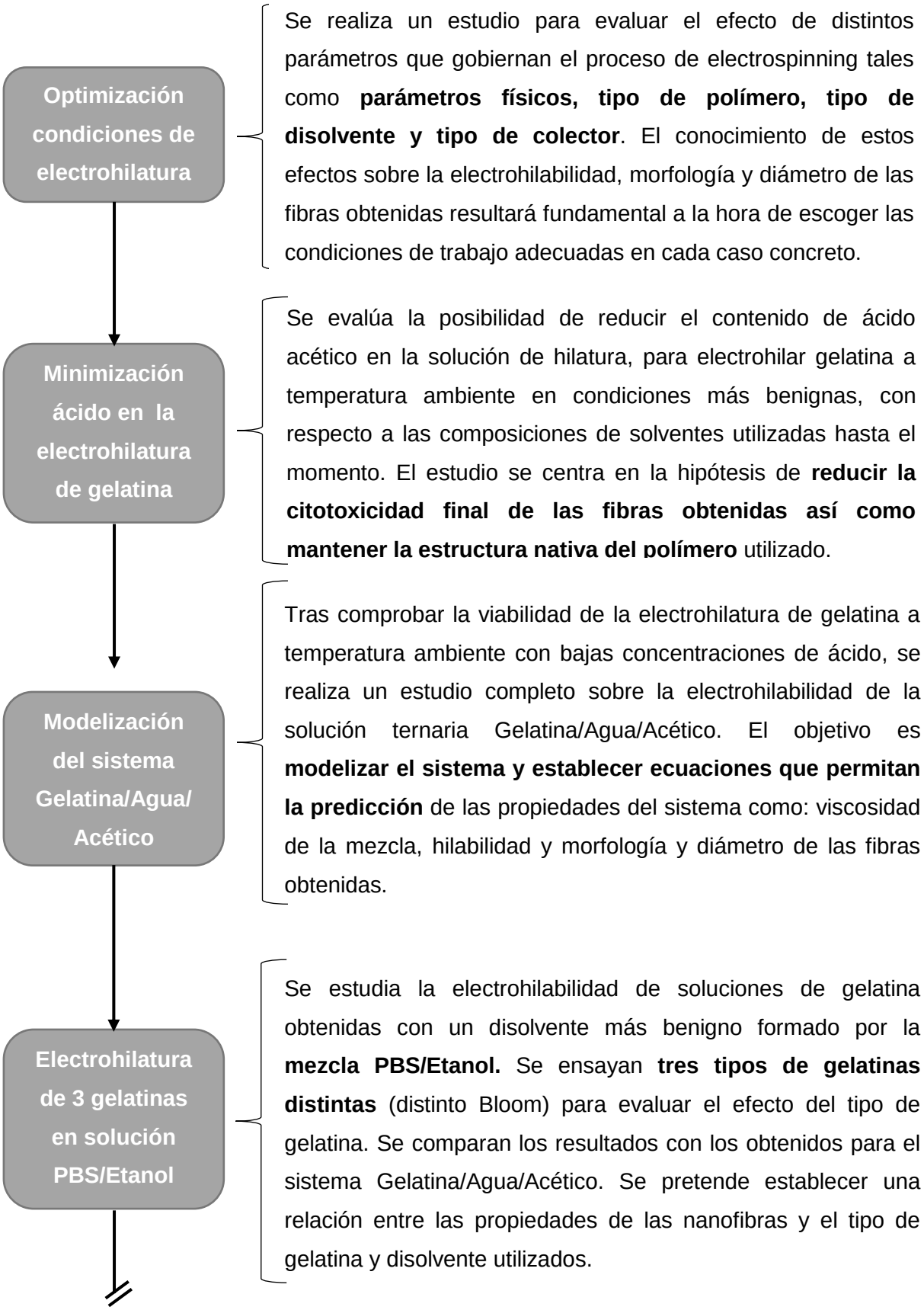

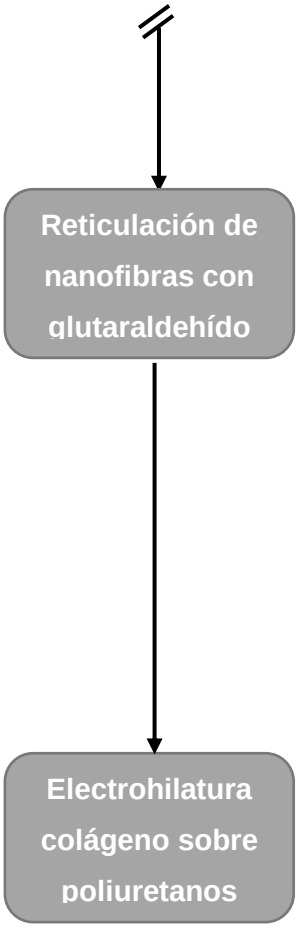

La reticulación de las nanofibras es fundamental para su estabilización y su posterior uso en medio acuoso. Se analiza el **efecto de tres métodos distintos de reticulación (vapor, inmersión e in-situ), basados en el uso de glutaraldehído como reticulante, sobre las propiedades de las fibras electrohiladas**. Se evalúa el efecto del tiempo de reticulación en las propiedades de las fibras obtenidas. Asímismo, con el objetivo de **simplificar el proceso,** se propone la aplicación de un nuevo método (in-situ) basado en la incorporación directa de glutaraldehído en la solución de hilatura que permita obtener nanofibras directamente reticuladas.

Se estudia la viabilidad para la deposición de una **nanocapa de fibras hiladas de colágeno sobre soportes biomateriales de poliuretano funcionalizados** con la idea de combinar las buenas propiedades mecánicas del film con la alta biocompatibilidad de la proteína. Se analiza el efecto del recubrimiento sobre las propiedades superficiales de los films, así como la influencia de los distintos poliuretanos sobre la distribución y diámetro de las nanofibras depositadas.

2.3. Materiales

En la **Tabla 2.1** se muestra un resumen de los diferentes productos químicos utilizados para la realización de la presente tesis doctoral. Se muestra el producto, sus características comerciales y su aplicación específica en el presente trabajo.

***Tabla 2.1**: Listado de los materiales utilizados para la realización de la presente tesis doctoral*

Producto	Proveedor	Tipo o Grado	Uso específico
Colágeno	Sigma Aldrich	Tipo I Calfskin	Formación de nanofibras
Gelatina	Sigma Aldrich	Bovine skin	Formación de nanofibras
	Rousselot	Bovine Bone	
	Sigma aldrich	Porcine Skin	
Agua bidestilada	Millipore	18.2 microsiemens	Preparación de disoluciones
Etanol	Panreac	99.5%	Disolución de la gelatina y reticulación nanofibras
PBS	Sigma Aldrich	-	Disolución de la gelatina
Ácido acético	Panreac	99.9%	Disolución de la gelatina
HIPF	Sigma aldrich	99 %	Disolución del colágeno y gelatina
KBr	Sigma aldrich	100%	Preparación muestras FTIR
DMEM	Panreac, ATCC	-	Análisis de biocompatibilidad y estabilidad
Tripsina-EDTA	AATCC	-	Análisis de biocompatibilidad
Cells BJ-5ta	AATCC	Human Foreskin Fibroblasts	Análisis de biocompatibilidad
Cells HEK 293T	ECACC	Human Embryonic Kidney	Análisis de biocompatibilidad
Alamar Blue	Invitrogen	-	Análisis de biocompatibilidad
Glutaraldehído	Panreac	25%	Reticulación de nanofibras
Poliuretanos	DSM Biomedical	B80A	Soportes biomateriales para la deposición de nanofibras de colágeno
	DSM Biomedical	B80A Sulfonado	
	DSM Biomedical	B80A C18	

2.4. Métodos y técnicas experimentales

2.4.1. Preparación de las nanofibras

2.4.1.1. Disolución

El primer paso para la obtención de nanofibras es la realización de la disolución del polímero a hilar en un solvente adecuado.

Independientemente del polímero utilizado (gelatina o colágeno), así como del disolvente elegido en cada caso (ácido acético, HIPF, PBS/etanol, etc.), el procedimiento de disolución es similar: el polímero se adiciona lentamente al recipiente que contiene el disolvente y se tapa para evitar la evaporación del disolvente. La mezcla se agita a una velocidad aproximada de 700 rpm (**Figura 2.1**).

Figura 2.1: *Agitador mecánico (Agimatic-n, Selecta)*

Todas las disoluciones utilizadas en la presente tesis se realizaron a temperatura ambiente (T=25ºC± 2ºC).

2.4.1.2. *Viscosidad*

Para determinados estudios será necesario el control de la viscosidad de la solución de polímero. Éste se ha realizado mediante un viscosímetro rotacional (Brookfield DVII+, **Figura 2.2**), conectado a un baño termostático con el objetivo de controlar la temperatura de medición. Para realizar la medida de viscosidad se utilizó el spin número 21 del viscosímetro con sus respectivos accesorios a fin de reducir la cantidad de solución necesaria (aprox 10 ml) y evitar de esta manera un consumo excesivo de material.

Figura 2.2*: Viscosímetro (Brookfield DVII+)*

2.4.2. Electrohilatura

Una vez completada la disolución del polímero ésta pasará al proceso central y más importante en la fabricación de las nanofibras: la máquina de electrohilatura. Para la obtención de nanofibras en la presente tesis se ha utilizado una máquina de fabricación propia diseñada e implementada por un grupo de investigación del Instituto de Investigación Textil de Terrassa (INTEXTER) (**Figura 2.3**). La máquina de electrohilatura está formada por cuatro partes fundamentales: la fuente de alimentación, la bomba de caudal, el colector y la jeringa que contendrá la

solución de polímero a hilar. Mediante un software desarrollado también por investigadores del INTEXTER, la máquina permite modificar los parámetros característicos del proceso de electrohilado, tales como posición de la jeringa, caudal y voltaje aplicado entre el cabezal de la aguja y el colector conectado a tierra. El software, además, permite incorporar datos tales como el diámetro de la jeringa, intensidad de corriente, etc., necesarios para controlar el proceso. Al trabajar con una máquina de fabricación propia, existe la posibilidad de realizar modificaciones mecánicas en función de las necesidades concretas. En este caso, con el objetivo de evitar el consumo excesivo de material se incorporó un mecanismo de transmisión de movimiento entre la bomba de caudal y la jeringa que contiene el polímero a hilar mediante un conducto con agua. En todos los casos se ha trabajado con un colector de cobre conectado a tierra, el cual se ha recubierto con el material específico sobre el que se depositarán las nanofibras en cada caso (aluminio, papel, poliuretano, etc.).

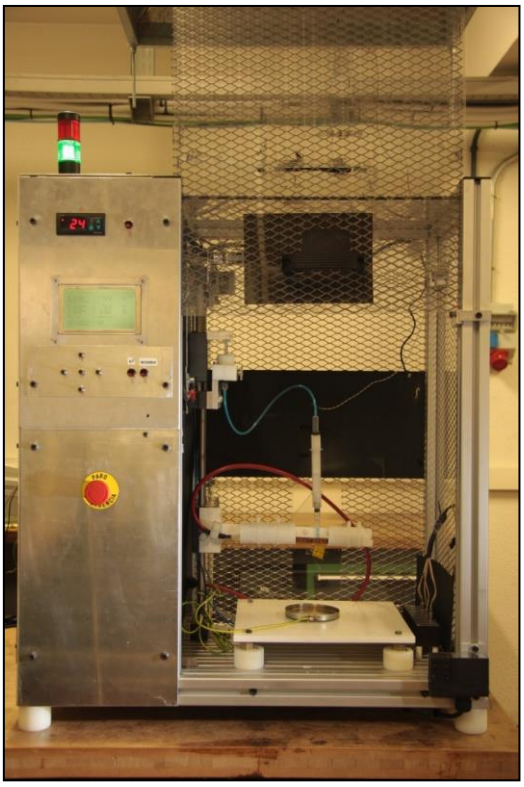

***Figura 2.3**: Máquina de electrohilatura diseñada y fabricada en INTEXTER*

2.4.3. Reticulación de las nanofibras

La estabilización de las nanofibras electro-hiladas resulta un paso esencial para permitir su uso en aplicaciones que requieran resistencia al agua y/o rendimiento termo-mecánico. Se ha estudiado el proceso de reticulación de films y/o nanofibras de gelatina con glutaraldehído (GA) mediante tres vías de aplicación distintas:

- GA vapor: Las muestras a reticular se colocan sobre el soporte perforado de un desecador que contiene una solución de GA a la concentración deseada (esquema en **Figura 2.4**)
- GA inmersión: Las muestras se sumergen directamente en una disolución de GA a una determinada concentración en etanol.
- GA in-situ: Se añaden pequeñas cantidades de GA a la disolución inicial de gelatina previamente a su electro-hilatura con el objetivo de obtener nanofibras ya reticuladas.

La reticulación se llevó a cabo a temperatura ambiente y a las muestras obtenidas se le aplicó un tratamiento de secado en estufa por aire a 37ºC durante 1 hora.

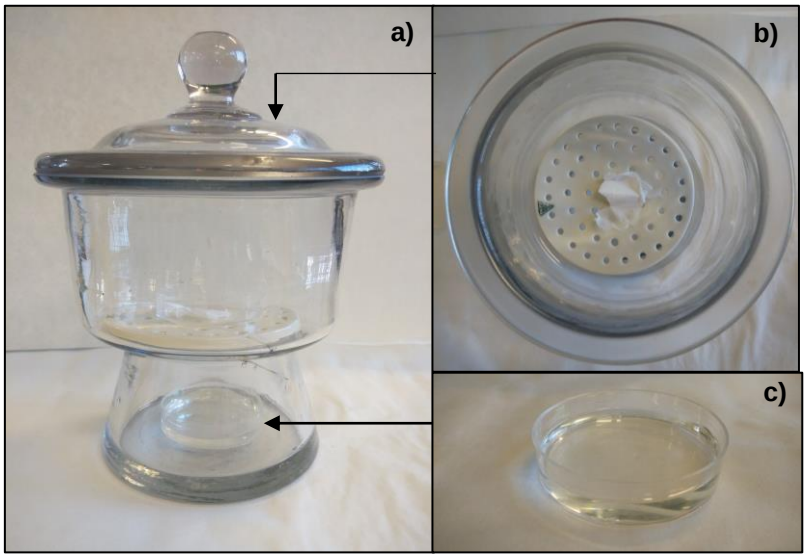

***Figura 2.4**: Montaje para la reticulación mediante vapor de glutaraldehído: a) desecador b) soporte perforado con muestra c) placa de Petri conteniendo la solución de glutaraldehído*

2.4.4. Caracterización de las nanofibras

La caracterización de las fibras obtenidas por electrospinning se ha realizado por distintas técnicas en función de la propiedad a analizar. A continuación se hace una pequeña descripción de las técnicas utilizadas y su uso específico para esta tesis.

2.4.4.1. Análisis microscópico

Debido al tamaño de las fibras obtenidas mediante electrohilatura, la microscopía resulta una técnica fundamental para su caracterización, tanto para evaluar su presencia y distribución, como para realizar un análisis más exhaustivo acerca de su morfología y tamaño.

- *Microscopía Óptica*

La microscopía óptica resulta un método eficaz y rápido para la determinación de nanofibras sobre un sustrato trasparente, tal y como los films de poliuretanos, puesto que el material debe permitir el paso de la luz para su correcta observación mediante esta técnica. Se trata de un tipo de microscopia que usa una fuente de luz visible combinada con un sistema de lentes para obtener imágenes magnificadas de muestras pequeñas.

***Figura 2.5**: Microscopio óptico. (JENAVAL, Carl-Zeiss)*

En la presente tesis se ha trabajado con un microscopio óptico vertical (Jenaval, Carl Zeiss, **Figura 2.5**) cuyo objetivo de máximo aumento es de X100, el cual combinado con el ocular de X25 permite obtener una imagen con un aumento total de X2500. Este microscopio se ha utilizado principalmente para la observación general de la orientación de las fibras electrohiladas sobre soportes transparentes de poliuretano. Además ha resultado una técnica útil y rápida para la determinar la formación de fibras.

- *Microscopía electrónica de barrido (SEM)*

La microscopía electrónica utiliza electrones en lugar de fotones o luz visible para formar imágenes de objetos diminutos. Los microscopios electrónicos permiten alcanzar una capacidad de aumento muy superior a los microscopios convencionales (alcanzando aumentos de más de 500.000X) debido a que la longitud de onda de los electrones es mucho menor que la de los fotones "visibles".

En la presente tesis se ha trabajado con dos microscopios electrónicos de barrido (SEM), modelos JSM-5610, JEOL y Phenom Standard, en función de su disponibilidad (**Figuras 2.6 y 2.7** respectivamente). El resultado de este análisis son imágenes de alta resolución de la topografía superficial de la muestra, las cuales pueden ser analizadas mediante softwares de imagen, tales como Image J, Photoshop, etc.

Debido a su proceso de funcionamiento, es condición necesaria que las muestras a observar en un microscopio electrónico sean conductoras. Con este objetivo, se utilizó un equipo de recubrimiento superficial por pulverización catódica de oro/paladio para proporcionar conductividad eléctrica a aquellas muestras recogidas sobre un soporte no conductor (papel, poliuretano, etc.), mientras que las muestras recogidas sobre papel de aluminio no necesitarán ser sometidas a este proceso de recubrimiento.

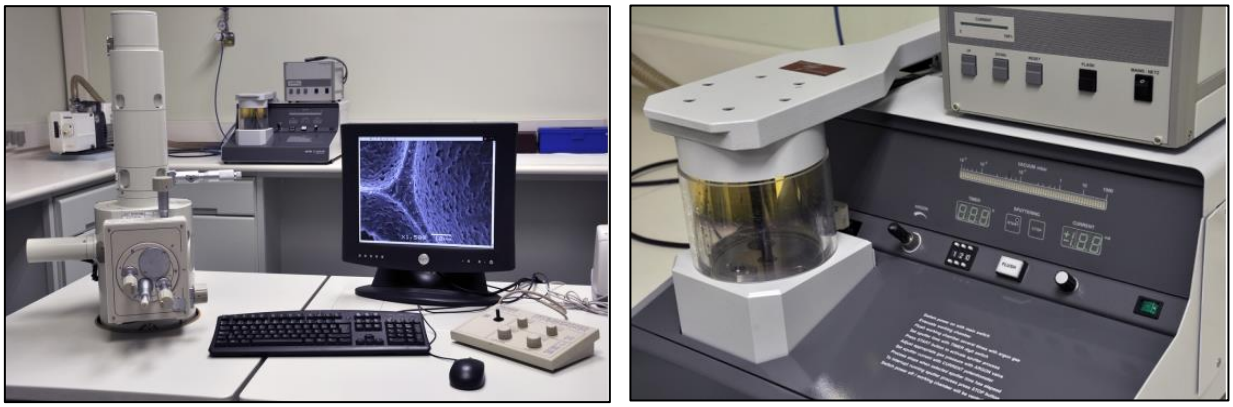

***Figura 2.6**: Microscopio electrónico de barrido (JEOL, JS-5610) y equipo de recubrimiento (SCD 005, Bal-Tec)*

***Figura 2.7**: Microscopio electrónico de barrido (Phenom Standard) y equipo de recubrimiento (SC7620, Quorum Technologies)*

2.4.4.2. Espectroscopia

- *Por transformada de Fourier (FTIR)*

La espectrometría de infrarrojos (espectroscopia IR) es un tipo de espectrometría de absorción que utiliza la región infrarroja del espectro electromagnético, basándose en el hecho de que los enlaces químicos de las sustancias tienen frecuencias de vibración específicas, que corresponden a los niveles de energía de la molécula. Como las demás técnicas espectroscópicas, puede ser utilizada para identificar un compuesto o investigar la composición de una muestra.

En la presente tesis se utilizó el espectrofotómetro por transformada de Fourier (FTIR, Avatar System 320, **Figura 2.8**) para identificar y comparar la estructura química de los polímeros (colágeno, gelatina) en sus tres estados: puros, en disolución y en forma de fibras (una vez electrohilada la disolución).

***Figura 2.8**: Espectofotometro FTIR (Avatar System 320)*

Las muestras sólidas (polímeros puros o nanofibras) se analizan mediante la formación de una pastilla a partir de prensar una mezcla del polímero con bromuro potásico (material transparente a la radiación incidente en la región infrarroja). Para el análisis FTIR de las muestras líquidas (disoluciones de polímeros) se utilizó el accesorio especial para tal efecto suministrado por el mismo fabricante del equipo, en el que dos cristales de NaCl forman una cavidad estanca donde se introduce el líquido mediante una jeringa. El esquema de la célula para realizar FTIR de líquidos se muestra en la **Figura 2.9**. Las condiciones generales de registro de los espectros realizados se especifican en la **Tabla 2.2**.

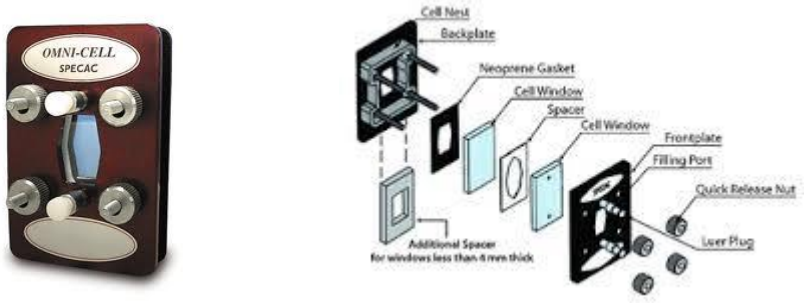

***Figura 2.9**: Célula medición FTIR líquidos. a) Fotografía b) Esquema de componentes (Fuente: www.speac.com)*

***Tabla 2.2**: Condiciones de registro de los espectros FTIR*

Número de barridos	32
Resolución	$4cm^{-1}$
Formato final	Absorbancia
Detector	DTGS KBr
Rango espectral	500-4000 cm^{-1}

- *Reflectancia total atenuada (ATR)*

Aunque la medida más común en el infrarrojo es la que se basa en la absorción (o intensidad transmitida), también se han desarrollado espectroscopias basadas en el fenómeno de la reflexión, como es la reflectancia total atenuada.

***Figura 2.10**: Accesorio ATR (Avatar System)*

El principio de esta medida (**Figura 2.11**) se basa en el fenómeno de la reflexión total interna y la transmisión de la luz a través de un cristal con un elevado índice de refracción. La radiación penetra (unos micrómetros) más allá de la superficie del cristal donde se produce la reflexión total, en forma de onda evanescente. Si en el lado exterior del cristal se coloca un material

absorbente (muestra), la luz que viaja a través del cristal se verá atenuada y se puede registrar el espectro de la muestra. El ángulo de la luz incidente y la geometría del cristal facilitan que se produzcan sucesivas reflexiones en sus caras internas. El espectro medido tiene una apariencia similar al espectro de transmisión, excepto por ciertas variaciones en la intensidad en función de la longitud de onda que se producen.

Se consideró el uso de esta técnica para el estudio de la estructura química de las fibras de colágeno tras su deposición sobre un film de poliuretano, teniendo en cuenta que la modificación sólo afectaba a la superficie del film. El análisis ATR se realizó mediante el accesorio Smart MIRacle ATR (cristal de ZnSe) (**Figura 2.10**) del espectrofotómetro Nicolet Avatar 320.

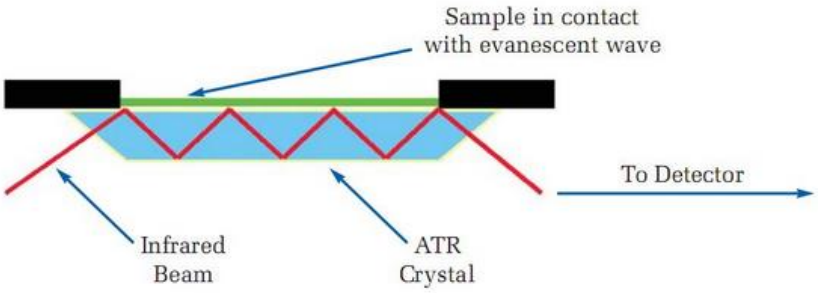

Figura 2.11. *Esquema del sistema de reflexión total atenuada (Fuente: www.alkor.net)*

2.4.4.3. Análisis térmico

- *Calorimetría diferencial de barrido (DSC)*

La calorimetría diferencial de barrido es una técnica termoanalítica basada en la determinación del flujo calorífico diferencial necesario para mantener una muestra de un material y una referencia inerte a la misma temperatura. Así cuando la muestra experimenta una transformación física (transición de fase) se necesitará que fluya más o menos calor a la muestra de referencia para mantener ambas a la misma temperatura.

El resultado del experimento es una curva de flujo calorífico en función de la temperatura o el tiempo.

Este equipo (modelo PerkinElmer DSC 7, **Figura 2.12**) se ha utilizado con el objetivo de determinar cambios significativos en la temperatura de degradación de los polímeros antes y después de ser electrohilados, analizando de esta manera el efecto de la disolución y el proceso de electrohilado en la estructura nativa de la proteína.

***Figura 2.12**: Calorímetro (DSC 7, PerkinElmer)*

- *Termogravimetría (TGA)*

La termogravimetría (TG) es un método de análisis que estudia los cambios de masa que experimenta una muestra en función de la temperatura, y puede realizarse a temperatura constante (régimen isotérmico) o a variaciones de temperatura (régimen dinámico). Las aplicaciones de este método de análisis van dirigidas al estudio de las transformaciones que implican absorción y desorción de gases, reacciones químicas, etc. Durante la termogravimetría se determina continuamente la masa y la temperatura de la muestra mientras aumenta la temperatura.

El termograma obtenido permite evaluar los cambios de masa que se producen a diferentes temperaturas, indicando las transformaciones que tienen lugar en cada momento.

El uso de esta técnica mediante el equipo Mettler Toledo TGA/SDTA851e (**Figura 2.13**) ha permitido determinar diferencias entre el comportamiento de los soportes de fibras antes y después de ser reticulados. Las especificaciones del equipo se resumen en la **Tabla 2.3**.

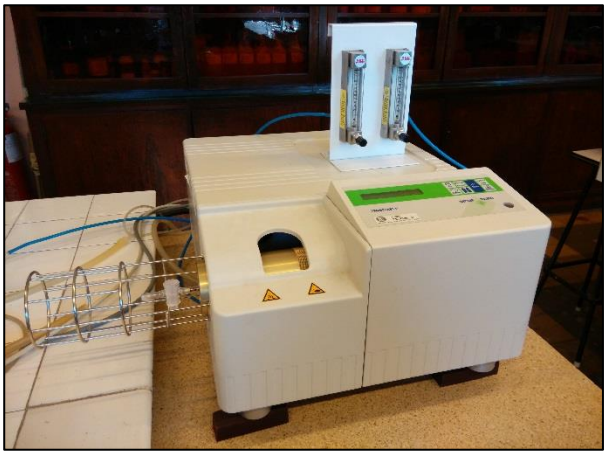

***Figura 2.13**: Termogravímetro (TGA/SDTA851e, Mettler Toledo)*

***Tabla 2.3**: Especificaciones TGA*

Temperatura máxima	1600ºC
Precisión	± 0.25 ºC
Peso máximo balanza	5 g
Resolución balanza	±1 µg
Material horno	Alúmina
Refrigeración	Agua

2.4.4.4. Ángulo de contacto

El ángulo de contacto es una medida cuantitativa de la humectabilidad de un sólido por un líquido. Medidas de ángulo inferiores a 90º indican que la mojabilidad es muy alta y el fluido se extenderá sobre la superficie, mientras que ángulos superiores a 90º significan que la mojabilidad es baja y el fluido disminuirá el contacto con la superficie, formando una gota compacta (**Figura 2.14**).

En el caso que el líquido utilizado sea agua se habla de materiales hidrofóbicos (con ángulo >90º) e hidrofílicos (<90º). La superficie de los films de poliuretano utilizados en la presente tesis se caracterizaron teniendo en cuenta este criterio de humectabilidad antes y después de ser cubiertos con una capa de fibras colágenas. La medición del ángulo se realizó mediante un software de edición de imágenes (Photoshop CS5) a partir de fotografías tomadas a una gota de agua sobre la superficie (cámara Canon EOS 40D).

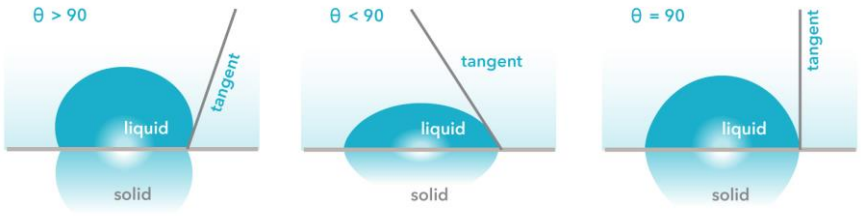

***Figura 2.14**: Ángulos de contacto para superficies con distinta humectabilidad*
(Fuente: www.biolinscientific.com)

2.4.4.5. Análisis de biocompatibilidad

La evaluación de la biocompatibilidad de las mallas de fibras proteicas electrohiladas se realizó mediante el denominado test de citotoxicidad por contacto indirecto. El ensayo permitió detectar pequeñas cantidades de solvente residual en las fibras electrohiladas, así como valorar el efecto de estas trazas de disolvente en la viabilidad celular. En este último caso, un medio de cultivo se puso en contacto con la malla de fibras electrohilada.

***Figura 2.15**: Cabina de seguridad biológica (NuAire)*

Considerando la posible aplicación de las fibras electrohiladas como soportes para aplicaciones biomédicas dentro de la ingeniería de tejidos se evalúa su citotoxicidad sobre células tisulares (fibroblastos(BJ-5ta) y/o células de riñón(HEK 293T)). Todos los ensayos en los que se manipulan células vivas se trabajan en el interior de una cabina de seguridad biológica (Type II Class Hood-cell culture, NuAire, **Figura 2.15**) y se sigue el procedimiento general de cultivo celular formado por las siguientes etapas:

- *Descongelación*

Las células se conservan en criotubos que se encuentran en un congelador a -80ºC. Para su uso, se llevan los criotubos a la cabina de seguridad biológica situados en hielo seco, con el objetivo de disminuir el shock térmico que supone el paso de bajas temperaturas a temperatura ambiente. Los criotubos se colocan en un baño de agua a 37ºC con agitación suave y una vez descongelado se transfiere su contenido a un tubo de centrífuga (**Figura 2.16**) conteniendo el medio de cultivo completo indicado por el fabricante (DMEM + Fetal Bovine Serum + Hygromycin B). Tras aproximadamente 5 minutos de centrifugación se retira el sobrenadante de la solución y se resuspenden las células en medio de cultivo fresco. Finalmente se añade esta suspensión a un recipiente de cultivo previamente preparado y se introduce en un incubador a 37ºC con atmosfera de 5% de CO_2 (**Figura 2.17**).

***Figura 2.16**: Centrífuga (Beckman)*

***Figura 2.17**: Incubadora CO_2 (Nuaire)*

- *Mantenimiento*

Esta etapa consiste en dos acciones fundamentales:

- Cambio periódico del medio de cultivo para reponer los nutrientes necesarios consumidos mediante la proliferación celular.
- Observación de las células por microscopia óptica (**Figura 2.18**) para evaluar el crecimiento y determinar el momento en que éstas se encuentran en confluencia (ocupando toda la superficie del frasco) y deben ser tripsinizadas.

***Figura 2.18**: Microscopio óptico (Olympus CK30)*

- *Tripsinización*

Una vez las células llegan a confluencia se retira el cultivo celular, se añade tripsina-EDTA y se mantiene el frasco en incubación durante aproximadamente 10 minutos con el objetivo de desengancharlas de su base. Mediante microscopia óptica se observa cuando las células se han desprendido de la superficie. En ese momento se añade medio de cultivo completo a la solución para inactivar la tripsina y se realizan las alícuotas deseadas de la suspensión en nuevos frascos de cultivo.

Las células procedentes del cultivo celular con un crecimiento óptimo se utilizan para los ensayos de citotoxicidad por contacto indirecto, para la evaluación de la biocompatibilidad de las mallas de fibras electrohiladas mediante el conocido como ensayo Alamar Blue. Este ensayo se basa en el recuento de las células viables mediante cambios de color en el medio producidos por el contacto del resazurin (compuesto que generan las células al respirar) con el reactivo AlamarBlue. Las mediciones se realizan con el lector de microplacas Infinite M200 (Tecan) (**Figura 2.19**).

***Figura 2.19**: Lector de microplacas (Infinite M200, Tecan)*

La morfología de las células usadas para los ensayos por contacto indirecto se analizan mediante el uso de un microscopio de contraste de fase (Eclipse Ti-S, Nikon) (**Figura 2.20**).

***Figura 2.20**: Microscopio de contraste de fase (Eclpse Ti-S, Nikon)*

CHAPTER 3:

Effect of operational and solution parameters on diameter of electrospun protein fibers

Effect of operational and solution parameters on diameter of electrospun protein fibers

SUMMARY

This study provides a complete knowledge about the effect of the main parameters governing the electrospinning process of protein solutions (gelatin/collagen) both in their electrospinnability such as the diameter of the obtained fibers. Regarding the operational parameters (voltage, flow rate and distance between needle and collector) the result showed that the protein solutions behaviour, unlike the common behavior of other polymers, can be defined as go/no go system. Thus, the electrospinnability of solution is affected by the operational parameters but not the diameter of electrospun fibers obtained working into an optimal condition rate, which didn't show significant differences regarding the operational conditions used. The solution parameters, however, along with the conductivity of collector used to collect the protein nanofibers, showed a high significant effect in the obtained results. It was noted the direct relationship between the polymer concentration in same solvent conditions and the polymer protein type (based on their molecular weight) in the diameter of resulted nanofibers. The effect of solvent conductivity was also tested and their effect in nanofiber diameter was stablished as significant for the same polymer protein, showing finest fibers for higher solvent conductivity even for solutions using higher polymer concentration. Finally, the effect of the material conductivity of collector used to receive the electrospun nanofibers was defined, which could be important to take into account in cases where an specific type of collector is needed.

Keywords: electrospinning, proteins, parameters optimization.

3.1. Introduction

Among the different techniques used for the fabrication of nanofibers, capable of acting as scaffolds into the field of tissue engineering (self-assembly, phase separation, template synthesis, drawing, etc. [3.1-3.4]), the electrospinning process has been postulated recently as the most widely studied technique due to their simple, versatile and inexpensive nature, exhibiting the most promising results on biomedical applications [3.5-3.6].

Although the electrospinning is an old technique, first observed in 1897 [3.7], it has gained popularity in the last 10 years due in large part to an increased interest in nanoscale properties and technologies. The process allows obtaining nano and micro-sized continuous fibers by applying a high voltage electrostatic field between a metal capillary syringe containing a polymer solution and a grounded collector where the fibers are deposited as a result of the solvent evaporation, forming a nonwoven fibrous webs of high porosity.

There are a wide range of polymers that used in electrospinning are able to form nanofibers on nano, micro range, used for varied applications. This process has been reported for both synthetic (PLA [3.8], PCL [3.9], Cellulose acetate [3.10], etc.), and natural polymers, and although the synthetic polymer are highly useful in biomedical field since their good mechanical properties, natural polymers can be considered as the first biodegradable biomaterials, having better bioactive properties. Into the natural polymers, including polysaccharides [3.11] and proteins [3.12], collagen [3.13-3.14] and gelatin [3.15-3.16] are some prominent biopolymers being used extensively due to its excellent biological and physico-chemical properties for tissue engineering applications.

From a technical point of view, the election of an appropriate solvent in function of the polymer type is one of the most important parameter influencing the electrospinning manufacturing process, due to their effect on the solution parameters, including viscosity, conductivity, molecular weight and surface tension. Regarding obtaining of electrospun collagen and gelatin nanofibers, first studies demonstrated the ability of dissolve and electrospin these natural polymers with some complex solvents such as 1,1,1,3,3,3-hexafluoro-2propanol (HIPF) and 2,2,2-trifluoroethanol (TFE) [3.12, 3.15, 3.17-3.23]. However, their potential cytotoxicity combined with their high cost, has promoted the search of alternative systems to electrospun protein polymers, where carboxylic acids as acetic acid have postulated recently as a good option [3.16, 3.24-3.27].

Beside the solution parameters, the electrospinning is also governed by operational parameters, including applied voltage, distance between tip and collector and flow rate, and ambient parameters such as humidity and temperature.

Many studies have been efforts to found the relationship between each parameter that govern electrospinning and the diameter of final electrospun fibers and the electrospinnability of solution. Although these studies allow to establish some general trends [3.7, 3.28-3.30], it is important to note that the particularly effect of each parameter has significant relationship with the solution system, due to the different behavior and interactions produced. So, a general forecast of the final diameter and morphology of electrospun fibers are quite difficult.

The aim of this study is to analyze the effect of the main operational parameters influencing the electrospinning process (voltage, flow rate and distance between needle and collector) and solution parameters (nature of the polymer, polymer concentration, type of solvent) for a system formed by gelatin/acetic acid/water, taking into account their recently potential as a benign solvent to form tissue engineering scaffolds, in order to have a complete control of the process making easier the production of nanofibers with desired morphology and diameter. Complementary, the effect of other important parameters are also analyzed, as the polymer type (gelatin/collagen), solvent type (HIPF, Acetic Acid) and the collector conductivity (aluminum, cellulose) on the diameter electrospun fibers. The experiments were carried out following an experiment design in order to determine each independent effect of these parameters and their interactions. The experimental results were summarized and analyzed with the software MODDE 8.0.2 (Umetrics AB).

3.2. Experimental

3.2.1. Materials

Gelatin powder from bovine skin (type B with Bloom ~ 225g) and Collagen type I from calfskin were purchased from Sigma Aldrich and used without further treatment or purification. Glacial acetic acid (99,99%, Panreac), 1,1,1, 3,3,3-hexafluoro 2-propanol (HIPF, Sigma) and bidestillate water were used as solvents. To evaluate the conductivity of collector on the fiber diameter, conductive aluminum and cellulose foils were used to cover the base.

3.2.2. Solution preparation

Two different solutions of gelatin in aqueous acetic acid solution (25% v/v) were prepared for the experiments designed to evaluate the effect of operational parameters and polymer concentration (300 and 400 mg/ml) on electrospun fiber diameter and solution spinnability (samples 1 and 2 of **Table 1**).

Moreover, for the study of the effect of other parameters on the electrospun fiber diameter many system polymer/solvent were prepared:

- Type of solvent: The same polymer (gelatin) was used to establish the effect of solvent on electrospun fibers for an optimal concentration in each one (80mg/ml in HIPF and 300 mg/ml in Acetic Acid 25%). (Samples 1 and 3 of **Table 3.1**)
- Polymer type: To determine the effect of the polymer type, gelatin and collagen solutions were dissolved on HIPF at same concentration (80mg/ml). (Samples 4 and 5 of **Table 3.1**)
- Collector conductivity: Two identical solutions (gelatin in HIPF at 80mg/ml) were electrospunned with different cover foil on collector (aluminum and polyurethane) to evaluate the effect of collector conductivity on the electrospinning process. (Samples 3 and 4 of **Table 3.1**)

All solutions were stirred at room temperature (25ºC ± 1ºC) for 1h. The control of the stirring time is crucial, especially for gelatin case, to avoid the gelation process occurring between gelatin and water, which could alter the viscosity of solution and consequently the diameter of their electrospinnability [3.31-3.32].

***Table 3.1**: Experimental conditions of solution properties and collector conductivity for each electrospun sample*

Sample	Polymer	Collector	Solvent	Polymer Concentration
1	Gelatin	Cellulose	Acetic 25%	300 mg/ml
2	Gelatin	Cellulose	Acetic 25%	400 mg/ml
3	Gelatin	PU	HIPF	80 mg/ml
4	Gelatin	Aluminum	HIPF	80 mg/ml
5	Collagen	Aluminum	HIPF	80 mg/ml

3.2.3. Electrospinning

Electrospinning was performed in a home-made device developed by INTEXTER [3.33-3.34]. Each sample described in the previous section (**Table 1**) was placed in a 2.5 mL syringe with a stainless steel syringe needle (0.6 mm of inner diameter), connected to the anode of power supply. The electrospun polymer fibers were collected on the copper collector (connected to the cathode of the power supply) covering by aluminum or cellulose foil, except on the experiment to evaluate the conductivity effect of collector, where it was covered by polyurethane film.

In attempt to evaluate the effect of operational process parameters of electrospinning (voltage, distance between needle and collector and flow rate) on the fiber diameter, two different gelatin concentration (300 and 400 mg/ml) were dissolved on aqueous acetic acid solution (25% v/v) and the solutions were electrospunned under 27 different conditions, according with a 3x3 experimental design, where each of the three factors studied have three levels, specified in each case through the paper.

All solutions were electrospun at room temperature (25ºC $\pm$ 1ºC).

3.2.4. Fiber characterization

The morphology of fibers obtained by electrospinning was analyzed by Scanning Electron Microscopy (SEM) using a Phenom Standard SEM (Phenom-World, Netherlands). Samples were observed without any metallic coating.

To obtain the average diameter for each experiment (single polymer-solvent system and single combination of Voltage-Distance-Flow rate), 50 arbitrary electrospun fibers were measured by an image analyzing software package (ImageJ) and average and standard deviation were calculated.

3.2.5. Statistical analysis

All experimental results were analyzed by MODDE 8.0.2 in order to find a relation between the input variables and the response. In each case the regression effect plots were consulted and interpreted in order to obtain information concerning whether the factors (both individually and their interactions) had a significant effect on the response.

3.3. Results and discussion

3.3.1. Effect of operational parameters and polymer concentration on electrospun gelatin diameter and solution electrospinnability

The use of aqueous acetic acid solution at 25 % v/v to electrospin gelatin has been reported recently as a benign solvent for the fabrication of electrospun gelatin mats [3.27]. In order to control the electrospinning process, the effect of the operational parameters, such as voltage, distance and flow rate, on the fiber diameter have been studied in a range of values for each one (voltage: 10, 14, 18 kV; Distance: 7, 11, 15 cm; Flow rate: 0.25, 0.5, 1 ml/h).

Beside the operational parameters, the effect of polymer concentration on electrospun fibers diameter is also one of the most studied parameters on the electrospinning process. Many literatures have demonstrated that the fiber diameter increase significantly with an increase of polymer concentration in the same polymer-solvent system [3.24, 3.26, 3.35-3.36], because of the increase of the viscosity of solution. To analyze the effect of the polymer concentration, two different concentrations of gelatin (300 and 400 mg/ml) were selected for the electrospinning of gelatin-acetic-water solutions at the chosen above mentioned different operational parameters.

The study was carried out according with an experimental design of 54 experiments (3 factors and 3 levels for operational parameters and 2 levels for polymer concentration).

On the one hand, the results shown in **Figure 3.1** confirm the general trend reported on literature above mentioned: for the same type of solvent, solutions with high concentration (400 mg/ml) of polymer resulted in higher (fiber diameter $\sim$ 350 nm $\pm$ 40) average fiber diameter compared with solutions with low concentration of gelatin (300 mg/ml) (fiber diameter $\sim$200 nm $\pm$ 25).

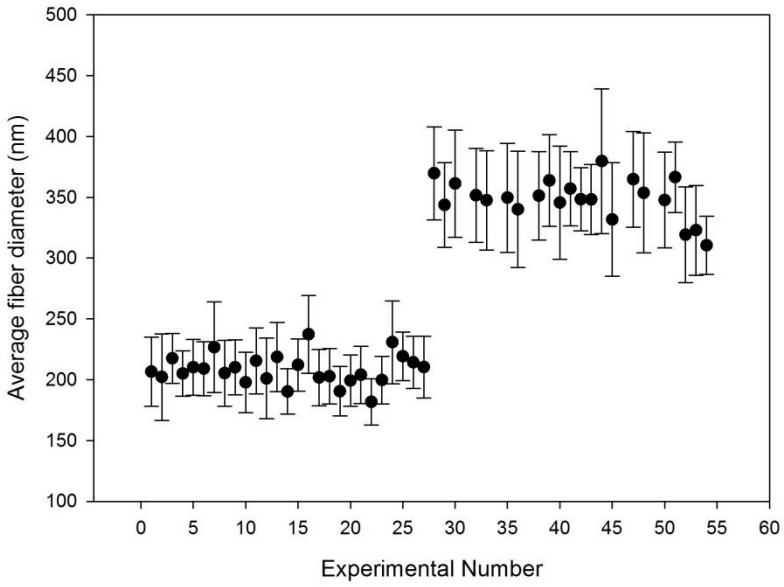

***Figure 3.1**: Experimental values of average fiber diameter with their standard deviation for two different gelatin concentration solutions at same conditions of solvent (25% AA)*

On the other hand, observing the standard deviation of each experiment it can be concluded that the operational parameters have not a significant effect on the diameter of the electrospun fiber for each group of experiments carried out with the same concentration of polymer, as had been reported previously for a similar acid system [3.37]. However, it is important to note that although the fiber diameter is not significant affected by the operational parameter values, their values controls de electrospinnability of the solution and therefore not all the conditions defined by the experiments are suitable to obtain fibers. This behavior is particularly relevant for solutions with 400 mg/ml of gelatin dissolved in 25% v/v acetic acid as it is shown in **Table 3.2**, where the feasibility of electrospinning for each experiment is defined (no fiber formation, nanofibers obtaining from optimum jet and nanofibers obtaining from unstable (intermittent) jet) . Thus, the electrospinnability of the different solutions is affected by the operational parameters and the electrospinning of gelatin on aqueous acetic acid solution (at 25% v/v) can be considered as a **go/no go system**, where the operational parameters and the polymer concentration control the feasibility of electrospinning. A 3-D graph (**Figure 3.2**) has been created with the aim of showing the electrospinnability results for the solution of 400 mg/ml of gelatin and water-acetic solvent in a more visual form depending on the three operational parameters studied (flow rate, distance and voltage).

***Table 3.2**: Average diameter and feasibility of electrospinning (Nanofibers/Unstable/No fibers) for experiments performed with solutions using 400 mg/ml of gelatin and water-acetic solvent at different combination of operational parameters*

Nº Experiment	Voltage (kV)	Distance (cm)	Flow rate (ml/h)	Average diameter (nm)	Feasibility of electrospinning
1	10	7	0.25	370 ± 38	Nanofibers
2	14	7	0.25	344 ± 35	Nanofibers
3	18	7	0.25	361 ± 44	Nanofibers
4	10	11	0.25	-	No fibers
5	14	11	0.25	352 ± 39	Nanofibers
6	18	11	0.25	347 ± 41	Nanofibers
7	10	15	0.25	-	No fibers
8	14	15	0.25	350 ± 45	Unstable
9	18	15	0.25	340 ± 48	Nanofibers
10	10	7	0.5	-	No fibers
11	14	7	0.5	351 ± 37	Nanofibers
12	18	7	0.5	364 ± 38	Nanofibers
13	10	11	0.5	346 ± 47	Unstable
14	14	11	0.5	357 ± 30	Nanofibers
15	18	11	0.5	348 ± 26	Nanofibers
16	10	15	0.5	348 ± 29	Unstable
17	14	15	0.5	380 ± 59	Unstable
18	18	15	0.5	332 ± 47	Nanofibers
19	10	7	1	-	No fibers

20	14	7	1	365 ± 39	Nanofibers
21	18	7	1	354 ± 49	Nanofibers
22	10	11	1	-	Unstable
23	14	11	1	348 ± 39	Nanofibers
24	18	11	1	366 ± 29	Nanofibers
25	10	15	1	319 ± 39	Unstable
26	14	15	1	323 ± 37	Nanofibers
27	18	15	1	311 ± 24	Nanofibers

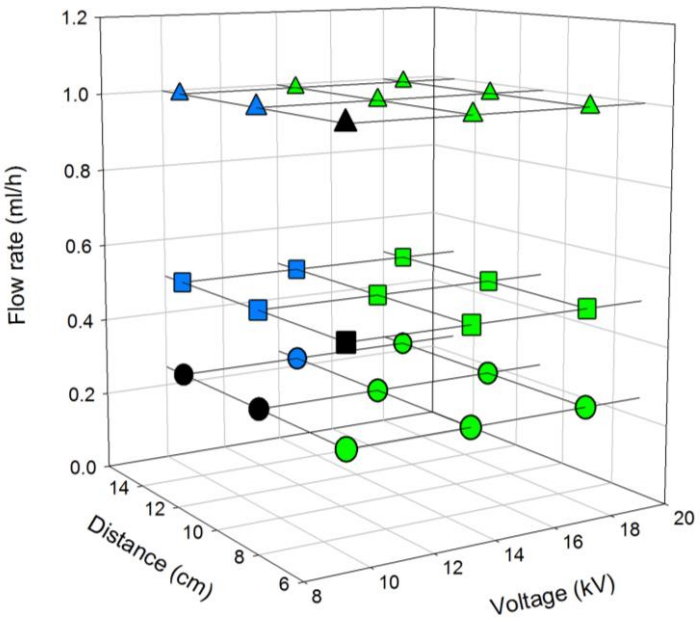

***Figure 3.2**: Electrospinnability (Green: Nanofibers; Blue: Unstable; Black: No fibers) for solution of 400 mg/ml of gelatin in aqueus acetic acid solution (25% v/v)*

Bearing in mind that the feasibility of the electrospinning is governed by the voltage, distance to the collector and flow rate, the following conclusions can be extracted from the analysis of the results shown in **Table 3.2**:

- **Effect of voltage**: Fixed the distance and the flow rate conditions, the value of voltage must be high enough to allow the stretching of polymer drop, but low enough to avoid the unstable jet (**Figure 3.3**). Similar behavior has be found in literature [3.38].

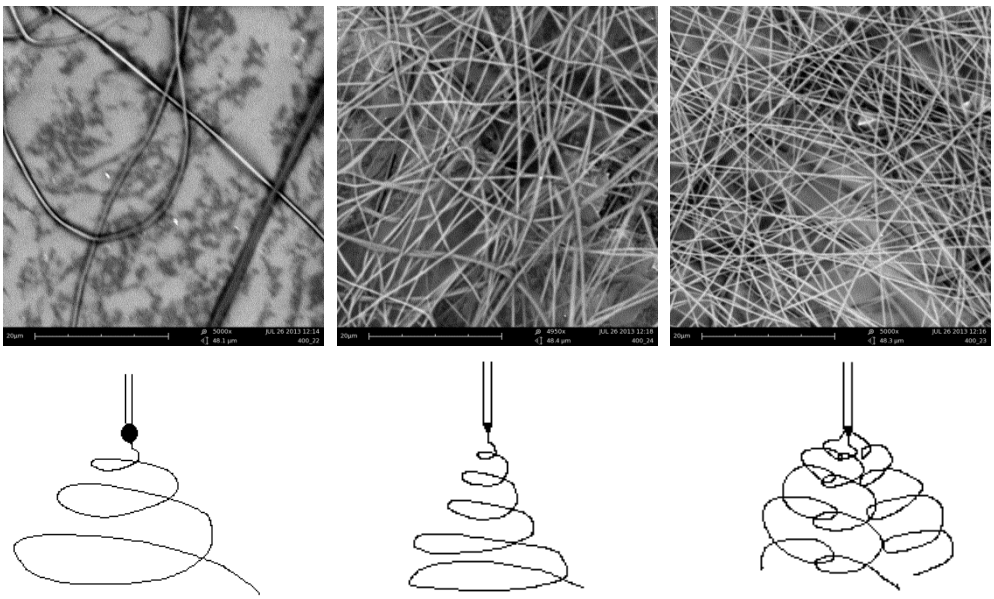

***Figure 3.3**: SEM images and schematic representation of electrospun nanofibers obtained increasing the voltage while maintaining the flow rate and distance (experiments 22, 23 and 24 of the **Table 3.2**)*

- **Effect of distance**: For the same conditions of voltage and flow rate, the distance between needle and collector must be high enough to not cause a short circuit, but low enough to allow the action of the electric field. Also, into the range of the electric field is acting, the increase of distance suppose an increase of the diameter of fiber distribution surface (**Figure 3.4**). Similar behavior has been reported on literature [3.39].

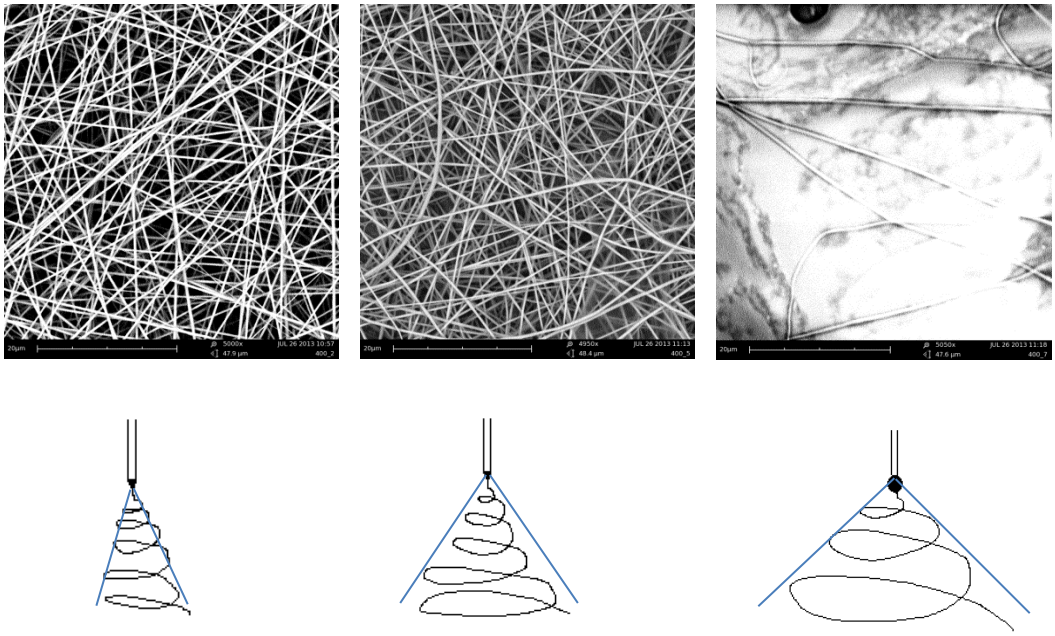

***Figure 3.4**: SEM images and schematic representations of electrospun nanofibers obtained increasing the distance while maintaining the flow rate and voltage (experiments 11, 14 and 17 of **Table 3.2**)*

- **Effect of flow rate**: For the same conditions of voltage and distance the obtaining of nanofibers the value of flow rate must be high enough to flow the polymer through the needle to form a drop at the tip, but low enough to allow the action of electric field before the drop fall by its own weight (**Figure 3.5**). Similar behavior has been reported on literature [3.40].

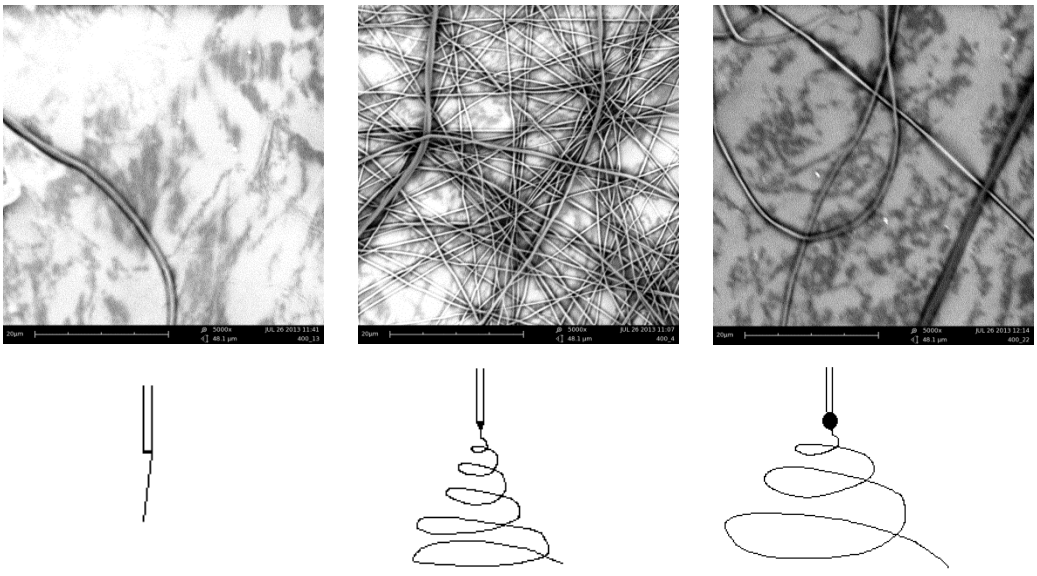

***Figure 3.5**: SEM images and schematic representation of electrospun nanofibers obtained increasing the flow rate while maintaining the distance and voltage (experiments 4, 13 and 22 of **Table 3.2**)*

To corroborate the influence and possible interaction of the four parameters studied on the diameter of the fibers formed using the feasible solutions, a statistical analysis was carried out using MODDE Software 8.0.2 (Umetrics AB). The results from the screening of interaction process model based on D-Optimal Design with 95% of uncertainty are shown in the effect plot represented in **Figure 3.6**.

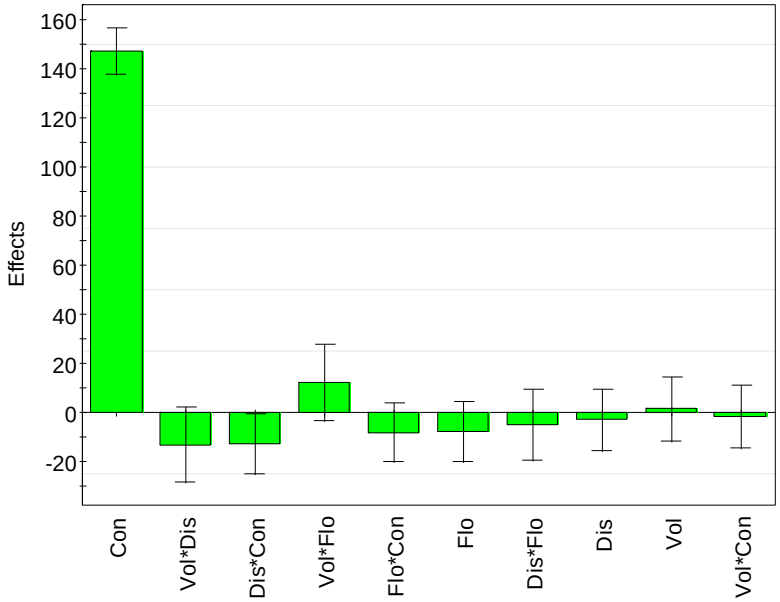

***Figure 3.6**: Analysis of operational parameters (Voltage, Distance, Flow rate) and polymer concentration on the electrospun fiber diameter for aqueous acetic acid (25%v/v) gelatin solution by multifactorial MODDE*

It is important to note that each bar on the effect plot is superimposed by a confidence interval, which indicates the uncertainty of each coefficient. Furthermore, the size of the confidence intervals depends on the size of the noise. When the confidence interval of one parameter include zero, it can be concluded that this parameter has not a significant effect on the response. Thus, the results of Figure 6 allow to determine, with 95% of uncertainty, that while the polymer concentration has a clear positive and significant influence on the fiber diameter (increasing with the increase of the polymer concentration), the rest of the operational parameters are not affecting the fiber diameter. In addition, it is observed that the diameter of the fiber is independent of the interactions between the parameters. So, as conclusion, the electrospinning of gelatin on aqueous acetic acid solution at 25% v/v can be considered as a go/no go system, where the polymer concentration, mainly affecting the viscosity of the solution, dominates the diameter of the electrospun fibers.

3.3.2. Effect of the type of solvent

The choice of solvent is other important parameters to consider affecting the electrospinning process. The solvent must be capable to dissolve the polymer at desired concentrations and providing good properties of viscosity, surface tension and conductivity to the solution.

Although recent studies have demonstrated that solutions formed by low concentration carboxylic acid are a benign alternative solvent system to electrospin gelatin, the most commonly solvents used to electrospinning protein polymers are the fluorinate compound as 1,1,1,3,3,3-hexafuoro-2-propanol and 2,2,2- trifluoroethanol. These complex solvents have a highly corrosive nature, which may affect the original protein structure [3.41] besides providing a potential cytotoxicity to the obtained scaffolds [3.31], because the presence of small amounts of residual solvent embedded on nanofibers is almost unavoidable [3.42-3.43]. However, these solvents can be a good option to electrospun gelatin fibers in certain cases where the remaining solvent may not be a problem, due to their good capacity to dissolve gelatin at room temperature.

To study the effect of the type of solvent on the electrospinnability of gelatin, gelatin powder was dissolved both in HIPF and acetic acid aqueous solution at 25% v/v before to electrospinning. Due to the different behavior of gelatin on these two solvents it was not possible to use the same concentration in both cases: gelatin solution of 300 mg/ml in HIPF it was not electrospinnable due to their too high viscosity, which avoid the pass of solution throw the needle; and gelatin solution of 80 mg/ml in acetic acid at 25% it was not electrospinnable due to their too low viscosity, which avoid the interaction of the polymer chains and provokes the formation of electrospray. The minimum concentration needed to obtain electrospun gelatin nanofibers in acetic acid solution at 25% is 200 mg/ml [3.27] and the reported maximum concentration that can be dissolved in HIPF is below 100 mg/ml [3.12, 3.44].

Despite this, the comparison of electrospun gelatin nanofibers obtained in HIPF and acetic acid solution at 25%, at their feasible concentration (80 and 300 mg/ml, respectively) is enough to extract some conclusions. The experiments were performed also following an experimental design in function of the operational parameters (in this case: voltage: 10, 14, 18 kV; Distance: 7, 11, 15 cm; Flow rate: 0,5, 2 ml/h) to confirm the results obtained in the previous section (effect of process parameters) at the same time that the solvent type effect is studied.

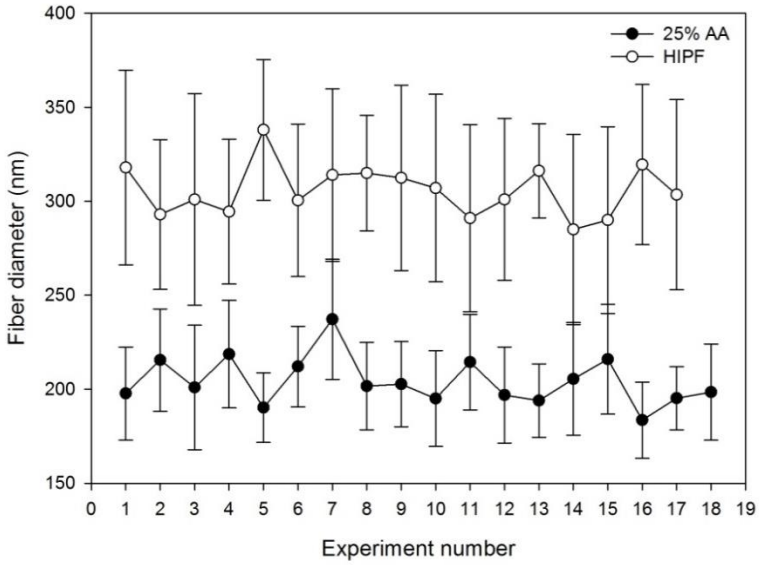

***Figure 3.7**: Experimental values of average fiber diameter with their standard deviation for two gelatin solutions using different solvents in their optimal concentration (80 mg/ml for HIPF and 300 mg/ml for 25% v/v aqueous acetic acid)*

The results (**Figure 3.7**) were analyzed by MODDE, confirming that the operational parameters have not a significant effect on fiber diameter for each group of experiments performed with the same solvent. By contrast, the effect of the type of solvent has a significant influence on the diameter of electrospun gelatin fibers. It was observed that although the concentration and viscosity of gelatin is highest in solutions formed with acetic acid solvent (300 mg/ml and 338 cP for acetic acid, in front of 80 mg/ml and 40 cP for HIPF, respectively), the diameter of electrospun gelatin nanofibers do not reflect the typical behavior expected in relation with the polymer concentration and viscosity of the solution that has been previously referenced (larger diameter forhigher viscosity solution [3.24, 3.45-3.46]). By contrast, in this case the fibers from HIPF solutions were slightly higher than the fiber electrospun from acetic acid based solutions, indicating that the effect of the viscosity and polymer concentration is comparable only between solutions with the same solvent system, where the interaction between the polymer and the solvent do not change.

For the cases of different solvent system like this, the effect of the solvent properties is more significant compared to the effect of polymer concentration and the given results can be explained taking into account the properties of different solvents that are shown in **Table 3.3** [3.7].

***Table 3.3**: Properties of different solvents used to dissolve gelatin and make electrospinning*

Solvent	Surface tension (mN/m)	Dielectric constant	Boiling point (ºC)	Density (g/ml)
HIPF	16.1	16.7	58.2	1.596
Water	72.8	80	100	1.000
Acetic Acid	26.9	6.2	118.1	1.049
25% AA	~40 [3.47-3.48]	~ 77 [3.48]	-	~1.060 [3.48]

Table 3 shows that the values of surface tension, dielectric constant, boiling point and density are significantly different from each solvent and these differences can explain the different diameter obtained when using HIPF or acetic acid-water mixture [3.7].

Considering that has not been demonstrated that surface tension has a significant influence on the nanofiber size [3.7, 3.29] it can be observed that the main parameter affecting the electrospinnability and fiber diameter is the conductivity of solution that is directly related with the dielectric constant. In this regard, the dielectric constant of HIPF solvent is lower (lower conductivity) compared with acetic-water mixtures and as a result the finest nanofibers were obtained for acetic acid aqueous solution at 25% v/v.

Figure 3.8 shows the values of the average diameter of electrospun gelatin fibers for different solutions (1) 300mg/ml gelatin on 25% AA; 2) 80 mg/ml gelatin on HIPF; 3) 400 mg/ml gelatin on 25%AA)) after corroborating that there is not significant influence of the operational parameters on fiber diameter:

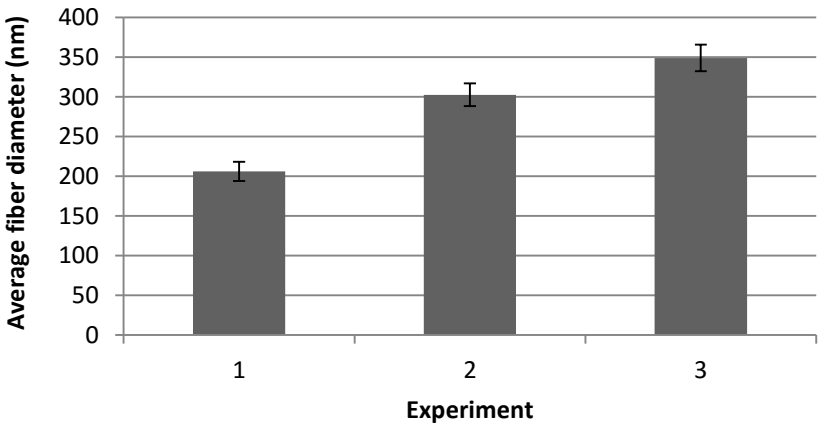

***Figure 3.8**: Average fiber diameter of gelatin electrospun nanofibers obtained from different solutions of gelatin: Experiment 1: 300 mg/ml of gelatin dissolved in acetic acid at 25 % v/v, Experiment 2: 80 mg/ml of gelatin in HIPF, Experiment 3: 400 mg/ml of gelatin in acetic acid at 25 % v/v*

From **Figure 3.8** it can be seen that the diameter of electrospun gelatin fiber using 400 mg/ml of gelatin in Acetic Acid at 25 % v/v is similar to the obtained using lower concentration of polymer (80 mg/ml) dissolved in HIPF solvent. In this case, the ratio of gelatin concentration for the two solvents ([gelatin in AA25]/[gelatin in HIPF]= 380/80 = 4.75) is very similar to the ratio of dielectric constant solvents ($\varepsilon_{AA25}/\varepsilon_{HIPF}$; 77/16.7 = 4.70), suggesting that the solution conductivity and polymer concentration parameters and this interaction is controlling the resulted fiber diameter.

3.3.3. Effect of Collector conductivity

Another interesting factor to control fiber diameter of electrospun fibers is the degree of conductivity of the collector piece. In addition, the deposition of electrospun fibers onto collector of different conductivity is an interesting issue for some applications such as the coating of non-conductive biomaterials (i.e. polyurethane, silicone) frequently used in tissue engineering applications. One example may be the use of the electrospun gelatin nanofibers as a surface coating of polyurethane biomaterial, taking into account the benefits to combine the properties of natural and synthetic polymers on the materials suitable for to be used as scaffold on tissue engineering [3.49].

For this reason, in function of the future application of the nanofibers mats formed by electrospinning, it may be interesting deposit them on a different type of collector, to prevent further manipulation. Therefore, the effect of collector conductivity on electrospinnability and diameter of electrospun fibers must be considered in order to control the characteristics of fiber mat obtained, which can be different depending on the further application. Bearing this purpose in mind, two gelatin solutions with the same concentration (80 mg/ml) and dissolved in the same solvent (HIPF) were electrospun onto the cupper collector part of the electrospinning device that was covered with two different materials to change their conductivity: 0.020 mm aluminum foil (high conductive material) and 0.135 mm polyurethane film (low conductive material). To confirm the non-significance of main operational parameters an experimental design was applied (in this case: voltage: 10, 14, 18 kV; Distance: 7, 11, 15 cm; Flow rate: 0,5, 2, 4 ml/h) and a statistical analysis was performed.

The experimental results are shown in **Figure 3.9** for both type of collectors used.

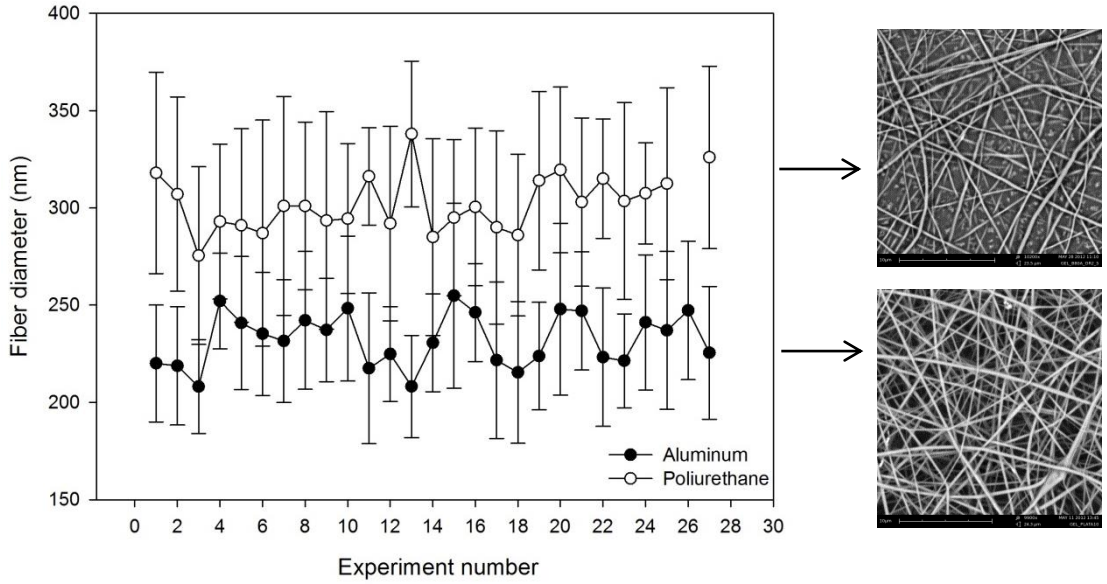

***Figure 3.9**: Experimental values of average fiber diameter with their standard deviation for two gelatin solutions at same conditions of solvent (HIPF), concentration (80 mg/ml) with different conductivity of collector covering (aluminum and polyurethane)*

It can be observed a slight difference between the fiber diameter results obtained for the electrospun fibers deposited onto a more conductive material (aluminum foil, $3.6x10^{7}$ S/m) compared to the diameter of the fibers deposited onto the less – conductive material (polyurethane film, $1.6x10^{-3}$ S/m). While the electrospun gelatin fibers deposited onto the aluminum foil have an average diameter between 200-250 nm±, the fibers deposited on the polyurethane film have a higher thickness (~ 300 nm±).

The conductivity of the collector is highly related with the electrostatic forces acting on the deposition of the charged fibers [3.50]. Some studies have demonstrated that fibers collected on the non-conducting material usually have a lower packing density compare to those collected on a conducting surface, caused by the repulsive forces of the accumulated charges on the collector as more fibers are deposited. For a conducting collector, charges on the fibers are dissipated thus allowing more fibers to be attracted to the collector [3.51-3.52]. The results observed on **Figure 3.9** confirm the above mentioned behavior: less density and more separate fibers were obtained for fibers deposited onto no-conductive collector (polyurethane) due to the charges repulsion while the covered collector covered with the aluminum foil are able to pack fibers closely together because for this latter case the charges on the fibers can be dissipated and there are attracted to the collector, also producing a slight decrease of the fiber diameter obtained.

The effect of collector type (conductivity) along with the different operational parameters (voltage, flow rate and distance between needle and collector) on the fiber diameter was statistically analyzed and the effect plot results are shown in **Figure 3.10**.

The results shown in **Figure 3.10** confirm that the operational parameters (both individually and their interactions) have still a non-significant effect on the fiber diameter for the studied ranges, unlike the conductivity of collector, which has a negative significant effect, since increasing the collector conductivity provokes a decrease of the fiber diameter.

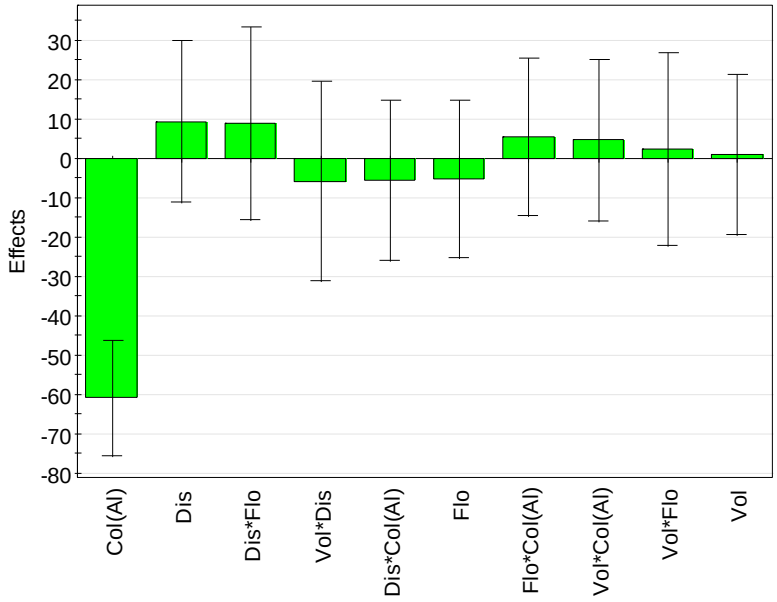

***Figure 3.10**: Analysis of operational parameters (Voltage, Distance, Flow rate) and type of collector of nanofibers on the electrospun fiber diameter for gelatin solution in HIPF by multifactorial MODDE*

3.3.4. Effect of polymer type

Gelatin is a natural polymer commonly used for the fabrication of nanofibers mats by electrospinning and suitable for biomedical applications due to their good properties of biocompatibility and biodegradability, combined with their low cost. Also, it can be considered as a model of behavior applicable subsequently to collagen, the most abundant protein in the human body. In this regard, being gelatin and collagen two of the most used protein based polymers in the field of biomedical engineering, a comparison of the electrospinnability of these two natural polymers is carried out in order to analyze the effect of the nature of the polymer on the properties of the resulted electrospun fibers.

The most commonly solvent used to dissolve these natural polymers is HIPF at optimal concentration of 80mg/ml, as it was pointed out in various studies [3.12-3.13, 3.53].

However, it is important to highlight that although both collagen and gelatin have demonstrated its potential to be electrospun using HIPF solvent, they behaves significantly different during electrospinning process due to the particular properties of each polymer [3.54].

Figure 3.11 shows the values of average fiber diameter with their standard deviation for each experiment based on an experimental design of three factors with three levels (Voltage: 10, 14, 18 kV; Distance: 7, 11, 15 cm; Flow rate: 0.5, 2, 4 ml/h) for electrospun gelatin and collagen solutions at same conditions of solvent system (HIPF), polymer concentration (80 mg/ml) and type of collector (aluminum foil). A representative SEM image of collagen and gelatin nanofibers was also shown.

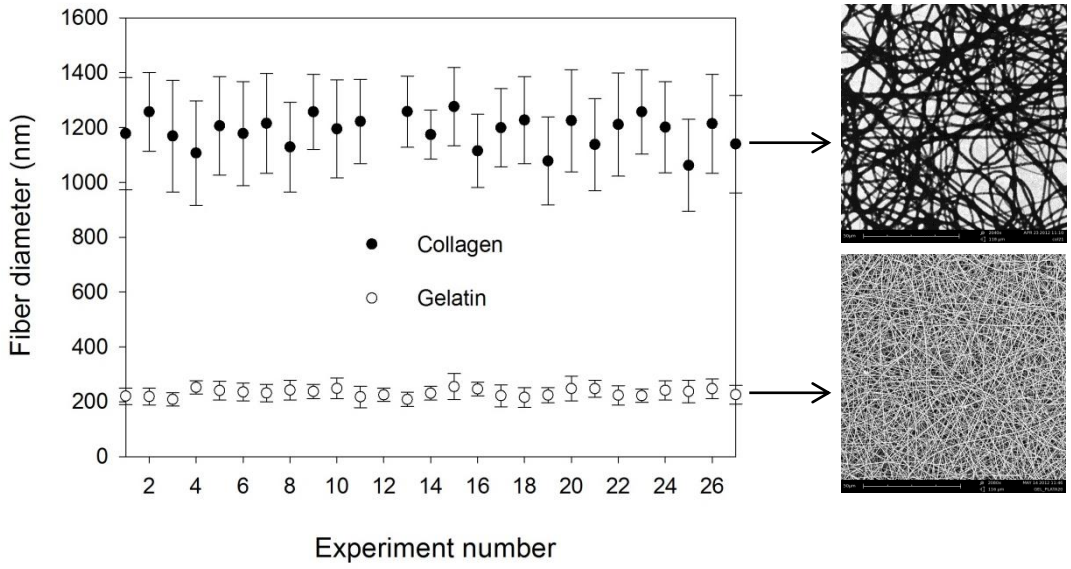

***Figure 3.11**: Experimental values of average fiber diameter with their standard deviation for gelatin and collagen electrospun solutions at same conditions of solvent (HIPF), concentration (80 mg/ml) and collector (aluminum foil)*

The differences on the average diameter between gelatin and collagen electrospun nanofibers obtained at same conditions were clear. While collagen shows an average diameter about 1200 nm ± 160 nm (this value is comparable to the range of values previously reported on the literature for collagen type I calfskin electrospun in HIPF as solvent [3.55-3.59]), gelatin nanofibers are significantly finer with an average diameter slightly higher than 200 nm ± 30 nm. These differences on the fiber diameter are directly related with the molecular weight of each natural polymer [3.60], taking into account that both polymer have the same chemical nature.

It is known that polymer molecular weight reflects the entanglement of polymer chains and has a significant effect on rheological properties of solution, such as viscosity

[3.61]. Many studies have demonstrated the influence of this parameter on the fiber morphology obtained by electrospinning, indicating that an increase of molecular weight of polymer implies a reduction of the number of beads and droplets [3.46, 3.62]. In this case, the concentration of each polymer was enough to avoid the formation of beads and droplets, which would appear to reduce the polymer concentration, as has been observed in other studies [3.27]. So, the increase of molecular weight implies directly the obtaining of fibers by electrospinning with a higher diameter. In this particular case the molecular weight of the collagen (300kDa) is 6-fold the molecular weight of the gelatin (>50 kDa) and, as a result, the fiber diameter of the collagen resulted higher compared to gelatin (**Figure 3.12**).

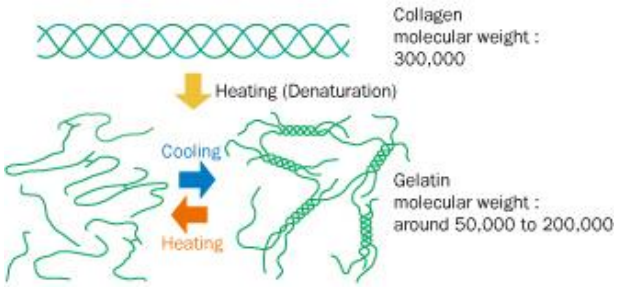

***Figure 3.12**: Schematic representation of collagen and gelatin structure with their average molecular weight*

Taking into account the aforementioned premises, an statistically analysis was carried out by MODDE in order to evaluate the effect of the use of either collagen or gelatin on fiber diameter of the electrospun fibers. At the same time, the influence of the operational parameters was analyzed. The results are shown in **Figure 3.13**, confirming the non-significance of operational parameters on electrospun fiber diameter independently of the polymer used, and indicating that only the effect of the type of polymer on the diameter was significant.

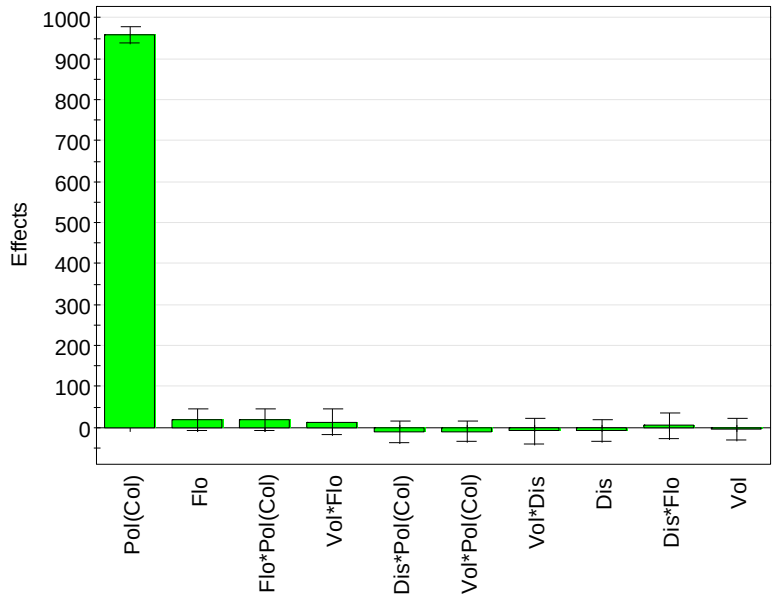

Figure 3.13: Analysis of operational parameters *(Voltage, Distance, Flow rate) and type of collector of nanofibers on the electrospun fiber diameter for gelatin solution in HIPF by multifactorial MODDE*

3.4. Conclusions

The effect of the main parameters that control the electrospinnability of protein solution (gelatin and collagen) at the usually used solvents was analyzed and the results allow obtaining a complete knowledge about the behavior of the process, including the obtained electrospun fibers diameters and solution electrospinnability.

The results obtained by the experimental designs evidence that although the effect of the operational parameters (voltage, flow rate and distance between needle and collector) has not a significant effect on the electrospun fiber independently of combination of polymer and solvent used in the range of this work, the behavior of process and electrospinnability of solutions can be different for each operational values combination. Thus, it was concluded that the protein (gelatin/collagen) polymer solutions (on HIPF and Acetic acid 25%) could be defined as a go/ no go system, which allows fabricating electrospun fibers with a given diameter for an operational parameter values capable for the electrospinnability. Also, the directly relationship between polymer concentration and electrospun gelatin fibers diameter was demonstrated, according to the literature, for the most benign solvent recently used to electrospun gelatin: aqueous acetic acid solution at low concentration (25% v/v).

Beside these, the study allows to determine the significance of other important parameters on the electrospun nanofibers fabricated to take into account on the electrospinning process as can be the solvent system, collector conductivity and

polymer type. On the one hand the use of the benign solvent formed by acetic acid/water mixture at 25% v/v allows fabricating electrospun gelatin fibers with a smaller diameter than the HIPF solvent, even used high polymer concentration, due the significant increase value of solvent conductivity. On the other hand it was demonstrated that a non-conductive layer onto the collector affects significant the fiber deposition and diameter, obtaining thicker and less compact fibers. Finally, the electrospun fibers obtained from collagen solution show a significant higher diameter than the obtained electrospun fibers from gelatin solutions at the same conditions, due to their different molecular weight.

3.5. References

[3.1] C.E. Ayres, B.S. Jha, S.A. Sell, G.L. Bowlin, D.G. Simpson, Nanotechnology in the design of soft tissue scaffolds: innovations in structure and function, Wiley Interdiscip Rev Nanomed Nanobiotechnol. 2 (2010) 20–34.

[3.2] R. Vasita, D.S. Katti, Nanofibers and their applications in tissue engineering., Int. J. Nanomedicine. 1 (2006) 15–30.

[3.3] L. a Smith, P.X. Ma, Nano-fibrous scaffolds for tissue engineering., Colloids Surf. B. Biointerfaces. 39 (2004) 125–31.

[3.4] N. Ashammakhi, a. Ndreu, Y. Yang, H. Ylikauppila, L. Nikkola, Nanofiber-based scaffolds for tissue engineering, Eur. J. Plast. Surg. 35 (2008) 135–149.

[3.5] M.R. Ladd, T.K. Hill, J.J. Yoo, S.J. Lee, Electrospun Nanofibers in Tissue Engineering, (2008).

[3.6] H. Liu, X. Ding, G. Zhou, P. Li, X. Wei, Y. Fan, Electrospinning of Nanofibers for Tissue Engineering Applications, J. Nanomater. 2013 (2013) 1–11.

[3.7] N. Bhardwaj, S.C. Kundu, Electrospinning: a fascinating fiber fabrication technique., Biotechnol. Adv. 28 (2010) 325–47.

[3.8] X.D.Z. Xian Tao Wen, Hong Song Fan, Yan Fei Tan, H.D. Cao, H. Li, B. Cai, Preparation of electrospun PLA nanofiber scaffold and the evaluation in vitro., Key Eng. Mater. 288-289 (2005) 139–142.

[3.9] A. Cipitria, A. Skelton, T.R. Dargaville, P.D. Dalton, D.W. Hutmacher, Design, fabrication and characterization of PCL electrospun scaffolds-a review, J. Mater. Chem. 21 (2011) 9419–9453.

[3.10] J.H.C. Hui Wang, Xiao Hong Qin, Study on Structures of electrospinning cellulose acetate nanofibers., Adv. Mat. Res. 175-176 (2011) 242–246.

[3.11] H. Homayoni, S.A.H. Ravandi, M. Valizadeh, Electrospinning of chitosan nanofibers: Processing optimization., Carbohydr. Polym. 77 (2009) 656–661.

[3.12] M. Li, M.J. Mondrinos, M.R. Gandhi, F.K. Ko, A.S. Weiss, P.I. Lelkes, Electrospun protein fibers as matrices for tissue engineering., Biomaterials. 26 (2005) 5999–6008.

[3.13] J.A. Matthews, G.E. Wnek, D.G. Simpson, G.L. Bowlin, Electrospinning of collagen nanofibers, Biomacromolecules. 3 (2002) 232–238.

[3.14] S.A. Sell, M.J. McClure, K. Garg, P.S. Wolfe, G.L. Bowlin, Electrospinning of collagen/biopolymers for regenerative medicine and cardiovascular tissue engineering., Adv. Drug Deliv. Rev. 61 (2009) 1007–19.

[3.15] Z.-M. Huang, Y.. Zhang, S. Ramakrishna, C.. Lim, Electrospinning and mechanical characterization of gelatin nanofibers, Polymer (Guildf). 45 (2004) 5361–5368.

[3.16] S. Panzavolta, M. Gioffrè, M.L. Focarete, C. Gualandi, L. Foroni, A. Bigi, Electrospun gelatin nanofibers: optimization of genipin cross-linking to preserve fiber morphology after exposure to water, Acta Biomater. 7 (2011) 1702–9.

[3.17] H.-W. Kim, J.-H. Song, H.-E. Kim, Nanofiber Generation of Gelatin-Hydroxyapatite Biomimetics for Guided Tissue Regeneration, Adv. Funct. Mater. 15 (2005) 1988–1994.

[3.18] Y. Zhang, H. Ouyang, C.T. Lim, S. Ramakrishna, Z.-M. Huang, Electrospinning of gelatin fibers and gelatin/PCL composite fibrous scaffolds., J. Biomed. Mater. Res. B. Appl. Biomater. 72 (2005) 156–65.

[3.19] Y.Z. Zhang, J. Venugopal, Z.-M. Huang, C.T. Lim, S. Ramakrishna, Crosslinking of the electrospun gelatin nanofibers., Polymer (Guildf). 47 (2006) 2911–2917.

[3.20] B. Su, J. Venugopal, S. Ramakrishna, Biomimetic and bioactive nano fi brous scaffolds from electrospun composite nanofibers, 1 (2007) 623–638.

[3.21] S.J. Kew, J.H. Gwynne, D. Enea, M. Abu-Rub, a Pandit, D. Zeugolis, et al., Regeneration and repair of tendon and ligament tissue using collagen fibre biomaterials., Acta Biomater. 7 (2011) 3237–47.

[3.22] B.S. Jha, C.E. Ayres, J.R. Bowman, T. a. Telemeco, S. a. Sell, G.L. Bowlin, et al., Electrospun Collagen: A Tissue Engineering Scaffold with Unique Functional Properties in a Wide Variety of Applications., J. Nanomater. 2011 (2011) 1–15.

[3.23] W. He, T. Yong, W.E. Teo, Z. Ma, S. Ramakrishna, Fabrication and endothelialization of collagen-blended biodegradable polymer nanofibers: potential vascular graft for blood vessel tissue engineering., Tissue Eng. 11 (2005) 1574–88.

[3.24] N. Choktaweesap, K. Arayanarakul, D. Aht-ong, C. Meechaisue, P. Supaphol, Electrospun Gelatin Fibers: Effect of Solvent System on Morphology and Fiber Diameters., Polym. J. 39 (2007) 622–631.

[3.25] S.-Y. Gu, Z.-M. Wang, J. Ren, C.-Y. Zhang, Electrospinning of gelatin and gelatin/poly(l-lactide) blend and its characteristics for wound dressing., Mater. Sci. Eng. C. 29 (2009) 1822–1828.

[3.26] J.-H. Song, H.-E. Kim, H.-W. Kim, Production of electrospun gelatin nanofiber by water-based co-solvent approach., J. Mater. Sci. Mater. Med. 19 (2008) 95–102.

[3.27] M. Erencia, F. Cano, J. a Tornero, J. Macanás, F. Carrillo, Resolving the electrospinnability zones and diameter prediction for the electrospinning of the gelatin/water/acetic Acid system., Langmuir. 30 (2014) 7198–205.

[3.28] Q.P. Pham, U. Sharma, A.G. Mikos, Electrospinning of polymeric nanofibers for tissue engineering applications: a review, Tissue Eng. 12 (2006) 1197–211.

[3.29] T. Subbiah, G.S. Bhat, R.W. Tock, S. Parameswaran, S.S. Ramkumar, Electrospinning of nanofibers, J. Appl. Polym. Sci. 96 (2005) 557–569.

[3.30] V. Pillay, C. Dott, Y.E. Choonara, C. Tyagi, L. Tomar, P. Kumar, et al., A Review of the Effect of Processing Variables on the Fabrication of Electrospun Nanofibers for Drug Delivery Applications., J. Nanomater. 2013 (2013) 1–22.

[3.31] M. Erencia, F. Cano, M.M. Tornero, Jose Antonio Fernandes, T. Tzanov, J. Macanás, F. Carrillo, Electrospinning of gelatin scaffolds with low acetic acid concentration effect of solvent composition on both diameter of nanofibers and cell viability, Summited. (2014).

[3.32] M.L. Ottone, M.B. Peirotti, J.A. Deiber, Rheokinetic model to characterize the maturation process of gelatin solutions under shear flow, Food Hydrocoll. 23 (2009) 1342–1350.

[3.33] A. Calleja, X. Granados, S. Ricart, J. Oró, J. Arbiol, N. Mestres, et al., High temperature transformation of electrospun BaZrO3 nanotubes into nanoparticle chains, CrystEngComm. 13 (2011) 7224.

[3.34] A.P.S. Immich, M.L. Arias, N. Carreras, R.L. Boemo, J.A. Tornero, Drug delivery systems using sandwich configurations of electrospun poly(lactic acid) nanofiber

membranes and ibuprofen, Mater. Sci. Eng. C. Mater. Biol. Appl. 33 (2013) 4002–8.

[3.35] S. Moon, R.J. Farris, Electrospinning of Heated Gelatin-Sodium Alginate-Water Solutions, Polym. Eng. Sci. 49 (2009) 1616–1620.

[3.36] K. Sisson, C. Zhang, M.C. Farach-Carson, D.B. Chase, J.F. Rabolt, Evaluation of cross-linking methods for electrospun gelatin on cell growth and viability., Biomacromolecules. 10 (2009) 1675–80.

[3.37] C.S. Ki, D.H. Baek, K.D. Gang, K.H. Lee, I.C. Um, Y.H. Park, Characterization of gelatin nanofiber prepared from gelatin–formic acid solution., Polymer (Guildf). 46 (2005) 5094–5102.

[3.38] M.M. Demir, I. Yilgor, E. Yilgor, B. Erman, Electrospinning of polyurethane ® bers, 43 (2002) 3303–3309.

[3.39] a. H. Hekmati, A. Rashidi, R. Ghazisaeidi, J.-Y. Drean, Effect of needle length, electrospinning distance, and solution concentration on morphological properties of polyamide-6 electrospun nanowebs, Text. Res. J. 83 (2013) 1452–1466.

[3.40] V. Beachley, X. Wen, Effect of electrospinning parameters on the nanofiber diameter and length, Mater Sci Eng C Mater Biol Appl. 29 (2009) 663–668.

[3.41] K. Gast, A. Siemer, D. Zirwer, G. Damaschun, Fluoroalcohol-induced structural changes of proteins: some aspects of cosolvent-protein interactions., Eur. Biophys. J. 30 (2001) 273–283.

[3.42] H. Lee, S. Ahn, H. Choi, D. Cho, G. Kim, Fabrication, characterization, and in vitro biological activities of melt-electrospun PLA micro/nanofibers for bone tissue regeneration, J. Mater. Chem. B. 1 (2013) 3670.

[3.43] J. Lannutti, D. Reneker, T. Ma, D. Tomasko, D. Farson, Electrospinning for tissue engineering scaffolds, Mater. Sci. Eng. C. 27 (2007) 504–509.

[3.44] D.I. Zeugolis, S.T. Khew, E.S.Y. Yew, A.K. Ekaputra, Y.W. Tong, L.-Y.L. Yung, et al., Electro-spinning of pure collagen nano-fibres - just an expensive way to make gelatin?, Biomaterials. 29 (2008) 2293–305.

[3.45] K. Nasouri, a. M. Shoushtari, a. Kaflou, Investigation of polyacrylonitrile electrospun nanofibres morphology as a function of polymer concentration,

viscosity and Berry number, Micro Nano Lett. 7 (2012) 423.

[3.46] P. Gupta, C. Elkins, T.E. Long, G.L. Wilkes, Electrospinning of linear homopolymers of poly(methyl methacrylate): exploring relationships between fiber formation, viscosity, molecular weight and concentration in a good solvent, Polymer (Guildf). 46 (2005) 4799–4810.

[3.47] X. Geng, O.-H. Kwon, J. Jang, Electrospinning of chitosan dissolved in concentrated acetic acid solution, Biomaterials. 26 (2005) 5427–32.

[3.48] Acetic Acid and its Derivatives - Google Libros, (n.d.).

[3.49] S.E. Kim, D.N. Heo, J.B. Lee, J.R. Kim, S.H. Park, S.H. Jeon, et al., Electrospun gelatin/polyurethane blended nanofibers for wound healing., Biomed. Mater. 4 (2009) 044106.

[3.50] N.M. Neves, Patterning of polymer nano fi ber meshes by electrospinning for biomedical applications, 2 (2007) 433–448.

[3.51] S. Ramakrishna, K. Fujihara, W.-E. Teo, T.-C. Lim, Z. Ma, An introduction to electrospinning and nanofibers., 2005.

[3.52] P. Kumar, Effect of collector on electrospinning to fabricate aligned nanofiber, 2012.

[3.53] L. Yang, C.F.C. Fitié, K.O. van der Werf, M.L. Bennink, P.J. Dijkstra, J. Feijen, Mechanical properties of single electrospun collagen type I fibers., Biomaterials. 29 (2008) 955–62.

[3.54] T.R. Keenan, Gelatin, in: Kirk-Othmer Encycl. Chem. Technol., 2003.

[3.55] O. Hartman, C. Zhang, E.L. Adams, M.C. Farach-Carson, N.J. Petrelli, B.D. Chase, et al., Microfabricated electrospun collagen membranes for 3-D cancer models and drug screening applications., Biomacromolecules. 10 (2009) 2019–32.

[3.56] N.S.F. Summer, U. Fellowship, S. Technologies, P. Tsing, P. Advisor, D.M. Elliott, Electrospinning natural polymers for tissue engineering applications., (n.d.) 1–15.

[3.57] D.. G.E.. Wnek, Polymer biomaterial constructs for regenerative medicine and functional biological systems., Case Western Reserve University, 2012.

[3.58] E. Boland, J. Matthews, K. Pawlowski, D. Simpson, G. Wnek, G. Bowlin, Electrospinning collagen and elastin: preliminary vascular tissue engineering., Front Biosci. 1 (2004) 10.

[3.59] S. a. Sell, P.S. Wolfe, K. Garg, J.M. McCool, I. a. Rodriguez, G.L. Bowlin, The Use of Natural Polymers in Tissue Engineering: A Focus on Electrospun Extracellular Matrix Analogues, Polymers (Basel). 2 (2010) 522–553.

[3.60] Z. Zhang, G. Li, B.I. Shi, Physicochemical properties of collagen, gelatin and collagen hydrosylate derived from bovine limed split wastes, J. Soc. Leather Technol. Chem. 90 (2006) 23.

[3.61] Z. Li, C. Wang, Effects of Working Parameters on Electrospinning, in: One-Dimensional Nanostructures, Springer Berlin Heidelberg, Berlin, Heidelberg, 2013: pp. 15–29.

[3.62] A. Koski, K. Yim, S. Shivkumar, Effect of molecular weight on fibrous PVA produced by electrospinning, Mater. Lett. 58 (2004) 493–497.

CHAPTER 4:

Electrospinning of gelatin fibers using solutions with low acetic acid concentration: effect of solvent composition on both diameter of electrospun fibers and cytotoxicity thereof

Electrospinning of gelatin fibers using solutions with low acetic acid concentration: effect of solvent composition on both diameter of electrospun fibers and cytotoxicity thereof

SUMMARY

Gelatin fibers were prepared by electrospinning of gelatin/acetic acid/water ternary mixtures with the aim of studying the feasibility of fabricating gelatin nanofiber mats at room temperature using an alternative benign solvent by significantly reducing the acetic acid concentration. The results showed that gelatin nanofibers can be optimally electrospun with low acetic acid concentration (25% v/v) combined with gelatin concentrations higher than 300 mg/ml. Both gelatin solutions and electrospun gelatin mats (prepared with different acetic acid aqueous solutions) were analyzed by FTIR and DSC techniques in order to determine the chemical and structure changes of the polymer. The electrospun gelatin mats fabricated from solutions with low acetic acid content showed some advantages as the maintenance of the decomposition temperature of the pure gelatin (~230ºC) and the reduction of the acid content on electrospun mats, which allowed to reach a cell viability upper than 90% (analyzed by cell viability test using human dermal fibroblast and embryonic kidney cells). This study has also analyzed the influence of gelatin and acetic acid concentration both on the solution viscosity and the electrospun fiber diameter, obtaining a clear relationship between these parameters.

Keywords: electrospinning, nanofibers, mat, cell viability, gelatin, acetic acid.

4.1. Introduction

In recent years, numerous reports in the field of tissue engineering have put the emphasis on the design and manufacturing of biocompatible and biodegradable supports with capacity of mimicking the structural and functional properties of extracellular matrices (ECM)[4.1-4.3]. For an optimal biocompatibility, scaffolds used for tissue engineering should possess special characteristics of degradation, porosity, microstructure, size, etc.[4.1, 4.3]. These characteristics highly depend on the fabrication method and, consequently, different techniques for the production of such scaffolds have been investigated and optimized (e.g. self-assembly, phase separation)[4.1-4.2, 4.4]. More recently, the electrospinning technique appeared as a versatile technique for manufacturing nanofibers and nanofibrous arrays with dimensions and scale similar to those of the native ECM[4.5-4.11], suitable for medical applications [4.12].

The electrospinning technique [4.11] allows the production of small diameter fibers (ranging from nanometers to micrometers) by applying a high voltage electrostatic field between a metal capillary syringe containing a polymer solution and a grounded collector where the fibers are deposited. During this process, as a result of solvent evaporation, electrospun fibers are deposited onto the collector in the form of nonwoven fibrous webs of high porosity. The properties of the obtained fibers depend on the operating conditions, e.g. flow rate, voltage, time, temperature and distance from the collector, as well as on the properties of the polymer solution, e.g. concentration, density, viscosity, conductivity, surface tension [4.7, 4.13].

Electrospinning can be applied to both synthetic [4.14-4.16] and natural polymers, including polysaccharides [4.17] and proteins, being collagen [4.18-4.19], silk fibroin [4.20] and gelatin [4.21] the most studied ones. Gelatin is known to have biocompatibility and biodegradability similar to collagen [4.22-4.23]. In fact, it is easily obtained by partial hydrolysis of collagen from animal tissues such as skin, muscle, and bone. Depending on the hydrolysis method, two different types of gelatin are produced: type A gelatin (acid process), type B (alkaline process). Both gelatins differ mainly in their amino acid composition, polypeptides pattern, bloom strength, turbidity and foaming properties [4.24-4.25].

From a technical point of view, the most important parameter influencing the electrospinning manufacturing process of gelatin nanofibers is the solvent selection [4.26] because, although gelatin is soluble in warm water, the electrospinning cannot be done at room temperature due to the gelation process that occurs between gelatin and water, which increase the solution viscosity avoiding the flow of aqueous gelatin solutions into the syringe [4.27].

With the aim of avoiding the gelation process and allow the electrospinnability of gelatin solutions, some complex solvent such as 1,1,1,3,3,3-hexafluoro-2-propanol (HIPF) or 2,2,2-trifluoroethanol (TFE) have been proposed for the fabrication of scaffolds made of natural polymer such as collagen [4.21, 4.28-4.32]. However, due to their highly corrosive nature, these solvents may affect the original protein structure [4.11, 4.33-4.34] besides providing a potential cytotoxicity to the obtained scaffolds, since the presence of small amounts of residual solvent embedded on the electrospun fibers is almost unavoidable [4.35-4.36]. This fact, combined with the high cost of these solvents, promoted the search of alternative systems to electrospin gelatin such as: i) the use of gelatin aqueous solution at high temperatures [4.37-4.38], ii) blending gelatin with another biopolymer (e.g. sodium alginate [4.38], poly(ethylene oxide), poly(e-caprolactone)) [4.11], PLA [4.39], iii) using solvent mixtures (acetic and ethyl acetate [4.40], and iiii) and using of carboxylic acid (formic acid [4.22, 4.41] or acetic acid [4.26, 4.39-4.43].

Among these alternatives, the use of aqueous solutions of carboxylic acids has been postulated recently as a preferable option to dissolve and electrospin gelatin at room temperature. The use of these acids implies a clear advantage over HIPF and TFE solvents due to their lower cytotoxicity and their simplicity of processing compared to other alternatives. However, the concentrations of acid proposed up to now to electrospin gelatin are quite high (minimum of 60% v/v), inducing the partial decomposition of gelatin and adversely affecting the structural integrity of the nanofibers [4.22].

This study analyzes the feasibility to electrospin nanofiber mats of gelatin at room temperature using an acetic acid based solvent characterized by a low concentration of acid. The effect of the acidity of the solvent on both the gelatin structure and the cytotoxicity of the final mat were tested. Finally, the relationship between reagents concentration, solution viscosity and fiber diameter was studied given that the diameter of the fibers is a crucial parameter for instance, to mimic the size of the fibers composing the extracellular matrix of connective tissue.

4.2. Experimental

4.2.1. Materials

Gelatin powder from bovine skin (type B with bloom ~225 g) was purchased from Sigma Aldrich (Spain) and used without further treatment or purification. Glacial acetic acid (99.99%, Panreac, Spain) and bi-distilled water were used as solvents. Solutions of gelatin with concentrations 200, 250, 300, 350, 400 mg/ml (kg/m^3) were prepared using acetic acid or mixtures of acid-water (25%, 50%, 75% v/v of acetic acid) as solvents. Gelatin was dissolved at room temperature (23 ºC) by stirring for 1 hour.

4.2.2. Electrospinning process

Electrospinning was performed in a home-engineered device [4.44-4.45]. Each gelatin solution was loaded into a 2.5 ml syringe with a stainless steel syringe needle (0.6 mm inner diameter) connected as an anode to a high voltage power supply. About 6-10 cm below the needle, a flat copper collector (connected as a cathode to the power supply) was placed to receive the electrospun fibers. The flow rate was controlled by a pump, and set between 1-1.5 ml/h, depending on the solution requirements. The applied voltage was in the range of 15-18 kV and all solutions were electrospun at room temperature (23 ºC).

Electrospun mats were not chemically cross-linked for mechanical stabilization to avoid interferences during their chemical and structural characterization.

4.2.3. Viscosity measurements

The viscosity of the different solutions was determined using a viscometer (Brookfield DV-II +, USA). After mixing for 1 h, samples were stored for different times (0 h, 1 h, 3 h, 24 h) before the measure of viscosity, in order to follow the gelation process. Each solution viscosity was measured three times and results shown a standard deviation below 2%.

4.2.4. Electrospun fibers characterization

The diameter and distribution of the electrospun gelatin fibers were directly examined by Scanning Electron Microscopy (SEM) (Phenom Standard, Phenom-World, Netherlands) without any metal coating. The obtained images were processed by image analyzing software (Photoshop CS6, Adobe, Ireland) so as to determine the average diameter and its standard deviation. Typically, 50 arbitrary fibers were measured.

Besides, both chemical structure and conformation of as-made fibers were analyzed by Fourier Transform Infrared Spectroscopy (FTIR) by using a Nicolet Avatar 320 spectrophotometer (Nicolet Instrument Corporation, USA). Samples were prepared by mixing 1 mg of fiber mat in a matrix of 300 mg of KBr followed by pressing (167 MPa). The spectrum was recorded in the range of 400 to 4000 cm^{-1} and averaging 32 scans at a resolution of 4 cm^{-1}.

Finally, the thermal properties of gelatin electrospun fibers were analyzed by Differential Scanning Calorimetry (DSC) by using a Perkin Elmer DSC7. During DSC measurements, a sample (about 4 mg) was heated from 50ºC to 300ºC at a heating rate 20ºC/min under a constant flow of a nitrogen atmosphere of 50 ml/min

4.2.5. Cytotoxicity evaluation

4.2.5.1. Cell culture

To determine the potential toxicity of the mats of gelatin fibers obtained from solutions with different acetic acid content, human foreskin fibroblasts (BJ-5ta) and Human Embryonic Kidney cells (HEK 293T) were used. Cells were maintained in 4 parts of Dulbecco's Modified Eagle's Medium (DMEM) containing 4 mM L-glutamine, 4500 mg/l glucose, 1500 mg/l sodium bicarbonate, 1 mM sodium pyruvate and 1 part of Medium 199, supplemented with 10 % (v/v) of fetal bovine serum (FBS), and 10 g/ml Hygromycin B at 37 ºC, in a humidified atmosphere with 5 % CO_2, according to the recommendations of the manufacturer. The culture medium was replaced every 2 days. At pre-confluence, cells were harvested using trypsin-EDTA (ATCC-30-2101) 0.25 % (w/v) trypsin/0.53 mM EDTA solution in Hank's BSS without calcium or magnesium. Both BJ-5ta (ATCC-CRL-4001) and DMEM (ATCC-30-2002) were purchased from American Type Culture Collection (LGC Standards S.L.U., Spain) whereas HEK 293T was purchased from the European Collection of Cell Culture.

4.2.5.2. Alamar Blue assay

Cells were seeded at a density of 4.5 x 10^4 cells/well on 96-well tissue culture-treated polystyrene plate (Nunc, Thermo Scientific, USA) the day before experiments. Then, they were exposed by indirect contact to the electrospun gelatin fibers, previously dissolved on medium (20 mg/mL in DMEM), at a final volume of 100 µL and incubated at 37 ºC in a humidified atmosphere with 5 % CO_2. Cells were examined for signs of toxicity, using Alamar Blue assay.

Resazurin, the active ingredient of AlamarBlue® reagent (Invitrogen, Life Technologies Corporation, Spain), is a non-toxic, cell-permeable compound that is blue in color and it can be reduced to resorufin by viable cells, developing a red color compound. After 24 h contact with cells, the solution of dissolved fiber mats was removed, the cells washed twice with PBS and stained with AlamarBlue® reagent. 100 µL of 10% (v/v) AlamarBlue® reagent in DMEM was added to the cells and incubated for 4 h at 37 ºC, after which the absorbance at 570 nm was measured, using 600 nm as a reference wavelength, in a microplate reader (Infinite M 200 plate reader, Tecan, USA). The quantity of resorufin formed is directly proportional to the number of viable cells. BJ5ta cells relative viability (%) was determined for each concentration of acetic acid and compared with that of cells incubated only with cell culture medium (negative control, C-) whereas H_2O_2 500 µM was used as a positive control (C+) of cell death. All tests were performed in triplicate.

4.2.5.3. Cells morphology

Morphological changes in cells were also followed by phase contrast microscopy using an Eclipse Ti-S microscope (Nikon Instruments Inc., Netherlands), after 24 h of contact with gelatin scaffolds.

4.3. Results and discussion

4.3.1. Viscosity of solutions

Regarding the electrospinning process, besides some technical parameters such as voltage, distance and flow rate, there are several other important parameters that influence the electrospinnability of solutions such as surface tension, conductivity, viscosity and molecular weight [4.11]. For instance, surface tension determines the upper and lower boundaries of electrospinning window if all other variables are held constant [4.46]. Previous studies concluded that the increase of an acid concentration provokes a surface tension decrease [4.40] that benefits the electrospinnability, normally impeded by high surface tensions.

In his case, to study the effect of viscosity on the electrospinnability, firstly, the viscosity changes over the storage time were analyzed for several gelatin solutions prepared with different solvent mixtures (25 - 100% v/v acetic acid). As shown in **Figure 4.1**, the viscosities of those solutions prepared with aqueous acetic acid at 50% and 75% and pure acetic acid (100%) vary depending on gelatin concentration (200 - 400 mg/ml) but they were very stable with time since no significant variation could be observed up to 24 h after mixing (the maximum increment of 15% was attained for the highest gelatin concentration solution,

400mg/ml, in 100% acetic acid), contrarily that occurs for pure formic acid system, where the viscosity of gelatin decreases after 5 hours of storage time [4.22]. In contrast, for the gelatin solutions containing 25% acetic acid, the viscosity clearly increased with time being the most important increment observed for the most concentrated solution in terms of gelatin content (about a 300% of increment). These changes of viscosity make sense taking into account the gelation phenomenon that gelatin undergoes in the presence of a high amount of water [4.47], which is well known that increases the helix formation in gelatin, and consequently the solution viscosity, proportionally to the gelatin concentration in solution [4.48]..

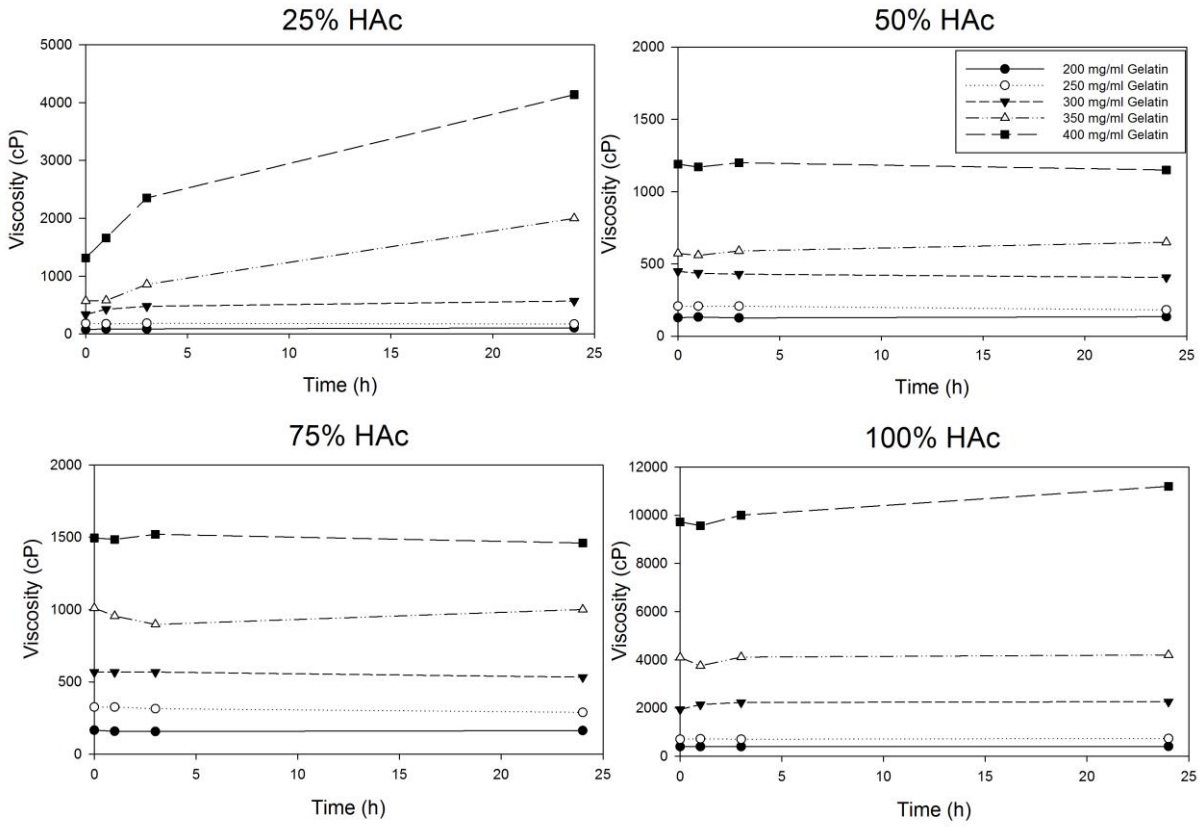

Figure 4.1: Viscosity changes with storage time for solutions of different gelatin and acetic concentration. All viscosity values have a standard deviation below 2%

From a practical point of view, these results suggest that performing the electrospinning at time zero (immediately after dissolving gelatin) is preferable in order to avoid any gelation process. The corresponding viscosities are summarized in **Table 4.1**. It is noteworthy to mention that the viscosity values obtained for the pure acetic acid solutions were in close agreement to those reported previously by

Choktaweesap et al. for gelatin solutions with concentrations in the range of 20 - 30% (200 - 300 mg/ml) [4.26].

Table 4.1: Viscosity (cP) of the gelatin solutions at time 0 h as a function of gelatin concentration and acetic acid concentration. All viscosity values have a standard deviation below 2%

		[Acetic acid] (% v/v)			
		100	**50**	**75**	**25**
[Gelatin] (mg/ml)	**200**	395	166	128	77
	250	704	325	208	183
	300	1940	567	448	338
	350	4100	1010	573	574
	400	9725	1495	1190	1317

4.3.2. Electrospinnability of gelatin solutions

The electrospinnability of gelatin solutions was examined by analyzing the morphology of electrospun fibers by SEM. Obtained results (**Figure 4.2**) confirmed the feasibility of electrospinning gelatin solutions with high acetic acid concentration combined with low gelatin concentration, previously reported by other authors [4.39, 4.42]. In this case the high acetic acid content promotes the interaction of gelatin with acetic inducing an increase of the viscosity of the solution, since the viscosity increases as the pH decreases [4.49], reaching the value of viscosity necessary for electrospinning. What is more relevant, electrospun fibers can also be obtained for aqueous solutions with low acetic acid concentrations (25% v/v) combined with high gelatin concentrations (>300 mg/ml). In this latter case, the concentration of gelatin is high enough to induce the necessary viscosity and polymer chain entanglement for adequate electrospinning. At the same time, the acetic acid content is high enough to provide electrical conductivity and, most important, to dissolve gelatin avoiding gelation (note that gelation occurs for gelatin in pure water and it absolutely impedes electrospinning).

On the contrary, other combinations were not suitable for electrospinning since they produced either very thick fibers (high acetic acid concentration and high gelatin concentration: images 2i, 2m, 2q and 2r) or did not produce fibers at all (low acetic acid concentration and low gelatin concentration: images 2c, 2d and 2h). In the first case the

viscosity of the solution is very high due to the high amount of gelatin and the acetic acid is only able to partially solvate it, just allowing the electrospinning of very thick fibers or microfibers [4.43]. In the second case the solutions did not reach the necessary viscosity and polymer chain entanglement to be electrospun. The characterization of some solutions (Figures 2b and 2g), which were partially able to produce nanofibers, also revealed the existence of beads, either as discrete beads or as beaded fibers due to fibers fusion at touching points. Similar behavior has been previously reported for gelatin solutions with a concentration between 200 mg/ml and 300 mg/ml using pure acetic acid as a solvent [4.26].

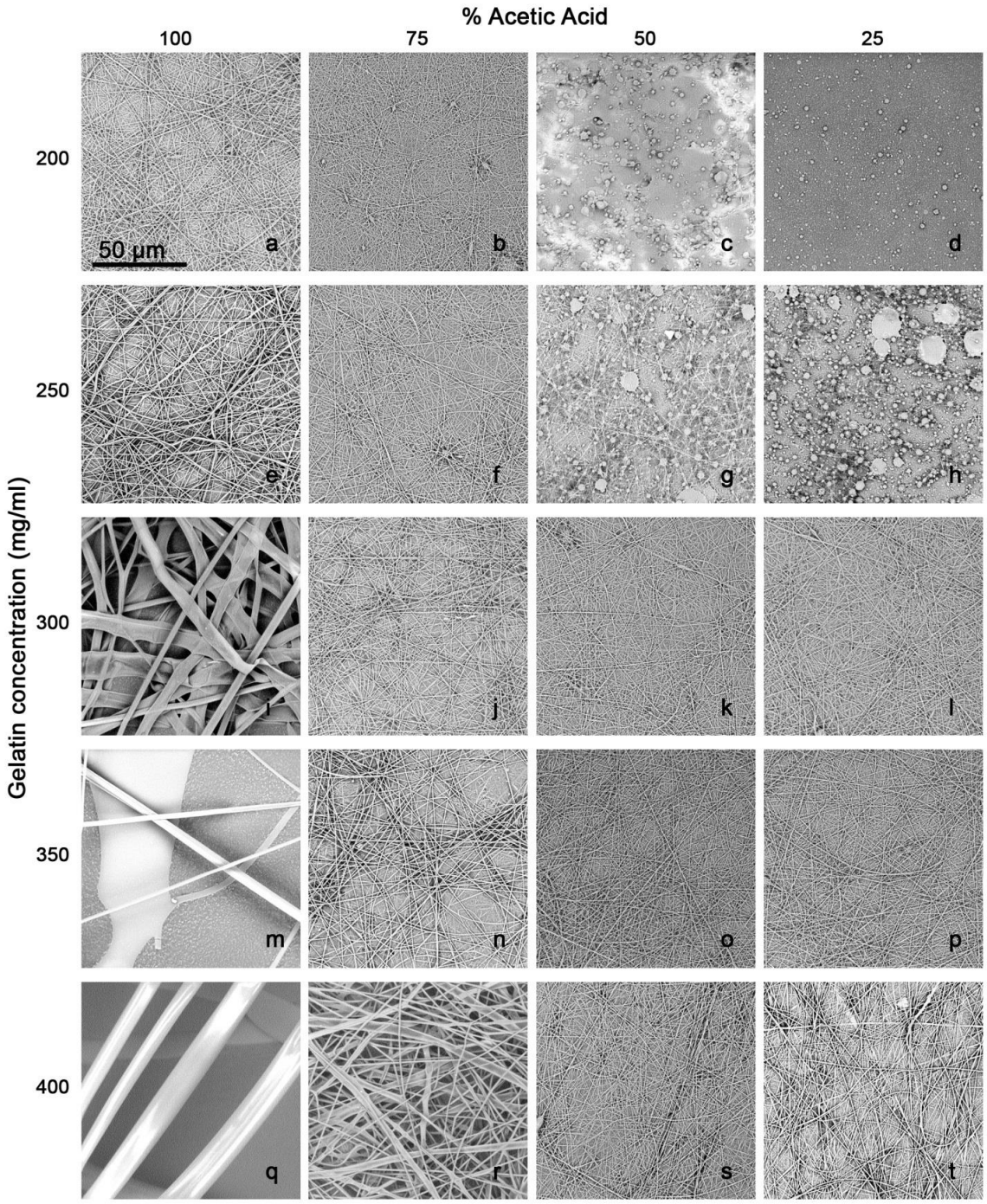

***Figure 4.2**: SEM images of electrospun gelatin fibers as a function of Acetic Acid percentage (100, 75, 50 and 25, arranged in columns) and Gelatin concentration in mg/ml (200, 250, 300, 350 and 400, arranged in rows). For instance, image (f) corresponds to fibers fabricated with 75% Acetic Acid and 250 mg/ml of Gelatin. The scale bar shown in microphotography (a) is valid for all the images*

4.3.2.1. Effect of gelatin concentration

It is obvious from the results that the gelatin concentration directly affects the viscosity of the mixture (**Table 4.1**), according with the literature [4.22, 4.26, 4.50]. The viscosity increased at higher gelatin content in the solution. The viscosity increased along with the gelatin content due to the high chain entanglement between the polymer chains induced by the increase of the polymer concentration. For homogeneous solutions of a linear polymer, the well-known Huggins equation describes this dependence of the solution viscosity with the concentration [4.51].

$$\frac{\eta_{sp}}{c} = [\eta] + K_H[\eta]^2 c \qquad \text{(Eq 4.1)}$$

where η_{sp} is the specific viscosity of the polymer solution, [η] is the intrinsic viscosity and K_H is the Huggins constant.

For practical purposes, it is important to obtain an optimum viscosity, neither too low so that the fibers cannot be formed (avoiding electrospray and beads-on-string structures) nor so high as to avoid stretching of the solution due to its high molecular weight (solution gelation hinders electrospinning). After having seen how the viscosity influence the electrospinnability of the gelatin fibers, it appears that the fabrication of gelatin electrospun fibers with a reproducible pattern was constrained to an operational window of viscosity in the range 200-1500 cP (mPa·s) which should coincide with suitable surface tension values as suggested by Geng et al [4.46].

In fact, most studies [4.22, 4.40] recommend to work with low gelatin concentration (lower than 120 mg/ml) at room temperature to avoid the gelation process and to facilitate the electrospinning. Our results showed that the viscosity of gelatin solution strongly depends on the percentage of acetic acid and it is possible and sometimes necessary, to work with high gelatin concentration at which gelation virtually does not occur.

The effect of gelatin concentration on the diameter of the electrospun fibers was further studied (Figure 4.3). The tendency to increase the viscosity of the solution and consequently the diameter of the obtained fibers was maintained, disregarding the exact content of acetic acid in solution. It is therefore concluded that the diameter of the fibers is directly related to the viscosity of the spinning solution used, as it has previously observed for different polymer/solvent systems [4.40, 4.52-4.53].

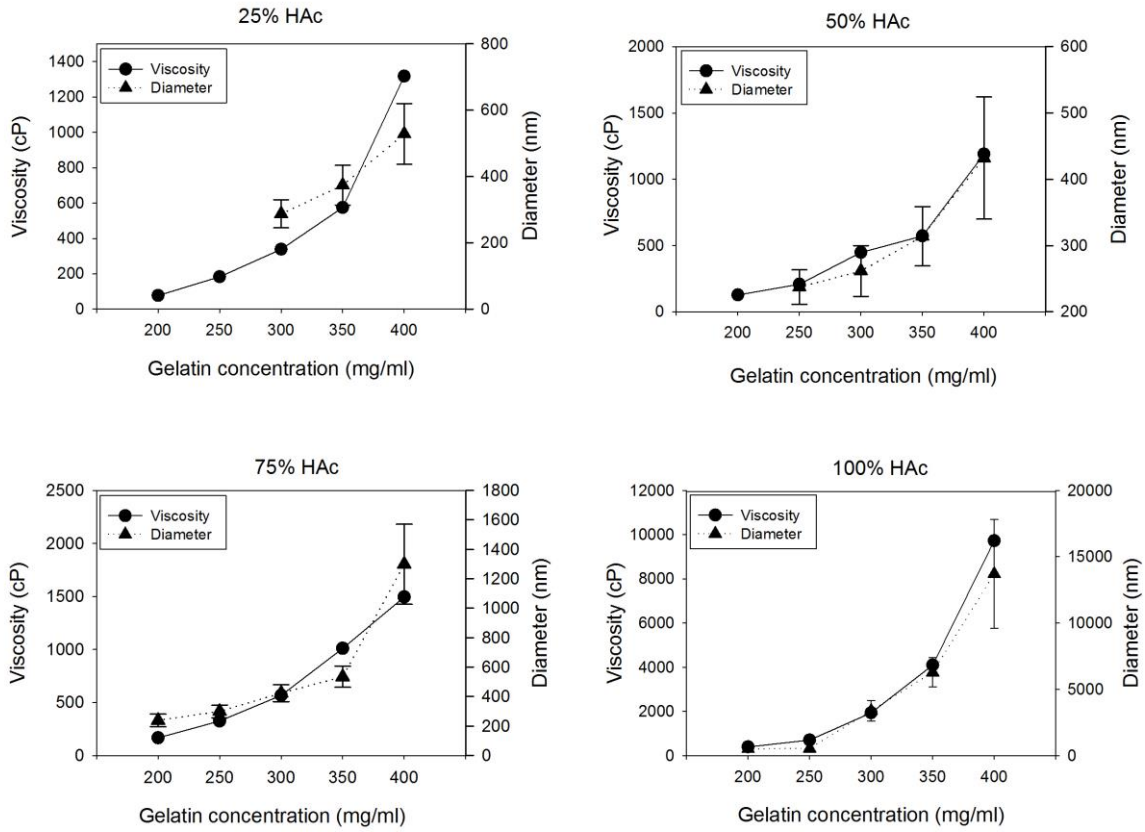

Figure 4.3: *Evolution of the viscosity of solution and the diameter of electrospun fibers obtained for each gelatin concentration. All viscosity values have a standard deviation below 2%. Electrospray was obtained at 200 and 250 mg/ml for 25% acetic acid solution and for this reason the diameter were not measured*

4.3.2.2. Effect of acetic acid concentration

It is well known that the presence of acetic acid influences the surface tension of solutions in a way that the surface tension could be reduced by increasing acetic acid concentration [4.22]. In this sense, one may expect that viscosity is also affected in a similar way but it is necessary to establish the exact relationship between both parameters, which concern electrospinnability.

Taking into account the experimental findings, at low concentrations of gelatin the acetic acid content did not affect significantly the viscosity. Accordingly, in these cases the electrospinning process is dominated by the surface tension. High surface tension (low acetic concentration) caused the formation of beads, in concordance with the behavior reported for

many different solution systems [4.46, 4.54-4.55] (see Figure 4.2 for solutions containing 25 and 50% v/v acetic acid combined with low concentration of gelatin, i.e. 200 or 250 mg/ml).

Conversely, increasing the gelatin concentration the effect of acetic acid concentration on viscosity is more noticeable and viscosity is the key parameter that controls electrospinnability, allowing solutions with low acetic acid concentration to spin. Yet, when viscosity was 1500 cP or higher, large diameter fibers with flawed distribution were obtained (see Figure 4.2 for solutions with 350 and 400 mg/ml gelatin and high concentration of acetic acid).

It is also important to note that the acetic acid content influences, in turn, the water content and thus, the gelling process. Performing the electrospinning immediately after dissolving the gelatin would avoid the spontaneous increase of viscosity, especially for solutions with high content of water (25 % acetic acid).

Similarly to the gelatin concentration, the effect of the acetic concentration was directly correlated to the fiber diameter (**Figure 4.4**), which had been previously observed for gelatin in other solvent systems [4.39-4.40]. Parallel to what happened with the viscosity trend, the diameter of the obtained electrospun fibers also follows a clear trend and this effect was observed independently of the gelatin concentration, thereby confirming the direct correlation between diameter of the fibers and the viscosity of the spinning solution.

Moreover, the influence of both working parameters (gelatin and acetic acid concentrations) on the viscosity of the spinning solution was statistically analyzed (software package Statgraphics Centurion XV, StatPoint, Inc., USA). The results from an ANOVA test with 95% of uncertainty (Table 4.2) determined that not only both parameters rule the solution viscosity (and, consequently, the diameter of electrospun fibers) but their interaction is also significant ($p = 0.0000 < 0.05$).

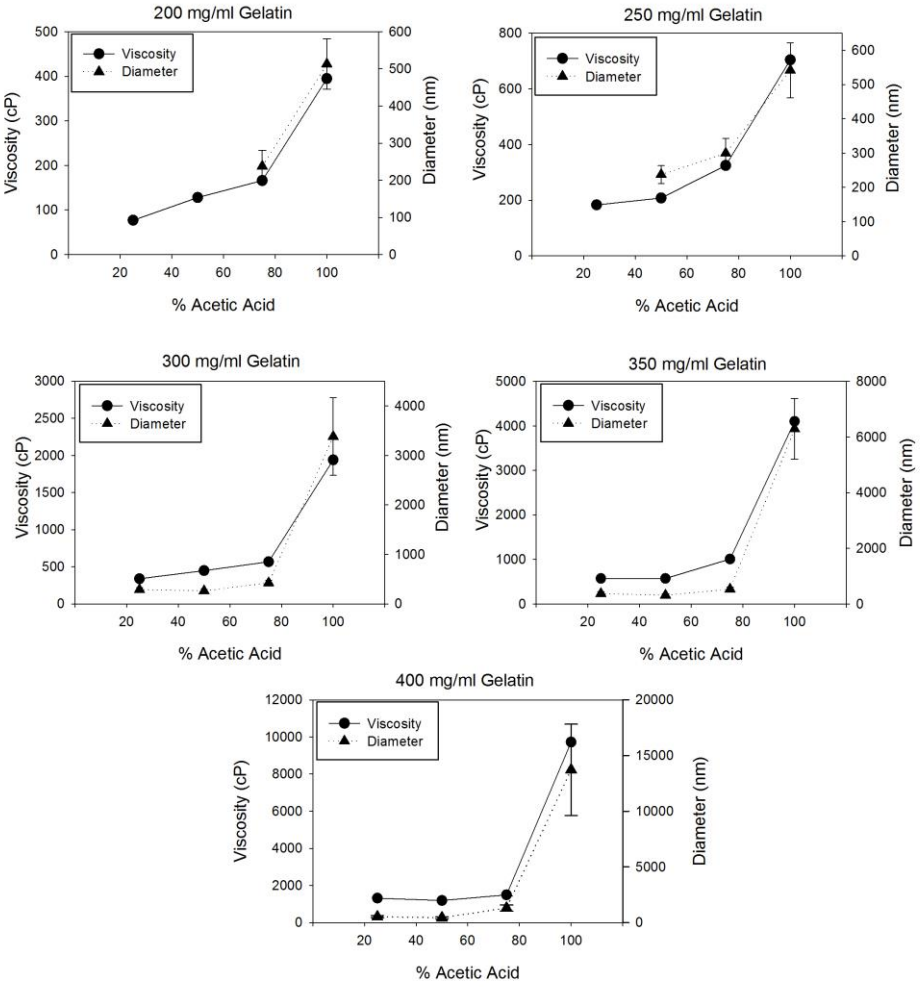

Figure 4.4: *Viscosity of solutions and diameter of electrospun fibers as a function of the acetic acid concentration. All viscosity values have a standard deviation below 2%*

***Table 4.2**: Analysis of gelatin concentration and acid acetic concentration effect on the viscosity of the spinning solution by multifactorial ANOVA*

Source of variance	Sum of Squares	Degrees of freedom	Mean square	F	F Critical (p=0.05)
[Acetic acid] (% v/v) (A)	$8.27 \cdot 10^7$	3	$2.91 \cdot 10^7$	1356.36	0.0000
[Gelatin] (mg/ml) (B)	$8.94 \cdot 10^7$	4	$2.23 \cdot 10^7$	1042.27	0.0000
A-B Interaction	$9.81 \cdot 10^7$	12	$8.18 \cdot 10^6$	381.35	0.0000
Error	857502	40	21437.5		
Total	$2.76 \cdot 10^8$	59			

4.3.3. Electrospun fibers characterization

4.3.3.1. FTIR

Samples prepared with a fixed gelatin concentration were analyzed by FTIR to determine the effect of acetic acid concentration on the chemical structure of the dissolved gelatin and of the electrospun fibers. Taking into account that a higher concentration of gelatin results in a high effect of the acetic acid on the solution properties [4.43] it was decided to use the highest gelatin concentration (400 mg/ml) to maximize and improve the characterization of the structural changes in solution state. However, for the characterization of electrospun gelatin mats, a concentration of 300 mg/ml was chosen due to the better electrospinnability of the dope solutions.

The characteristic gelatin IR bands are: amide I, II and III. Amide I (1650 cm^{-1}) is related to C=O stretching vibration coupled with the C-N stretch, amide II (1540 cm^{-1}) arises from out-of-phase combination of C-N stretch and in-plane N-H deformation modes, and amide III (1234 cm^{-1}) reveals the combination peaks between C-N stretching vibrations and N-H deformation from amide linkages as well as absorptions arising from wagging vibrations from CH_2 groups from close amino acid residues [4.56]. On the other hand, the typical bands for glacial acetic acid are 1706 cm^{-1} (C=O stretching), 1271 cm^{-1} (C-O stretching), 1388 cm^{-1} (CH_2 scissors deformation) and, finally, 3020 cm^{-1} and 2645 cm^{-1} (C-H asymmetric stretching) [4.57].

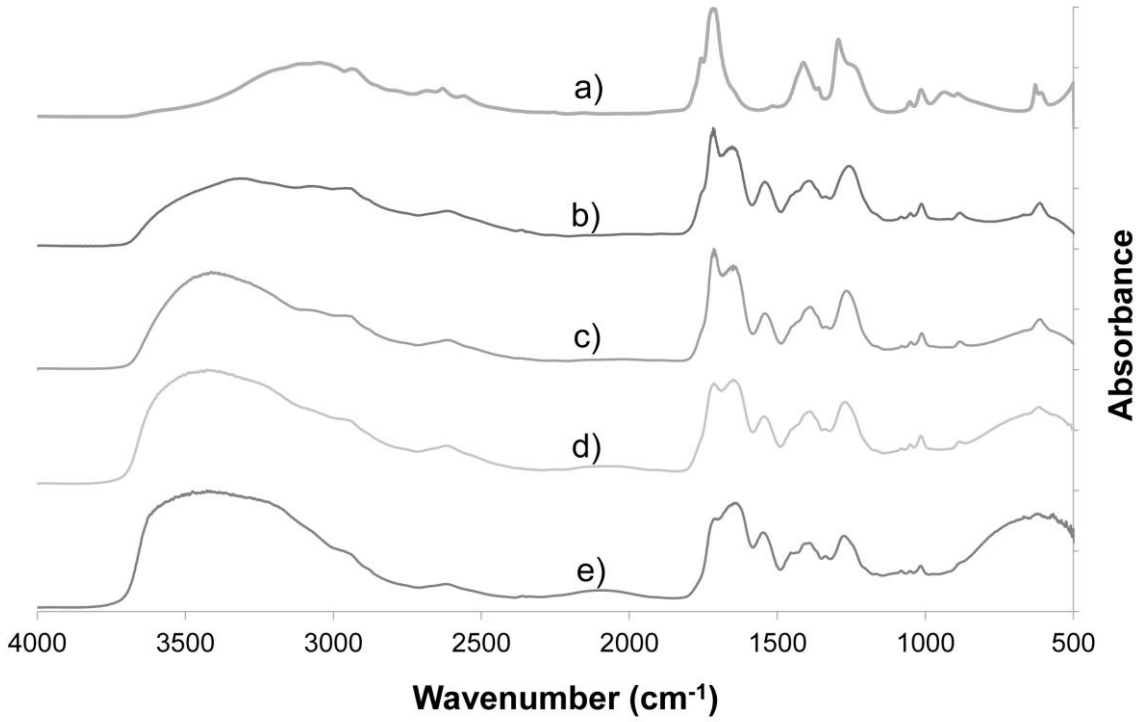

***Figure 4.5**: FTIR spectra of gelatin solutions (400 mg/ml) at different acetic acid concentration (% v/v); a) glacial acetic acid b) 100% c) 75% d) 50% e) 25%*

Figure 4.5 shows the FTIR spectra of gelatin solutions prepared using solvents with different acetic acid concentration and pure acetic acid. It was observed that the IR spectra of the four samples prepared with solutions of increasing concentrations of acetic acid (25% (Figure 4.5e), 50% (Figure 4.5d), 75% (Figure 4.5c) and 100% (Figure 4.5b)) are an overlapping of the characteristic spectral bands of both gelatin and acetic acid. Additionally, the relative intensity of the characteristic peaks of acetic acid (1706 cm^{-1} and 1271 cm^{-1}, Figure 4.5a) increased proportionally when increasing the acetic acid content of the electrospinning solutions. Accordingly, the relative absorption peak was minimum for the solution prepared with 25% of acetic acid as solvent (Figure 4.5e) while the maximum was observed for those solutions prepared with pure acetic acid (Figure 4.5b)**.**

On the other hand, none of the characteristic peaks of the acetic acid were detected in the FTIR spectra of the electrospun fibers specimens prepared by electrospinning of the abovementioned solution (**Figure 4.6**), except in the spectra of gelatin electrospun mats fabricated with 100% v/v acetic acid as solvent, where a slight change in shape of Amide I, suggesting the appearance of a new peak about 1702 cm^{-1}, related with the presence of residual acid. Despite this, the results corroborate the difficulty to detect the remaining acetic

acid in the electrospun fibers by FTIR. Yet, FTIR might not be accurate enough to confirm the latter conclusion, as it was suggested by Chang et al. [4.22] and, therefore, we carried out a DSC analysis to check whether the chemical structure of gelatin was affected by acetic acid in solution.

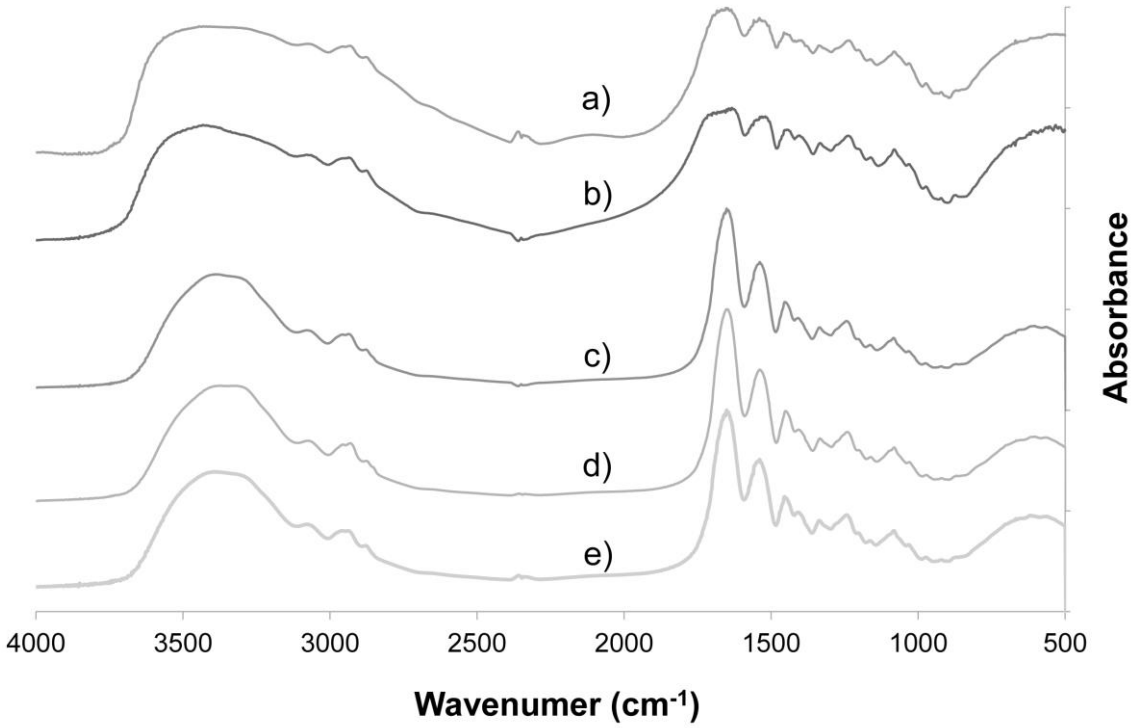

***Figure 4.6**: FTIR spectra of electrospun gelatin fibers obtained from solutions containing 300 mg/ml of gelatin and different acid acetic concentration (% v/v); a) powder gelatin b) 100% c) 75% d) 50% e) 25%*

4.3.3.2. DSC

DSC thermograms of electrospun fibers prepared with solutions containing 25, 50, 75 and 100 % v/v acetic acid and 300 mg/ml gelatin are plotted in **Figure 4.7**, together with the data corresponding to pure powder gelatin. The peak found about 230 ºC for pure gelatin (Figure 4.7a) agree with the reported value for gelatin decomposition [4.22, 4.40-4.41]. This peak was also found (although slightly shifted) for the nanofiber mats prepared with the lowest acetic acid concentration (25%, Figure 4.7b)). Oppositely, in the other solutions (50%, Figure 4.7c; 75%, Figure 4.7d; 100% Figure 4.7e) this peak was not detected, and a wider and shorter peak appeared offset to 200 °C (more deflected at higher acetic acid content). These changes suggest an increase in the amorphous part of the gelatin structure, i.e a decrease in its crystallinity. On the one hand it could be simply explained by the nanoscopic size of fibers,

but according with the literature [4.22], the changes are attributed to alterations of the random coil conformations of the protein.

Thus, despite FTIR spectra did not show many differences for the electrospun fiber mats prepared with different acetic acid concentrations, the chemical structure of gelatin was certainly altered, resulting in lower protein stability, as the DSC results show. Accordingly, it seems necessary to reduce the acid concentration as much as possible in order to produce nanofibers more analogous to the pristine gelatin.

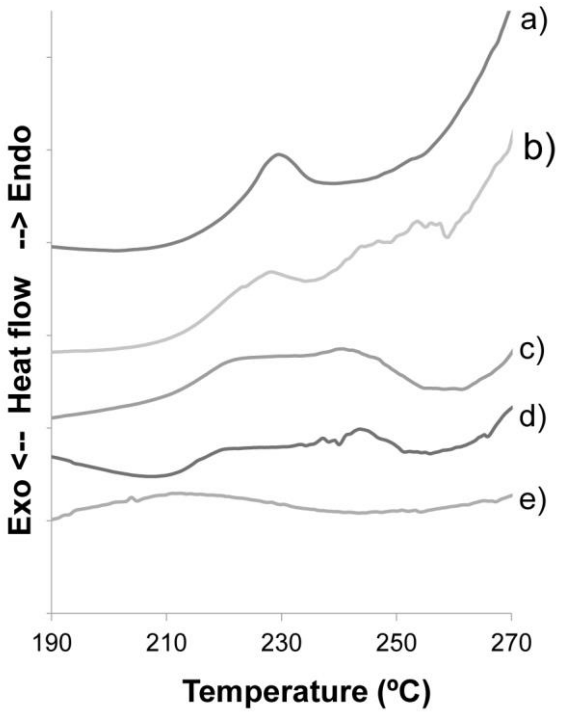

Figure 4.7: DSC of electrospun fibers obtained for solutions containing 300 mg/ml gelatin and different acetic acid concentrations (% v/v): b) 25 % c) 50 % d) 75 % e) 100 %. Data in a) correspond to powder gelatin

4.3.4. Cytotoxicity evaluation

The culture medium used to dissolve the mats of electrospun gelatin fibers contains Phenol Red, a pH indicator frequently used in cell biology that allows for detecting any chemical or microbiological contamination in the medium, which could affect the cells, basing on the color changes. This indicator spans the pH range from 6.8 (yellow) to 8.4 (purple) [4.58] and is useful to detect any possible trace amounts of acetic acid in fiber mats (**Figure 4.8**).

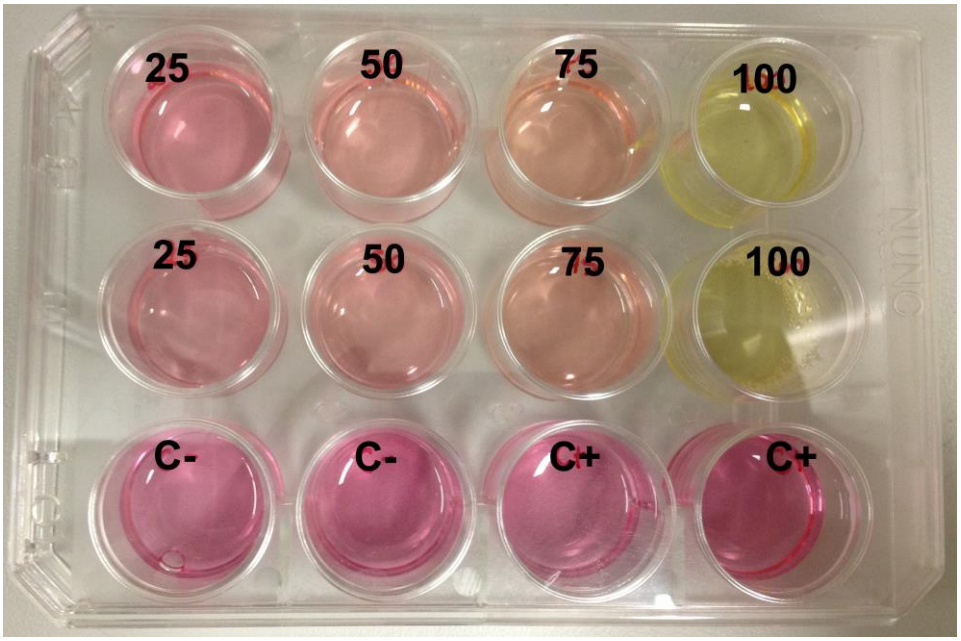

***Figure 4.8**: Color changes in culture medium after dissolving the mats of electrospun fibers produced by different acetic acid content solution (25, 50, 75 and 100%). C+ and C- are samples without any electrospun mats dissolved, showing the original color of culture medium, which will used to evaluate the positive and negative control, respectively*

The pH of the cell medium affects the proliferation of skin cells, being the optimal range of pH between 7.2 and 8.3 [4.59]. In this case, the color changes in the medium after exposure to electrospun gelatin fibers fabricated from different acid content solutions were obvious. For the control samples (without gelatin fibers) the color of the medium was pink/purple (4 well below in **Figure 4.8**), indicating a pH around 7.8 based on the Phenol Red scale, where the proliferation is optimal. Increasing the acetic acid content, the color of medium turned gradually from red (for 25% sample with pH 7.6) to yellow for 100% acetic acid sample (pH 6), passing through orange for intermediate acid content (50 and 75%) (pH between 7.2 and 7.6). These results confirmed the presence of residual acetic acid in the electrospun gelatin fibers in direct proportion to the acid content in the spinning solution. These observations constituted a preliminary assessment of the toxicity of the developed materials towards the cells.

4.3.4.1. Alamar Blue assay

To assess the influence of residual acetic acid content in the fibers on the cell viability the Alamar Blue assay was performed on two different types of cells - fibroblasts and HEK (**Figure 4.9**). The found trend was similar for both cell types: a high cell viability for mats

obtained from gelatin solutions with 25% acetic acid content, a slight decrease of cell viability for samples made of 50 and 75% of acetic acid, and a dramatically decrease for a those mats electrospun from solutions of 100 % acetic acid. The confirmed cytotoxicity of the traces of acetic acid contained in gelatin electrospun fibers reinforces the importance of using minimum acetic acid concentration in the future for the electrospinning of gelatin solutions in order to obtain gelatin nanofibers suitable as scaffolds for tissue engineering (i.e. cell viability higher than 90%).

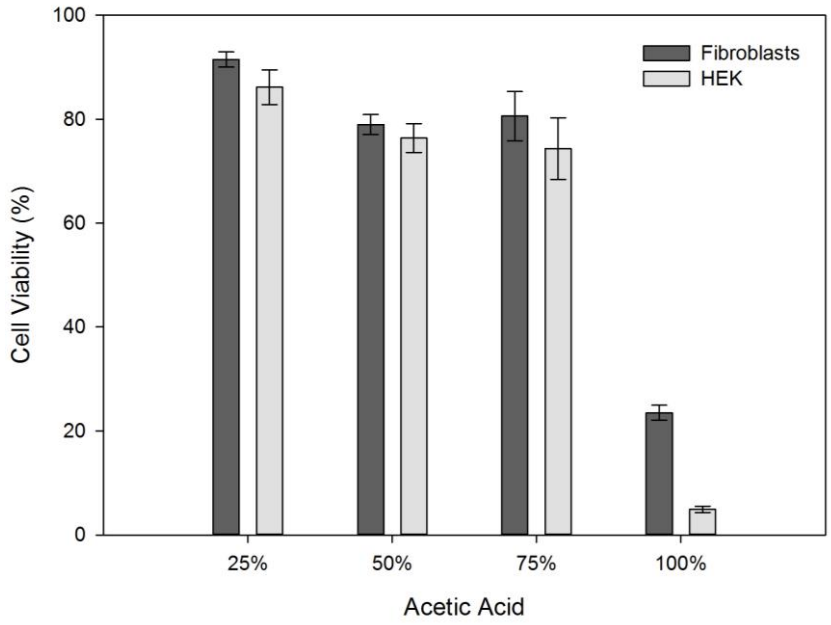

***Figure 4.9**: Evaluation of the average cell viability (with the standard deviation) of BJ-5ta fibroblasts and HEK293T cells as a function of acetic acid contained in the electrospun solution*

4.3.4.2. Cell morphology

The morphology of BJ-5ta fibroblast cells after indirect contact with the different electrospun gelatin fibers was examined after 24 h by phase contrast microscopy (**Figure 4.10**). The images corroborated the quantitative Alamar Blue assay values, showing low density of cells for the samples that were electrospun with high acetic acid concentration solutions. Moreover, the acid content of electrospun gelatin solutions affected the cell morphology [4.60] as follows: cells in contact with nanofiber mats formed from solutions with a low concentration of acetic acid had comparable morphology to those displayed in the negative control (elongated, spindle-shape and good attachment), indicating high cell biocompatibility. In contrast, those cells that were in contact with the electrospun fibers obtained from solutions with a high concentration of acetic acid shown a clearly disturbed morphology

which was more similar to those cells distributed in positive control (rounded-shape and evidence of cell detachment).

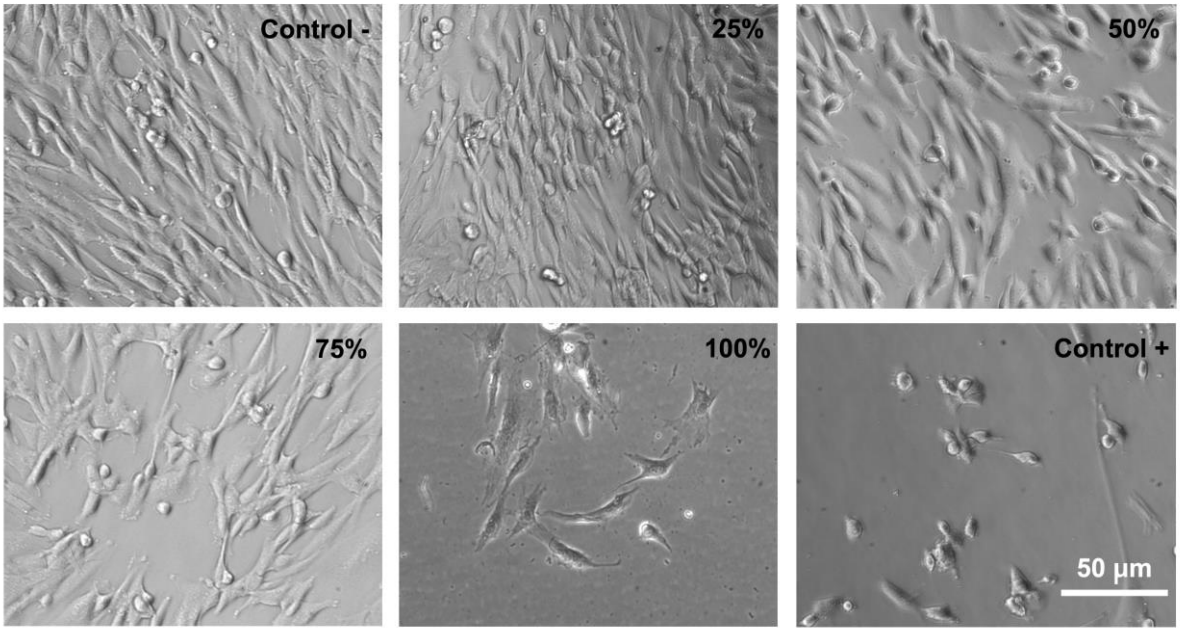

***Figure 4.10**: Cell morphology for BJ-5ta fibroblast cells after 24 h in contact with different solutions of mats of electrospun fibers. The scale bar shown in Control + is valid for all the images*

4.4. Conclusions

The feasibility of electrospinning gelatin nanofibers from solutions with different concentrations of acetic acid and gelatin at room temperature was tested.

The results showed the viability to obtain electrospun gelatin nanofibers at low acetic acid concentration (25%) combined with gelatin concentration of 300 mg/ml or higher. Both acetic acid content and gelatin concentration exhibited a clear influence on the viscosity solution, which trend was directly correlated with electrospun fiber diameter. Moreover, the study of viscosity solution in front of time determined that the solutions with low acetic acid and high gelatin concentration were those showed the higher rheology instability, due to the gelation process, suggesting the importance to develop the electrospinning just after 1h of stirring the solution.

Although the FTIR spectra did not show many differences on the electrospun gelatin mats in function of acetic content, the DSC analysis allows to determine the benefit to work at low acetic acid concentration, being the electrospun mat from 25% of acetic acid the only sample that keeps showing the characteristic degradation peak of pure gelatin at 230ºC, related with the crystallinity conformation of polymer.

Finally, the indirect cytotoxicity assay demonstrated the direct relationship between the acetic concentration of the solution and the acid traces found in the final mats revealed by the pH indicator changes. Also, the greatest cell viability (upper than 90%) was achieved for mats from solutions at 25% acetic acid concentration.

4.5. References

[4.1] B. Dhandayuthapani, Y. Yoshida, T. Maekawa, D.S. Kumar, Polymeric Scaffolds in Tissue Engineering Application: A Review, Int. J. Polym. Sci. 2011 (2011) 1–19.

[4.2] D.W. Hutmacher, Scaffolds in tissue engineering bone and cartilage, Biomaterials. 21 (2000) 2529–43.

[4.3] M.P. Lutolf, J. a Hubbell, Synthetic biomaterials as instructive extracellular microenvironments for morphogenesis in tissue engineering, Nat. Biotechnol. 23 (2005) 47–55.

[4.4] C.E. Ayres, B.S. Jha, S.A. Sell, G.L. Bowlin, D.G. Simpson, Nanotechnology in the design of soft tissue scaffolds: innovations in structure and function, Wiley Interdiscip Rev Nanomed Nanobiotechnol. 2 (2010) 20–34.

[4.5] X. Yang, H. Wang, Electrospun Functional Nanofibrous Scaffolds for Tissue Engineering, in: Tissue Eng., InTech, 2010: pp. 159–178.

[4.6] Q.P. Pham, U. Sharma, A.G. Mikos, Electrospinning of polymeric nanofibers for tissue engineering applications: a review, Tissue Eng. 12 (2006) 1197–211.

[4.7] W.-J. Li, C.T. Laurencin, E.J. Caterson, R.S. Tuan, F.K. Ko, Electrospun nanofibrous structure: a novel scaffold for tissue engineering, J. Biomed. Mater. Res. 60 (2002) 613–21.

[4.8] A.G. Kanani, S.H. Bahrami, Review on Electrospun Nanofibers Scaffold and Biomedical Applications, Trends Biomater. Artif. Organs. 24 (2010) 93–115.

[4.9] S. a. Sell, P.S. Wolfe, K. Garg, J.M. McCool, I. a. Rodriguez, G.L. Bowlin, The Use of Natural Polymers in Tissue Engineering: A Focus on Electrospun Extracellular Matrix Analogues, Polymers (Basel). 2 (2010) 522–553.

[4.10] Z.-M. Huang, Y.-Z. Zhang, M. Kotaki, S. Ramakrishna, A review on polymer nanofibers by electrospinning and their applications in nanocomposites, Compos. Sci. Technol. 63 (2003) 2223–2253.

[4.11] N. Bhardwaj, S.C. Kundu, Electrospinning: a fascinating fiber fabrication technique., Biotechnol. Adv. 28 (2010) 325–47.

[4.12] L.T.H. Nguyen, S. Chen, N.K. Elumalai, M.P. Prabhakaran, Y. Zong, C. Vijila, et al., Biological, Chemical, and Electronic Applications of Nanofibers, Macromol. Mater. Eng. 298 (2013) 822–867.

[4.13] A. Greiner, J.H. Wendorff, Electrospinning: a fascinating method for the preparation of ultrathin fibers, Angew. Chem. Int. Ed. Engl. 46 (2007) 5670–703.

[4.14] X.T. Wen, H.S. Fan, Y.F. Tan, H.D. Cao, H. Li, B. Cai, et al., Preparation of Electrospun PLA Nanofiber Scaffold and the Evaluation In Vitro, Key Eng. Mater. 288-289 (2005) 139–142.

[4.15] A. Cipitria, A. Skelton, T.R. Dargaville, P.D. Dalton, D.W. Hutmacher, Design, fabrication and characterization of PCL electrospun scaffolds-a review, J. Mater. Chem. 21 (2011) 9419–9453.

[4.16] J.H.C. Hui Wang, Xiao Hong Qin, Study on Structures of electrospinning cellulose acetate nanofibers., Adv. Mat. Res. 175-176 (2011) 242–246.

[4.17] H. Homayoni, S.A.H. Ravandi, M. Valizadeh, Electrospinning of chitosan nanofibers: Processing optimization., Carbohydr. Polym. 77 (2009) 656–661.

[4.18] S.A. Sell, M.J. McClure, K. Garg, P.S. Wolfe, G.L. Bowlin, Electrospinning of collagen/biopolymers for regenerative medicine and cardiovascular tissue engineering., Adv. Drug Deliv. Rev. 61 (2009) 1007–19.

[4.19] J.A. Matthews, G.E. Wnek, D.G. Simpson, G.L. Bowlin, Electrospinning of collagen nanofibers, Biomacromolecules. 3 (2002) 232–238.

[4.20] H. Wang, H. Shao, X. Hu, Structure of silk fibroin fibers made by an electrospinning process from a silk fibroin aqueous solution, J. Appl. Polym. Sci. 101 (2006) 961–968.

[4.21] M. Li, M.J. Mondrinos, M.R. Gandhi, F.K. Ko, A.S. Weiss, P.I. Lelkes, Electrospun protein fibers as matrices for tissue engineering, Biomaterials. 26 (2005) 5999–6008.

[4.22] C.S. Ki, D.H. Baek, K.D. Gang, K.H. Lee, I.C. Um, Y.H. Park, Characterization of gelatin nanofiber prepared from gelatin–formic acid solution., Polymer (Guildf). 46 (2005) 5094–5102.

[4.23] T.R. Keenan, Gelatin, in: Kirk-Othmer Encycl. Chem. Technol., 2003.

[4.24] R.M. Hafidz, Chemical and functional properties of bovine and porcine skin gelatin, Int. Food Res. J. 817 (2011) 813–817.

[4.25] S. Hermanto, L.O. Sumarlin, W. Fatimah, Differentiation of Bovine and Porcine Gelatin Based on Spectroscopic and Electrophoretic Analysis, 1 (2013) 68–73.

[4.26] N. Choktaweesap, K. Arayanarakul, D. Aht-ong, C. Meechaisue, P. Supaphol, Electrospun Gelatin Fibers: Effect of Solvent System on Morphology and Fiber Diameters., Polym. J. 39 (2007) 622–631.

[4.27] E. Doi, Gels and gelling of globular proteins, Trends Food Sci. Technol. 4 (1993) 1–5.

[4.28] Z.-M. Huang, Y.. Zhang, S. Ramakrishna, C.. Lim, Electrospinning and mechanical characterization of gelatin nanofibers, Polymer (Guildf). 45 (2004) 5361–5368.

[4.29] H.-W. Kim, J.-H. Song, H.-E. Kim, Nanofiber Generation of Gelatin-Hydroxyapatite Biomimetics for Guided Tissue Regeneration, Adv. Funct. Mater. 15 (2005) 1988–1994.

[4.30] Y. Zhang, H. Ouyang, C.T. Lim, S. Ramakrishna, Z.-M. Huang, Electrospinning of gelatin fibers and gelatin/PCL composite fibrous scaffolds., J. Biomed. Mater. Res. B. Appl. Biomater. 72 (2005) 156–65.

[4.31] Y.Z. Zhang, J. Venugopal, Z.-M. Huang, C.T. Lim, S. Ramakrishna, Crosslinking of the electrospun gelatin nanofibers., Polymer (Guildf). 47 (2006) 2911–2917.

[4.32] B. Su, J. Venugopal, S. Ramakrishna, Biomimetic and bioactive nano fi brous scaffolds from electrospun composite nanofibers, 1 (2007) 623–638.

[4.33] S. Agarwal, J.H. Wendorff, A. Greiner, Use of electrospinning technique for biomedical applications, Polymer (Guildf). 49 (2008) 5603–5621.

[4.34] K. Gast, A. Siemer, D. Zirwer, G. Damaschun, Fluoroalcohol-induced structural changes of proteins: some aspects of cosolvent-protein interactions., Eur. Biophys. J. 30 (2001) 273–283.

[4.35] H. Lee, S. Ahn, H. Choi, D. Cho, G. Kim, Fabrication, characterization, and in vitro biological activities of melt-electrospun PLA micro/nanofibers for bone tissue regeneration, J. Mater. Chem. B. 1 (2013) 3670.

[4.36] J. Lannutti, D. Reneker, T. Ma, D. Tomasko, D. Farson, Electrospinning for tissue engineering scaffolds, Mater. Sci. Eng. C. 27 (2007) 504–509.

[4.37] S. Zhang, Y. Huang, X. Yang, F. Mei, Q. Ma, G. Chen, et al., Gelatin nanofibrous membrane fabricated by electrospinning of aqueous gelatin solution for guided tissue regeneration., J. Biomed. Mater. Res. A. 90 (2009) 671–9.

[4.38] S. Moon, R.J. Farris, Electrospinning of Heated Gelatin-Sodium Alginate-Water Solutions, Polym. Eng. Sci. 49 (2009) 1616–1620.

[4.39] S.-Y. Gu, Z.-M. Wang, J. Ren, C.-Y. Zhang, Electrospinning of gelatin and gelatin/poly(l-lactide) blend and its characteristics for wound dressing., Mater. Sci. Eng. C. 29 (2009) 1822–1828.

[4.40] J.-H. Song, H.-E. Kim, H.-W. Kim, Production of electrospun gelatin nanofiber by water-based co-solvent approach., J. Mater. Sci. Mater. Med. 19 (2008) 95–102.

[4.41] L. Ren, J. Wang, F.-Y. Yang, L. Wang, D. Wang, T.-X. Wang, et al., Fabrication of gelatin–siloxane fibrous mats via sol–gel and electrospinning procedure and its application for bone tissue engineering, Mater. Sci. Eng. C. 30 (2010) 437–444.

[4.42] S. Panzavolta, M. Gioffrè, M.L. Focarete, C. Gualandi, L. Foroni, A. Bigi, Electrospun gelatin nanofibers: optimization of genipin cross-linking to preserve fiber morphology after exposure to water, Acta Biomater. 7 (2011) 1702–9.

[4.43] M. Erencia, F. Cano, J. a Tornero, J. Macanás, F. Carrillo, Resolving the electrospinnability zones and diameter prediction for the electrospinning of the gelatin/water/acetic Acid system., Langmuir. 30 (2014) 7198–205.

[4.44] A. Calleja, X. Granados, S. Ricart, J. Oró, J. Arbiol, N. Mestres, et al., High temperature transformation of electrospun BaZrO3 nanotubes into nanoparticle chains, CrystEngComm. 13 (2011) 7224.

[4.45] A.P.S. Immich, M.L. Arias, N. Carreras, R.L. Boemo, J.A. Tornero, Drug delivery systems using sandwich configurations of electrospun poly(lactic acid) nanofiber membranes and ibuprofen, Mater. Sci. Eng. C. Mater. Biol. Appl. 33 (2013) 4002–8.

[4.46] X. Geng, O.-H. Kwon, J. Jang, Electrospinning of chitosan dissolved in concentrated acetic acid solution, Biomaterials. 26 (2005) 5427–32.

[4.47] M. Djabourov, J. Leblond, P. Papon, Gelation of aqueous gelatin solutions. I. Structural Investigation., J. Phys. Fr. 49 (1988) 319–332.

[4.48] P.N. Magee, E. Farber, Citrate-Promoted Helix Formation in Gelatin, (1962) 124–129.

[4.49] M.A. Masuelli, M.G. Sansone, D.F. Aplicada, Hydrodynamic Properties of Gelatin – Studies from Intrinsic Viscosity Measurements, in: Prod. Appl. Biopolym., 2012: pp. 85–116.

[4.50] M.A. Oraby, A.I. Waley, A.I. El-dewany, E.A. Saad, M.A. El-hady, Electrospun Gelatin Nanofibers : Effect of Gelatin Concentration on Morphology and Fiber Diameters., Polym. J. 9 (2013) 534.

[4.51] C. Abrusci, a. Martín-González, a. Del Amo, T. Corrales, F. Catalina, Biodegradation of type-B gelatine by bacteria isolated from cinematographic films. A viscometric study, Polym. Degrad. Stab. 86 (2004) 283–291.

[4.52] P. Gupta, C. Elkins, T.E. Long, G.L. Wilkes, Electrospinning of linear homopolymers of poly(methyl methacrylate): exploring relationships between fiber formation, viscosity, molecular weight and concentration in a good solvent, Polymer (Guildf). 46 (2005) 4799–4810.

[4.53] K. Nasouri, a. M. Shoushtari, a. Kaflou, Investigation of polyacrylonitrile electrospun nanofibres morphology as a function of polymer concentration, viscosity and Berry number, Micro Nano Lett. 7 (2012) 423.

[4.54] Q. Yang, Z. Li, Y. Hong, Y. Zhao, S. Qiu, C. Wang, et al., Influence of solvents on the formation of ultrathin uniform poly(vinyl pyrrolidone) nanofibers with electrospinning, J. Polym. Sci. Part B Polym. Phys. 42 (2004) 3721–3726.

[4.55] S. V Fridrikh, J.H. Yu, M.P. Brenner, G.C. Rutledge, Controlling the fiber diameter during electrospinning., Phys. Rev. Lett. 90 (2003) 144502.

[4.56] P.F. De Almeida, B. Farias, FTIR Characterization of Gelatin from Chicken Feet, J. Chem. Chem. Eng. 6 (2012) 1029–1032.

[4.57] J.-J. Max, C. Chapados, Infrared Spectroscopy of Aqueous Carboxylic Acids: Comparison between Different Acids and Their Salts, J. Phys. Chem. A. 108 (2004) 3324–3337.

[4.58] Sudha Gangal, Principles and Practice of Animal Tissue Culture, Second Edi, Orient Black Swan, London, 2010.

[4.59] J.R. Sharpe, K.L. Harris, K. Jubin, N.J. Bainbridge, N.R. Jordan, The effect of pH in modulating skin cell behaviour, Br. J. Dermatol. 161 (2009) 671–3.

[4.60] K. Ramaesh, F. a Billson, M.C. Madigan, Effect of bile acids on fibroblast proliferation and viability, Eye (Lond). 12 (Pt 4) (1998) 717–22.

CHAPTER 5:

Resolving the electrospinnability zones and diameter prediction for the electrospinning of the gelatin/water/acetic acid system

Resolving the electrospinnability zones and diameter prediction for the electrospinning of the gelatin/water/acetic acid system

SUMMARY

The development of suitable biomimetic scaffolds is a fundamental requirement of tissue engineering. Although electrospinning has emerged as an effective method for producing such scaffolds of nanometer-sized fibers, the influence of solution characteristics on the morphology of the resulting nanofibers depends on each polymer solution system. In this study, gelatin nanofibers and microfibers were prepared via electrospinning using mixtures of water and acetic acid at different ratios as solvents. The viscosities of gelatin solutions before electrospinning were analyzed and two different behaviors were found as a function of the solvent composition, taking into account classic models of polymer science. A power law relationship between viscosity and gelatin concentration was found for each solvent system and an empirical model including the influence of acetic acid was obtained for aqueous systems.

Moreover, a ternary diagram considering gelatin, water and acetic acid mass fractions was constructed as a tool to establish the difficult electrospinnability domains in terms of fiber occurrence and morphology. Also, the isodiametric curves were defined in the fibers region.

Finally, in order to correlate the diameter of electrospun nanofibers and the electrospinnability zones, the Berry number was used. However, as its only allows the range of electrospinnability to be established for a fixed solvent composition, a new dimensionless parameter ($B_{e,mod}$) was suggested to take into account all the acetic acid aqueous solutions as a single solvent.

Keywords: electrospinning, nanofibers, gelatin, acetic acid, modeling, Berry number.

5.1. Introduction

The design of scaffolds able to mimic extracellular matrices and allowing cell cultures is one of the most important challenges in the tissue engineering field [5.1-5.3]. Among the different possible structures, nanofibrous scaffolds are clearly preferred due to their similarity to extracellular matrices fibrils in both dimensions and morphology [5.4-5.5]. The major techniques used nowadays for the fabrication of such nanofibrous scaffolds are self-assembly, phase-separation and electrospinning, the last one being the most widely applied technique due to its simplicity and versatility [5.6-5.9].

In the electrospinning process, a high voltage is applied to a polymer solution so that the particles can be electrically loaded and attracted from a nozzle cone (positively charged) to the surface of a ground collector. As the solvent evaporates during the passage from one electrode to the other, the nanofiber is deposited onto the counter-electrode [5.9]. Despite its conceptual simplicity, the electrospinning process is very intricate and it is controlled by several parameters, which can be classed in two main categories: solution parameters (concentration, molecular weight, surface tension, conductivity and viscosity) and operating parameters (voltage, distance between tip and collector, flow rate, ambient humidity and temperature) [5.7-5.8, 5.10]. Therefore, considerable effort has been devoted to understand and control the electrospinning process so as to obtain fibers with reproducible morphology and diameter. A number of models of electrified and electrospun jets have been reported in literature, but their complexity makes the forecast of the final products quite difficult [5.11-5.12].

Experimental evidence shows that the diameter of electrospun fibers is influenced by molecular conformation and that solution concentration and viscosity are the critical keys in determining the final fiber morphology [5.13-5.14]. The relationship between the solution viscosity and the polymer concentration is highly dependent on the nature of the polymer (e.g. molecular structure and molecular weight) and the intermolecular interactions within the polymer solution (polymer-polymer, polymer-solvent). Because of these variants, it is almost impossible to establish a universal formula to include all polymer-solvent systems in a given electrospinning process [5.15]. In the literature, an attempt to combine concentration and viscosity parameters in a dimensionless number named Berry number (B_e) can be found [5.16]. B_e is defined as the product of the polymer concentration (c) and the solution intrinsic viscosity ($[\eta]$) (equation 5.1) and it has been used to establish the ranges of electrospinnability and predict the diameter of the electrospun fibers [5.14, 5.17-5.18]. The relationship between B_e and electrospun fiber diameter (d) is usually considered as allometric and it is expressed as a power

law equation (equation 5.2), where α and ß are experimental coefficients [5.14, 5.17, 5.19]:

$$B_e = c \cdot [\eta] \quad \text{(Eq.5.1)}$$

$$d = \alpha \cdot (B_e)^{\beta} \quad \text{(Eq. 5.2)}$$

Besides, among the typical natural polymers used for electrospinning (collagen, chitosan, silk fibroin, etc..), gelatin is one of the most recently studied, because of its good properties of biodegradability and biocompatibility combined with a low cost [5.20-5.25]. However, gelatin electrospinning is not a trivial procedure because of the gelation process that occurs between gelatin and water, which limits the range of solvents that can be used [5.26-5.28]. Complex solvents such as fluoroalcohols have demonstrated their potential to avoid gelation and allow electrospinning of gelatin solution at room temperature, but their high cytotoxicity affects the original protein structure [5.29]. Consequently, some carboxylic acids (e.g. formic acid, acetic acid) have recently been tested as solvents, and have yielded good results, especially for a low acid concentration [5.23].

This research has been focused on the gelatin-water-acetic acid system (G-W-AA system) in order to determine those compositions that can be electrospun and to determine the relationship between nanofiber morphology and solution composition. The approach is not merely practical, in the sense of establishing the electrospinnability boundaries and predicting the characteristics of the as-obtained nanofibers, but it also seeks to provide a complete analysis regarding the rheological properties of the studied system.

5.2. Experimental

5.2.1. Materials

Powder type B gelatin (G) from bovine skin, with reported bloom of ca. 225 g and suitable for a cell culture was obtained from Sigma-Aldrich (Alcobendas, Madrid). Glacial acetic acid (AA) of 99.99% was purchased from Panreac (Castellar del Vallés, Barcelona). Doubly distilled water (W) was used for solution preparation.

5.2.2. Solutions preparation

Test solutions were prepared dissolving different amounts of powder gelatin in acetic acid aqueous solutions. Gelatin concentration (C_G, mg/ml) was in the range from 100 to 650 mg/ml whereas the acetic acid percentage in the solvent (C_{AA}, v/v%) was always between 12.5% and 100%.

The composition of solutions was often expressed as the mass fractions (F_i) of the components, calculated according equation 5.3, where m_i is the mass of each of the solution constituents (G, W or AA):

$$F_i = \frac{m_i}{m_G + m_W + m_{AA}} \qquad \text{(Eq. 5.3)}$$

Solutions were stirred at room temperature (25ºC) for 1 hour, the control of the stirring time being crucial in order to avoid the gelation process which could alter the viscosity measurements. Previous studies showed that gelation by maturation usually occurs during times longer than 1 hour of contact between gelatin and solvent [5.23, 5.28].

5.2.3. Viscosity measurement

Dynamic viscosity was measured for each sample using a rotating viscometer (RVDV-II+, Brookfield Engineering Laboratories, USA), connected with a thermostatic bath at 25ºC. For the case of very dilute solutions (C_G in the range 0.002-0.01 mg/ml) viscosity was measured by a Cannon-Fenske viscometer. Intrinsic viscosity [η] was calculated by the four most commonly used equations employed in the literature for the study of viscosimetric properties of a dilute polymer solution by graphical extrapolation (equations 5.4 to 5.7) giving rise to different but close values $[\eta]_i$. Accordingly, an average value for intrinsic viscosity ($[\eta]_{average}$) was also calculated. In all equations *c* is the polymer concentration (g/ml), η_{sp} stands for specific viscosity, whereas η_r stands for relative viscosity and K_i are empirical constants [5.26]:

$$\frac{\eta_{sp}}{c} = [\eta]_H + K_H \cdot [\eta]_H^2 \cdot c \qquad \text{Huggins' equation} \qquad \text{(Eq. 5.4)}$$

$$\frac{ln(\eta_r)}{c} = [\eta]_K - K_H \cdot [\eta]_K^2 \cdot c \qquad \text{Kreamer's equation} \qquad \text{(Eq. 5.5)}$$

$$\frac{\eta_{sp}}{c} = [\eta] + K_{S-B} \cdot [\eta] \cdot \eta_{sp} \qquad \text{Schulz-Blaschke's equation} \qquad \text{(Eq. 5.6)}$$

$$\frac{\eta_{sp}}{c} = [\eta] \cdot e^{K_M \cdot [\eta] \cdot c} \qquad \text{Martin's equation} \qquad \text{(Eq. 5.7)}$$

5.2.4. Electrospinning

Electrospinning was performed in a home-made device developed by INTEXTER. Each dope solution was placed in a 2.5 ml syringe with a stainless steel syringe needle (0.6 mm of inner diameter), connected to the anode of a power supply. A pump controlled the flow rate of the spinning solution and mat samples produced were directly collected on carbon tapes to facilitate microscopic analysis, thus avoiding the manipulation of the fibers. Carbon tapes were fastened onto the copper collector of the electrospinning device and connected to the cathode of the power supply.

The operational parameters were maintained within a range of values that had proved not to significantly affect the nanofiber diameter [5.30], in accordance with the results obtained by Ki et al. [5.24] for a similar system of gelatin/acid.

In our case, the ranges were: voltage 10-18 kV; distance between needle and collector 7-14cm, and flow rate 0.5-2 ml/h. All solutions were electrospun at room temperature (25 ± 1ºC).

5.2.5. Fiber Characterization

The morphology of fibers in the electrospun mats was inspected by Scanning Electron Microscopy (SEM) using a Phenom Standard SEM. Samples were observed without any metallic coating.

Typically, 30 arbitrary fibers were measured by an image analyzing software package (Image J,) so as to determine the fiber average diameter. Each tested solution was measured three times and the standard deviation always remained below 2%.

5.2.6. Data analysis

Viscosity and diameter data were analyzed and plotted using different statistic software packages: Statsgraphics Centurion (ICS Centurion, StatPoint Technologies, Inc, Richmond, VA, USA), Origin Pro 9 (OriginLab, Northampton, MA, USA), Sigmaplot 12 (Systat Software, San José, CA, USA).

5.3. Results and discussion

5.3.1. Solution viscosity

Many studies have demonstrated the strong influence of some solution parameters on the electrospinning process, such as surface tension, conductivity, viscosity and polymer molecular weight [5.8]. Among them, viscosity and polymer concentration are suggested to be the most decisive in determining the final fiber diameter [5.31]. However, it is difficult to predict the viscosity of ternary systems such as the one studied here (G-W-AA) [5.32-5.33]. That is why, as a first approach, the modelling of viscosity as a function of solution composition was carried out.

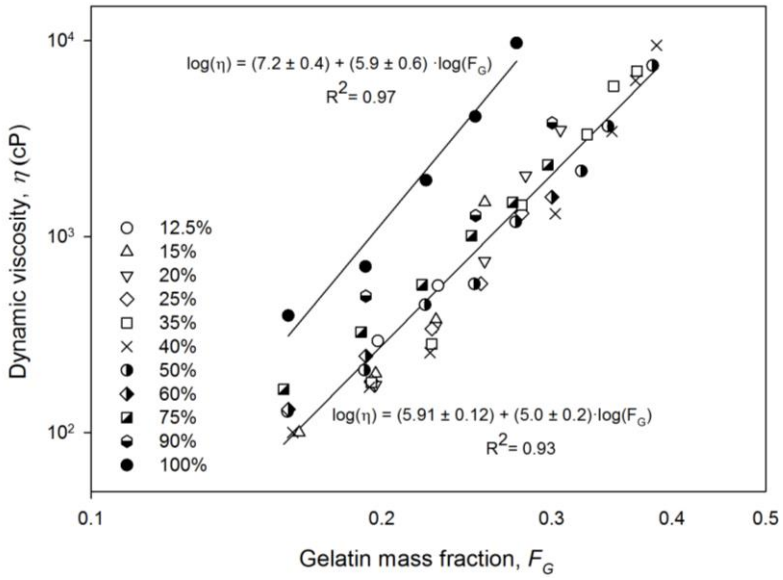

***Figure 5.1**: Dynamic viscosity (η) versus gelatin mass fraction (F_G) for the tested solutions. All water-acetic acid mixtures were fitted to a single regression*

Figure 5.1 shows the plot of dynamic viscosity of solutions as a function of gelatin mass fraction. At first glance, those solutions prepared with pure acetic acid can be distinguished from the rest as two different regression lines were revealed. The obtained data suggested that dynamic viscosity followed a clear trend with F_G. Yet, in addition to the polymer concentration, acetic acid content also controlled the intermolecular interaction between the gelatin-solvent pair. In fact, both parameters are the main variables that have been combined in the literature to develop practical equations to predict the viscosity of polymer solutions in dilute (at very small values of *c*) or semi-dilute solutions. Basically, these equations assume a strong dependence on the concentration, the intrinsic viscosity and on the dynamic viscosity of the pure

solvent. In this sense, De Gennes' equation [5.34-5.36] has been applied to model the viscosity of the solution in the semi-dilute regime (see equation 5.8):

$$\frac{\eta}{\eta_s} = \eta_r = \left(\frac{c}{c^*}\right)^{\frac{3}{3\nu-1}} \quad \text{(Eq. 5.8)}$$

where η is the dynamic viscosity of the solution, η_s is the dynamic viscosity of the solvent, ν is the Flory exponent (3/5 for good solvents, 1/2 for theta solvents and 1/3 for poor solvents) [5.37] and *c** is the critical chain overlap concentration which marks the onset of significant polymer chain overlap in solution. In other words, c* is the crossover concentration between the dilute and the semi-dilute regimes and its estimate has shown to be inversely proportional to $[\eta]$ [5.38-5.39], i.e. equation 5.9:

$$c^* = \frac{2.5}{[\eta]} \quad \text{(Eq. 5.9)}$$

Intrinsic viscosity for each composition was estimated by the Huggins', Kreamer's, Schulz-Blashke's and Martin's relationships and the average of the four estimated values was reported in **Table 5.1**. Based on these $[\eta]$ values, the c* concentration was then theoretically calculated for each system by equation 9, and the results were also reported in the same table.

***Table 5.1**: Intrinsic viscosities, [η], of tested solutions calculated by Huggins', Kraemer's, Schulz-Blashke's and Martin's equations, average intrinsic viscosity and the calculated critical chain concentration with its standard deviation*

C_{AA} (%)	$[\eta]_H$ (ml/g)	$[\eta]_K$ (ml/g)	$[\eta]_{SB}$ (ml/g)	$[\eta]_M$ (ml/g)	$[\eta]_{average}$ (ml/g)	c* (g/ml)
15	102.6	99.2	102.7	102.5	101.8 ± 1.7	0.0246 ± 0.0004
20	94.3	90.4	94.0	93.6	93.1 ± 1.8	0.0269 ± 0.0005
25	97.4	93.5	97.2	96.5	96.1 ± 1.8	0.0260 ± 0.0005
35	94.2	91.0	94.1	93.6	93.2 ± 1.5	0.0268 ± 0.0004
50	100.0	95.7	100.0	99.5	99 ± 2	0.0252 ± 0.0005
75	120.8	112.5	121.4	120.3	119 ± 4	0.0210 ± 0.0007
90	124.1	115.1	120.1	120.3	120 ± 4	0.0208 ± 0.0007
100	51.1	50.4	51.1	50.9	50.9 ± 0.3	0.0491 ± 0.0001

The values for [η] were noticeably low when using pure acetic acid (AA) instead of water-acetic acid mixtures as solvent (W-AA). For W-AA systems, the increase of AA content produced an initial decrease of [η] followed by a noticeable increase, particularly at high concentration of AA. As a result, the *c** value for pure acetic acid solution was higher, by a factor of almost two, (c^*_{AA} ~ 0.05 g/ml) than those calculated for water-acetic acid ($c^*_{water\text{-}AA}$ ~ 0.025 g/ml). Accordingly, two main types of gelatin–solvent intermolecular interactions can be differentiated depending on the presence or absence of water. Actually, these intermolecular interactions comprise hydrogen bonding and Van der Waals interactions which can be hold among the different molecules: water, acetic acid and gelatin. Firstly, in the presence of water, chain overlap occurred at lower concentrations of gelatin compared to solutions in AA solvent ($c^*_{water\text{-}AA} < c^*_{AA}$), indicating that intermolecular interactions between gelatin chains and water molecules cause the gelatin coils to expand. Secondly, differently from W-AA solutions, a higher concentration of gelatin was required for chain overlapping in pure acetic acid ($c^*_{AA} > c^*_{water\text{-}AA}$) since for the AA solvent solution the interactions cause the polymer coils to contract. Finally, it is noteworthy that for c>c* (i.e. semi-dilute regime) the concentration of gelatin will be high enough to induce a significant degree of entanglement between polymer chains.

To facilitate a better interpretation, the relative viscosity of polymer semi-dilute solutions was plotted as a function of c/c* (recall that $c^* \sim 2.5/[\eta]$, i.e. $B_e = 2.5 \cdot c/c^*$) in **Figure 5.2**. The plotted values were within the range of applicability of equation 8 at c>c* (i.e. semi-dilute regime), so a linear regression of the data was made to estimate and compare the scaling exponent, which is directly related to the Flory exponent (ν), for studying the viscosity dependence on both the c/c* ratio and the concentration of AA in solution.

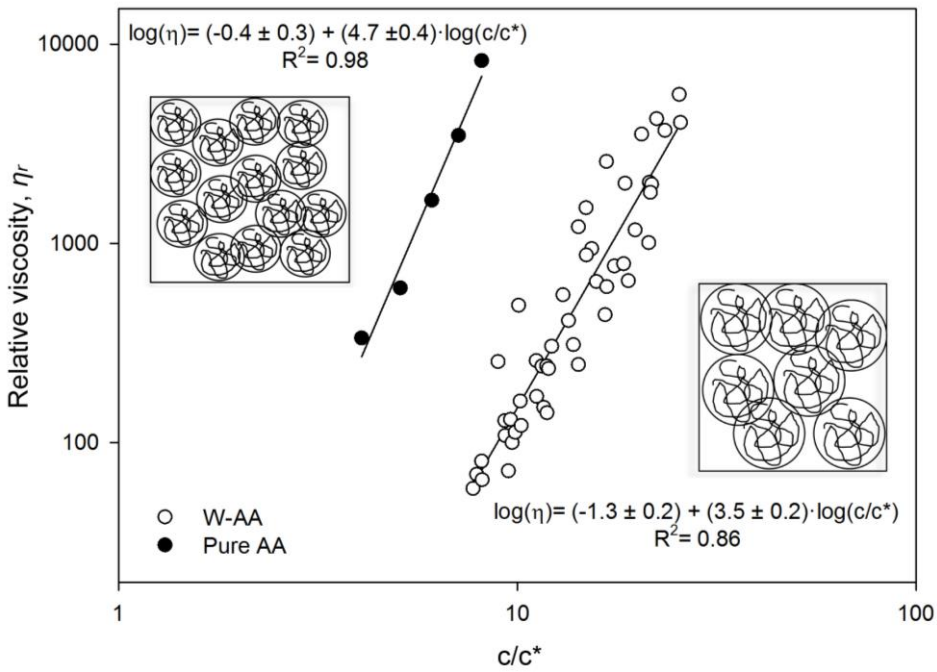

***Figure 5.2**: Relative viscosity (η_r) versus c/c* for semi-dilute entanglements solutions of pure acetic acid (black) and for water-acetic acid mixtures (white). Each system was fitted to a different regression*

From the results, it can be seen that η_r behavior was in close agreement with the relationship previously shown in **Figure 5.1** as viscosity was influenced by both *c* and AA content in solution. Regarding the AA content, it was pointed out that the presence of water in the solvent had a crucial effect on the final viscosity of the gelatin solutions but all the water-acetic acid mixtures tested showed a similar trend and, therefore, they were modeled all together as a single system. Taking that into account just two different systems are necessary to model the viscosity of solutions (either made of pure acetic acid or made of water-acetic acid solutions).

Besides, **Figure 5.2** also showed that for semi-dilute solutions of W-AA solvents, a significant degree of entanglement was noticed from c/c*~10, while for solutions using just AA as solvent the entanglement occurred always for a lower c/c* value. That is, for any c/c*, the η_r of AA-based solutions is always higher than for W-AA-based solutions (e.g. for a c/c* ~10 η_{rAA} ~10000 > $\eta_{rW\text{-}AA}$ ~100). These results are consistent with the above discussion, which highlighted the major influence of the composition of the solvent in controlling the gelatin-solvent intermolecular interactions.

On the other hand, a stronger dependence of the viscosity with the c/c* value was observed for AA system compared to the W-AA system because the estimated scaling exponents were 4.7 ± 0.4 and 3.5 ± 0.2, respectively. This scaling exponent is related to the known Flory exponent (ν) which has been widely used to characterize polymer-

solvent intermolecular interactions, the so-called good, theta and poor solvent behavior [5.37]. Flory exponent was calculated from the relationship given in equation 8 and values of 0.55 and 0.60 resulted for AA and W-AA solvents, respectively. Thus, all the W-AA-based solutions behaved like a good solvent for gelatin (chain segments swell, i.e. cause coils to expand) while pure AA solvent interacted as a theta solvent for gelatin (chain segments stay close to each others, i.e. cause coils to contract). As can be seen, these results also confirm the higher c* value found for AA system compared with W-AA (recall that $c^*_{AA} \sim 2\ c^*_{water\text{-}AA}$).

In summary, these results confirm that the presence or absence of water molecules in the solvent was crucial for establishing the final conformation of gelatin chains.

Likewise, it was pointed out that the effect of AA content on the dynamic viscosity of W-AA-based solutions was more significant at high concentrations of gelatin. In order to model the dependence of η on gelatin and AA content, an empirical equation was proposed taking into account the hypothesis that the relationship between η and the mass fraction of gelatin could be expressed as a power law function, as has been observed in some studies [5.18, 5.24-5.25, 5-40] (equations 5.10 and 5.11):

$$\eta = k \cdot (F_G)^a \qquad \text{(Eq. 5.10)}$$

$$\log(\eta) = \log(k) + a \cdot \log(F_G) \qquad \text{(Eq. 5.11)}$$

where *k* and the scaling exponent *a* are assumed to depend on the acetic acid mass fraction (F_{AA}). The best linear regression was achieved using the following equation (equation 5.12):

$$\log(\eta) = (2.5 \pm 0.5 \cdot F_{AA}^2 - 3.4 \pm 0.7 \cdot F_{AA} + 6.8 \pm 0.2) + (-3.1 \pm 0.9 \cdot F_{AA} + 6{,}2 \pm 0.3) \cdot \log(F_G) \qquad \text{(Eq. 5.12)}$$

As expected, the resulting model obtained by statistical software (Statgraphics) showed that *k* and *a* are both functions of F_{AA}. Furthermore, it was proved that the *k* parameter followed a quadratic dependence on the F_{AA}, which agrees with the quadratic relationship also reported in the literature between the viscosity of aqueous acetic acid solutions and the acid content [5.41-5.42], attaining a maximum around 80% w/w of acetic acid. Conversely, the scaling factor was found to be directly proportional to F_{AA}.

Data calculated by equation 12 are plotted in **Figure 5.3a** where a 3-D surface plot (Matlab software) illustrates the effect of F_{AA} and F_G on the dynamic viscosity of solutions.

For high F_G content a quadratic profile was observed that can be related to the balance of two different factors. On the one hand for $F_{AA} < 0.5$ the high water content promotes the interaction with gelatin and water, it is being the main mechanism that influences the viscosity in this range. On the other hand, for $F_{AA} > 0.5$ the viscosity follows the typical trend of gelatin viscosity as a function of pH (for the range 2-3.5), increasing as the pH decreases, reaching the minimum viscosity on the isoelectric point (pH 4.6-5.2 for type B gelatin) [5.26].

Additionally, **Figure 5.3b** shows the regression between experimental and predicted viscosities and it can be seen that data points fit well to a straight line of slope 1 with a high correlation coefficient ($R^2 = 0.97$), proving the usefulness of the model.

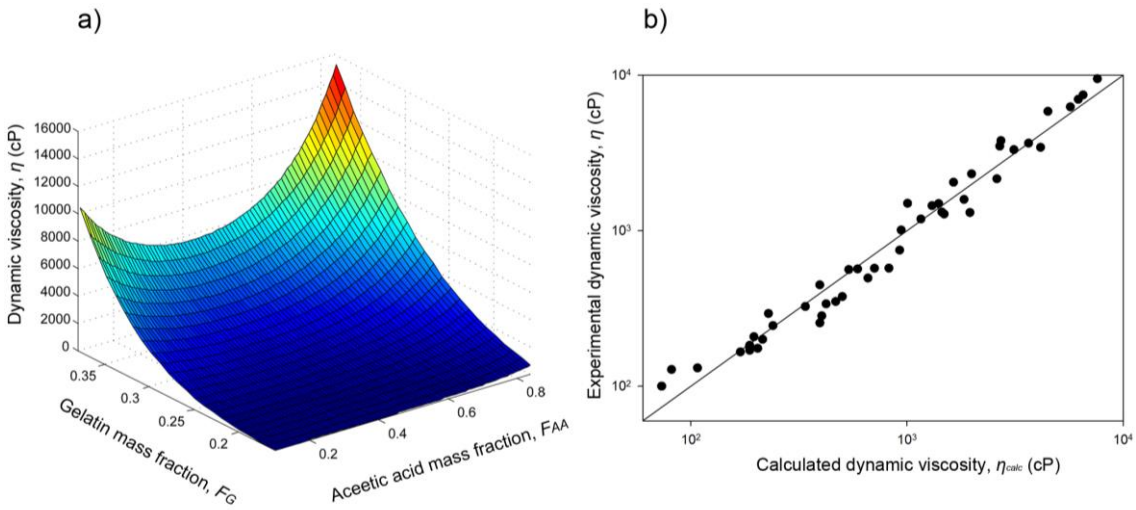

***Figure 5.3**: Response surface plot of dynamic viscosity (η) as a function of gelatin mass fraction (F_G) and acetic acid mass fraction (F_{AA}) (3a, left). Experimental intrinsic viscosity values (η) vs. calculated (η_{calc}) ones using the suggested model. The proximity to the diagonal line of slope 1 indicates a very agreement between the two values (3b, right)*

5.3.2. Electrospinnability boundarie

Data from the results of the electrospinning process and from the nanofibers diameter assessment (when they were obtained) were plotted in a ternary diagram (**Figure 5.4**) in order to better identify and predict the electrospinnability domains or composition regions and the borders thereof, similarly to what has been done recently by Ago et al

[5.43]. In **Figure 5.4** the mass fraction of each component (F_i) is plotted along one axis and dots are categorized depending on the fibers (or other structure if any) morphology.

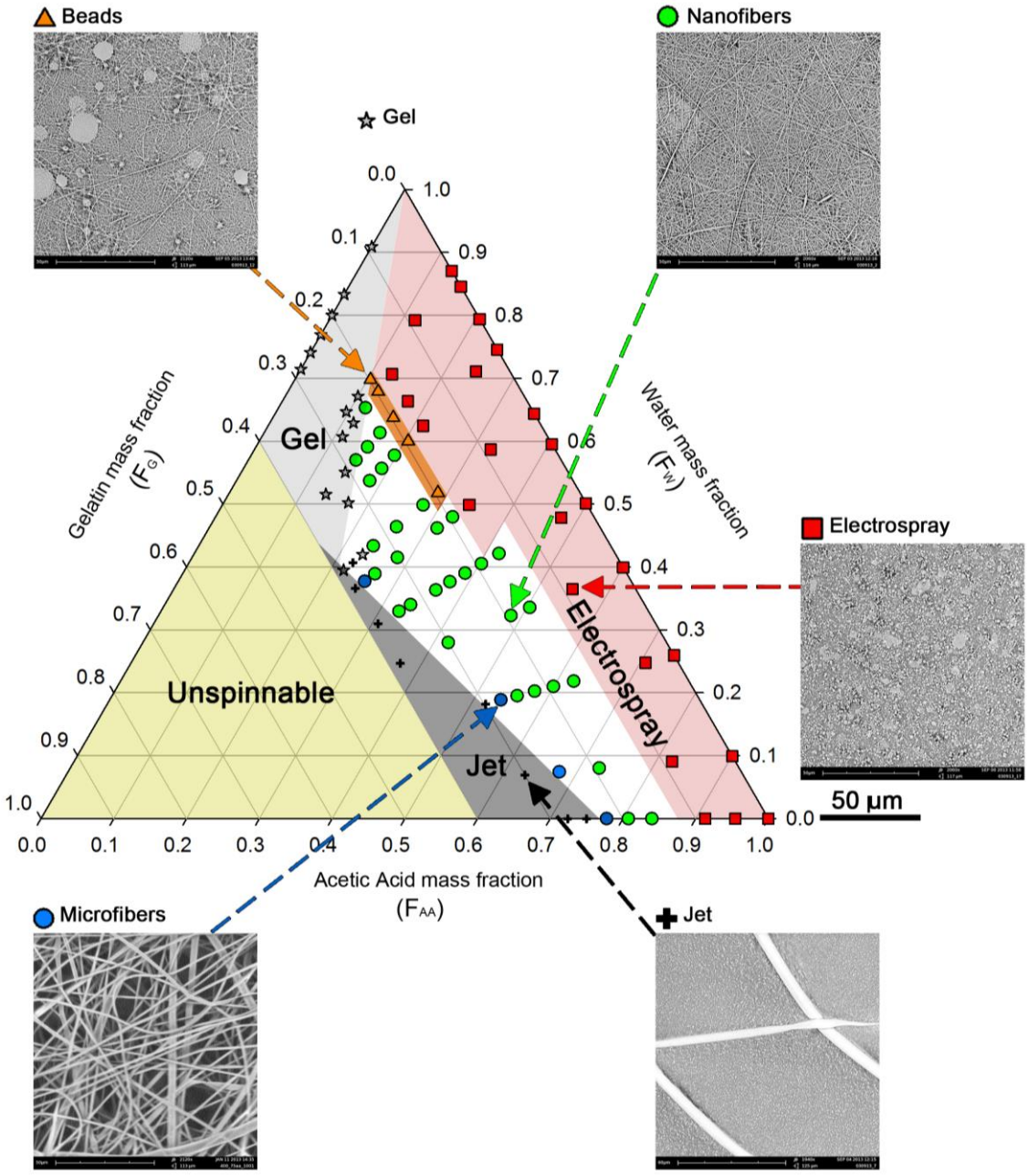

***Figure 5.4**: Ternary diagram showing the electrospinnability domains according to the composition of the precursor solution (gelatin (F_G), acetic acid (F_{AA}) and water (F_W) mass fractions). Colours are used as a guide of the different domains and a representative SEM image of each domain was included*

For the G-AA-W system, six different regions were identified:

- ***I. Unspinnable region***: this was the area of the diagram where dispersions were obtained, instead of homogeneous mixtures of the three components. From the ternary diagram it can be seen that macroscale phase-separation occurred for mixtures with F_G values higher than 0.4, indicating the gelatin solubility limit.
- ***II. Gel region***. This region comprised those homogenous mixtures of very high viscosity that do not flow through the syringe of the electrospinning device and, therefore, electrospinning failed. This domain was characterized by solutions that satisfied the following conditions: $F_G < 0.4$ and $F_G/F_{AA} \geq 1.75$. In other words, the amount of gelatin went below the phase separation limit but greatly exceeds the amount of acetic acid, so gelation occurred due to the surrounding and tightly bond water molecules [5.27].
- ***III. Electrospray region***. Those solutions belonging to this domain did not produce a continuous jet when being electrospun and a spray of the solution onto the ground collector was obtained in its place. The commonly suggested explanation is that the viscoelastic force in the jet was too small to hold the fibrous structure [5.15]. In terms of composition, this region was related to the minimum gelatin amount in the mixture, since very dilute solutions did not have the necessary viscosity and polymer chain entanglement. The threshold F_G value required to obtain the transition from electrospraying to electrospinning was found to be ca. 0.15. Indeed, two different borders were observed in the diagram: $F_G = 0.175$ for solutions with F_{AA} lower than 0.4 and $F_G = 0.125$ for solutions with F_{AA} higher than 0.4.
- ***IV. Beaded fibers region***. The progressive change from individual scattered beads to continuous electrospun fibers is usually observed as the chain entanglement density increases in polymer solution [5.44]. However, just in this transition range, beaded fibers (also called beads-on-string) are often observed [5.36]. In this case, solutions with $F_G \sim 0.2$ and $F_{AA} < 0.3$ and $F_W > 0.5$ produced these beaded fibers. According to the above mentioned electrospray limits, it is possible that beaded fibers could also be obtained for solutions of lower F_G (~0.15) but higher F_{AA}, even if they were not experimentally found.
- ***V. Unstable jet region***. In this area of the diagram, solutions were very viscous (due to the high amount of gelatin) but also contained enough acetic acid to allow electrospinning. Nevertheless, the electrospinning of such solutions still presented some problems since the syringe was frequently occluded thus provoking an intermittent flow. This region was defined by those solutions that satisfied the following conditions: $F_G < 0.4$ and $F_{AA} \geq 1.45 - 3.2 \cdot F_G$. This region slightly

overlapped the gel region.

- ***VI. Fibers region***. Once regions I to V were delimited, the remaining area included all solutions that resulted in the formation of nanofibers and microfibers, the latter being found in the boundaries of the unstable jet region. This approximately, this triangle-shape region could be described by three simple mathematical relations involving F_G and F_{AA} (equations 5.13 to 5.15):

$$0.15 < F_G < 0.4 \quad \text{(Eq. 5.13)}$$

$$F_G/F_{AA} \leq 1.75 \quad for \ F_{AA} \leq 0.2 \quad \text{(Eq. 5.14)}$$

$$F_G/F_{AA} \leq 0.45 - 0.29 \cdot F_{AA} \quad for \ F_{AA} > 0.2 \quad \text{(Eq. 5.15)}$$

According to the obtained results, nano and microfibers with a diameter ranging from 200 to 3000 nm can be successfully obtained. By using statistical software Origin Pro 9, it was possible to define isodiametric curves in the fiber region (**Figure 5.5)**. As can be seen, the contour lines do not run parallel to the gelatin mass fraction but they are askew and twisted. Therefore, it seems that it is not possible predict to directly the diameter of the electrospun fibers by exclusively taking into account the mass fraction of the solution components and their relations.

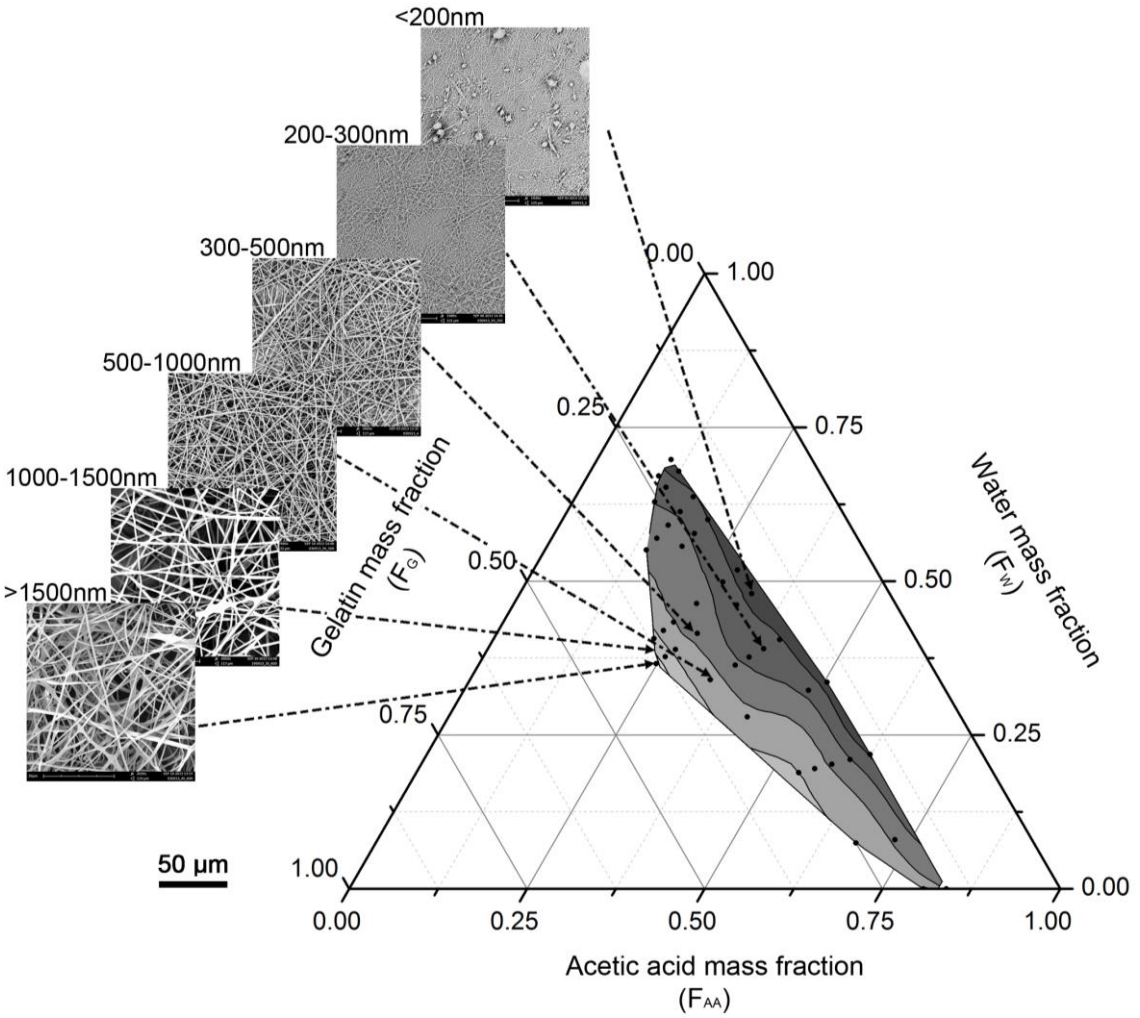

***Figure 5.5**: Isodiametric contour lines for the nanofibers and microfibers electrospinning domain according to the composition of the precursor solution (gelatin (F_G), acetic acid (F_{AA}) and water (F_W) mass fractions). A representative SEM image of each diameter range was included*

5.3.3. Diameter modeling

Besides the ranges of electrospinnability of the studied system, the diameter of the electrospun fibers is another essential feature that must be controlled for further biomedical developments due to the experimental evidence of the sensibility of cells to fiber size [5.45].

In regard to the relationship between the fiber diameter and electrospinning process parameters, the power law potential dependence of the Berry dimensionless number (equation 5.2) has proved to be of practical importance for establishing the ranges of electrospinnability and predicting the diameter of the electrospun fibers [5.17-5.18, 5.36, 5.46-5.48]. So, to evaluate the correlation between the experimental data and the model described by equation 5.2, the average diameter of the fibers was determined

for each previously characterized electrospun gelatin solution and plotted versus the $C_G \cdot [\eta]$ product (see Table 5.1 for intrinsic viscosity) in log-log scale (**Figure 5.6**).

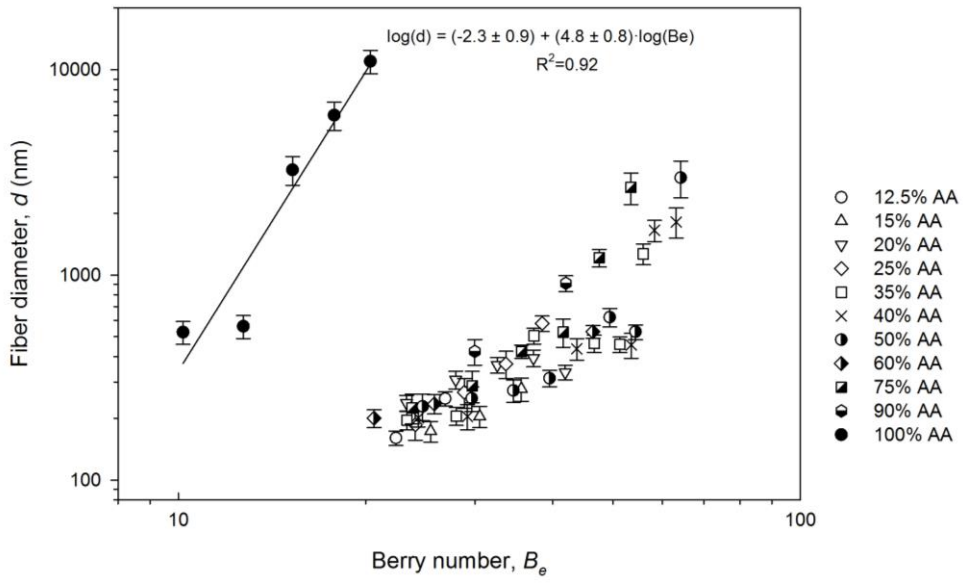

***Figure 5.6**: log-log relationship between the diameter of electrospun fibers (d) and B_e number for the tested solutions*

From the results, two main behaviors can be clearly differentiated depending on whether the solvent used was pure AA or W-AA mixtures, as was seen also for the dynamic viscosity (**Figure 5.1** and **Figure 5.2**). For the W-AA-based solutions it was observed that for each solvent composition (i.e. 50% AA) the fiber diameter correlated well with the Be number according to the power law given by equation 2, evidencing a clear relationship between the fiber diameter and the dynamic viscosity of the solution, which in many other cases has been reported as a power law dependence [5.18, 5.25, 5.36].

A detailed analysis of the data plotted in **Figure 5.6** showed that it was not possible to define a practical value or range of B_e to define the different regions of electrospinnability for all the W-AA based solutions, independently of the gelatin-solvent pair under study. So, in order to find a practical and alternative relationship that would help to predict these electrospinnability domains regardless of the acid content, some alternative formulations of the Berry number were proposed to include the effect of the acetic acid content on the diameter of the electrospun gelatin fibers. Among the different proposals, the following equation (equation 5.16) was chosen since it provided the best fit to the experimental data while maintaining the dimensionless character of the relationship. Moreover, the first term ($[\eta] \cdot F_G$) of this new expression is analogous to

the traditional Berry number ([η]·C) since F_G is proportional to C, thus preserving the meaning of the dimensionless number for a pure solvent (when FAA = 0):

$$B_{e,mod} = [\eta] \cdot F_G + {}^{F_{AA}}/_{F_G} \quad \text{(Eq. 5.16)}$$

The correlation between fiber diameter and $B_{e,mod}$ is shown in **Figure 5.7**. In this case, $B_{e,mod}$ helped to predict the change in electrospinnability regimes for all the polymers solutions tested, which were directly related to their rheology. In particular, four regimes were distinguished. For $B_{e,mod}$ values lower than about 20 ($B_{e,mod}$<20), the solutions were in the semi-dilute unentangled regime, where the concentration was large enough to have some chain overlap but not enough to cause any significant degree of entanglement, so electrospray and very low diameter nanofibers with droplets or beads were obtained. Conversely, for $B_{e,mod}$> 20 the concentration of gelatin was further increased reaching the semi-dilute entangled regime and the topological constraints induced by the larger occupied fraction of the available hydrodynamic volume in the solution induced chain entanglements, so continuous fibers were produced, i.e. nanofibers (<1000 nm) for 20<$B_{e,mod}$<35 and microfibers for 35<$B_{e,mod}$<40. Finally, when the chain entanglements were very high ($B_{e,mod}$>40) electrospinning became unstable, and jets with fibers of an average diameter greater than 3000 nm were obtained.

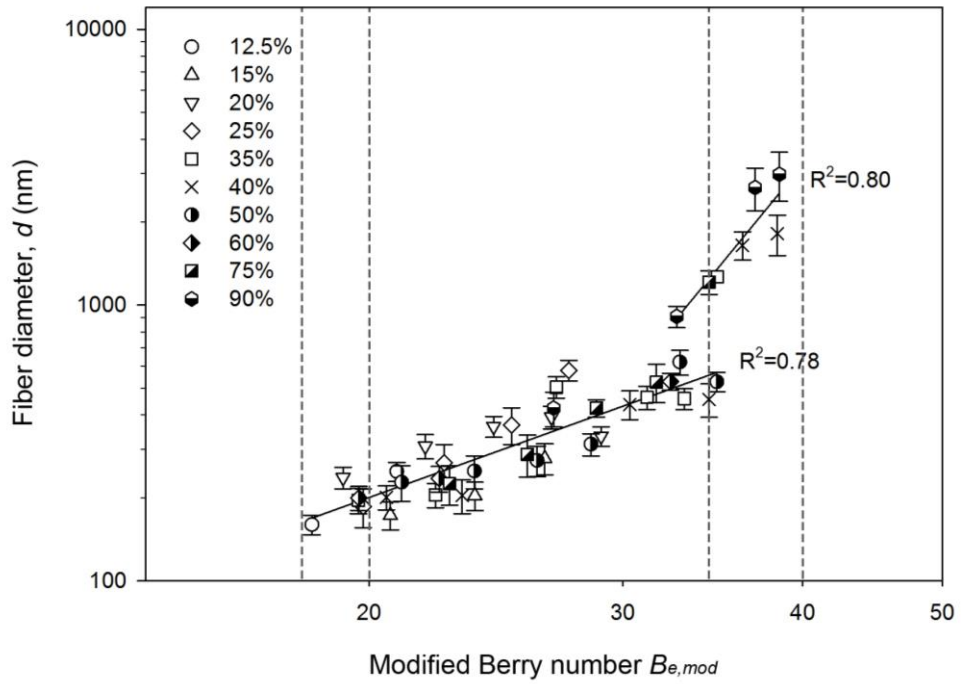

***Figure 5.7**: Relationship between the modified Berry number ($B_{e,mod}$) and electrospun fiber diameter (d) for the tested solutions (only W-AA mixtures) with ranges of electrospinnability (E: Electrospray; B: Beads; N: Nanofibers (<1000 nm); M: Microfibers (>1000 nm); U: Unstable Jet)*

It is worth mentioning that two different trends between fiber diameter and $B_{e,mod}$ were displayed, depending on whether $B_{e,mod}$ was lower or greater than about 35. That is, the dependence of the diameter on the $B_{e,mod}$ was lower for the regions producing nanofibers and beads (scaling exponent of 1.9) than for the regions producing microfibers (scaling exponent of 6.4). In addition, data were successfully fitted by a linear regression to a power law, i.e. $d=A\cdot(B_{e,mod})^B$, similar to the relationship between the diameter and the Be that is often reported in the literature [5.14, 5.17]. The regression analysis of the data led to the following power-law relationships:

- for nanofibers (d<1000 nm and $20<B_{e,mod}<35$):

$$d = 0.7\cdot(B_{e,mod})^{1.9} \qquad \text{(Eq. 5.17)}$$

- for micrometers (d>1000 nm and $B_{e,mod}>35$):

$$d = 2.10^{-7}\cdot(B_{e,mod})^{6.4} \qquad \text{(Eq. 5.18)}$$

A correlation of 92% was found between experimental and calculated diameters using these equations proving that the predicted values of the proposed models were in good agreement with the experimental observations, even if the fit was less good for microfibers with diameters greater than 2000 nm and the standard deviation for these fibers was larger (see **Figure 5.8**).

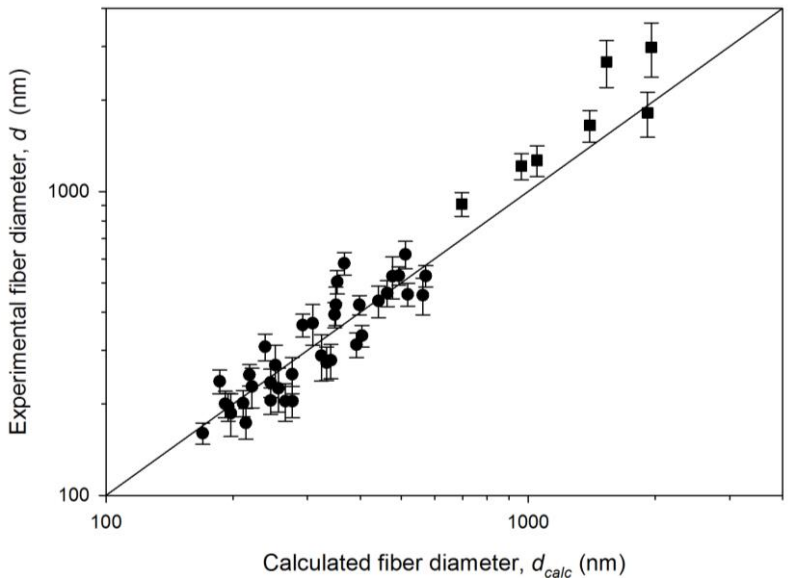

***Figure 5.8**: Experimental fiber diameter (d) values vs. values calculated by the models expressed in equations 16 (●) and 17 (■). The proximity to the diagonal line indicates a good agreement between the two values*

5.4. Conclusions

Gelatin solutions prepared by different mixture ratios of doubly distilled water and acetic acid were used to explore the relationship between viscosity, electrospinability regions and electrospun fiber diameter with the solution composition.

The analysis of viscosity distinguished between two different solvent systems (pure acid acetic and aqueous solutions) with significantly different behaviors corroborated by the Flory exponent (ν), which has been used to physically characterize polymer-solvent intermolecular interactions: $\nu = 0.6$ for W-AA system (good solvent) and $\nu = 0.55$ for AA system (stating an intermediate situation between theta and good solvent). Moreover, an empirical model including both the effect of acetic acid and gelatin concentration was found, which allowed the prediction of the viscosity with a correlation coefficient of 97%.

The results of the electrospinning process identified six different regions of electrospinnability in a ternary Gelatin-Water-Acid diagram. From such a diagram it could be seen that the solution composition necessary for obtaining gelatin nano and microfibers (ranging from 200 to 3000 nm) can be described by three simple mathematical relations involving F_G and F_{AA}. Moreover, the isodiametric curves were obtained within this area.

Finally, a modification of the Berry number was proposed to take into account the effect of acetic acid in order to establish the electrospinnability domains for aqueous solutions. The values of this new dimensionless number should be between 20 and 40 to guarantee that nano and microfibers are obtained. The relationship between fiber diameter and $B_{e,mod}$ was also established and two power law models were able to predict the nano and microfiber diameters, respectively.

5.6. References

[5.1] S.-W. Choi, Y. Zhang, Y. Xia, Three-dimensional scaffolds for tissue engineering: the importance of uniformity in pore size and structure., Langmuir. 26 (2010) 19001–6.

[5.2] F.J. O'Brien, Biomaterials & scaffolds for tissue engineering, Mater. Today. 14 (2011) 88–95.

[5.3] B. Dhandayuthapani, Y. Yoshida, T. Maekawa, D.S. Kumar, Polymeric Scaffolds in Tissue Engineering Application: A Review, Int. J. Polym. Sci. 2011 (2011) 1–19.

[5.4] K.M. Woo, J.-H. Jun, V.J. Chen, J. Seo, J.-H. Baek, H.-M. Ryoo, et al., Nano-fibrous scaffolding promotes osteoblast differentiation and biomineralization., Biomaterials. 28 (2007) 335–43.

[5.5] Y. Ji, K. Ghosh, X.Z. Shu, B. Li, J.C. Sokolov, G.D. Prestwich, et al., Electrospun three-dimensional hyaluronic acid nanofibrous scaffolds., Biomaterials. 27 (2006) 3782–92.

[5.6] S. Cai, H. Xu, Q. Jiang, Y. Yang, Novel 3D electrospun scaffolds with fibers oriented randomly and evenly in three dimensions to closely mimic the unique architectures of extracellular matrices in soft tissues: fabrication and mechanism study., Langmuir. 29 (2013) 2311–8.

[5.7] Q.P. Pham, U. Sharma, A.G. Mikos, Electrospinning of polymeric nanofibers for tissue engineering applications: a review, Tissue Eng. 12 (2006) 1197–211.

[5.8] N. Bhardwaj, S.C. Kundu, Electrospinning: a fascinating fiber fabrication technique., Biotechnol. Adv. 28 (2010) 325–47.

[5.9] A. Greiner, J.H. Wendorff, Electrospinning: a fascinating method for the preparation of ultrathin fibers, Angew. Chem. Int. Ed. Engl. 46 (2007) 5670–703.

[5.10] T. Subbiah, G.S. Bhat, R.W. Tock, S. Parameswaran, S.S. Ramkumar, Electrospinning of nanofibers, J. Appl. Polym. Sci. 96 (2005) 557–569.

[5.11] C.J. Thompson, G.G. Chase, a. L. Yarin, D.H. Reneker, Effects of parameters on nanofiber diameter determined from electrospinning model, Polymer (Guildf). 48 (2007) 6913–6922.

[5.12] S. Rafiei, S. Maghsoodloo, B. Noroozi, V. Mottaghitalab, A.K. Haghi, Mathematical modeling in electrospinning process of nanofibers: a detailed review, Cellul. Chem. Technol. 47 (2013) 323–338.

[5.13] Z. Li, C. Wang, Effects of Working Parameters on Electrospinning, in: One-Dimensional Nanostructures, Springer Berlin Heidelberg, Berlin, Heidelberg, 2013: pp. 15–29.

[5.14] F.K. Ko, Nanofiber Technology in Gogotsi Nanomaterials Handbook, in: Nanomater. Handb., 2006: pp. 553–564.

[5.15] T. Lin, X.G. Wang, Controlling the morphologies of electrospun nanofibers., in: Nanofibers Nanotechnol. Text., 2007: pp. 90–110.

[5.16] B.L. Hager, G.C. Berry, Moderately concentrated solutions of polystyrene. I. Viscosity as a function of concentration, temperature, and molecular weight, J. Polym. Sci. Polym. Phys. Ed. 20 (1982) 911–928.

[5.17] J. Tao, S. Shivkumar, Molecular weight dependent structural regimes during the electrospinning of PVA, Mater. Lett. 61 (2007) 2325–2328.

[5.18] K. Nasouri, a. M. Shoushtari, a. Kaflou, Investigation of polyacrylonitrile electrospun nanofibres morphology as a function of polymer concentration, viscosity and Berry number, Micro Nano Lett. 7 (2012) 423.

[5.19] F. Cengiz, I. Krucińska, E. Gliścińska, Comparative Analysis of Various Electrospinning Methods of Nanofibre Formation, 17 (2009) 13–19.

[5.20] M. Gulfam, J.M. Lee, J.-E. Kim, D.W. Lim, E.K. Lee, B.G. Chung, Highly porous core-shell polymeric fiber network., Langmuir. 27 (2011) 10993–10999.

[5.21] M. Li, M.J. Mondrinos, M.R. Gandhi, F.K. Ko, A.S. Weiss, P.I. Lelkes, Electrospun protein fibers as matrices for tissue engineering, Biomaterials. 26 (2005) 5999–6008.

[5.22] T.R. Keenan, Gelatin, in: Kirk-Othmer Encycl. Chem. Technol., 2003.

[5.23] M. Erencia, F. Cano, M.M. Tornero, Jose Antonio Fernandes, T. Tzanov, J. Macanás, F. Carrillo, Electrospinning of gelatin scaffolds with low acetic acid concentration effect of solvent composition on both diameter of nanofibers and cell viability, Summited. (2014).

[5.24] C.S. Ki, D.H. Baek, K.D. Gang, K.H. Lee, I.C. Um, Y.H. Park, Characterization of gelatin nanofiber prepared from gelatin–formic acid solution., Polymer (Guildf). 46 (2005) 5094–5102.

[5.25] N. Choktaweesap, K. Arayanarakul, D. Aht-ong, C. Meechaisue, P. Supaphol, Electrospun Gelatin Fibers: Effect of Solvent System on Morphology and Fiber Diameters., Polym. J. 39 (2007) 622–631.

[5.26] M.A. Masuelli, M.G. Sansone, D.F. Aplicada, Hydrodynamic Properties of Gelatin – Studies from Intrinsic Viscosity Measurements, in: Prod. Appl. Biopolym., 2012: pp. 85–116.

[5.27] M. Djabourov, J. Leblond, P. Papon, Gelation of aqueous gelatin solutions. I. Structural Investigation., J. Phys. Fr. 49 (1988) 319–332.

[5.28] M.L. Ottone, M.B. Peirotti, J.A. Deiber, Rheokinetic model to characterize the maturation process of gelatin solutions under shear flow, Food Hydrocoll. 23 (2009) 1342–1350.

[5.29] K. Gast, A. Siemer, D. Zirwer, G. Damaschun, Fluoroalcohol-induced structural changes of proteins: some aspects of cosolvent-protein interactions., Eur. Biophys. J. 30 (2001) 273–283.

[5.30] M. Erencia Millan, Propuesta de tesis: Preparación de soportes biomateriales con estructuras fibrilares obtenidas mediante electro-hilatura., Universitat Politecnica de Catalunya, 2013.

[5.31] S.K. Tiwari, S.S. Venkatraman, Importance of viscosity parameters in electrospinning: Of monolithic and core–shell fibers, Mater. Sci. Eng. C. 32 (2012) 1037–1042.

[5.32] K. Sollman, E. Marschall, W. Mi, Viscosity of selected binary, ternary, and quaternary liquid mixtures, J Chem Eng. 35 (1990) 375–381.

[5.33] M.-R. Fatehi, S. Raeissi, D. Mowla, Estimation of viscosity of binary mixtures of ionic liquids and solvents using an artificial neural network based on the structure groups of the ionic liquid, Fluid Phase Equilib. 364 (2014) 88–94.

[5.34] P.G. De Gennes, Dynamics of Entangled Polymer Solutions. II. Inclusion of Hydrodynamic Interactions, Macromolecules. 9 (1976) 594–598.

[5.35] R.. Colby, M. Rubinstein, Two-Parameter scaling for polymers in theta solvents, Macromolecules. 23 (1990) 2753–2757.

[5.36] P. Gupta, C. Elkins, T.E. Long, G.L. Wilkes, Electrospinning of linear homopolymers of poly(methyl methacrylate): exploring relationships between fiber formation, viscosity, molecular weight and concentration in a good solvent, Polymer (Guildf). 46 (2005) 4799–4810.

[5.37] P.J. Flory, Principles of Polymer Chemistry, Cornell University Press, New York, 1953.

[5.38] S. Matsuoka, M.K. Cowman, Equation of state for polymer solution, Polymer (Guildf). 43 (2002) 3447–3453.

[5.39] A.M. Jamieson, R. Simha, Newtonian viscosity of dilute, semidilute and concentrated polymer solution, in: L.A. Ultracki, A.M. Jamieson (Eds.), Polym. Phys. from Suspens. to Nanocomposites Beyond., Wiley, 2010: pp. 15–88.

[5.40] X. Geng, O.-H. Kwon, J. Jang, Electrospinning of chitosan dissolved in concentrated acetic acid solution, Biomaterials. 26 (2005) 5427–32.

[5.41] G. Bolat, G. Lisa, I.M. Popa, Experimental dynamic viscosities of binary mixtures: acetic acid + water, benzene, toluene, n-hexane, n-heptane AT 296.15, 302.15, 308.15, 314.15 and 319.15 K, Sci. Study Res. VI (2005) 181–190.

[5.42] P.B. Davis, H.C. Jones, The viscosities of binary mixtures of the associated liquids, water, formic acid and acetic acid, J. Am. Chem. Soc. 37 (1915) 1194–1198.

[5.43] M. Ago, K. Okajima, J.E. Jakes, S. Park, O.J. Rojas, Lignin-based electrospun nanofibers reinforced with cellulose nanocrystals., Biomacromolecules. 13 (2012) 918–26.

[5.44] M.L. Focarete, C. Gualandi, M. Scandola, M. Govoni, E. Giordano, L. Foroni, et al., Electrospun scaffolds of a polyhydroxyalkanoate consisting of omega-hydroxylpentadecanoate repeat units: fabrication and in vitro biocompatibility studies., J. Biomater. Sci. Polym. Ed. 21 (2010) 1283–1296.

[5.45] V. Chaurey, F. Block, Y.H. Su, P.C. Chiang, E. Botchwey, C.F. Chou, et al., Nanofiber size-dependent sensitivity of fibroblast directionality to the

methodology for scaffold alignment, Acta Biomater. (2012).

[5.46] C.L. Casper, J.S. Stephens, N.G. Tassi, D.B. Chase, J.F. Rabolt, Controlling surface morphology of electrospun polystyrene fibers: Effect of humidity and molecular weight in the electrospinning process., Macromolecules. 37 (2004) 573–578.

[5.47] A. Koski, K. Yim, S. Shivkumar, Effect of molecular weight on fibrous PVA produced by electrospinning, Mater. Lett. 58 (2004) 493–497.

[5.48] C.-M. Hsu, S. Shivkumar, Nano-sized beads and porous fiber constructs of Poly(ε-caprolactone) produced by electrospinning, J. Mater. Sci. 39 (2004) 3003–3013.

CHAPTER 6:

Preparation of electrospun nanofibers from solutions of different gelatin types using a benign solvent mixture composed of water/PBS/ethanol

Preparation of electrospun nanofibers from solutions of different gelatin types using a benign solvent mixture composed of water/PBS/ethanol

SUMMARY

The feasibility of using Phosphate Buffer Saline (PBS)/ethanol mixtures as a benign solvent to electrospin three type of gelatins was studied. Gelatins with different chemical properties, such as Bloom, were selected and the effect of the gelatin type and its concentration on the electrospinnability of the dope solution and on the fiber diameter of the electrospun mats were studied. Viscosity of the gelatin solution, which follows a power law relationship with the gelatin concentration, was found to significantly influence the morphology of the mats and the fiber diameter. It was demonstrated that the PBS/ethanol solvent interacted with the gelatins as a good solvent with a Flory exponent of 0.65. In addition, the effect of the solvent composition on the fiber formation process was evaluated corroborating that the ionic strength of the medium and the PBS/ethanol ratio significantly affected the morphology and the diameter of the electrospun fibers. Chemical structure and thermal stability of the electrospun gelatin mats were characterized by Fourier Transform Infrared Spectroscopy (FTIR) and Differential Scanning Calorimetry (DSC). Finally, cytotoxicity of the electrospun mats was analyzed by the Alamar Blue assay, using human foreskin fibroblasts (BJ-5ta), resulting in a high cell viability (80-90%) regardless the type of gelatin.

Keywords: electrospinning, nanofibers, gelatin, Phosphate Buffer Saline, ethanol.

6.1. Introduction

The electrospinning process has proved to be an interesting technique to fabricate polymer fibers with diameter ranging from few nanometers to micrometers. Although electrospinning is an old technique, first observed in 1897 by Rayleigh and patented on 1934 by Formhals [6.1], it has gained popularity in the last 10 years due to the recent interest in nanoscale technologies and to its potential applicability for the development of applications in several fields such as biomedical, pharmaceutical, biotechnological and environmental engineering [6.2-6.3].

Nano- and micro-electrospun fibers are fabricated by applying a high voltage electrostatic field between a capillary syringe containing a polymer solution and a grounded collector where the polymer fibers are deposited [6.4]. As a result, a nonwoven fibrous web or mat is obtained, which properties depend on parameters related to the process, the polymer solution and the ambient conditions [6.5-6.6].

Among the different possible applications of such mats, in recent years numerous reports have proposed the design and manufacturing of scaffolds made of electrospun fibers for tissue engineering applications using solutions of natural polymers due to their capacity of mimicking the structural and functional properties of extracellular matrices [6.7-6.8]. Among the various natural polymers that could be electrospun into fibrous scaffolds [6.9-6.10], gelatin is one of those most extensively investigated since it has properties comparable to those of collagen and it is also an abundant and low cost material.

Gelatin is derived from the parent protein collagen by chemical or biochemical processes that break up the secondary and further structures with varying degrees of hydrolysis of the polypeptide backbone [6.11]. For gelatin production the raw material may be any collagen-containing tissue such as skin, muscle and bone and, depending on the hydrolysis method used, two different types of gelatin are produced: type A (acid-treatment) and type B (alkali-treatment). Accordingly, the chemical properties of the gelatin products are affected by the animal species they come from, the nature of the tissue as well as by the type of treatment carried out for its extraction [6.12-6.13]. Those factors determine some important parameters such as the amino acid composition, the molecular weight distribution and the gel strength of each gelatin which are the key parameters controlling the viscosity of gelatin solutions. Since viscosity is one of the major parameters ruling electrospinnability, the aforementioned parameters are also decisive [6.14].

Regardless the type of gelatin, other crucial factor influencing the electrospinnability is the solvent selection [6.15]. Particularly, in order to successfully electrospin gelatin, the solvent system must be capable of avoiding the gelation process that occurs between gelatin and cold water (< 37 ºC) [6.16] and inducing an optimal viscosity to the dope solution, facilitating its movement through the syringe during electrospinning. In this regard, some complex solvents such as 1,1,1,3,3,3-hexafluoro-2-propanol or 2,2,2-trifluoroethanol were initially used to dissolve and electrospin natural polymers such as gelatin at room temperature [6.17-6.20], but their ability to form strong hydrogen bonds with protein based polymers hinders the complete removal of these solvents from the obtained fibers. As a result, not only the protein chemical structure is affected but undesirable reactions can also occur due to the high cytotoxicity of such solvents [6.21]. Alternatively, solvents based on carboxylic acids, such as formic acid [6.22-6.23] and acetic acid [6.15, 6.24-6.26], have been recently proposed for electrospinning of protein-based polymers [6.14, 6.27]. However, in most of reported cases a high concentration of acid (more than 60% v/v) is required, inducing the partial decomposition of gelatin and adversely affecting the structural integrity of nanofibers [6.22].

In order to overcome the disadvantages of using fluoroalcohols or carboxylic acids, a solvent consisting of a dilution of phosphate buffer saline in ethanol (hereafter water/PBS/ethanol) has already been proposed to prepare collagen or gelatin solutions for electrospinning [6.10, 6.28-6.29]. Such mixed solvent effectively dissolves gelatin, disrupting both hydrophobic and hydrogen bonding interactions between amino acids of gelatin as well as it provides an adequate medium for electrospinning [6.30]. A proper balance of the three components of the mixture may change some properties of the dope solution such as viscosity, surface tension, conductivity and degree of gelation [6.31], therefore determining their electrospinnability.

The purpose of this study was to assess the feasibility of using water/PBS/ethanol mixture as a benign and advantageous solvent for the electrospinning of different gelatins. Specifically, the three studied gelatins were obtained from bovine skin (BS), bovine bone (BB) or porcine skin (PS). BS and BB gelatins are type B gelatin whereas PS gelatin was obtained by acid treatment (type A). The effects of the gelatin type its concentration and the composition of the solvent were studied regarding the electrospinnability of the dope solutions and the diameter of the obtained fibers. In addition, the effect of those variables on the chemical structure and cytotoxicity of the resulted electrospun gelatin mats was analyzed.

6.2. Experimental

6.2.1. Materials

Gelatin type B from bovine skin (BS) (Bloom ~ 225 g) and gelatin type A from porcine skin (PS) (Bloom ~ 300 g) were purchased in their powder form from Sigma Aldrich (Madrid, Spain). Gelatin type B from bovine bone (BB) (Bloom ~ 250 g) was provided by Rousselot Gelatin S.L (Girona, Spain). All gelatins were used without further treatment or purification. Note that Bloom value is a currently used test to measure the strength of a gelatin and is directly related to molecular weight of the polymer [6.32].

Phosphate buffer saline (PBS) solution was also purchased in form of tablets from Sigma Aldrich. One tablet dissolved in 200 mL of deionized water yields 1X PBS solution (0.01 M phosphate buffer, 0.0027M potassium chloride and 0.137 M sodium chloride), with pH 7.34 at 25ºC. Different PBS buffers were obtained by diluting 20X PBS stock (10 tablets in 100ml) using bidistilled water. To prepare the dope solution, each gelatin was dissolved at room temperature in PBS/ethanol mixtures of different composition.

6.2.2. Nanofibers mats preparation

Electrospun gelatin nanofibers were obtained by the electrospinning process, performed in a home-made device developed by INTEXTER [6.14, 6.33]. Each gelatin solution was placed in a 2.5 ml syringe with a stainless steel syringe needle (0.6 mm of inner diameter) connected to the anode of a power supply. The electrospun gelatin fibers were collected on aluminum foil covering the copper collector that is connected to the cathode of the power supply. All solutions were electrospun at room temperature (~25ºC).

Firstly, to study the effect of the type and concentration of gelatin on the electrospinnability and fiber diameter of the electrospun fibers, the following procedure was followed: each gelatin was dissolved at different concentration (100, 120, 140, 160, 180 and 200 mg/ml) on the same solvent system formed by aqueous solution of PBS(10X) and ethanol, at ratio 1:1 v/v. The resulting solutions were subsequently electrospun at the selected conditions of voltage, flow rate and distance between the needle and the collector that contributes to better electrospinnability. It is noteworthy to mention that for two different concentrations of gelatins (100 and 120 mg/ml) there was not a significant influence of operational parameters in the ranges of study: voltage

(15, 18 and 21.5 kV), flow rate (0.75 and 1 ml/h), and distance between the needle and the collector at (9 cm).

Secondly, to evaluate the influence of the composition of the ternary solvent on the electrospinnability and fiber diameter, gelatin solutions of a fixed concentration (120 mg/ml) were prepared using two different series of solvent mixtures. On the one hand, solutions with different PBS/ethanol ratios (3:2, 1:1, 2:3) maintaining the PBS concentration (10X) were tested. On the other hand, solutions with different PBS concentration (5X, 10X, 20X) were prepared maintaining the PBS/ethanol ratio (1:1).

6.2.3. Fiber characterization

The diameter and morphology of electrospun gelatin fibers were analyzed by Scanning Electron Microscopy (SEM) using a Phenom Standard SEM. Samples were observed without any metallic coating. The average fiber diameter was estimated by measuring the diameter of 50 arbitrary electrospun fibers using an image analyzing software package (ImageJ).

Besides, chemical structure of the electrospun fibers was analyzed by Fourier Transform Infrared Spectroscopy (FTIR) by using a Nicolet Avatar 320 spectrophotometer (Nicolet Instrument Corporation, USA). Samples were prepared by mixing 1 mg of fibers taken from the mat in a matrix of 300 mg of KBr followed by pressing (167 MPa). The spectrum was recorded in the range of 500 to 4000 cm^{-1}, averaging 32 scans at a resolution of 4 cm^{-1}.

Finally, the thermal properties of gelatin electrospun fibers were analyzed by Differential Scanning Calorimetry (DSC) by using a Perkin Elmer DSC7. During DSC measurements, a specimen (~ 4 mg) was heated from 50ºC to 300ºC at a heating ratio 20 ºC/min under a constant flow of a nitrogen atmosphere of 50 ml/min.

6.2.4. Cytotoxicity evaluation

Human foreskin fibroblasts (BJ-5ta) were used to determine the potential toxicity of the electrospun gelatin mats.

6.2.4.1. Cell culture

Cells were maintained in 4 parts Dulbecco's Modified Eagle's Medium (DMEM) containing 4 mM L-glutamine, 4500 mg/l glucose, 1500 mg/l sodium bicarbonate, 1 mM sodium pyruvate and 1 part of Medium 199, supplemented with 10 % (v/v) of fetal

bovine serum (FBS), and 10 g/ml Hygromycin B at 37 ºC, in a humidified atmosphere with 5 % CO_2, according to the recommendations of the manufacturer. The culture medium was replaced every 2 days. At pre-confluence, cells were harvested using trypsin-EDTA (ATCC-30-2101), 0.25 % (w/v) trypsin/0.53 mM EDTA solution in Hank's BSS without calcium or magnesium. Both BJ-5ta (ATCC-CRL-4001) and DMEM (ATCC-30-2002) were purchased from American Type Culture Collection (LGC Standards S.L.U, Spain).

6.2.4.2. Alamar Blue assay

Cultured cells were seeded at a density of 4.5 x 10^4 cells/well on 96-well tissue culture-treated polystyrene plate (Nunc) the day before experiments, exposed to gelatin mats in solution (20 mg/mL in DMEM) at a final volume of 100 µL and incubated at 37 ºC in a humidified atmosphere with 5 % CO_2. Cells were examined after 24 h for signs of toxicity, using Alamar Blue assay. Resazurin, the active ingredient of AlamarBlue® reagent (Invitrogen, Life Technologies Corporation, Spain), is a non-toxic, cell-permeable compound that is blue in color and reduced to resorufin by viable cells, developing a red color compound.

After 24 h of contact with cells, the solution of dissolved scaffolds was removed, the cells washed twice with PBS and stained with AlamarBlue® reagent. 100 µL of 10 % (v/v) AlamarBlue® reagent in DMEM was added to the cells and incubated for 4 h at 37 ºC, after which the absorbance at 570 nm was measured, using 600 nm as a reference wavelength, in a microplate reader (Infinite M 200 plate reader, Tecan). The quantity of resorufin formed is directly proportional to the number of viable cells.

BJ5ta cells relative viability (%) was determined for each mat of electrospun fiber and compared with that of cells incubated only with cell culture medium. Hydrogen peroxide (500 µM) was used as a positive control for cell death.

All tests were performed by triplicate.

6.2.5. Statistical analysis

One-way analysis of variance (ANOVA) was used to determine the statistically significant differences between the average diameters of the electrospun fibers. The confidence interval was set at 95% and a p value less than 0.05 was considered to be a statistically significant difference. All statistical analyses were performed using Statgraphics Centurion XV.

6.3. Results and discussion

6.3.1. Effect of the operational parameters, type and gelatin concentration on the solutions electrospinnability

It has been reported that the physicochemical properties of the dope solution (i.e. viscosity) are much more crucial for controlling the degree of electrospinnability and the final diameter of the electrospun fibers than the operational conditions (i.e. voltage or flow) [6.14, 6.22, 6.34-6.36]. Accordingly, for the present system the observed differences should be due to both the type and concentration of the electrospun gelatin or the nature and composition of the solvent.

To validate the aforementioned hypothesis, a preliminary study was carried out to evaluate the effect of voltage and flow rate on the fiber properties. The average diameter of electrospun gelatin nanofibers obtained at different operational conditions are reported in (**Table 6.1**) and results were analyzed by ANOVA **(Table 6.2)**.

***Table 6.1**. Average diameter of gelatin fibers obtained at different operational conditions of voltage (15, 18, 21.5 V) and flow rate (0.75, 1 ml/h). Three types of gelatins (BS, BB, PS) and two concentrations (100 and 120 mg/ml) were tested**.** Uncertainty corresponds to the standard deviation of 50 measures*

Flow Rate (ml/h)	Voltage (kV)	Type of Gelatin	[Gelatin] (mg/ml)	Average diameter (nm)
0.75	18	BS	100	97 ± 12
0.75	21.5	BS	100	102 ± 14
0.75	15	BS	100	105 ± 14
0.75	15	BS	120	130 ± 15
0.75	18	BS	120	127 ± 13
0.75	21.5	BS	120	123 ± 12
0.75	21.5	BB	100	168 ± 17
0.75	18	BB	100	164 ± 15
0.75	15	BB	100	164 ± 17
0.75	18	BB	120	186 ± 21

1.0	15	BB	120	194 ± 18
0.75	15	BB	120	206 ± 21
075	15	PS	100	304 ± 37
1.0	15	PS	100	316 ± 43
1.0	18	PS	100	319 ± 38
1.0	18	PS	120	429 ± 68
1.0	15	PS	120	418 ± 79
0.75	15	PS	120	413 ± 72

***Table 6.2**. ANOVA analysis to assess the effect of voltage, flow rate and type and concentration of gelatin on the diameter of electrospun fibers*

Source of variance	Sum of Squares	Degrees of freedom	Mean square	F	Critical value of F (p=0.05)
Flow Rate	2014.95	2	1007.48	2.09	0.1741
Voltage	52.3409	2	26.1705	0.05	0.9474
Gelatin Type	96119.2	2	48059.6	99.83	0.0000
Concentration	9863.57	1	9863.57	20.49	0.0011
Error	4814.23	10	481.423		
Total	225274.	17			

Taking into account the obtained results, it was demonstrated that only the type and concentration of gelatin had a significant effect on the electrospun fiber diameter ($F_{critical}$ < 0.05). Thus, hereafter, all the solutions were electrospun selecting the optimal operational parameters (voltage and flow rate) that provided the best degree of electrospinnability in terms of the stability of the jet.

Besides, the SEM micrographs shown in **Figure 6.1** display the morphology of the electrospun mats obtained from the three types of gelatin at different concentrations using a single solvent composition, namely PBS(10X)/Ethanol, 1:1 v/v.

As it can easily observed, some differences on morphology occurred and were associated to both the gelatin concentration and its type, as it was initially suggested. For instance, nanofibers with beads were more often found in those mats prepared with a low concentration of gelatin BS, which had the lowest Bloom. The reason is that at low concentrations of polymer the viscosity of the solution was also low (see **Figure 6.2**) and the high surface tension of polymer solutions leaded to the instability and the breakup of the solution jet into droplets [6.37]. It is worth to mention that the incidence of beads decreased either when increasing the concentration or when increasing the Bloom of the gelatin. Both factors (concentration and Bloom) improved the quality of fibers because the electrospining jet was stabilized due to the increase of the solution viscosity that, in turn, was related to the intensification of polymer chain entanglement. As a result, bead-free nanofibers were obtained for BS gelatin at 200 mg/ml and for BB and PS gelatins at any of the tested gelatin concentrations.

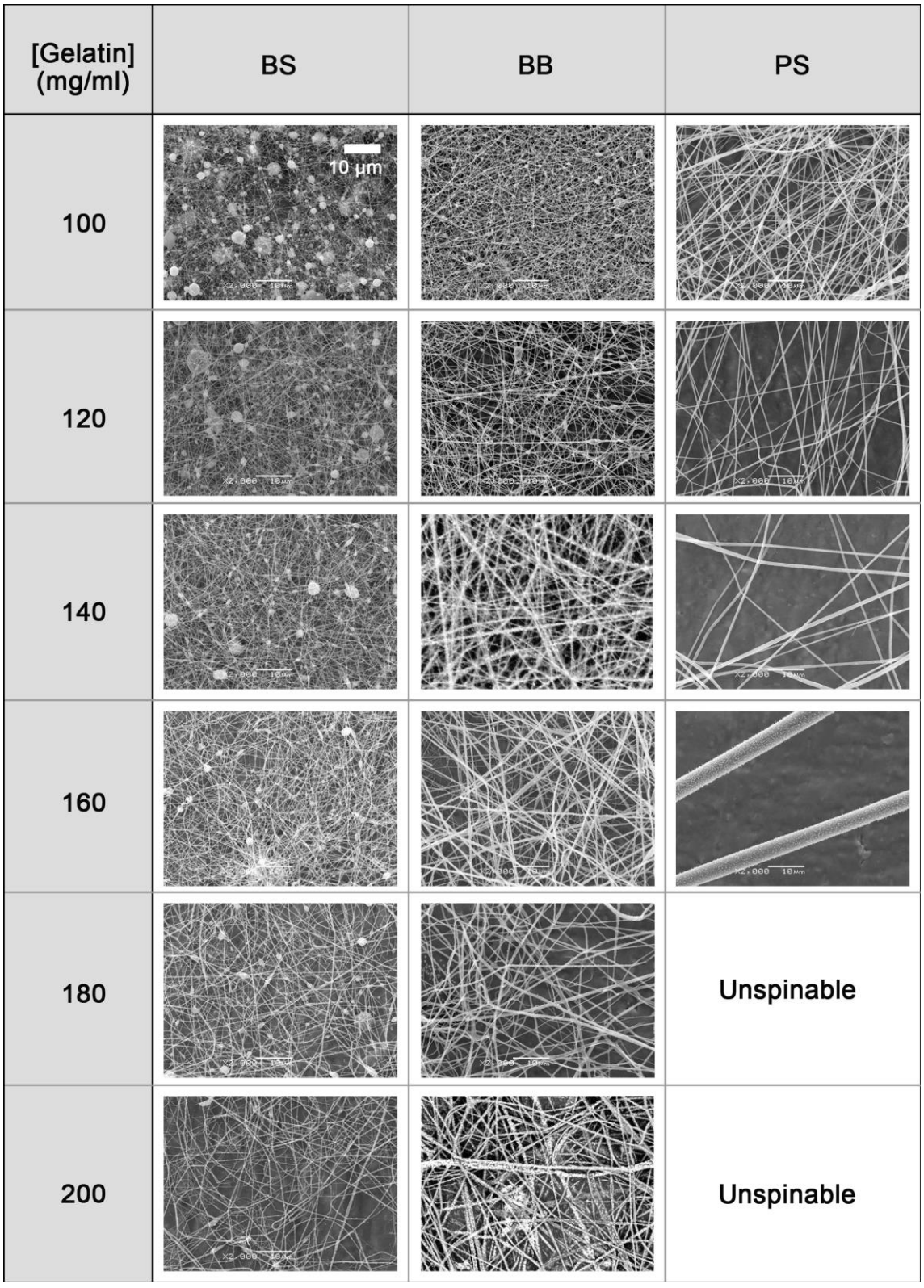

Figure 6.1. *SEM images of electrospun fibers obtained from BS, BB and PS gelatin solutions at different concentration showing morphology and electrospinnability. PBS (10X)/ethanol ratio 1:1 v/v*

However, when viscosity was too high the gelatin solutions were found unspinnable. This was the case for solutions of the gelatin with the highest Bloom (PS) at concentration ≥ 180 mg/ml.

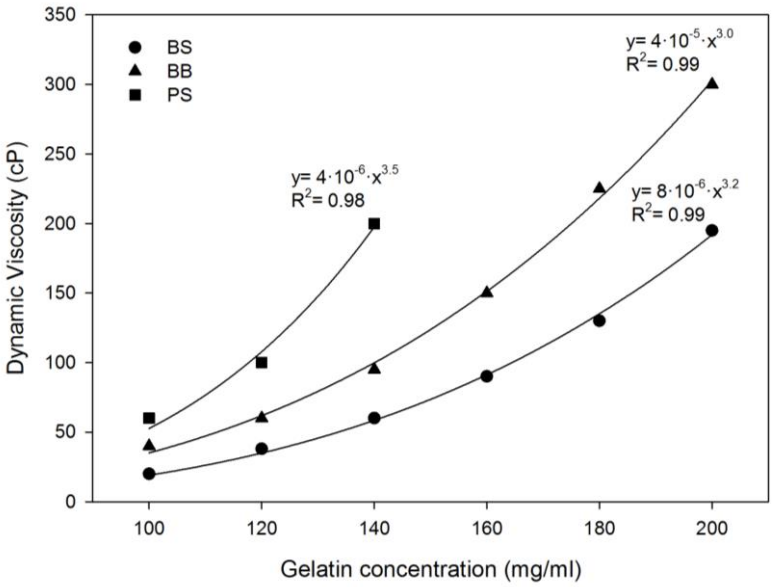

***Figure 6.2**: Dynamic viscosity of solutions vs. gelatin concentration for each gelatin type*

Figure 6.2 depicts the evolution of dynamic viscosity versus gelatin concentration for the three different gelatin tested. As it has been reported previously, viscosity follows an allometric ($\eta = \alpha c^{ß}$) relationship with the concentration of gelatin [6.15, 6.22, 6.34, 6.38]. More concretely, the relationship between dynamic viscosity and concentration of gelatin in semidilute regime is usually given by the equation proposed by De Gennes (Equation 6.1):

$$\frac{\eta}{\eta_s} = \eta_r = \left(\frac{c}{c^*}\right)^{3/(3\nu-1)} \qquad \textit{(Eq. 6.1)}$$

where η_r stands the relative viscosity, η_s stands for the viscosity of the solvent, c* stands for the critical chain overlap concentration and ν stands for the Flory exponent, which has been widely used to characterize polymer-solvent intermolecular interaction giving yield to the so-called good, theta and poor solvent behavior [6.39].

The parameter c* marks the onset of significant polymer chain overlap in solution and can be estimated by using Equation 6.2 [6.40]:

$$c^* = \frac{2.5}{[\eta]} \qquad \textit{(Eq. 6.2)}$$

where [η] is the intrinsic viscosity, defined as the increase in viscosity of a solvent through the addition of an infinitesimal amount of solute. In our case, [η] was experimentally determined by measuring the dynamic viscosity of diluted solutions and extrapolating to infinite dilution by the well-known Huggins equation (Equation 6.3), where η_{sp} is the specific viscosity of the polymer solution and K_H is the Huggins constant [6.41-6.42].

$$\frac{\eta_{sp}}{c} = [\eta] + K_H[\eta]^2 c \qquad \textit{(Eq. 6.3)}$$

The intrinsic viscosities of the different gelatin, [η], estimated for the solutions using PBS(10X)/ethanol 1:1 v/v as a solvent, are reported in **Table 6.3**. Based on the estimated [η] values, the c* concentration was then theoretically calculated for each system by using Equation 6.2 and the corresponding values are also reported in the same table. It is worth to note that c* was lower for gelatins with higher Bloom ($c^*_{PS} < c^*_{BB} < c^*_{BS}$) indicating that in this case chain overlapping occurred at lower concentration of gelatin compared to solutions prepared using gelatin of lower Bloom.

***Table 6.3**. Intrinsic viscosities, [η] of the tested gelatins calculated by Huggin's equation and the calculated critical chain concentration (c*)*

Gelatin type	Bloom (g)	[η] (ml/mg)	c* (g/ml)
BS	225	0.29	8.6
BB	250	0.33	7.5
PS	300	0.43	5.8

Following De Gennes' equation (Equation 6.1) the relationship between relative viscosity and c/c* ration allows to establish the regime of work (dilute, semidilute untentangled or semidilute entangled) based on the changes in the slope of the plot of **Figure 6.3** [6.43]. In this case, taking into account that c/c* > 1 for all the experiments and that these data fitted well to a single straight line of slope 3.11, it can be concluded that all the experiments were carried out on a semidilute entangled regime, where the gelatin concentration was high enough to induce a significant degree of entanglement between polymer chains. As it has been said before, the scaling exponent is directly related to the Flory exponent (Equation 6.1). Here, the estimated Flory exponent was 0.65 indicating that the PBS(10X)/Ethanol 1:1 v/v solvent behaves similarly to as a good solvent for the three tested gelatins (the theoretical value for a good solvent is

0.6). Note that the same behavior has been corroborated for alternative systems such as gelatin/acetic acid solutions [6.14].

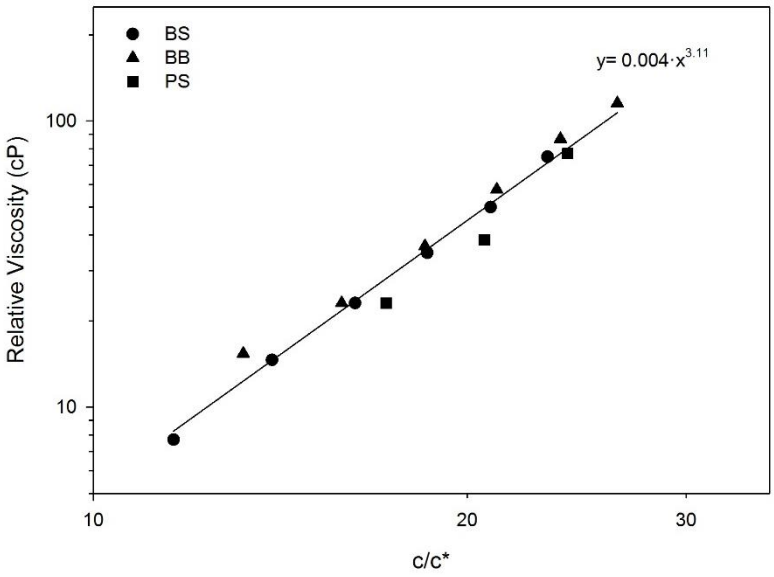

***Figure 6.3**: Relative viscosity versus c/c* of the three gelatins*

6.2.6. Effect of the type and gelatin concentration on the fiber diameter

After having seen how the type and concentration of the gelatin solution determined the viscosity of the dope solution and, as a result, influenced the electrospinnability and morphology of gelatin mats, a comprehensive study of the effect of the viscosity on the diameter of the electrospun fibers was carried out.

The influence of the gelatin concentration on the diameter of the electrospun fibers is depicted in **Figure 6.4**. Results indicated that an increase of the average diameter of the nanofibers was produced with the increasing of gelatin concentration. This behavior was the same independently of the type of gelatin considered and was in agreement with the results obtained by Zha et al. based on the electrospinning of porcine skin gelatin [6.31].

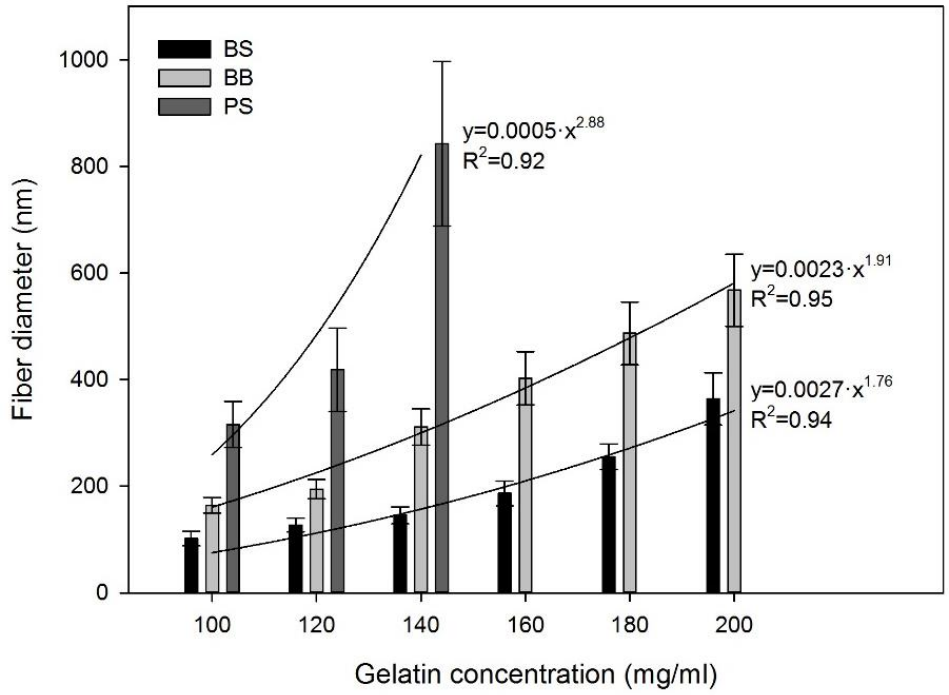

Figure 6.4. *Average diameter of the electrospun gelatin fibers obtained from BS, BB and PS gelatins at different concentration*

As regard to the relationship between the diameter of the electrospun fibers and the concentration of the gelatin solutions, the following allometric equation is often used to correlate the data [6.34, 6.44-6.46]:

$$d = \alpha(Be)^{\beta} \qquad \textit{(Eq. 6.4)}$$

where Be is a dimensionless number called Berry number (Be) defined as the product of the polymer concentration (c) and the solution intrinsic viscosity (Be=c*[η]) and it accounts for the regime of electrospinnability and the diameter of the resulted fibers.

The average diameter of the fibers was plotted against the Be number in **Figure 6.5** (both axes at logarithmic scale). As it can be observed, a linear relationship was found for each type of gelatin although the scaling exponent β varied from one polymer to another. Thus, it was not possible to obtain a unique relationship between the diameter and the dimensionless number Be that encompassed the behaviour of the three solvent-gelatin systems. This fact is quite coherent since each of the tested polymers bears a different chain length and, therefore, a different molecular weight and dissimilar rheological properties.

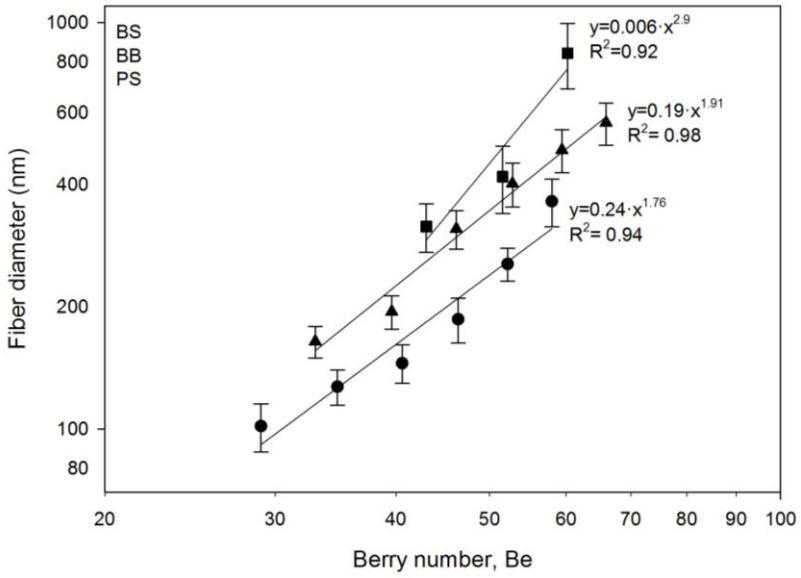

***Figure 6.5**: Average diameter of electrospun fiber versus Berry number for the three tested gelatins*

However, from a practical point of view, it would be advantageous of find a simple way to consider the three gelatins as if they were a single system so that knowing Be (or a similar parameter) one could predict the average diameter of the obtained fibers. Empirically, among several possible approaches, it was observed that the product Be·[η] provided a single and acceptable fitting (R^2 = 0.94) for the data of the three tested gelatins, thus unifying the behaviour of the three systems (see Equation 6.5 and **Figure 6.6**).

$$d = \alpha(Be[\eta])^{\beta} \qquad \textit{(Eq. 6.5)}$$

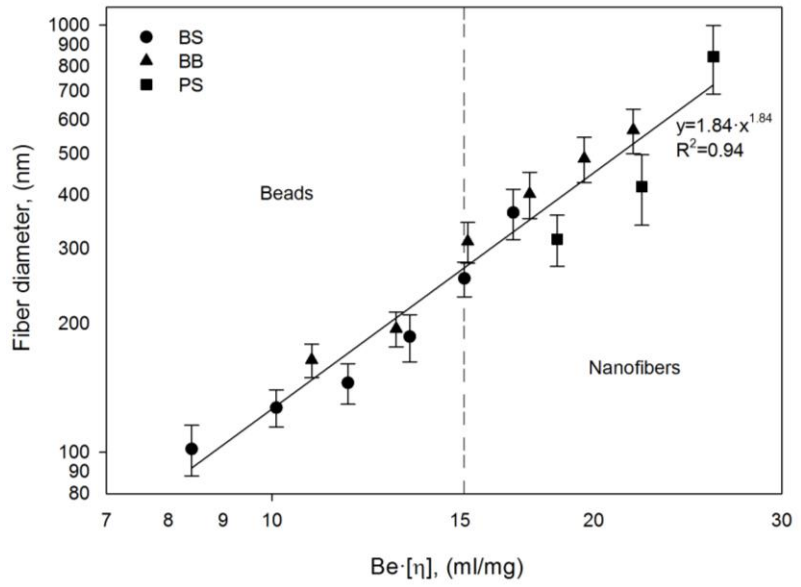

***Figure 6.6**: Average diameter of electrospun fiber versus Be·[η] for the three tested gelatins*

Taking into account that studied proteins mainly differ from the molecular w eight which strongly influences the value of [η]; it seems consistent that the correction of Be is made precisely with [η]. Moreover, thanks to this representation, it is feasible to clearly identify two different electrospinability domains: nanofibers for Be·[η] > 15 and beaded-fibers for Be·[η] < 15. Therefore, this kind of representation results in a useful tool for predicting not only the nanofiber diameter but also their morphology.

6.2.7. Effect of the solvent composition

Solvent properties have an important role in the electrospinning of gelatin at room temperature since the medium determines the polymer-solvent intermolecular interactions [6.4]. In this regard, any change in the composition of the water/PBS/ethanol ternary mixture would directly affect the physicochemical properties of the dope solution. For that reason, the effect of the solvent composition on the electrospinnability of gelatin and fiber diameter was studied.

Firstly, the influence of ethanol concentration was studied by electrospinning some solutions prepared with different amount of ethanol and PBS(10X) and containing any of the three studied gelatins at a fixed polymer concentration (120 mg/ml). A this point it is important to state that, on the one hand, gelatin is not soluble on pure ethanol, so a minimal amount of PBS might be necessary to prepare the solutions. Conversely, high concentrations of PBS induce the gelation process (what would hinder electrospinnig process) so a noticeable amount of ethanol is indeed required to break down hydrogen bonding between gelatin and water [6.47]. Considering this, three PBS(10X)/ethanol volume ratios (3:2, 1:1 and 2:3) were chosen to prepare the tested gelatin solutions. Within the selected ranges of composition, which were in agreement with previous works [6.31], homogeneous solutions were produced for each gelatin type.

The morphology of the mats and the average diameter of the resulted nanofibers are illustrated in **Figure 6.7** and **Figure 6.8**, respectively. From the results it can be seen that gelatins showed a similar behavior when the ratio PBS/ethanol decreased: free-beads nanofibers mats with fiber of higher diameter were obtained when electrospinning solutions with the lowest PBS/ethanol ratio. According to the literature [6.48] , the observed trend is due to the decrease of conductivity of the dope solution that occurs when increasing the amount of ethanol or decreasing the amount of salts coming from PBS solution. Both effects are maximized for the 2:3 PBS/ethanol medium. As a result of the decrease of conductivity, the solution jet is less stretched under a high electric field increasing the diameter of the electrospun fibers.

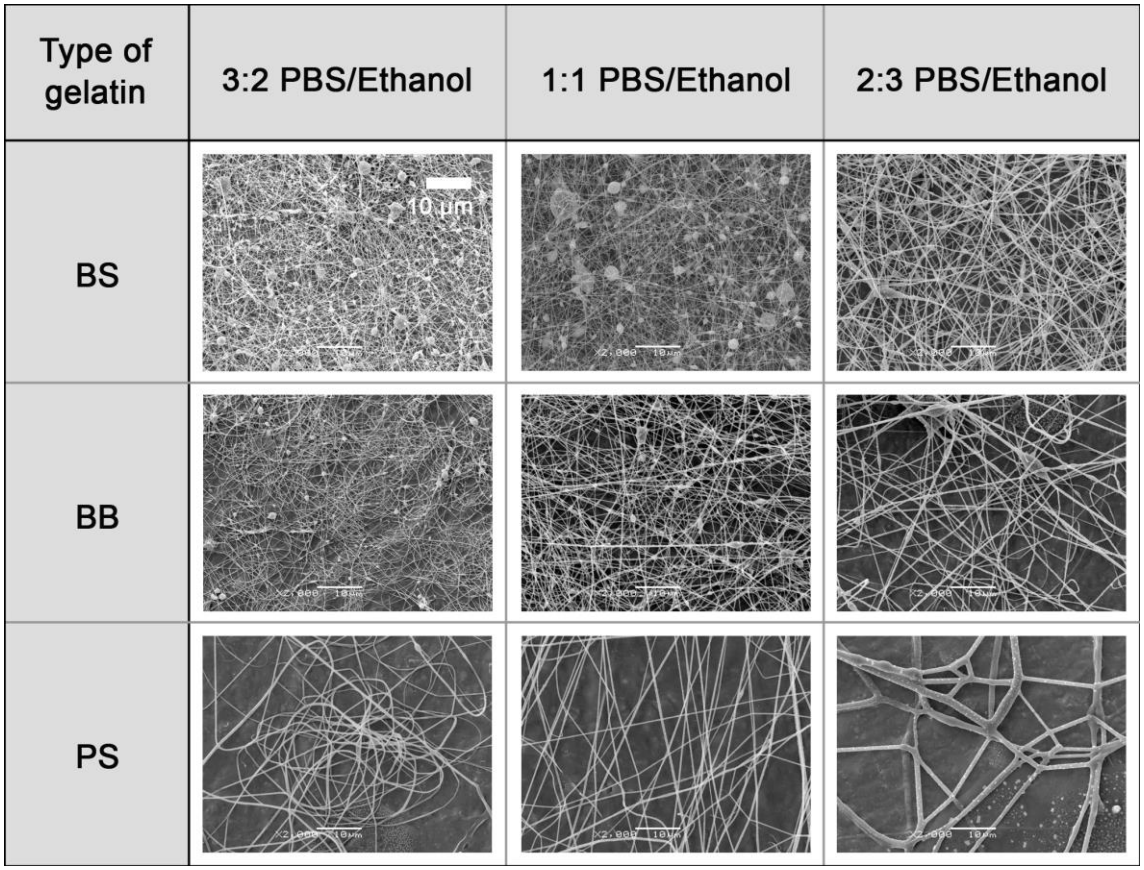

***Figure 6.7**: SEM micrographs of nanofibers mats from different gelatin type and ratio PBS/ethanol*

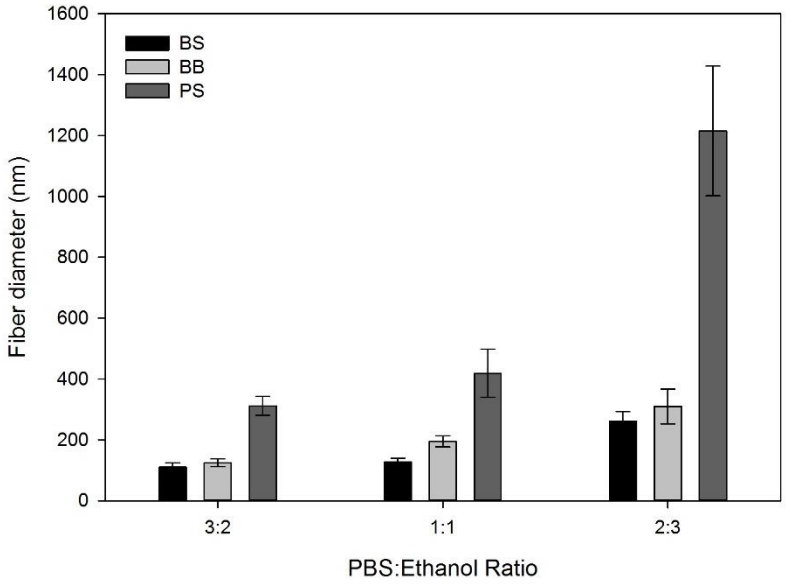

***Figure 6.8**. Average fiber diameter as a function of PBS(10X)/ethanol ratio*

Secondly, the influence of the ionic strength of the solvent on the electrospinnability of gelatin solutions and on the morphology of the obtained nanofibrous mats was analyzed in detail. For that purpose, gelatin solutions at a concentration of 120 mg/ml were prepared in 1:1 PBS/Ethanol solvent using solutions of PBS of different

concentration (5X, 10X and 20X). In this case, the total amount of ethanol was the same for all the studied samples, as well as the gelatin/ethanol ratio. The studied concentrations of the PBS solutions were chosen taking into account that gelatins are not soluble on pure ethanol nor in 1:1 water/ethanol mixtures [6.31] and therefore a minimal amount of ions (Na^+ and K^+) must be added to break down the gelatin networks and form the solution.

Results regarding the morphology of the nanofibers mats and their average fiber diameter can be seen in **Figure 6.9** and **Figure 6.10**, respectively. In this case, the solutions containing a lower salt concentration (<10X) form uneven fiber mats with large amount of beads, where, in addition, the salt crystals are very noticeable. Increasing the ionic strength the uniformity of the mats increases at the same time that fiber diameter decreases (**Figure 6.10**), along with the presence of the crystals. These results are in agreement with the previous literature [6.31] and are also related with the change of the solution conductivity: an increase of the ionic strength enhances the solution conductivity and, consequently, the solution jet is stretched under high electric voltage, which lead to fabricate a smaller fibers and more uniform fiber mats.

Although the behavior of both morphology and diameter of electrospun fibers as a function of PBS concentration is similar for the three gelatins, it is important to note that the amount of salt necessary to obtain a homogeneous solution (for the same gelatin concentration) is different in function of the type of gelatin and directly related with the gelatin gel strength. For this reason, solutions of PS gelatin in 5X PBS were not suitable for electrospinning (**Figure 6.9**).

Type of gelatin	1:1 PBS(5X)/Ethanol	1:1 PBS(10X)/Ethanol	1:1 PBS(20X)/Ethanol
BS	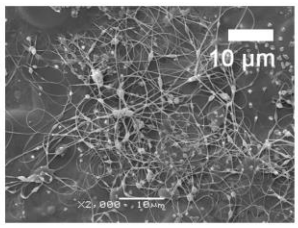	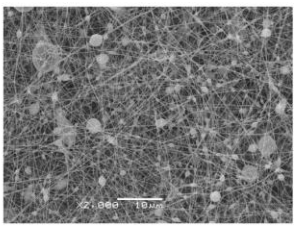	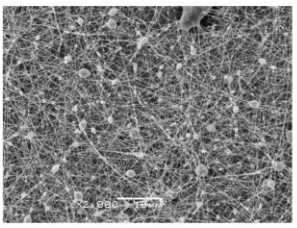
BB	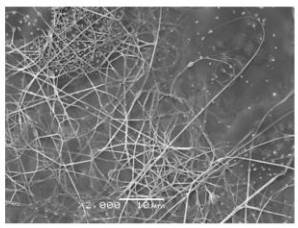	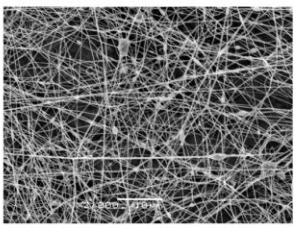	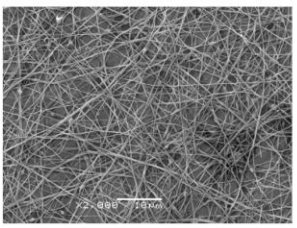
PS	Unspinable	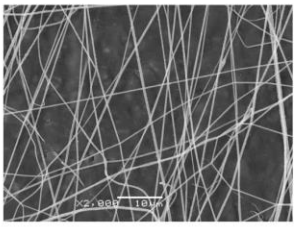	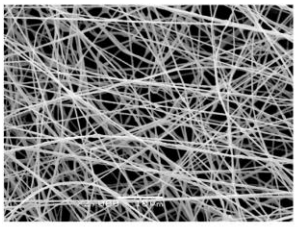

***Figure 6.9**: SEM micrographs of nanofibers mats of the three types of gelatins obtained varying the PBS concentration*

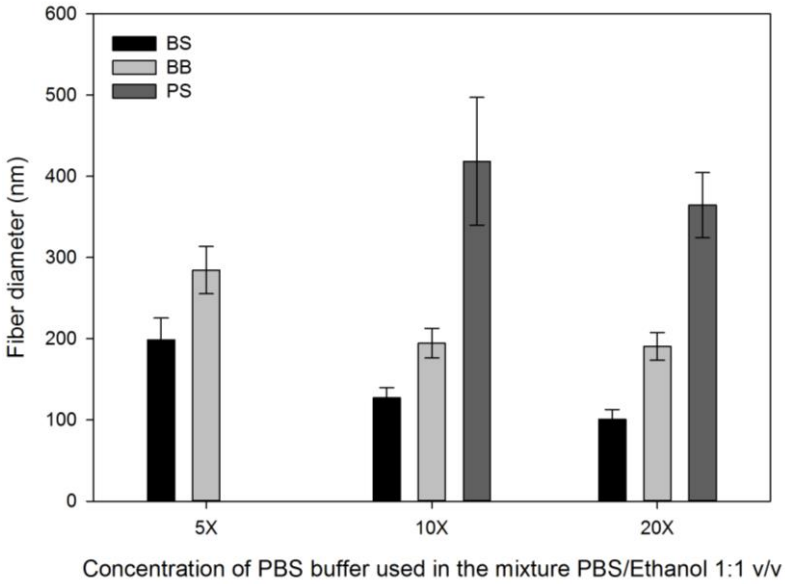

***Figure 6.10**: Average fiber diameter as a function of PBS solution concentration*

6.2.8. Nanofibers characterization

So as to compare the chemical structure of electrospun gelatins and their original counterparts in powder form were analyzed by FTIR. Specimens of nanofibers mats with a similar average diameter were selected to avoid any differences related to fiber solvent sorption on the analysis. Hence, the mats samples were prepared by electrospinning solutions of 200 mg/ml for BS, 140 mg/ml for BB and 100 mg/ml for PS gelatin. The solvent composition and ionic strength was the same for all three samples (PBS (10X)/Ethanol, 1:1).

The results are shown in **Figure 6.11** and, despite the fact that the spectra of powder gelatins were much more attenuated and smooth, all the spectra showed the characteristic IR bands of gelatin at ~3300, ~1650, ~1540 and ~1240 cm^{-1} corresponding to the Amide A (N-H stretching vibration), Amide I (C=O stretch), Amide II (N-H bend and C-N stretch) and Amide III (C-N stretch plus and N-H deformation), respectively [6.49].

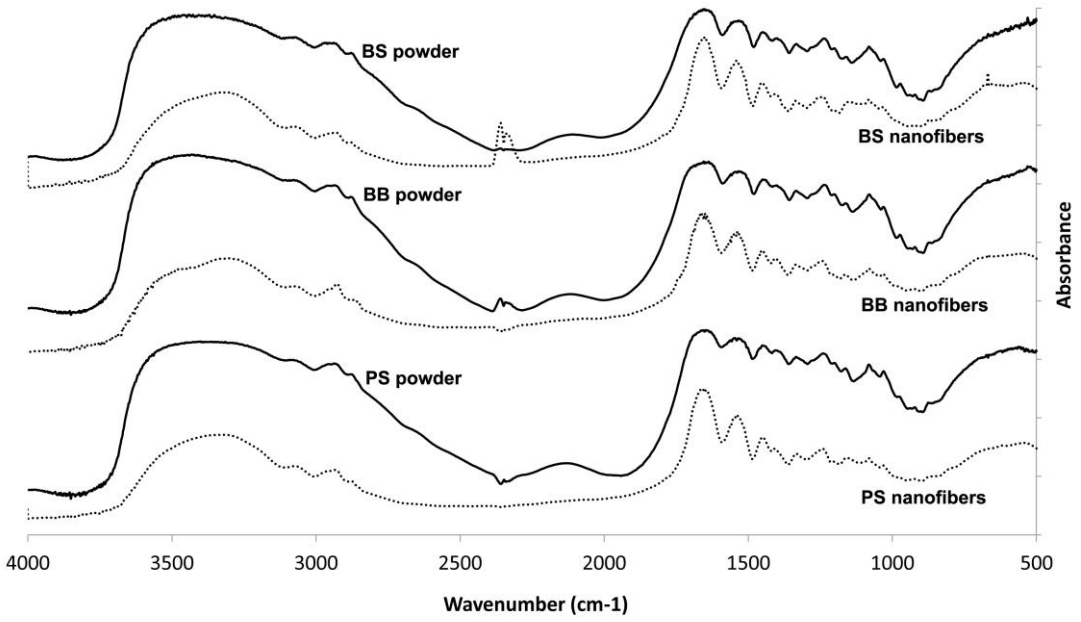

***Figure 6.11**: FTIR spectra of different gelatin type solutions dissolved in PBS(10X)/ethanol 1:1 v/v before (powder) and after (mat) the electrospinning process*

From these results it could be concluded that no change in the chemical structure of the gelatin occurred during the electrospinning process, as it had also been reported previously on many cases [6.22, 6.49]. However, the FTIR technique might not be sensitive enough to underline small structural differences between samples, particularly those related to protein conformation. Therefore, Differential Scanning Calorimetry

(DSC) analyses were carried out to check whether any denaturalization process affected the chemical structure of three different gelatins either by the dissolution step or by the electrospinning process. The DSC thermograms of the three studied gelatins, both before and after their dissolution on the ternary mixture based solvent (PBS(10X)/ethanol, 1:1v/v), are shown in **Figure 6.12**.

Conversely to what happened by FTIR analysis, strong differences between pure gelatins and their analogue fiber mats were clearly observed at the characteristics peaks corresponding to the glass transition temperature (T_g, first peak in the range 90-110ºC) and to the melting point (T_m, second peak in the range 200-230ºC).

Both T_g and T_m were significantly lower for all the gelatin nanofiber mats ($T_{g,n}$ = 95 ºC and $T_{m,n}$ = 200 ºC) compared to the thermal properties of the three powder gelatins ($T_{g,p}$ = 110 ºC and $T_{m,p}$ = 230 ºC). In fact, for the nanofibers, the T_m was only partially identified as a shoulder in the thermograms. According with the literature [6.50-6.52], the dissolution step or/and the electrospinning process negatively affect the gelatin thermal stability due to the destabilization of its original chemical structure. Based on previous results carried out with acetic acid as a solvent [6.27], which confirm that electrospinning process is not the main issue affecting the chemical structure of the gelatin fibers, it can be concluded that dissolution step of gelatin is the responsible of the loss of thermal properties of gelatin.

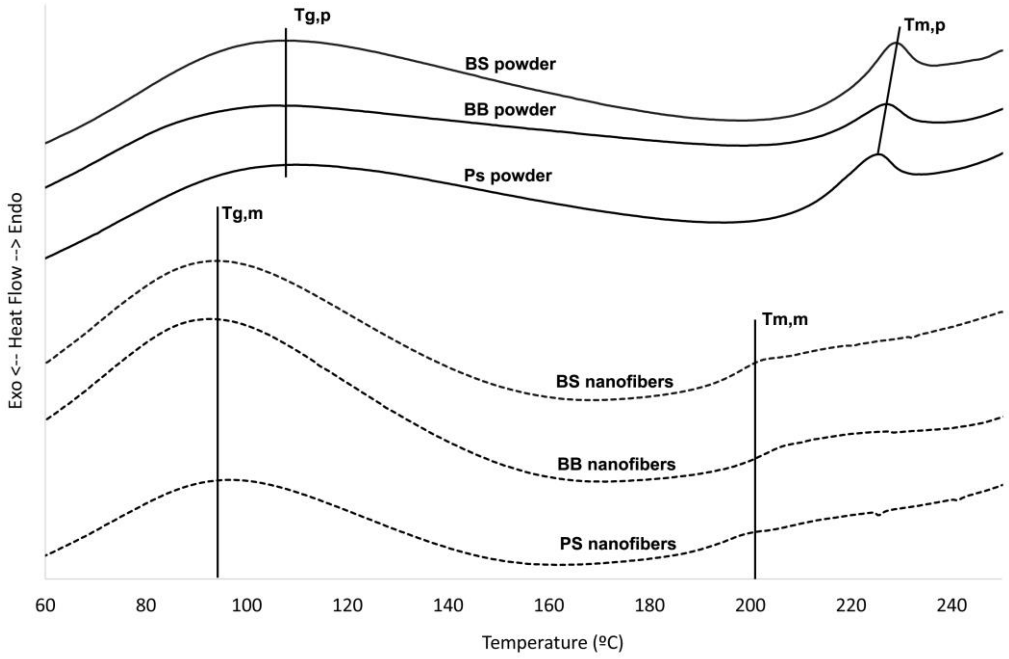

***Figure 6.12**: Differential Scanning Calorimetry (DSC) thermograms of the three different gelatins dissolved in PBS(10X)/ethanol 1:1 v/v solvent before (powder) and after (mat) the electrospinning process*

Nonetheless, it is worth to note that the decomposition peaks of the original gelatins agreed with the ones published in the literature [6.22, 6.25]: ~ 230ºC for BS gelatin, ~ 228 ºC for BB and ~ 225 for PS, indicating an indirect relationship between the gelatin Bloom and the decomposition temperature.

6.2.9. Cytotoxicity evaluation

To assess cytotoxicity of the nanofibers mats, which may be caused by the presence of traces of solvent in the electrospun fibers, the Alamar Blue cell viability assay [6.53] was carried out using BJ-5ta fibroblasts cells. Cell viability was determined after dissolving the nanofibers mats in the culture medium and results are shown in **Figure 6.13**. The results of Alamar blue assay demonstrated that the cell viability was high (higher than 90%) regardless the gelatin type. Consequently, it is possible to affirm that PBS/ethanol solvent mixture was not negatively affecting cell viability. These results were comparable those recently obtained for a similar system which used acetic acid aqueous solutions as alternative solvent where a cell viability of 90% was achieved [6.27].

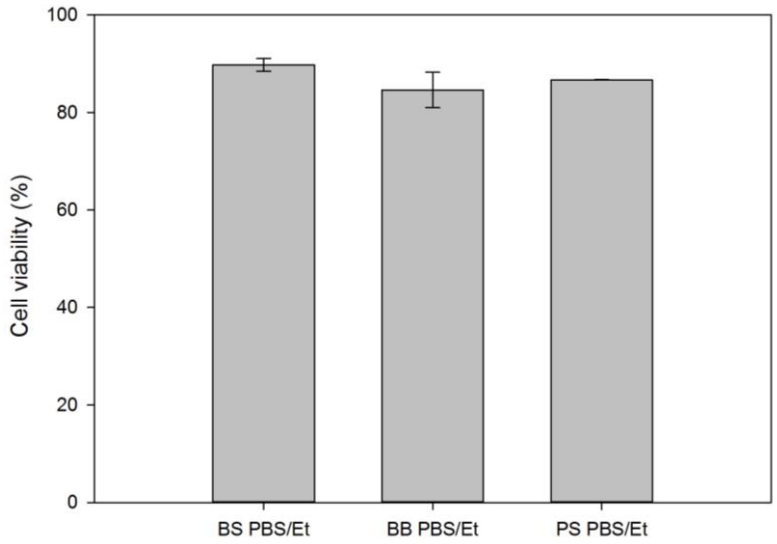

***Figure 6.13**: Cell viability of BJ-5ta fibroblast cells as a function of gelatin type*

6.4. Conclusions

By this research, different compositions of PBS/Ethanol solvent mixture were investigated so as to determine their feasibility to dissolve and electrospin three different gelatins at room temperature. Results demonstrated that the PBS/Ethanol solvent is able to dissolve all the studied gelatins and to form the corresponding stable

dope solutions. As a main conclusion, it was demonstrated that the size of electrospun nanofibers decreased due to the high stretching of the solution jet when increasing the ionic strength or the PBS/ethanol ratio. In this sense, slight variations of the solvent composition could be applied to tune the final diameter of the electrospun fibers.

In addition, both gelatin concentration and gelatin type (characterized by their Bloom value) strongly influence the morphology of the gelatin mats and on the fiber diameter mainly due to the changes on the viscosity of the solutions. An increase of the gelatin concentration or the gelatin Bloom induces an increase of the solution viscosity and consequently, the formation of beads on the electrospun mats is reduced and at the same time the average fiber diameter increases.

Besides, the calculation of intrinsic viscosity for each gelatin type in the PBS(10X)/ethanol 1:1v/v solvent allowed us to determine that the experiments were carried out on a semidilute entangled regime and that the solvent mixture acted as a good solvent for all the tested gelatins. Regarding the relationship between the rheological properties of the solutions and the technical characteristics of the obtained mats, the allometric relationship between the Berry number and the diameter of the electrospun fiber was demonstrated for each individual gelatin. Moreover, thanks to a simple modification of the Berry number (namely the use of $Be\cdot[\eta]$), a new allometric relationship was found, able to take into account the effect of the different type of gelatin in order to stablish the electrospinnability domains for solutions in PBS(10X)/ethanol 1:1v/v solvent. By doing so, two electrospinnability domains were clearly identified, resulting in nanofibers for $Be\cdot[\eta]>15$ and fibers with beads for $Be\cdot[\eta]<15$.

When evaluating the physic-chemical properties of the obtained nanofibers, it was proved that even if FTIR spectra were practically identical for all the gelatin types, gelatins were affected by either the dissolution or the electrospinning processes since a change on the thermal properties was noticed by DSC with a slight decrease of both transition temperature (T_g) and melting point (T_m) of the electrospun mats compared with the pure gelatins. That fact suggests that a negative effect of the solvent on the thermal stability takes place but it does not highly harms the chemical structure of the polymer; instead it might affect proteins conformation.

Finally, gelatin mats fabricated with PBS/ethanol solvent mixture perform well in relation to cytotoxicity as all the fabricated mats obtained cell viability values above 90%, regardless the gelatin type.

6.5. References

[6.1] A. Formhals, Process and apparatus for preparing artificial threads., US Patent No. 1,975,504, 1934.

[6.2] S. Agarwal, J.H. Wendorff, A. Greiner, Use of electrospinning technique for biomedical applications, Polymer (Guildf). 49 (2008) 5603–5621.

[6.3] J.J. Doyle, S. Choudhari, S. Ramakrishna, R.P. Babu, Electrospun Nanomaterials : Biotechnology , Food , Water , Environment , and Energy., Conf. Pap. Mater. Sci. 2013 (2013) 1–14.

[6.4] N. Bhardwaj, S.C. Kundu, Electrospinning: a fascinating fiber fabrication technique., Biotechnol. Adv. 28 (2010) 325–47.

[6.5] W.-J. Li, C.T. Laurencin, E.J. Caterson, R.S. Tuan, F.K. Ko, Electrospun nanofibrous structure: a novel scaffold for tissue engineering, J. Biomed. Mater. Res. 60 (2002) 613–21.

[6.6] A. Greiner, J.H. Wendorff, Electrospinning: a fascinating method for the preparation of ultrathin fibers, Angew. Chem. Int. Ed. Engl. 46 (2007) 5670–703.

[6.7] J. Lannutti, D. Reneker, T. Ma, D. Tomasko, D. Farson, Electrospinning for tissue engineering scaffolds, Mater. Sci. Eng. C. 27 (2007) 504–509.

[6.8] B. Dhandayuthapani, Y. Yoshida, T. Maekawa, D.S. Kumar, Polymeric Scaffolds in Tissue Engineering Application: A Review, Int. J. Polym. Sci. 2011 (2011) 1–19.

[6.9] H. Homayoni, S.A.H. Ravandi, M. Valizadeh, Electrospinning of chitosan nanofibers: Processing optimization., Carbohydr. Polym. 77 (2009) 656–661.

[6.10] J.A. Matthews, G.E. Wnek, D.G. Simpson, G.L. Bowlin, Electrospinning of collagen nanofibers, Biomacromolecules. 3 (2002) 232–238.

[6.11] D. Meyer, J.-P. Blaauwhoed, Handbook of Hydrocolloids, CRC Press, 2009.

[6.12] R.M. Hafidz, Chemical and functional properties of bovine and porcine skin gelatin, Int. Food Res. J. 817 (2011) 813–817.

[6.13] S. Hermanto, L.O. Sumarlin, W. Fatimah, Differentiation of Bovine and Porcine

Gelatin Based on Spectroscopic and Electrophoretic Analysis, 1 (2013) 68–73.

[6.14] M. Erencia, F. Cano, J. a Tornero, J. Macanás, F. Carrillo, Resolving the electrospinnability zones and diameter prediction for the electrospinning of the gelatin/water/acetic Acid system., Langmuir. 30 (2014) 7198–205.

[6.15] N. Choktaweesap, K. Arayanarakul, D. Aht-ong, C. Meechaisue, P. Supaphol, Electrospun Gelatin Fibers: Effect of Solvent System on Morphology and Fiber Diameters., Polym. J. 39 (2007) 622–631.

[6.16] M. Djabourov, J. Leblond, P. Papon, Gelation of aqueous gelatin solutions. I. Structural Investigation., J. Phys. Fr. 49 (1988) 319–332.

[6.17] M. Li, M.J. Mondrinos, M.R. Gandhi, F.K. Ko, A.S. Weiss, P.I. Lelkes, Electrospun protein fibers as matrices for tissue engineering., Biomaterials. 26 (2005) 5999–6008.

[6.18] H.-W. Kim, J.-H. Song, H.-E. Kim, Nanofiber Generation of Gelatin-Hydroxyapatite Biomimetics for Guided Tissue Regeneration, Adv. Funct. Mater. 15 (2005) 1988–1994.

[6.19] Y. Zhang, H. Ouyang, C.T. Lim, S. Ramakrishna, Z.-M. Huang, Electrospinning of gelatin fibers and gelatin/PCL composite fibrous scaffolds., J. Biomed. Mater. Res. B. Appl. Biomater. 72 (2005) 156–65.

[6.20] Y.Z. Zhang, J. Venugopal, Z.-M. Huang, C.T. Lim, S. Ramakrishna, Crosslinking of the electrospun gelatin nanofibers., Polymer (Guildf). 47 (2006) 2911–2917.

[6.21] K. Gast, A. Siemer, D. Zirwer, G. Damaschun, Fluoroalcohol-induced structural changes of proteins: some aspects of cosolvent-protein interactions., Eur. Biophys. J. 30 (2001) 273–283.

[6.22] C.S. Ki, D.H. Baek, K.D. Gang, K.H. Lee, I.C. Um, Y.H. Park, Characterization of gelatin nanofiber prepared from gelatin–formic acid solution., Polymer (Guildf). 46 (2005) 5094–5102.

[6.23] L. Ren, J. Wang, F.-Y. Yang, L. Wang, D. Wang, T.-X. Wang, et al., Fabrication of gelatin–siloxane fibrous mats via sol–gel and electrospinning procedure and its application for bone tissue engineering, Mater. Sci. Eng. C. 30 (2010) 437–444.

[6.24] S.-Y. Gu, Z.-M. Wang, J. Ren, C.-Y. Zhang, Electrospinning of gelatin and gelatin/poly(l-lactide) blend and its characteristics for wound dressing., Mater. Sci. Eng. C. 29 (2009) 1822–1828.

[6.25] J.-H. Song, H.-E. Kim, H.-W. Kim, Production of electrospun gelatin nanofiber by water-based co-solvent approach., J. Mater. Sci. Mater. Med. 19 (2008) 95–102.

[6.26] S. Panzavolta, M. Gioffrè, M.L. Focarete, C. Gualandi, L. Foroni, A. Bigi, Electrospun gelatin nanofibers: optimization of genipin cross-linking to preserve fiber morphology after exposure to water, Acta Biomater. 7 (2011) 1702–9.

[6.27] M. Erencia, F. Cano, M.M. Tornero, Jose Antonio Fernandes, T. Tzanov, J. Macanás, F. Carrillo, Electrospinning of gelatin scaffolds with low acetic acid concentration effect of solvent composition on both diameter of nanofibers and cell viability, Summited. (2014).

[6.28] S.J. Kew, J.H. Gwynne, D. Enea, M. Abu-Rub, a Pandit, D. Zeugolis, et al., Regeneration and repair of tendon and ligament tissue using collagen fibre biomaterials., Acta Biomater. 7 (2011) 3237–47.

[6.29] Q. Jiang, N. Reddy, S. Zhang, N. Roscioli, Y. Yang, Water-stable electrospun collagen fibers from a non-toxic solvent and crosslinking system., J. Biomed. Mater. Res. A. 101 (2013) 1237–47.

[6.30] B. Dong, O. Arnoult, M.E. Smith, G.E. Wnek, Electrospinning of collagen nanofiber scaffolds from benign solvents, Macromol. Rapid Commun. 30 (2009) 539–542.

[6.31] Z. Zha, W. Teng, V. Markle, Z. Dai, X. Wu, Fabrication of gelatin nanofibrous scaffolds using ethanol/phosphate buffer saline as a benign solvent., Biopolymers. 97 (2012) 1026–1036.

[6.32] R. Schrieber, H. Gareis, Gelatin handbook- Theory and Insutrial Practice, Wiley, 2007.

[6.33] A.P.S. Immich, M.L. Arias, N. Carreras, R.L. Boemo, J.A. Tornero, Drug delivery systems using sandwich configurations of electrospun poly(lactic acid) nanofiber membranes and ibuprofen, Mater. Sci. Eng. C. Mater. Biol. Appl. 33 (2013) 4002–8.

[6.34] K. Nasouri, a. M. Shoushtari, a. Kaflou, Investigation of polyacrylonitrile electrospun nanofibres morphology as a function of polymer concentration, viscosity and Berry number, Micro Nano Lett. 7 (2012) 423.

[6.35] M.A. Oraby, A.I. Waley, A.I. El-dewany, E.A. Saad, B.M.A. El-hady, E.T. Al, Electrospinning of Gelatin Functionalized with Silver Nanoparticles for Nanofiber Fabrication, 2013 (2013) 95–105.

[6.36] M. Erencia Millan, Propuesta de tesis: Preparación de soportes biomateriales con estructuras fibrilares obtenidas mediante electro-hilatura., Universitat Politecnica de Catalunya, 2013.

[6.37] M.M. Hohman, M. Shin, G. Rutledge, M.P. Brenner, Electrospinning and electrically forced jets. II. Applications, Phys. Fluids. 13 (2001) 2221.

[6.38] X. Geng, O.-H. Kwon, J. Jang, Electrospinning of chitosan dissolved in concentrated acetic acid solution, Biomaterials. 26 (2005) 5427–32.

[6.39] P.J. Flory, Principles of Polymer Chemistry, Cornell University Press, New York, 1953.

[6.40] A.M. Jamieson, R. Simha, Newtonian viscosity of dilute, semidilute and concentrated polymer solution, in: L.A. Ultracki, A.M. Jamieson (Eds.), Polym. Phys. from Suspens. to Nanocomposites Beyond., Wiley, 2010: pp. 15–88.

[6.41] A. Saxena, K. Sachin, H.B. Bohidar, A.K. Verma, Effect of molecular weight heterogeneity on drug encapsulation efficiency of gelatin nano-particles., Colloids Surf. B. Biointerfaces. 45 (2005) 42–8.

[6.42] C. Abrusci, a. Martín-González, a. Del Amo, T. Corrales, F. Catalina, Biodegradation of type-B gelatine by bacteria isolated from cinematographic films. A viscometric study, Polym. Degrad. Stab. 86 (2004) 283–291.

[6.43] P. Gupta, C. Elkins, T.E. Long, G.L. Wilkes, Electrospinning of linear homopolymers of poly(methyl methacrylate): exploring relationships between fiber formation, viscosity, molecular weight and concentration in a good solvent, Polymer (Guildf). 46 (2005) 4799–4810.

[6.44] F.K. Ko, Nanofiber Technology in Gogotsi Nanomaterials Handbook, in: Nanomater. Handb., 2006: pp. 553–564.

[6.45] J. Tao, S. Shivkumar, Molecular weight dependent structural regimes during the electrospinning of PVA, Mater. Lett. 61 (2007) 2325–2328.

[6.46] F. Cengiz, I. Krucińska, E. Gliścińska, Comparative Analysis of Various Electrospinning Methods of Nanofibre Formation, 17 (2009) 13–19.

[6.47] B. Mohanty, H.B. Bohidar, Systematic of alcohol-induced simple coacervation in aqueous gelatin solutions., Biomacromolecules. 4 (2003) 1080–6.

[6.48] C.J. Angammana, S. Member, S.H. Jayaram, Analysis of the Effects of Solution Conductivity on Electrospinning Process and Fiber Morphology., IEEE Trans. Ind. Appl. 47 (2011) 1109–1117.

[6.49] K. Sisson, C. Zhang, M.C. Farach-Carson, D.B. Chase, J.F. Rabolt, Evaluation of cross-linking methods for electrospun gelatin on cell growth and viability., Biomacromolecules. 10 (2009) 1675–80.

[6.50] J. Garcia, M.-F. Hsieh, B. Doma, D. Peruelo, I.-H. Chen, H.-M. Lee, Synthesis of Gelatin-γ-Polyglutamic Acid-Based Hydrogel for the In Vitro Controlled Release of Epigallocatechin Gallate (EGCG) from Camellia sinensis, Polymers (Basel). 6 (2013) 39–58.

[6.51] H.-C. Chen, W.-C. Jao, M.-C. Yang, Characterization of gelatin nanofibers electrospun using ethanol/formic acid/water as a solvent., Polym. Adv. Technol. 20 (2009) 98–103.

[6.52] A. Bigi, G. Cojazzi, S. Panzavolta, N. Roveri, K. Rubini, Stabilization of gelatin films by crosslinking with genipin., Biomaterials. 23 (2002) 4827–4832.

[6.53] S.N. Rampersad, Multiple applications of Alamar Blue as an indicator of metabolic function and cellular health in cell viability bioassays., Sensors (Basel). 12 (2012) 12347–60.

CHAPTER 7:

Glutaraldehyde based crosslinking methods for stabilization of gelatin electrospun fibers: effect on the fiber diameter

Glutaraldehyde based crosslinking methods for stabilization of gelatin electrospun fibers: effect on the fiber diameter

SUMMARY

Three glutaraldehyde (GA) based crosslinking methods were studied in order to stabilize two types of electrospun gelatin mats fabricated from different dope solutions prepared using either aqueous acetic acid at 25% (AA) and a mixture of ethanol and PBS salts (PBS/Ethanol). The three crosslinking methods analyzed were: i) GA vapor method in which the electrospun mats were in contact with vapor of GA, ii) GA immersion method in which the mats were immersed in GA solution and iii) GA in-situ method that was based on the introduction of little amounts of GA in the dope gelatin solution prior to electrospin. The effect of each crosslinking method on the diameter and morphology of the fibers as well as on the water stability of the treated mats was studied. Besides that, the parameters influencing the GA in-situ method were optimized demonstrating the viability to obtain crosslinked fibers directly by electrospinning. The behavior of the crosslinking reaction was found to be dependent of the solvent used to dissolve gelatin, regardless the method used. In particular, crosslinking reaction occurs with higher intensity at neutral pH (PBS/Ethanol solvent) than at acid pH (Acetic Acid solvent) and the diameter of the resulted fibers was also higher when working at basic conditions. In addition, the results show that the GA vapor method was the treatment causing the higher changes on the morphology of the fibers due to its higher content of water. Finally, Fourier Transform Infrared Spectroscopy (FTIR) analyses corroborated that all the crosslinked mats have the same chemical structure. However, differences in the thermal behavior between mats before and after crosslinking were observed by thermogravimetry (TGA).

Keywords: electospinning, nanofibers, crosslinking, glutaraldehyde.

7.1. Introduction

The interest in creating biopolymer scaffolds with ability to mimic the structural, mechanical and biological characteristics of extracellular matrix (ECM) is increasing in recent years due to its potential applications in several fields as drug delivery and tissue engineering [7.1-7.4].

Electrospinning has been postulate as a simple and cost-effective technique that allows the fabrication of three-dimensional nanofibrous scaffolds from both synthetic and natural polymers, based on the application of a high voltage electrostatic field between a capillary syringe containing a polymer solution and a grounded collector where the polymer fibers are deposited [7.5].

Among the different polymers capable to be electrospun into nanofibrous scaffolds, gelatin is an interesting option to take into account due to its outstanding properties and its demonstrated uses in the biomedical field such as the wound dressing and adsorbent pad for surgical [7.6]. Gelatin is derived from the parent protein collagen by its partial hydrolysis [7.5] and it shows the same advantages over synthetic polymer such as biological origin, biodegradability and biocompatibility, combined with a lower cost and higher commercial availability than collagen. The possibility to fabricate three-dimensional gelatin-based polymer scaffolds with the mentioned properties is an appealing approach for tissue-engineering research and is being extensively investigated [7.8-7.11].

An important technical point in order to electrospun gelatin is the solvent selection, which must be capable of avoiding the gelation process that occurs between gelatin and water at room temperatures (<37ºC) [7.12-7.13] allowing the movement of the solution through the syringe during the electrospinning maintaining the viscosities into the optimal range. Typical solvent systems used to this purpose include 1,1,1,3,3,3-hexafluoro-2-propanol (HIPF) [7.14-7.15] and 2,2,2-trifluoroethanol (TFE) [7.16-7.18]. However, their high cytotoxicity, based on their ability to form strong hydrogen bonds with gelatin, present a challenge to the complete removal of the residual solvent on the fibers, which can affect the protein chemical structure [7.19]. Many alternative solvents have been investigated in order to obtain a benign system to electrospin protein-based polymers [7.20-7.21], including the aqueous acetic acid solution at low concentrations, which prevents the partial decomposition of gelatin produced at high concentrations, and the mixtures based on phosphate buffer saline(PBS) and ethanol composition. These two benign solvent systems have been used in recent studies with good preliminary results to fabricate gelatin electrospun scaffolds [7.22-7.24].

Despite numerous attempts to use the gelatin-based scaffolds on tissue engineering, some drawbacks still hinder their applications such as their poor mechanical properties and water sensitivity [7.25-7.26]. Therefore, the resulting gelatin nanofibrous mats must be stabilized in order to use in long-term application improving both water-resistant ability and thermo-mechanical performance.

Although there are different reported methods that can be applied to crosslinking collagenous materials such as physical methods including dehydrothermal treatment [7.27] and UV-irradiation [7.28], the most widely used and efficient technique is the chemical cross-linking, based on a reactive molecules used to modify gelatin via its amino, carboxyl or hydroxyl groups. Among the wide variety of chemical reactive such as carbodiimides [7.29-7.31], glyoxal [7.32], genipin [7.30-7.31,7.33-7.34], transglutamine [7.30, 7.35], glutaraldehyde (GA) is the most used because its low cost and excellent efficiency on the protein stabilization, achieving strength and water resistance of the obtained structure reducing its cytotoxicity when it is used at low concentration [7.36-7.37].

The crosslinking of protein samples, such as gelatin, with GA involves the reaction of free amino groups of lysine or hydroxylysine amino acid residues of the polypeptide chains with the aldehyde groups of GA [7.38-7.40]. The samples can be crosslinked by different ways including contact with vapor of GA [7.18, 7.23, 7.34, 7.41] or soaking on GA-based solution [7.37, 7.40, 7.42-7.44]. However, all these methods require further washing and drying treatments in order to remove any residual amount of GA present on the scaffold, thus extending the process. Despite some studies [7.32, 7.45] have proposed the fabrication of crosslinked electrospun gelatin mats directly by the electrospinning process including little amounts of GA on the polymer solution, their experimental test were very terse and consequently, the results were very poor.

The aim of the present study is to perform a comprehensive analysis about the crosslinking of electrospun gelatin nanofibers obtained from two different benign solvents (diluted acetic acid and PBS/Ethanol aqueous mixture). The crosslinking was carried out by different ways: vapor GA at different times (GA vapor method), soaking in GA solution (GA immersion method) and incorporation of GA on previous electrospun solution (GA in-situ method). The diameter of electrospun fibers before and after crosslinking were evaluated and compared for each crosslinking method and for both solvents used to form mats. Finally, the chemical structure and the thermal stability of electrospun gelatin nanofibers before and after crosslinking were analyzed.

7.2. Experimental

7.2.1. Materials

Gelatin type B from bovine skin (BS) (Bloom ~ 225 g) were purchased in their powder form from Sigma Aldrich (Madrid, Spain) and was used without further treatment or purification. Phosphate buffer saline (PBS) solution was also purchased from Sigma Aldrich in form of tablets. One tablet dissolved in 200 mL of deionized water yields 1X PBS solution (0.01 M phosphate buffer, 0.0027M potassium chloride and 0.137 M sodium chloride), with pH 7.34 at 25ºC. Glacial acetic acid (AA) of 99.99%, ethanol absolute of 99.5% and aqueous GA solution 25% were purchased from Panreac (Castellar del Vallés, Barcelona).

7.2.2. Fabrication of gelatin scaffolds

7.2.2.1. Electrospun gelatin mats

Electrospun gelatin fibers were obtained by the electrospinning process, performed in a home-made device developed by INTEXTER used in previous research [7.22, 7.46]. Each gelatin solution was placed in a 2.5 ml syringe with a stainless steel syringe needle (0.6 mm of inner diameter) connected to the anode of a power supply. The electrospun gelatin fibers were collected on aluminum foil covering the copper collector that is connected to the cathode of the power supply.

Two different types of electrospun gelatin mats were fabricated based in two different benign solvent systems. On the one hand gelatin was dissolved on PBS/Ethanol solution (ratio 1:1, PBS 0.1M) at concentration of 180 mg/ml and the solution was electrospun using the following conditions according to previous published work [7.24]: applied voltage 18kV, needle to collector distance 9cm and solution flow rate 1 ml/h. On the other hand a solution of gelatin at concentration 300 mg/ml on aqueous acetic acid solvent (25% v/v) was electrospun into non-woven mats according to the conditions established in previous work and published elsewhere [7.22]: applied voltage 15kV, needle to collector distance 9cm and solution flow rate 0.8 ml/h.

All gelatin solutions were stirred about 1h and electrospun at room temperature (25ºC).

7.2.2.2. Gelatin films

Gelatin solutions were prepared at the same way and concentrations that have been described in the previous section for the two different solvent systems. Films were obtained on the bottom of Petri dishes (diameter 5.5 cm) after water evaporation at 37ºC from 2 ml of gelatin solution.

7.2.3. Cross-linking methods

The stabilization of electrospun gelatin mats were carried out by three different GA based cross-linking methods:

7.2.3.1. GA vapor

Gelatin films and electrospun mats with the supporting aluminum foil, obtained from two different solvent systems (AA and PBS/Ethanol aqueous solutions), were placed on a holed ceramic shelf in a desiccator which contains 10 ml of aqueous GA solution (25% v/v) in a Petri dish, following the procedure published elsewhere [7.18]. The films and mats were crosslinked in the GA vapor at room temperature at different contact times. After that, samples were dried at 37ºC during 1h and subsequently they were analyzed carrying out the water-stability test described in section 7.2.4.

7.2.3.2. GA immersion

Gelatin electrospun mats from two different solvent systems (AA and PBS/Ethanol aqueous solutions) were soaked in 10 ml solution of 1.2% GA in ethanol during 20h at room temperature, following the procedure published elsewhere [7.42]. After that, the mats were dried at 37ºC during 1h and subsequently they were analyzed carrying out the water-stability test described in section 7.2.4.

7.2.3.3. GA in situ

Different amounts of GA solution were added to the gelatin solution and stirred at room temperature. Each solution was fabricated by duplicate to obtain, on the one hand, a gelatin film by the process described above, and on the other hand, a nanofiber mat by the electrospinning process. After that, the samples were dried during 1h at 37ºC and subsequently they were analyzed carrying out the water-stability test described in section 7.2.4.

7.2.4. Water-stability test

The crosslinked gelatin films or nanofibrous mats were immersed into warm bidestillate water at 37ºC for certain period of time to test their dissolvability.

7.2.5. Characterizations

The morphology of electrospun gelatin fibers were analyzed by Scanning Electron Microscopy (SEM) using a Phenom Standard SEM. Prior to SEM, samples were

sputter coated for 120 s with platinum using a coater (SC7620 Quorum Technologies). Based on the SEM photos, fiber diameters of electrospun mats were analyzed using an image analyzing software package (ImageJ). The average diameter for each experiment was obtained from 50 arbitrary measures of electrospun fibers.

The cross-linked gelatins were characterized by Fourier Transform Infrared Spectroscopy (FTIR) using a Nicolet Avatar 320 spectrophotometer (Nicolet Instrument Corporation, USA). Samples were prepared by mixing 1 mg of nanofibers mat in a matrix of 300 mg of KBr followed by pressing (167 MPa). The spectrum was recorded in the range of 500 to 4000 cm^{-1} and averaging 32 scans at a resolution of 4 cm^{-1}.

Finally, thermal properties of the electrospun fibers were measured by Thermogravimetry (TGA/851e, Mettler Toledo).The instrument was calibrated with an indium/aluminum standards and the analysis were conducted using a sample weight of 5-10 mg under a nitrogen atmosphere (15 cm^3/min) and at a scanning speed of 10ºC/min, heating from 25ºC to 500ºC.

7.3. Results and discussion

7.3.1. Morphology and diameter of uncross-linked and cross-linked gelatin by using GA vapor method

7.3.1.1. Gelatin Films

To determine a proper crosslinking condition, grouped of gelatin films (samples of 1x1 cm) obtained from PBS/Ethanol and aqueous acetic acid solvent were exposed in the GA vapor for a timescale of 0, 10, 30, 60, 120, 150, 180 and 1200 min and their respective water-resistant behaviors were evaluated and summarized in **Table 7.1**.

***Table 7.1**: Water-stability results of gelatin films crosslinked with GA vapor at different times and obtained from different solvents (AA and PBS/Ethanol)*

	PBS/Ethanol solvent (PBSET mats)				**Acetic acid 25% solvent (AA mats)**			
Crosslinking time / Stability Time	**1h**	**2h**	**24h**	**5 days**	**1h**	**2h**	**24h**	**5 days**
0 min	N	-	-	-	N	-	-	-
10 min	I	I/N	I/N	I/N	I	I/N	N	-
30 min	I	I/N	I/N	I/N	I	I/N	N	-
1 h	I	I	I/N	I/N	I	I	I/N	N
2 h	I	I	I	I	I	I	I	I/N
2,5 h	I	I	I	I	I	I	I	I/N
3 h	I	I	I	I	I	I	I	I/N
20 h	Y	Y	Y	Y	Y	Y	Y	Y

"N" denotes gelatin film completely disappears after the specified period
"Y" denotes gelatin film remain after the specified period
"I" denotes gelatin film is an intermediate stage between "N" and "Y", observed as a formless gel

Two different conclusions can be extracted from these results. On the one hand, comparing the type of solvent used to prepare de film, the PBS/Ethanol films always have an equal or greater stability than the AA films regardless the time of exposition with the GA vapor. This behavior may be related with the final pH of the prepared mats, since as reported in the literature [7.38] it is expected higher reactivity of GA with gelatin at neutral pH (mats prepared with PBS/Ethanol aqueous solution) compared with their reactivity at acid pH (mats obtained from acetic acid solutions) due to the induction of a different reaction mechanism between the reactive residues in proteins and the GA vapor. Therefore, the results suggest the presence of small amount of residual solvent on the final mats that determines its pH, influencing the crosslinking reaction mechanism.

On the other hand, it is noteworthy that for the both type of mats the cross-linking begins to be detectable from a contact time of 2 hours, but the complete cross-linking, which maintain the overall dimensional stability of the film, is not reached until 20 h. Consequently, time of exposition of 20 h are required to obtain stable gelatin films which is in agreement with the range of crosslinking exposure times proposed in the literature to guarantee the stabilization of gelatin scaffolds with GA vapor [7.18, 7.23, 7.34, 7.41].

7.3.1.2. Gelatin electrospun mats

Different samples of electrospun gelatin mats fabricated from PBS/Ethanol and AA solvents were exposed to GA vapor for a timescale of 5, 10, 20, 30, 60, 120 min. After the drying step, the water stability test was carried out during 2h and subsequently the samples were analyzed by SEM. The results are shown in **Figure 7.1** and **Figure 7.2** for PBS/Ethanol and AA mats, respectively.

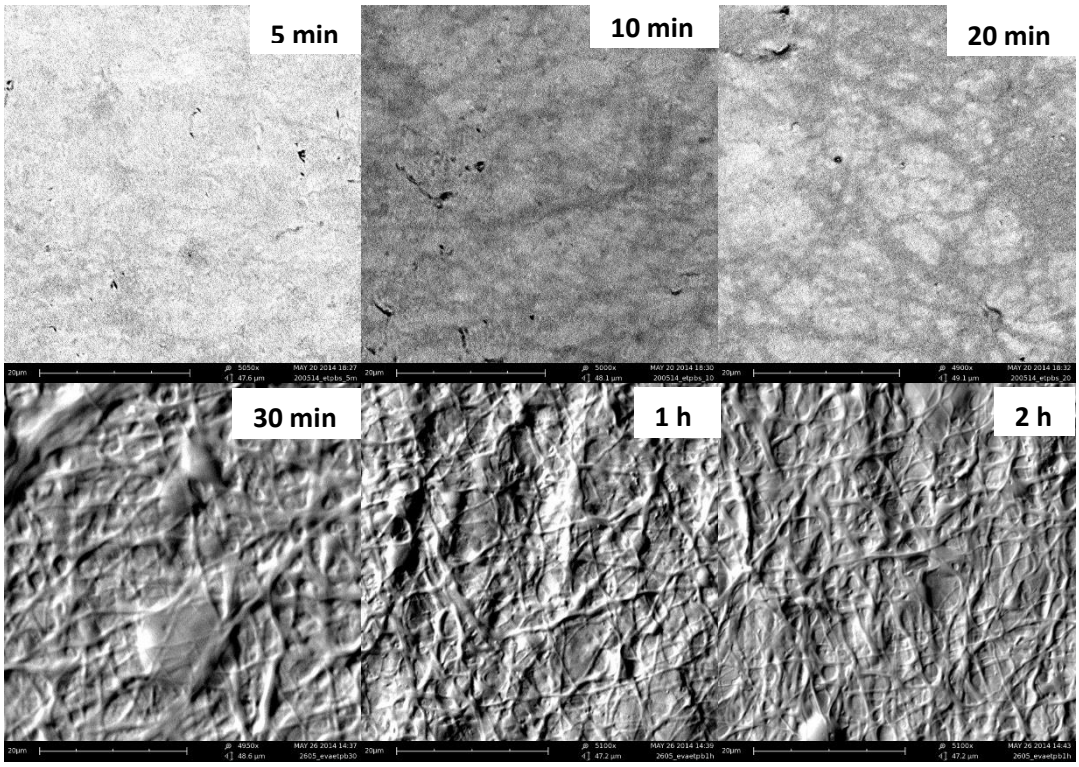

***Figure 7.1**: Morphologies of gelatin nanofibers fabricated from PBS (0.1M)/Ethanol (1:1) solution crosslinked at different times with GA vapor (25% v/v) after the water-stability test*

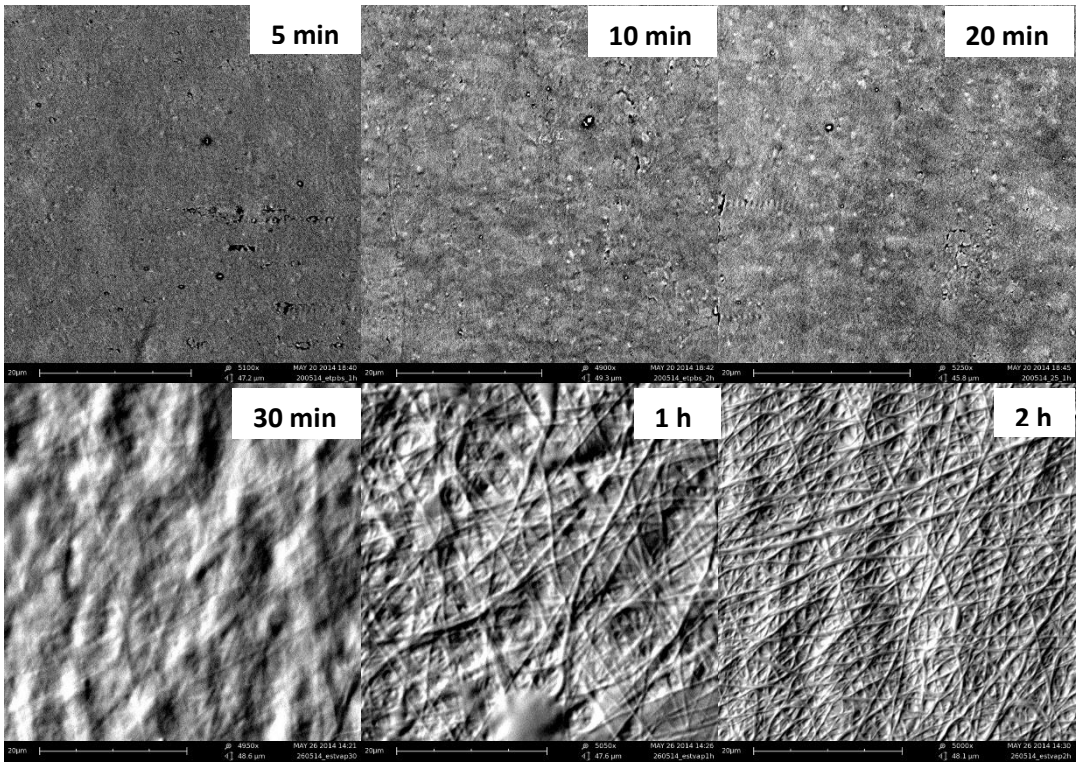

***Figure 7.2**: Morphologies of gelatin nanofibers fabricated from aqueous acetic acid aqueous solution crosslinked at different times on GA vapor (25% v/v) after the water-stability test*

From results it can be observed that for both types of electrospun gelatin the cross-linking methods (GA vapor) stabilize the mats from 30 min, unlike what was happening with gelatin films, when the time necessary to start the cross-linking process was significantly higher (2h). This behavior may be due to two different factors: on the one hand, the different amount and thickness of the gelatin samples which both are higher for gelatin films than for the electrospun mats. As a result, the ratio GA/sample is lower for the films samples and more time is necessary to complete the crosslinking. On the other hand, the different specific surface exposed to the GA vapor. In this sense, the contact area available to react with GA is significate higher for electrospun mats than gelatin films, thanks to their nanofibrous structure, making more effective the cross-linking reaction process. Similar results were obtained by Wu et al. [7.47] for gelatin crosslinked with GA vapor with a slight reduction of crosslinking time needed to stabilize nanofibers due to the higher concentration of GA used (50% instead of 25%).

A comprehensive SEM analysis of PBS/Ethanol and AA mats (only for the samples that showed stability, that is for GA contact times of 30 min, 1h and 2h) was carried out at different steps: i) before contact with GA, ii) after contact with GA and after drying and iii) after the water-stability test. The analysis aims to study the effect of each state on the morphology and diameter of electrospun gelatin fibers. The results are shown in **Figure 7.3** for PBS/Ethanol mats and in **Figure 7.4** for AA mats.

Although the morphology of electrospun fibers before the crosslinking treatment is very similar for the two different solvent system used (Figures 7.3A and 7.4A) it is worth to note that the effect of GA vapor is significant different in both cases. Nanofibers formed using PBS/Ethanol solvent experience swelling and fusion, which creates a surface layer of polymer where fibers are, embedded (Figures 7.3B, 7.3C and 7.3D). Conversely, AA mats did not experience significant swelling and fusion between nanofibers after being in contact with GA vapor (Figures 7.4B, 7.4C and 7.4D). In this regard, the GA treatment seems slightly affect the nanofibers after 2 hours of treatment. These results demonstrated the greater capacity of PBS/Ethanol mats to absorb the water vapor present in the air during cross-linking process, which may have caused the change in morphology.

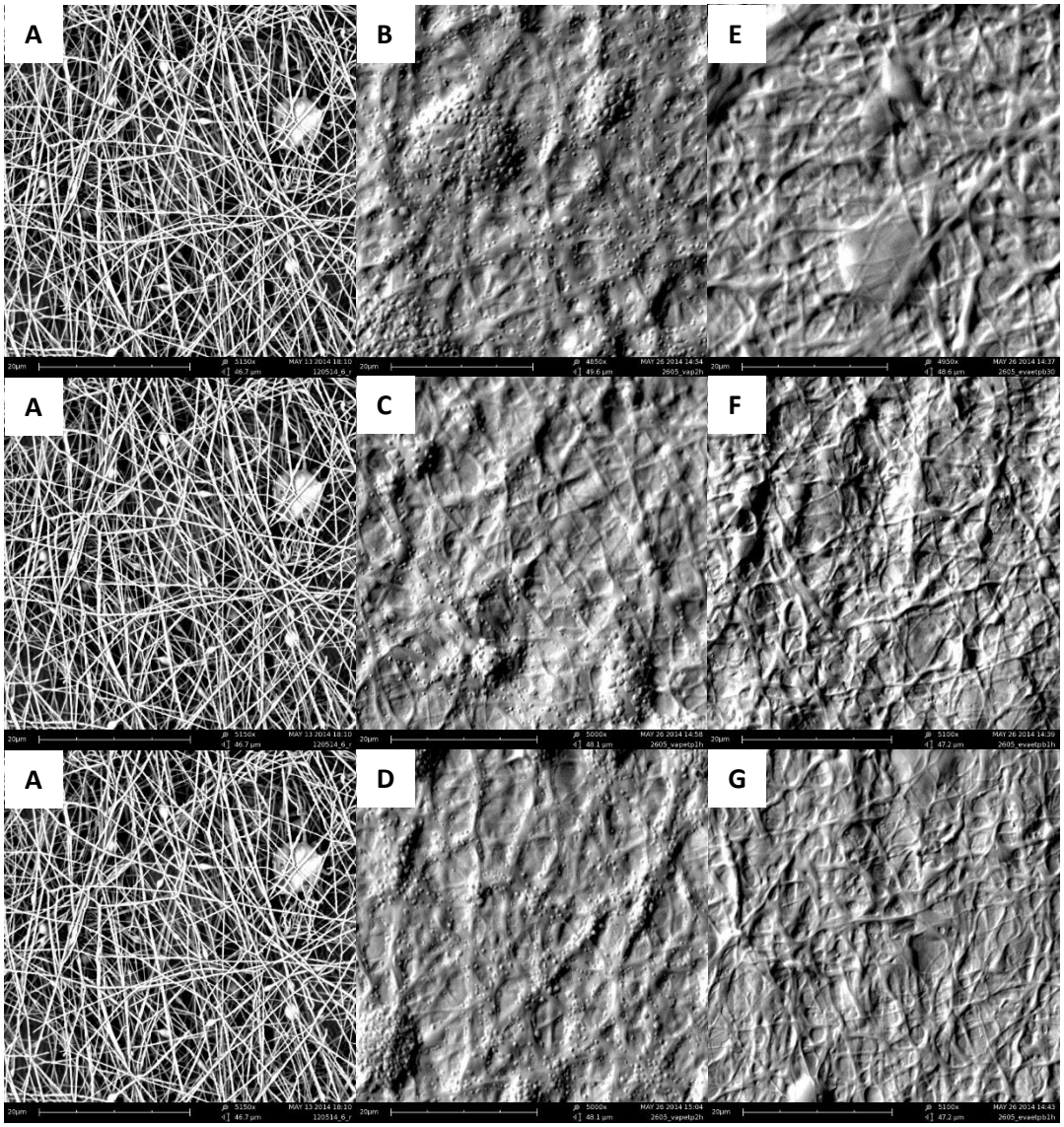

***Figure 7.3**: Morphologies of gelatin nanofibers fabricated from PBS (0.1M)/Ethanol (1:1) solution: before the crosslinking process (image A), after being in contact with GA vapor 25% at 30, 60 and 120 min (images B, C and D, respectively) and the respective samples after water-stability test (2h) (images E, F, G)*

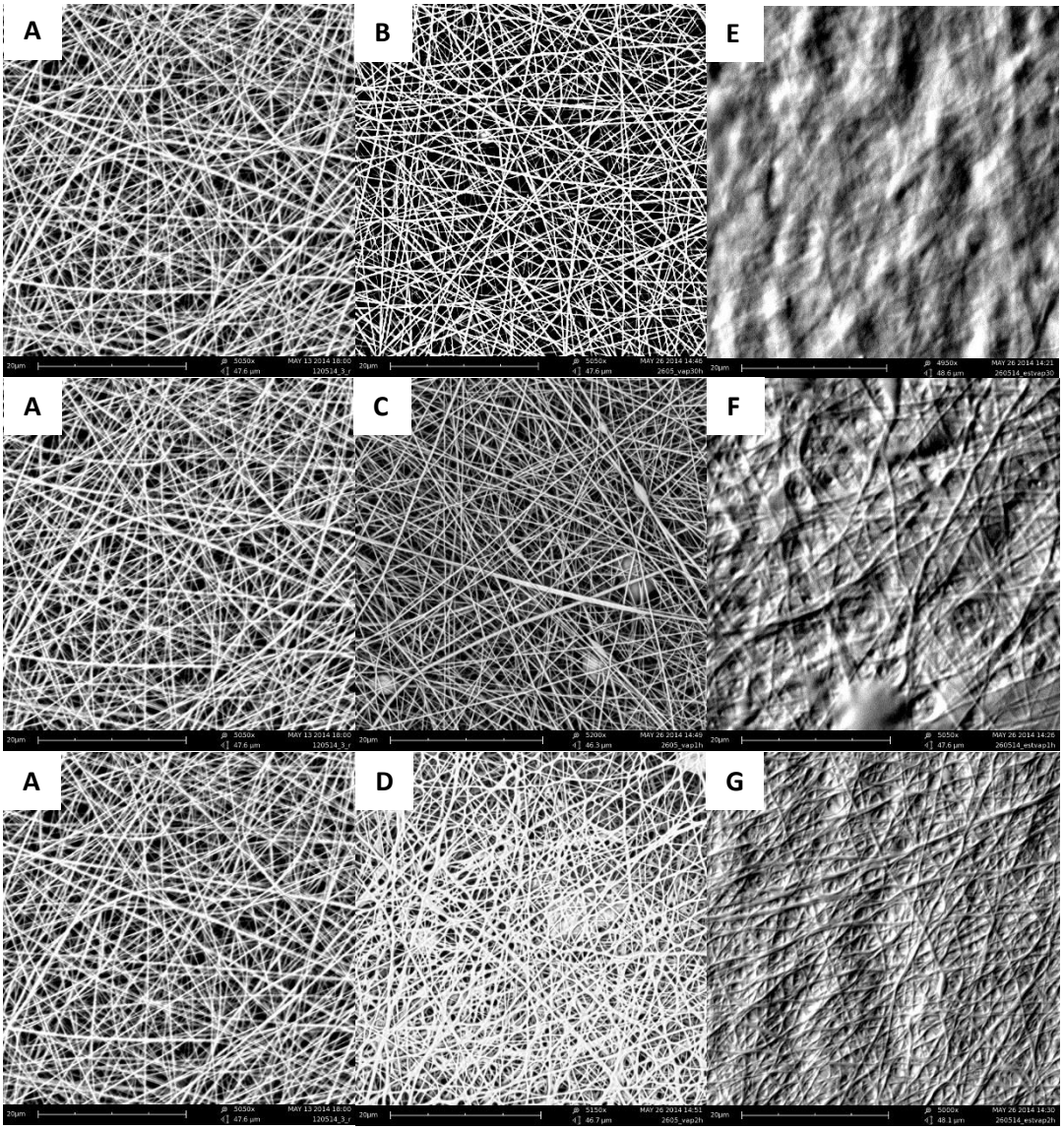

***Figure 7.4**: Morphologies of gelatin nanofibers fabricated from aqueous acetic acid solution: before the crosslinking process (image A),after being in contact with GA vapor 25% at 30, 60 and 120 min (images B, C and D, respectively) and the respective samples after water-stability test (2h) (images E, F, G)*

As regard to the effect of the water stability test is worth to note that for PBS/Ethanol mats show a slightly broken surface with fibers more defined and without the presence of salts crystals from PBS solution, confirming the effect of the crosslinking process even for low contact times (30 min). As opposed to PBS/Ethanol mats, AA mats did not show stability at 30 min and required 1 h of treatment with GA vapor, confirming that residual acid inhibits the crosslinking reaction as it was observed for gelatin films. Nevertheless, fusion between the fibers was observed as a result of the swelling process occurred during the water-stability test.

Apart from the morphology of the mats, the diameter of electrospun gelatin fibers for both types of mats was also analyzed for the different crosslinking stages represented on **Figures 7.3 and 7.4**. The averages diameters with their standard deviation are

shown in **Figure 7.5** and allow to corroborate the changes observed on the fiber morphology.

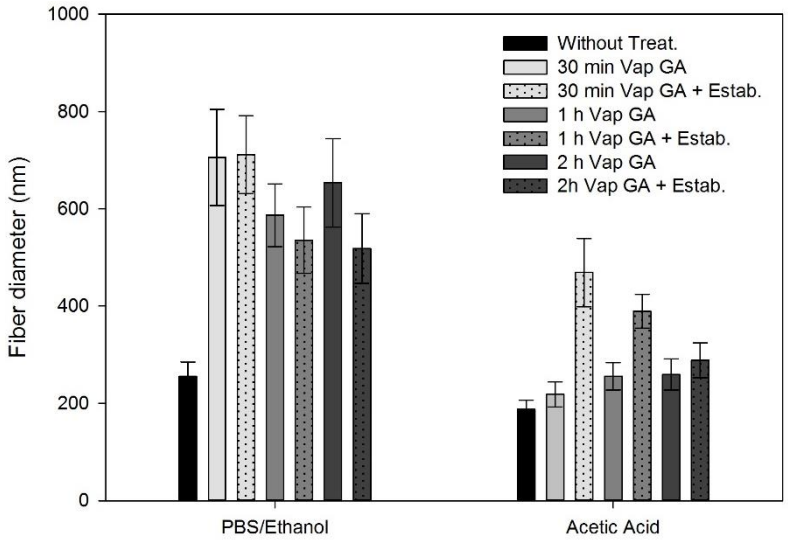

***Figure 7.5**: Average electrospun fiber diameter of mats from PBS/Ethanol and AA solutions at different stages during the process of crosslinking using the GA vapor method*

The electrospun fibers from both solvents have a similar diameter, being slightly higher the obtained for the PBS/Ethanol mats (≈ 250 nm) compared with the fiber diameter of AA mats (≈ 200 nm). These observed values agree with the obtained in previous studies for the same conditions [7.24, 7.46] . However, the effect of GA treatment on the fiber diameter of both mats significantly differs for each case. On the one hand, the diameter of electrospun fibers from PBS/Ethanol solvent increases dramatically after GA vapor exposure, and it remains stable after the dissolvability test, only showing a slightly decrease which is non-significant. On the other hand, the diameter of electrospun fibers from AA solvent remains very similar to the original fibers after GA contact, with slight increment in function of the contact time. Moreover, the fiber diameter significantly increases after the water-stability test due to the swelling of the fibers caused by the low degree of crosslinking of the samples due to the acid pH. In fact, the observed increase is less pronounced when increasing the GA contact time due to the higher degree of crosslinking achieved for longer times as it was observed previously [7.47].

All in all, it can be concluded that the electrospun fibers obtained from PBS/Ethanol solvent have a higher capacity to crosslink with GA vapor at the same conditions than AA fibers, but their changes on morphology and diameter experienced by mats are also higher.

7.3.2. *Morphology and diameter of uncross-linked and cross-linked gelatin by immersion on GA solution*

The morphology of electrospun gelatin fibers obtained from PBS/Ethanol and AA solvent system were analyzed by SEM at different steps of another crosslinking method usually used on the literature based on the immersion of polymer on a diluted GA solution [7.37, 7.40, 7.42-7.44]. In this particular case gelatin was immersed in ethanol solution with 1.2% of GA for 20 h to guarantee the stabilization of the mats and to study the effect of this treatment on the fiber diameter. The results are shown in **Figure 7.6**.

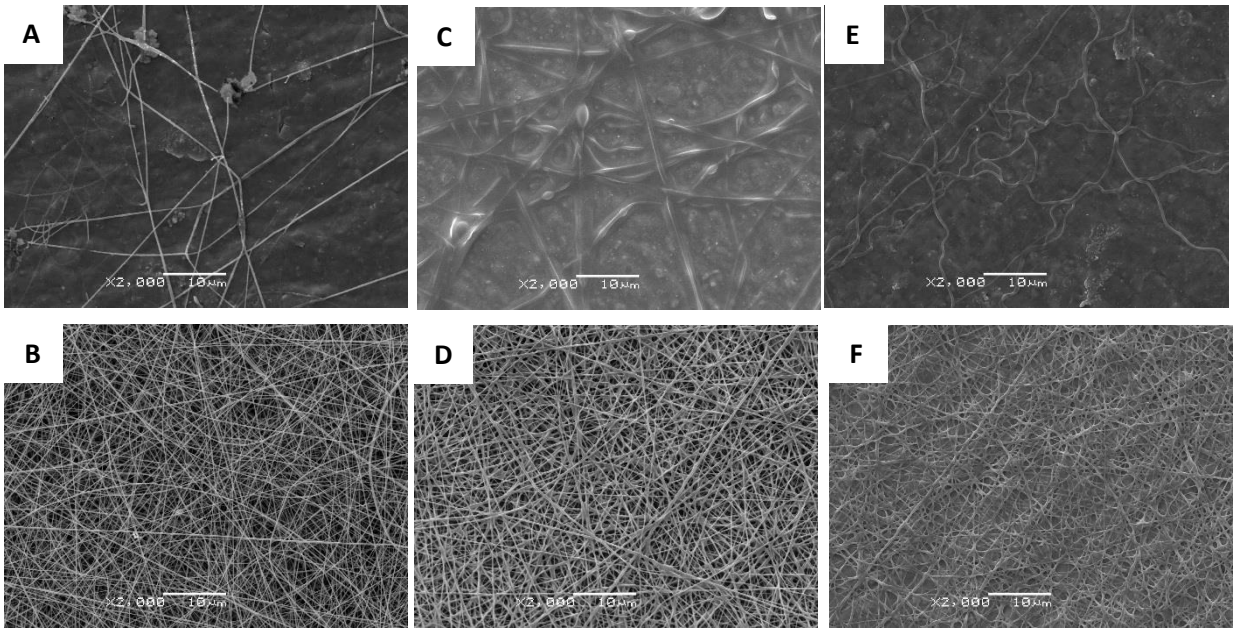

***Figure 7.6**: Morphologies of gelatin nanofibers fabricated from PBS (0.1M)/Ethanol (1:1) and AA solution: before the crosslinking process (images A and B, respectively), after the immersion on diluted GA in ethanol (1.2% GA) for 20h (images B and C) and after water-stability test (images D, E)*

The SEM images reveal a similar behavior of the mats in front of the treatments compared to the mats crosslinked by GA vapor method. On the one hand, the electrospun gelatin fibers fabricated using PBS/Ethanol solution swell after their immersion on GA solution and this fiber deformation remains after the dissolvability test, indicating a good grade of crosslinking. On the other hand, the nanofibers of AA mats show a similar morphology in all stages of crosslinking method, only with small changes after dissolvability test because of the swelling of the fibers in water. These changes on fiber morphology were contrasted with the analysis of the fiber diameter, whose results are shown in **Figure 7.7**.

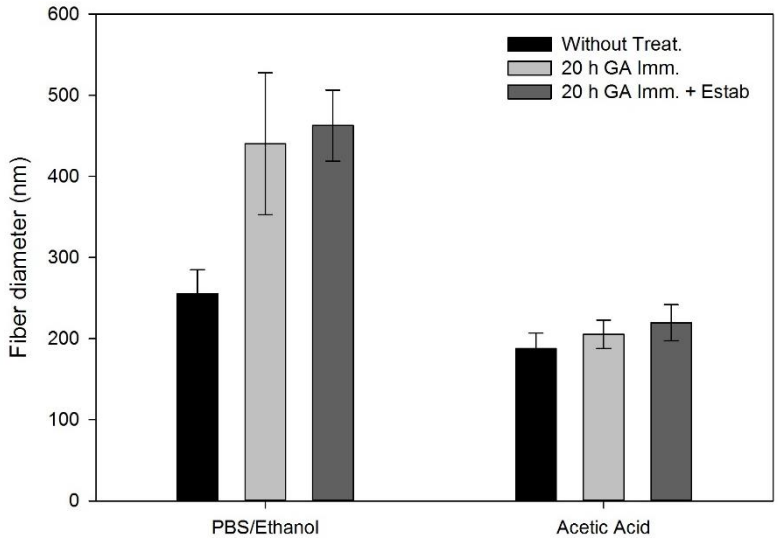

***Figure 7.7**: Average electrospun fiber diameter of mats from PBS/Ethanol and AA solutions at different stages during the process of cross-linking using the GA immersion method*

At this point is important to note that, although the trend is similar than observed for GA vapor method, the absolute values of average diameter after the GA treatment are significantly different. The electrospun gelatin fibers cross-linked by GA vapor method have a further increase in their diameter after being in contact with GA than fibers cross-linked by GA immersion method, for both types of mats independently of the solvent system used in their fabrication. This behavior is probably due to the effect of the presence of ethanol on the crosslinking solution, which dehydrates the sample preserving the fiber structure since gelatin is not soluble on pure ethanol. Also, it is noteworthy to mention the impossibility to crosslink the electrospun nanofibers using the same aqueous solution used for GA vapor method owing to the high solubility of gelatin nanofibers in water.

These results suggest the possibility to work with a GA/ethanol solution on GA vapor method on futures studies and compare the morphology and diameter of electrospun nanofibers obtained after the cross-linked with GA/water and GA/ethanol solution. However, it will be important to take into account the concentration of GA on GA/ethanol solution, considering that the GA is supplied at 25% in water by the manufacturers, so, in order to reduce the water content significantly to avoid the dissolution of gelatin, the concentration in ethanol will be low and it could affect the crosslinking reaction.

7.3.3. Morphology and diameter of uncross-linked and cross-linked gelatin by GA incorporation in situ

Apart from the GA methods above mentioned, obtaining electrospun gelatin nanofibers crosslinked directly in situ through the electrospinning process is a challenge and an important objective for the development of scaffolds into the tissue engineering field. Despite this can be a complicated process involving structural changes on the electrospinning machine (UV-in situ) [7.48], some studies have proposed the option to work with the incorporation of little amounts of crosslinking agent directly into the dope solution [7.32, 7.45]. Nevertheless the preliminary results based on the application of the GA in-situ method were not too good, suggesting that an optimization of the process is needed.

Taking it into account, the viability of crosslinking gelatin using GA by an in situ electrospinning process was proposed and analyzed. Firstly, in situ crosslinking experiments were carried out with gelatin films in order to evaluate the effect of the gelatin and GA concentration along with the solvent system on the crosslinking reaction. According to the obtained results some of these solutions were electrospun and the morphology of the obtained nanofibers were analyzed.

7.3.3.1. Gelatin films

Gelatin films were prepared by dissolution of gelatin in AA solution and their water stability at different times were measured (**Table 7.2**). In addition, the physical state of the films during the water stability test was controlled by photographing the films (**Figure 7.8**).

***Table 7.2**: Water-stability results at different times for gelatin films from aqueous acetic acid solution at different acid percentage and gelatin and GA concentrations, crosslinked with GA in situ method*

Ref.	% AA v/v	[Gel] mg/ml	%[GA] mM/ml	Aspect	1h	2h	3h	24h	5 d
FA0	25	300	0	Fluid	N	-	-	-	-
FA1	25	300	$1.25 \cdot 10^{-5}$	Fluid	I	I	I/N	N	-
FA2	25	300	$2.50 \cdot 10^{-5}$	Fluid/Gel	I	I	I	I/N	I/N
FA3	25	300	$3.75 \cdot 10^{-5}$	Gel	Y	Y	Y	Y	Y
FA4	100	300	$3.75 \cdot 10^{-5}$	Gel	Y	Y	Y	Y	Y
FA5	25	100	$3.75 \cdot 10^{-5}$	Fluid	Y	Y	Y	Y	Y
FA6	**25**	**200**	$\mathbf{3.75 \cdot 10^{-5}}$	**Fluid/Gel**	**Y**	**Y**	**Y**	**Y**	**Y**

"N" denotes gelatin film completely disappears after the specified period
"Y" denotes gelatin film remain after the specified period
"I" denotes gelatin film is an intermediate stage between "N" and "Y", observed as a formless gel

***Figure 7.8**: Physical state of the gelatin films (FA0-FA6) after the immersion in water for 5 days*

The rheology of the dope solution is an important parameter because is related to the electrospinnability of the samples. Solutions that become into a gel after the addition of GA could not be suitable to fabricate electrospun gelatin mats since their rheology avoid the flow through the syringe. From the results shown in **Table 7.2** it can be seen that gelation occurs at high gelatin concentration (300mg/ml) combined with the necessary amounts of GA to reach the stability of films in water (0.375 %v/v). Therefore, it is necessary to reduce the gelatin concentration maintaining the percentage of GA in order to obtain solutions with both an adequate fluid rheology, so that they can be electrospun, and that result in films with good water stability. Both conditions are met in the case of the samples FA5 and FA6 (see **Table 7.2**). However,

previous studies established that for obtaining nanofibers by electrospinning the minimum gelatin concentration on aqueous AA solution at 25%v/v has to be at least of 200 mg/ml, which makes discard sample FA5 and choose sample FA6 as the solution with capacity to be electrospun.

Similarly to AA based films, alternative gelatin films were obtained from gelatin solutions using a 1:1 PBS/Ethanol mixture with PBS concentration of 0.1M. The results of the water stability test are shown in **Table 7.3**. In addition a photography of the films immersed in water after 5 days is presented on **Figure 7.9**.

***Table 7.3**: Water-stability results at different times for gelatin films from PBS(0.1M)/Ethanol (1:1) solution at different gelatin and GA concentrations, crosslinked with GA in situ method*

Ref.	[Gel] mg/ml	%[GA] mM/ml	Aspect	1h	2h	3h	24h	5 d
FP0	180	0	Fluid	N	-	-	-	-
FP1	180	$1.25 \cdot 10^{-5}$	Fluid/Gel	I	I	I	I/N	N
FP2	180	$2.50 \cdot 10^{-5}$	Gel	Y	Y	Y	Y	Y
FP3	180	$3.75 \cdot 10^{-5}$	Gel	Y	Y	Y	Y	Y
FP4	100	$3.75 \cdot 10^{-5}$	Gel	Y	Y	Y	Y	Y
FP5	120	$3.75 \cdot 10^{-5}$	Gel	Y	Y	Y	Y	Y
FP6	**100**	**$1.25 \cdot 10^{-5}$**	**Fluid/Gel**	**Y**	**Y**	**Y**	**Y**	**Y**
FP7	100	$6.25 \cdot 10^{-6}$	Fluid	N	-	-	-	-

"N" denotes gelatin film completely disappears after the specified period
"Y" denotes gelatin film remain after the specified period
"I" denotes gelatin film is an intermediate stage between "N" and "Y", observed as a formless gel

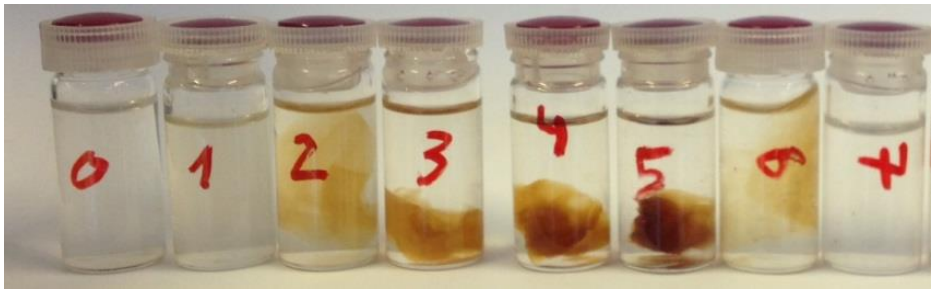

***Figure 7.9**: Physical state of the gelatin films (FP0-FP6) after the immersion in water for 5 days*

The first clearly conclusion that can be extracted from these results is that the gelatin capacity of crosslinking is higher in films obtained from PBS/Ethanol solvent compared with the prepared using AA solvent due to the different acidity of the samples. This behavior agrees with the results observed for both GA vapor and immersion methods. Hence, for the same gelatin and GA concentration, the dope solution behaves as a gel when using PBS/Ethanol solvent while it behaves as a fluid for AA based solutions (compare Sample FA5 and FP4).

The high crosslinking capacity of gelatin regenerated using PBS/Ethanol solvent is an advantage from the point of view of stability of the films. However, this behavior is a disadvantage in relation to the application of the GA in situ-method during electrospinning due to the strong tendency to form gels gel even at low concentration of gelatin and GA (see sample FP6).

7.3.3.2. Gelatin electrospun mats

Taking on board the results discussed for gelatin films, which have determined the rheology of the dope solutions and the stability of the films after the addition of GA, one composition of each solvent system was chosen as suitable solution to go through the electrospinning process in order to fabricate directly crosslinked nanofibers. Particularly conditions corresponding to samples FA6 and FP6 were selected to prepare the dope solutions that subsequently will be electrospun. Rheology of the solution and morphology of the fibers are shown in **Table 7.4** along with samples prepared without the presence of GA.

***Table 7.4**: Electrospinnability of two different gelatin solutions (200mg/ml of gelatin in AA (EA) and 100 mg/ml in PBS/Ethanol(EP)) with and without the addition of GA in situ*

Ref.	Solvent	[Gel] mg/ml	% [GA] mM/ml	Aspect	Electrospinnig
EA1	AA25	200	$3.75 \cdot 10^{-5}$	Fluid/Gel	Unspinnable
EA2	AA25	200	0	Fluid	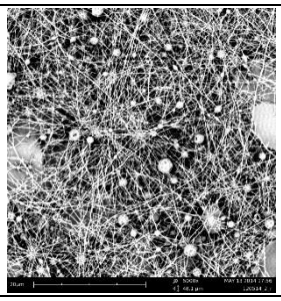
EP1	ETPBS	100	$1.25 \cdot 10^{-5}$	Fluid/Gel	Unspinnable
EP2	ETPBS	100	0	Fluid	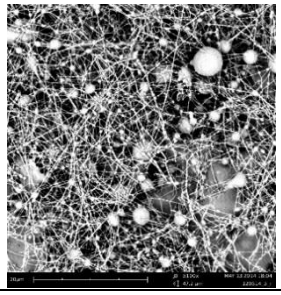

From the results it was observed that the addition of GA to the dope solution hinders their electrospinnability due to the increase of the solution viscosity, which prevents the pass of the gelatin through the syringe, as it was previously observed by Angarano et al. [7.32]. Consequently, the GA in situ method coupled to the electrospinning step failed for the selected conditions. Moreover, taking into account that for concentration below 100 mg/ml is not possible to electrospin the PBS/Ethanol based solution, the electrospinning of these solutions was discarded.

These results also suggest the impossibility to electrospun gelatin nanofibers directly crosslinked by the GA in situ method for solutions based on PBS/Ethanol solvent taking into account that the solution with the minimum amount of gelatin needed to electrospin (100mg/ml) becomes unspinnable after the incorporation of the minimum GA concentration (EP1 sample) needed to provide water resistance to the fibers. Thus, the optimization of GA in situ method was focused on gelatin solutions using aqueous acetic acid solvent since there is still scope for reducing the viscosity of the solution by decreasing the concentration of gelatin.

The experiments described on **Table 7.5** were carried out based on the idea to reduce the solution viscosity and allow the electrospinnability. The actions to reduce the viscosity were concentrated on decreasing the gelatin concentration, decreasing the GA concentration and decreasing the stirring time to prevent that the crosslinking reaction occurs in the solution before the electrospinning.

***Table 7.5**: Electrospinnability and water-stability results for gelatin films from aqueous acetic acid (25%) solution at different gelatin and GA concentrations and stirring time, crosslinked with GA in situ method*

Ref.	[Gel] mg/ml	% [GA] mM/ml	Stirring time	[GA]/[Gel] (mM /mg)	Aspect	Electrospinning	Dissolvability
EA3	100	$1.88 \cdot 10^{-4}$	1 h	$18.8 \cdot 10^{-7}$	Fluid	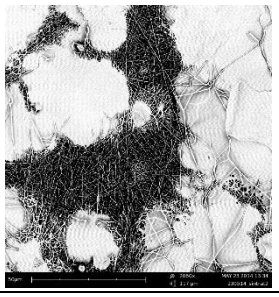	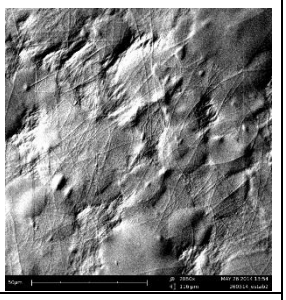
EA4	200	$2.50 \cdot 10^{-5}$	1 h	$1.25 \cdot 10^{-7}$	Fluid/Gel	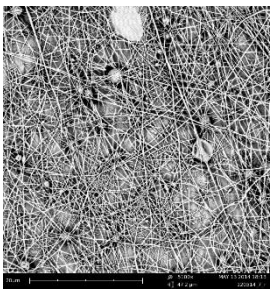	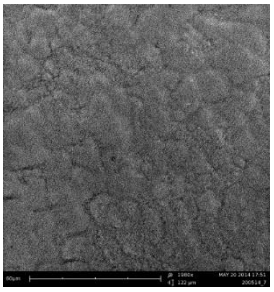
EA5	200	$3.75 \cdot 10^{-5}$	1h	$1.88 \cdot 10^{-7}$	Gel	Unspinnable	-
EA6	200	$3.75 \cdot 10^{-5}$	5 min	$1.88 \cdot 10^{-7}$	Fluid	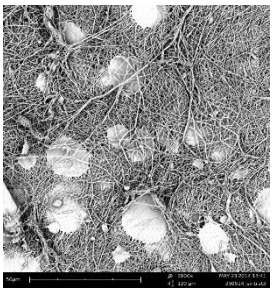	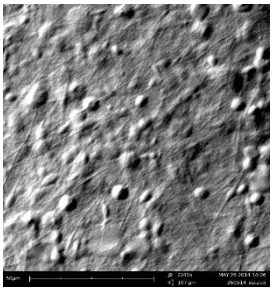
EA7	200	$1.88 \cdot 10^{-4}$	1 h	$9.38 \cdot 10^{-7}$	Gel	Unspinnable	-
EA8	300	$2.50 \cdot 10^{-5}$	5 min	$0.83 \cdot 10^{-7}$	Fluid	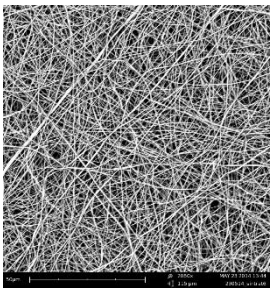	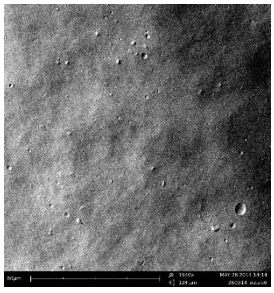
EA9	300	$3.75 \cdot 10^{-5}$	5 min	$1.25 \cdot 10^{-7}$	Fluid	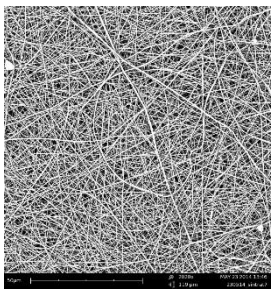	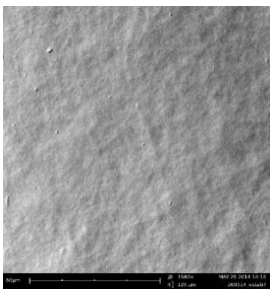

The results show that only two samples, EA3 and EA6, are stable to the water stability test. Nevertheless, after the test the samples appeared swollen and fused as it was confirmed by SEM images. In addition, fiber diameter significantly increases after the water stability test (**Figure 7.10**) which corroborates the poor stability of the electrospun fibers.

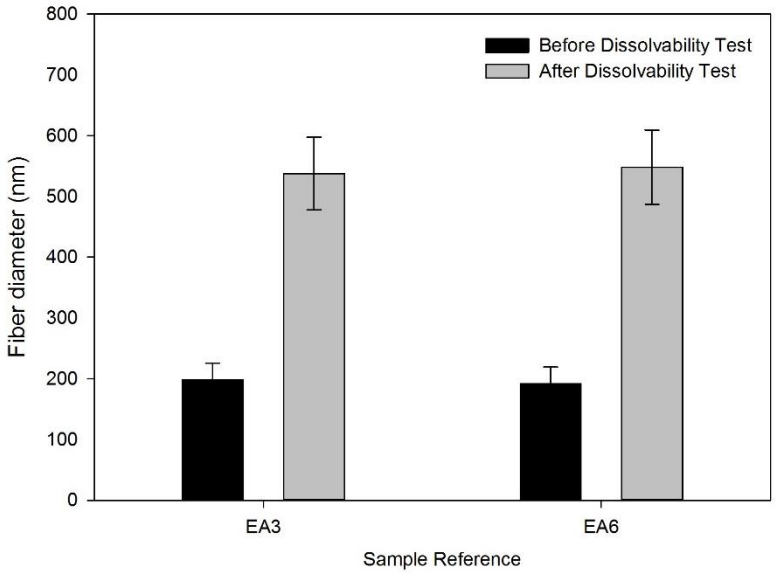

***Figure 7.10**: Average electrospun fiber diameter (from GA crosslinking in situ method) before and after the water-resistant test for samples EA3 and EA7 described on Table 7.5*

Although the ratio between GA and gelatin concentration can be considered the most important in order to control the crosslinking reaction, the results for this GA in situ method allow to conclude that both the gelatin concentration and the stirring time are also interesting parameter to take into account in order to obtain solutions with a suitable rheology (viscosity) for electrospinning. On the one hand it was observed that, for the same gelatin concentration, the stirring time allowed to mix the reagents maintaining the solution viscosity into an electrospinnable range was inversely proportional to the [GA]/[Gel] ratio (EA4 vs EA6) since the crosslinking reaction is faster for solutions with high concentration of the reagents. On the other hand, the results show that for the same stirring time, gelation occurs before for higher the ratio [GA]/[Gel] allowed before to form a gel is higher for solutions with lower gelatin concentration (EA3 vs EA7). Thus, the process optimization must be a compromise between three parameters: ratio GA/Gel, gelatin concentration and stirring time.

7.3.4. Electrospun fibers characterization

FT-IR analysis was carried out to characterize the chemical structure of the electrospun gelatin fibers and it changes after the crosslinking with GA. FTIR spectra of the resulted fibers are shown in **Figure 7.11** where the uncrosslinked samples are compared with the crosslinked samples using the GA vapor method.

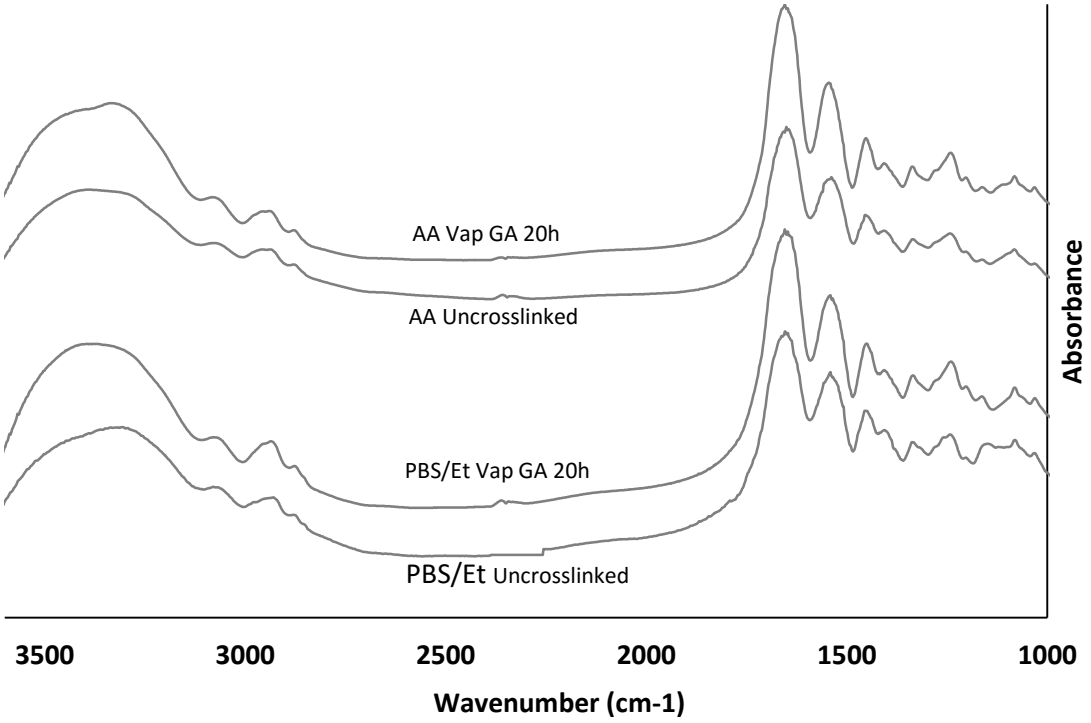

***Figure 7.11**: FT-IR spectra of electrospun gelatin nanofibers obtained from two different solvent (Acetic acid and PBS/Ethanol) before and after being crosslinked by the GA vapor method during 20 h*

Firstly, it can be noted that the FTIR spectra of the un-cross-linked electrospun gelatins revealed a structure that was similar to raw gelatin, reported in many literature [7.22-7.23, 7.34], showing the following characteristic peaks: Amide I (C=O stretch) at 1636-1640 cm^{-1}, Amide II (N-H bend and C-H stretch) at 1542-1544 cm^{-1} , Amide III (C-N stretch plus N-H in phase bending) at 1240 cm^{-1} and Amide A (N-H stretching vibration) at 3300 cm^{-1}. However, it can be observed slight differences in the peaks related with the O-H (around 3300 cm^{-1}) and C-O stretches (around 3300 cm^{-1} and 1100 cm^{-1}) between the spectra of un-crosslinked gelatins depending on the solvent system used. While the changes on the band affecting the O-H peak (between 3200 and 3600 cm^{-1}) is related with differences in the water content of the samples, the changes related with the C-O group are probably due to the presence of traces of ethanol from PBS/Ethanol solvent, which causes the emergence of a new peak around the 1100 cm^{-1}.

Regarding the difference between samples before and after crosslinking, it can be note that the spectra are very similar. Many literature have analyzed the effect of GA crosslinking reaction of gelatin samples on infrared spectra, indicating small differences on characteristics peaks [7.36, 7.42, 7.45, 7.49]. Glutaraldehyde have an aldehyde group (-CHO) that reacts with the amino group of the lysine residues of proteins [7.37], turning to yellow the color of sample because the aldimine linkage (CH=N) reactions formed during the crosslinking process. The characteristic absorption of the aldimine groups occurred at 1450 cm^{-1} , so, increasing the amount of CH=N groups on the spectra along with changes on the amide peaks, due to their involvement on the crosslinking reaction, determine the differences between crosslinked and uncrosslinked sample. However, in this case, like in the previously reported studies mentioned, the differences on the spectra before and after crosslinking are so small that it is difficult to assert that are due to the crosslinking process and not to the accuracy of the measure, as it was assumed by other reported study which indicate that the chemical structure of gelatin was largely preserved in the process of GA crosslinking [7.23].

For this reason, a complementary study with TGA to evaluate the thermal stability of electrospun gelatin fibers was carried out in order to find the effect of GA crosslinking on nanofibers. The results (**Figure 7.12**) allowed observing two type of differences between the thermograms, especially related with the residual mass of the samples after the thermal treatment. On the one hand, the nanofibers fabricated using AA showed a lower percentage of residual mass than the electrospun fibers from PBS/Ethanol solvent due to the presence of inorganic salts in nanofibers from PBS/Ethanol. On the other hand, comparing the results obtained for nanofibers from the same solvent system it can be note significant differences between the thermograms before and after the crosslinking process by GA vapor. In both cases, the residual weight of the electrospun mats treated with GA vapor during 20h was lower compared with the obtained for the non treated mats, suggesting the presence of an amount of free GA. The presence of GA on the samples is corroborated by the onset degradation temperature observed which occurs around 185ºC, close to the boiling point of GA (187 ºC). Also, the results show that the amount of free GA is higher for samples of AA mats (higher difference between the residual masses), suggesting that the amount of free GA is lower in mats from PBS/Ethanol since crosslinking reactions are promoted at neutral pH. So, although the results suggest a decrease in thermal stability by the crosslinked mats, the removing of free GA must be necessary to compare the real stability of crosslinked mats.

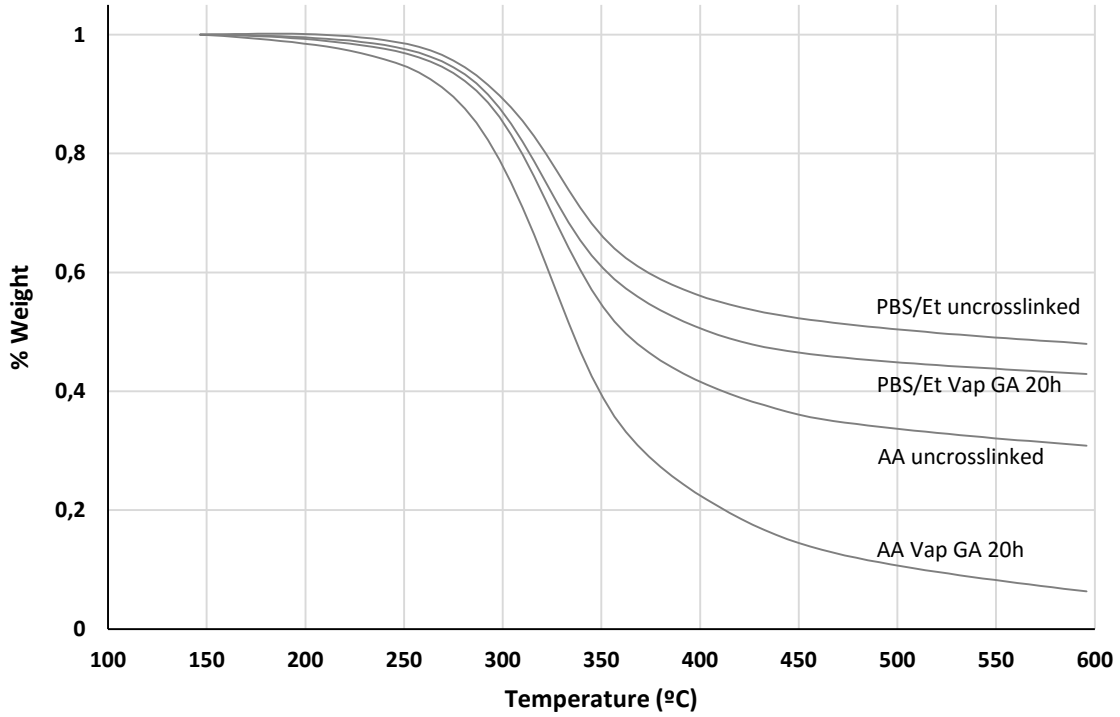

***Figure 7.12**: Thermograms of electrospun gelatin nanofibers obtained from two different solvent (Acetic acid and PBS/Ethanol) before and after being crosslinked by the GA vapor method during 20 h*

7.4. Conclusions

The viability of crosslinking electrospun gelatin mats fabricated using two different benign solvent by three different GA based methods was demonstrated. So, the effect of each crosslinking method on the electrospun fiber morphology and diameter was analyzed. In addition, for the GA vapor method the effect of time on the degree of crosslinking was determined.

The results indicated that the electrospun gelatin fibers were stable to water after 30 minutes of contact with GA vapor, being virtually complete after 2 hours. Comparing these times with the obtained for the stabilization of gelatin films (minimum of 24 h) it was demonstrated the importance to take into account both the thickness and the surface area of sample to establish the crosslinking conditions. Despite the different behavior of gelatin films and electrospun mats regarding to the time to achieve stability, the behavior in front of the solvent used for the fabrication of samples (AA or PBS/ethanol) was the same in both cases. The crosslinking reaction was more effective for samples from PBS/ethanol (neutral pH), suggesting the presence of residual solvent on final gelatin samples, which determine their pH and as a result, the crosslinking degree.

Besides this, the effect of GA vapor on the morphology of the fibers was also significantly different for both type of mats. GA vapor method induces a slight swelling of the fibers fabricated using AA solvent after the water-stability test while the PBS/Ethanol fibers showed a high swelling and fusion just after contact with GA vapor because its greater capacity to absorb the water vapor. Therefore, an increase of fiber diameter was observed after the crosslinking process by GA vapor, being higher for fiber from PBS/Ethanol solvent, which practically triplicates its size. Similar trends were obtained for mats crosslinked using GA immersion method, observing higher swelling for fibers treated with GA vapor since the presence of ethanol in the PBS/ethanol mixture causes dehidratation of the samples.

The viability of a novel method based on the incorporation of GA directly on the dope solution in order to obtain electrospun fibers directly crosslinked was analyzed for mats fabricated using AA solvent. However, this method could not be applied to obtain fibers from PBS/Ethanol solvent due to its strong tendency to form gels even at low concentrations of GA, which hinders the movement of the solution through the syringe of the electrospinning machine. The results of in-situ crosslinking method for AA fibers suggested that the ability to obtain crosslinking fibers directly by electrospinning was a compromise between three solution parameters: the gelatin concentration, the ratio between GA and gelatin concentration and the stirring time before electrospin. Although this study demonstrated the viability to obtain electrospun gelatin nanofibers directly crosslinked for two combination of solution parameters used, the swelling and increased diameter of these fibers were similar than the obtained for mats crosslinked by GA vapor during 30 minutes, indicating the poor grade of stability and the need to make a comprehensive study to optimize this method.

Finally, the chemical structure of electrospun gelatin was confirmed by FTIR analysis, which pointed up the main characteristics peaks of pure gelatin. Some structural differences between crosslinked and uncrosslinked mats, which were no detected by FTIR, were observed comparing the thermograms of the samples.

7.5. References

[7.1] E.S. Place, N.D. Evans, M.M. Stevens, Complexity in biomaterials for tissue engineering., Nat. Mater. 8 (2009) 457–70.

[7.2] M.M. Stevens, J.H. George, Exploring and engineering the cell surface interface., Science. 310 (2005) 1135–8.

[7.3] M. PX, Biomimetic materials for tissue engineering, Adv Drug Deliv. Rev. 60 (2008) 184–198.

[7.4] T. Garg, O. Singh, S. Arora, R.S.R. Murthy, Scaffold: A Novel Carrier for Cell and Drug Delivery, Crit. Rev. Ther. Drug Carr. Syst. 29 (2012) 1–63.

[7.5] N. Bhardwaj, S.C. Kundu, Electrospinning: a fascinating fiber fabrication technique., Biotechnol. Adv. 28 (2010) 325–47.

[7.6] R. Schrieber, H. Gareis, Gelatin handbook- Theory and Insutrial Practice, Wiley, 2007.

[7.7] D. Meyer, J.-P. Blaauwhoed, Handbook of Hydrocolloids, CRC Press, 2009.

[7.8] S.-M. Lien, W.-T. Li, T.-J. Huang, Genipin-crosslinked gelatin scaffolds for articular cartilage tissue engineering with a novel crosslinking method, Mater. Sci. Eng. C. 28 (2008) 36–43.

[7.9] S.-W. Choi, Y. Zhang, Y. Xia, Three-dimensional scaffolds for tissue engineering: the importance of uniformity in pore size and structure., Langmuir. 26 (2010) 19001–6.

[7.10] S. Gautam, A.K. Dinda, N.C. Mishra, Fabrication and characterization of PCL/gelatin composite nanofibrous scaffold for tissue engineering applications by electrospinning method., Mater. Sci. Eng. C. Mater. Biol. Appl. 33 (2013) 1228–35.

[7.11] S. Baiguera, C. Del Gaudio, E. Lucatelli, E. Kuevda, M. Boieri, B. Mazzanti, et al., Electrospun gelatin scaffolds incorporating rat decellularized brain extracellular matrix for neural tissue engineering., Biomaterials. 35 (2014) 1205–14.

[7.12] M. Djabourov, J. Leblond, P. Papon, Gelation of aqueous gelatin solutions. I. Structural Investigation., J. Phys. Fr. 49 (1988) 319–332.

[7.13] M. Djabourov, J. Leblond, P. Papon, Gelation of aqueous gelatin solutions . II . Rheology of the sol-gel transition To cite this version : Gelation of aqueous transition Rheology of the sol-gel, (1988).

[7.14] M. Li, M.J. Mondrinos, M.R. Gandhi, F.K. Ko, A.S. Weiss, P.I. Lelkes, Electrospun protein fibers as matrices for tissue engineering, Biomaterials. 26 (2005) 5999–6008.

[7.15] H.-W. Kim, J.-H. Song, H.-E. Kim, Nanofiber Generation of Gelatin-Hydroxyapatite Biomimetics for Guided Tissue Regeneration, Adv. Funct. Mater. 15 (2005) 1988–1994.

[7.16] Z.-M. Huang, Y.. Zhang, S. Ramakrishna, C.. Lim, Electrospinning and mechanical characterization of gelatin nanofibers, Polymer (Guildf). 45 (2004) 5361–5368.

[7.17] Y. Zhang, H. Ouyang, C.T. Lim, S. Ramakrishna, Z.-M. Huang, Electrospinning of gelatin fibers and gelatin/PCL composite fibrous scaffolds., J. Biomed. Mater. Res. B. Appl. Biomater. 72 (2005) 156–65.

[7.18] Y.Z. Zhang, J. Venugopal, Z.-M. Huang, C.T. Lim, S. Ramakrishna, Crosslinking of the electrospun gelatin nanofibers., Polymer (Guildf). 47 (2006) 2911–2917.

[7.19] K. Gast, A. Siemer, D. Zirwer, G. Damaschun, Fluoroalcohol-induced structural changes of proteins: some aspects of cosolvent-protein interactions., Eur. Biophys. J. 30 (2001) 273–283.

[7.20] C.S. Ki, D.H. Baek, K.D. Gang, K.H. Lee, I.C. Um, Y.H. Park, Characterization of gelatin nanofiber prepared from gelatin–formic acid solution., Polymer (Guildf). 46 (2005) 5094–5102.

[7.21] J.-H. Song, H.-E. Kim, H.-W. Kim, Production of electrospun gelatin nanofiber by water-based co-solvent approach., J. Mater. Sci. Mater. Med. 19 (2008) 95–102.

[7.22] M. Erencia, F. Cano, M.M. Tornero, Jose Antonio Fernandes, T. Tzanov, J. Macanás, F. Carrillo, Electrospinning of gelatin scaffolds with low acetic acid concentration effect of solvent composition on both diameter of nanofibers and cell viability, Summited. (2014).

[7.23] Z. Zha, W. Teng, V. Markle, Z. Dai, X. Wu, Fabrication of gelatin nanofibrous

scaffolds using ethanol/phosphate buffer saline as a benign solvent., Biopolymers. 97 (2012) 1026–1036.

[7.24] M. Erencia, F. Cano, J. a Tornero, J. Macanás, F. Carrillo, Preparation of electrospun nanofibers from solutions of different gelatin types using a benign solvent mixture composed of water/salt/ethanol., To Be Summited. (2014).

[7.25] K.Y. Lee, J. Shim, H.G. Lee, Mechanical properties of gellan and gelatin composite films, Carbohydr. Polym. 56 (2004) 251–254.

[7.26] K. Yasuda, J. Ping Gong, Y. Katsuyama, A. Nakayama, Y. Tanabe, E. Kondo, et al., Biomechanical properties of high-toughness double network hydrogels., Biomaterials. 26 (2005) 4468–75.

[7.27] M.G. Haugh, M.J. Jaasma, F.J. O'Brien, The effect of dehydrothermal treatment on the mechanical and structural properties of collagen-GAG scaffolds., J. Biomed. Mater. Res. A. 89 (2009) 363–9.

[7.28] D. Lew, P.H. Liu, D.P. Orgill, Optimization of UV Cross-Linking Density for Durable and Nontoxic Collagen GAG Dermal Substitute., J Biomed Mater Res B Appl Biomater. 82 (2007) 51–56.

[7.29] S. Zhang, Y. Huang, X. Yang, F. Mei, Q. Ma, G. Chen, et al., Gelatin nanofibrous membrane fabricated by electrospinning of aqueous gelatin solution for guided tissue regeneration., J. Biomed. Mater. Res. A. 90 (2009) 671–9.

[7.30] S. Torres-Giner, J. V Gimeno-Alcañiz, M.J. Ocio, J.M. Lagaron, Comparative performance of electrospun collagen nanofibers cross-linked by means of different methods., ACS Appl. Mater. Interfaces. 1 (2009) 218–23.

[7.31] H. Liang, W. Chang, H. Liang, M. Lee, H. Sung, Crosslinking Structures of Gelatin Hydrogels Crosslinked with Genipin or a Water-Soluble Carbodiimide, (2003).

[7.32] M. Angarano, S. Schulz, M. Fabritius, R. Vogt, T. Steinberg, P. Tomakidi, et al., Layered Gradient Nonwovens of In Situ Crosslinked Electrospun Collagenous Nanofibers Used as Modular Scaffold Systems for Soft Tissue Regeneration, Adv. Funct. Mater. 23 (2013) 3277–3285.

[7.33] S. Panzavolta, M. Gioffrè, M.L. Focarete, C. Gualandi, L. Foroni, A. Bigi, Electrospun gelatin nanofibers: optimization of genipin cross-linking to preserve

fiber morphology after exposure to water, Acta Biomater. 7 (2011) 1702–9.

[7.34] K. Sisson, C. Zhang, M.C. Farach-Carson, D.B. Chase, J.F. Rabolt, Evaluation of cross-linking methods for electrospun gelatin on cell growth and viability., Biomacromolecules. 10 (2009) 1675–80.

[7.35] R.. de Carvalho, C.R.. Grosso, Characterization of gelatin based films modified with transglutaminase, glyoxal and formaldehyde., Food Hydrocoll. 18 (2004) 717–726.

[7.36] S. Farris, J. Song, Q. Huang, Alternative reaction mechanism for the cross-linking of gelatin with glutaraldehyde., J. Agric. Food Chem. 58 (2010) 998–1003.

[7.37] A. Bigi, G. Cojazzi, S. Panzavolta, K. Rubini, N. Roveri, Mechanical and thermal properties of gelatin films at different degrees of glutaraldehyde crosslinking., Biomaterials. 22 (2001) 3–8.

[7.38] I. Migneault, C. Dartiguenave, M.J. Bertrand, K.C. Waldron, Glutaraldehyde : behavior in aqueous solution , reaction with proteins , and application to enzyme crosslinking, 37 (2004).

[7.39] L.H.H.O. Damink, P.J. Dijkstra, M.J.A. Van Luyn, P.B. Van Wachem, P. Nieuwenhuis, J. Feijen, Glutaraldehyde as a crosslinking agent for collagen-based biomaterials, J. Mater. Sci. Mater. Med. 6 (1995) 460–472.

[7.40] A. Talebian, S.S. Kordestani, A. Rashidi, F. Dadashian, M. Montazer, The Effect of Glutaraldehyde on the Properties of Gelatin Films, 56 (2007) 537–541.

[7.41] L. Jeong, W.H. Park, Preparation and characterization of gelatin nanofibers containing silver nanoparticles., Int. J. Mol. Sci. 15 (2014) 6857–79.

[7.42] M.A. Oraby, A.I. Waley, A.I. El-dewany, E.A. Saad, M.A. El-hady, Electrospun Gelatin Nanofibers : Effect of Gelatin Concentration on Morphology and Fiber Diameters., Polym. J. 9 (2013) 534.

[7.43] M. Skotak, S. Noriega, G. Larsen, A. Subramanian, Electrospun cross-linked gelatin fibers with controlled diameter: the effect of matrix stiffness on proliferative and biosynthetic activity of chondrocytes cultured in vitro., J. Biomed. Mater. Res. A. 95 (2010) 828–36.

[7.44] H.-C. Chen, W.-C. Jao, M.-C. Yang, Characterization of gelatin nanofibers electrospun using ethanol/formic acid/water as a solvent., Polym. Adv. Technol. 20 (2009) 98–103.

[7.45] T.-H. Nguyen, Fabrication and characterization of cross-linked gelatin electro-spun nano-fibers., J. Biomed. Sci. Eng. 03 (2010) 1117–1124.

[7.46] M. Erencia, F. Cano, J. a Tornero, J. Macanás, F. Carrillo, Resolving the electrospinnability zones and diameter prediction for the electrospinning of the gelatin/water/acetic Acid system., Langmuir. 30 (2014) 7198–205.

[7.47] S.-C. Wu, W.-H. Chang, G.-C. Dong, K.-Y. Chen, Y.-S. Chen, C.-H. Yao, Cell adhesion and proliferation enhancement by gelatin nanofiber scaffolds., J. Bioact. Compat. Polym. 26 (2011) 565–577.

[7.48] W.-H. Lin, W.-B. Tsai, In situ UV-crosslinking gelatin electrospun fibers for tissue engineering applications., Biofabrication. 5 (2013) 035008.

[7.49] M.A. Oraby, A.I. Waley, A.I. El-dewany, E.A. Saad, B.M.A. El-hady, E.T. Al, Electrospinning of Gelatin Functionalized with Silver Nanoparticles for Nanofiber Fabrication, 2013 (2013) 95–105.

CHAPTER 8:

Electrospinning of collagen nanofibers onto the surface of end-group-modified polyurethanes

Electrospinning of collagen nanofibers onto the surface of end-group-modified polyurethanes

SUMMARY

The electrospinning of collagen nanofibers and their deposition onto three different end-group-modified polyurethane biomaterials has been studied. Stable nanofibers were obtained using a 8% w/v collagen solution in 1,1,1,3,3,3-hexafluoro-2-propanol when operational parameters (voltage, flow and distance between needle and collector) were set at 15 kV, 0,5 ml/h and 15 cm, respectively. Using these conditions, the polyurethanes were successfully coated by a nanofiber layer of collagen nanofibers with a distribution of the fibers, aligned or random, that depends of the manner of arranging the polyurethane samples in the collector device of the electrospinning machine. Moreover, it was demonstrated that the deposition process of the collagen nanofibers was not dependent of the end group of the modified polyurethane. The resulted collagen coating were not stable to PBS solution, so the treatment with glutaraldehyde vapor atmosphere was necessary to achieve stability to water treatments such as simulated cell culture solution. Both the properties of coated polyurethanes and collagen deposited fibers were analyzed by different characterization techniques such as contact angle and scanning electron microscopy. The results showed that it was possible to deposit a layer of collagen nanofibers onto polyurethane biomaterials, regardless the chemical end-group characteristic of the surface. After the crosslinking reaction with glutaraldehyde, the collagen nanofibers show stability to wet treatments. Moreover, it was shown that the coating of the polyurethanes with the collagen nanofibers did not change the surface properties of the biomaterials as it was corroborated by contact angle measurements. Also, the morphology and diameter of the collagen nanofibers were not influenced by the characteristic polyurethane end-group. Finally, the IR absorption bands of electrospun collagen fibers were analyzed and compared to the bands of the original lyophilized collagen, observing slight differences between them that suggests denaturation of collagen caused by the solution and electrospinning processes.

Keywords: electrospinning, nanofibers, collagen, coating, polyurethane.

8.1. Introduction

One of the most important objectives in tissue engineering field falls in obtaining an adequate scaffold, which may be permanently integrated into or bioresorbed by the body and must be capable of mimicking the conditions and characteristics present in local microenvironment throughout the mammalian organ system. Ideally, tissue engineering scaffold should mimic the chemical composition, the physical morphology and the biological functions of native extracellular matrix (ECM), which provides mechanical support to cells and regulates cell activities.

Advancements in nanotechnology, specifically in the field of nanofiber fabrication, have shown great promise with respect to developing clinically relevant scaffolds [8.1]. In this way, the electrospinning process, well known for many years in the textile industry and in organic polymer science [8.2-8.5] has re-emerged in the last years running as one of the best techniques for generating biopolymer scaffolding for tissue engineering, due to the closely mimics of the topology of the electrospun scaffols to the native ECM. Many studies, most of them based on biodegradable polymers materials, have been carried out in the application of polymer nanofibers in the tissue enginnering of bone [8.6], blood vessels [8.7-8.8], cartilage [8.9], skin [8.10], etc.

Electrospinning technique has demonstrated their ability to fabricate nanofiber from solutions of different polymer type, both synthetic [8.11-8.13] as natural polymers, including polysaccharides [8.14] and proteins such as collagen [8.15-8.16], silk fibroin [8.17] and gelatin [8.18]. Among the natural polymers with the ability to perform nanofibers by electrospinning, collagen is one of the best candidates for the fabrication of tissue scaffolds for its excellent properties of biodegradation and biocompatibily. The solvent used for the production of collagen electrospun scaffolds is an important parameter to take into account, which should be able to dissolve the protein and to be evaporated during the electrospinning process. Although recently new benign solvent has been studied for the production of collagen nanofibers by electrospinning [8.19-8.20] in order to avoid the potential denaturation of collagen native structure [8.21] in solution, the most common solvent used for electrospun collagen and their blends is still fluoroalchols, such as 1,1,1,3,3,3 hexafluoro-2-propanol due to its good solvent properties [8.22-8.23].

But an ideal tissue-engineered scaffold not should only be capable of functioning biologically in the implant site, but they must be mechanical stable, which is mainly dependent primarily on the section of the biomaterial, the architectural design of the

scaffold and the cell material interactions. The scaffold must be able to withstand the forces exerted by, e.g. pulsed blood flow [8.24].

Although polymer fibers have been successfully used in the preparation of scaffolds, few recently studies have focused on the mechanical properties of single fibers in the submicron range [8.25-8.27], highlighting the low mechanical and structural properties of support to perform well after implantation of the natural proteins such collagen alone. In this way, recent developments has been focused in the blending of natural proteins with synthetic (PCL [8.28], PVA [8.29], PLGA [8.30], etc.) or natural (silk [8.31], etc.) biodegradable polymers, polysaccharides (HA [8.32], chitosan [8.33], etc.), etc. The process of obtaining these copolymers is based on the electrospinning of a solution directly including the two different types of polymers in a certain proportion.

However, taking into account that the cell attachment and compatibility is a surface phenomenon, this study explore the possibility to modify surface properties of polyurethane biomaterials (which has been also used as a copolymer to create a blending with collagen by electrospinning [8.34]) by depositing a nanolayer of collagen electrospun fibers onto their surface. In this way, it will be possible to obtain a scaffold with adequate mechanical properties due to the presence of polyurethane and with improved biocompatibility promoted by the collagen layer. Although the coating of polyurethane scaffold with collagen has been previously investigated using a bulk collagen solution [8.35], it is expected that the local application of collagen nanofibers by electrospinning onto the surface of different modified polyurethanes allow to distribute the nanofibers according to a predefined concentration and orientation which will control the final properties of these biomaterials.

The aim of this study was to optimize the electrospinning process to obtain stable collagen nanofibers by controlling the main operational parameters (voltage, flow rate, distance between needle and collector) in order to modify the surface of polyurethane biomaterials by depositing a nanolayer of collagen fibers onto their surface. The deposition of nanofibers were optimized, in order to create a random distribution onto the polyurethane surface, and the coating was stabilized using glutaraldehyde vapor as a crosslinking agent. Finally, the properties of the resulted coated materials were analyzed by SEM, IR spectroscopy and contact angle to determine their final properties.

8.2. Experimental

8.2.1. Materials

Acid soluble, lyophilized collagen type I of bovine skin and 1,1,1,3,3,3-hexafluoro-2-propanol (HIPF) (>99%) were purchased from Sigma Aldrich (Madrid, Spain) and were used without further treatment or purification. Three types of polyurethane films (0,135 mm of thickness, Figure 8.1) were purchased from DSM Biomedical (Bionate 80A UR) and the surface treatments to incorporate sulfonate and octadecyl end functional groups were carried out by the polymer technology group of DSM, from Berkley, USA. The collagen nanofibers were stabilized by crosslinking reaction using aqueous glutaraldehyde solution 25% from Panreac (Castellar del Vallés, Barcelona) and the resulted stability was controlled by treatment with Dulbecco's Modified Eagle's Medium (DMEM) from Sigma Aldrich (Madrid,Spain).

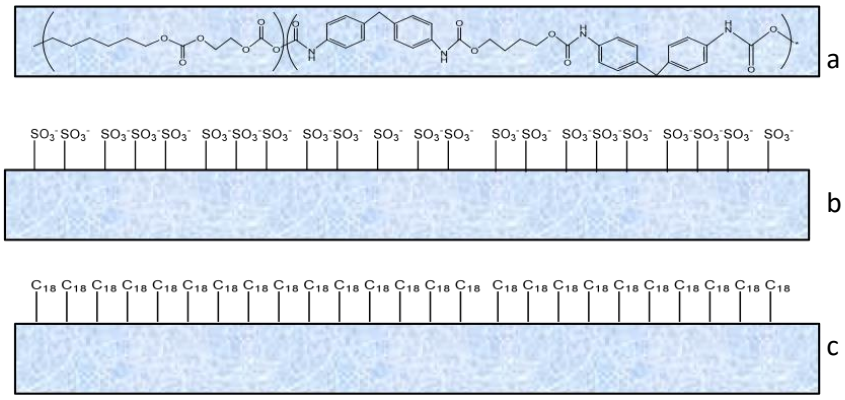

Figure 8.1. *Chemical structure of unmodified polyurethane (a) and modified incorporating sulfonate (b) and octadecyl (c) end-groups*

8.2.2. Electrospun collagen nanofibers

Electrospinning was carried out in a home-made device developed by INTEXTER [8.36-8.37]. Operational parameters and conditions of the dope solution were adjusted taking into account some previous articles [8.16, 8.24, 8.38-8.40]. In this sense, acid soluble collagen was dissolved in HIPF at a concentration of 8% w/v by stirring for 1 h at room temperature (25 ºC) and the solution was placed in a 2.5 ml syringe with a stainless steel syringe needle (0.6 mm of inner diameter) connected to the anode of a power supply. Electrospinning operational parameters were initially set to: 15 kV of applied voltage, 0.5 ml/h of flow rate and 12 cm of distance between needle and collector. After that the operational parameters were adjusted until the formation of a

stable jet of nanofibers. To assess the stability of the jet of collagen nanofibers a high definition camera was coupled to the electrospinning machine (Figure 8.2). Once the jet was stabilized, the nanofibers were projected over the surface of the polyurethane samples and their distribution was analyzed by optical microscope and SEM (see 8.2.4.3.) The electrospun collagen nanofibers were deposited on the surface of polyurethane films which were previously fixed on the copper collector connected to the cathode of the power supply. The arrangement of the sample to the collector was adapted in order to obtain aligned or random distribution of the nanofibers. Nanofibers were collected for a time of 1 minute, ensuring the formation of a nanolayer of collagen fibers on the polyurethane surface.

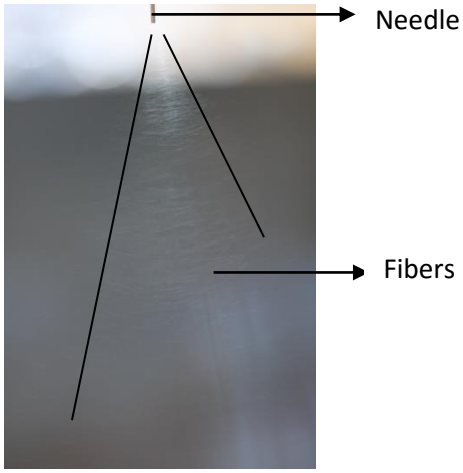

Figure 8.2: *Image captured by a digital camera of a jet of nanofibers leaving the needle of an electrospinning machine (8% w/v collagen in HIPF)*

8.2.3. Crosslinking

The stabilization of electrospun collagen nanofibers were carried out by a glutaraldehyde (GA) based cross-linking method. Coated polyurethane films were placed on a holed ceramic shelf in the desiccator which contains 10 ml of aqueous glutaraldehyde solution (25% v/v) in a Petri dish. The fibers were crosslinked by reaction with the glutaraldehyde vapor at room temperature during 24h. After that, samples were rinsed with bidestillate water to quench unreacted glutaraldehyde and immersed in DMEM solution for 2h at 37ºC under CO_2 atmosphere. Finally, the

samples were removed from DMEM medium and put on the air dryer at 37ºC during 1h and the integrity of the nanofibers was evaluated by SEM analysis.

8.2.4. Characterization: Chemical structure and morphology

8.2.4.1. Fourier transform infrared spectroscopy (FT-IR)

Spectra of both lyophilized and electrospun collagen were collected by a Nicolet Avatar 320 spectrophotometer (Nicolet Instrument Corporation, USA) in order to characterize their chemical structure. Samples were prepared by mixing 1 mg of collagen with 300 mg of KBr followed by pressing (167 MPa). The spectrum was recorded in the range of 500 to 4000 cm^{-1} and averaging 32 scans at a resolution of 4 cm^{-1}.

8.2.4.2. Attenuated total reflectance spectroscopy (ATR)

Nicolet Avatar 320 spectrophotometer using the Smart MIRacle ATR accessory (ZnSe crystal) was used to characterize coated polyurethane films.

8.2.4.3. Microscopic analysis

A general view of the nanofiber distribution was analyzed by optical microscopy. In this case, 15 images were taken for each sample according to the scheme shown in Figure 8.3. Moreover, detailed images of the coated surfaces of polyurethane samples were observed under a scanning electron microscope (Phenom Standard SEM), allowing to determine the average diameter of the nanofibers by using an image software package (Image J). The average diameter was estimated from 50 arbitrary measures of electrospun fibers.

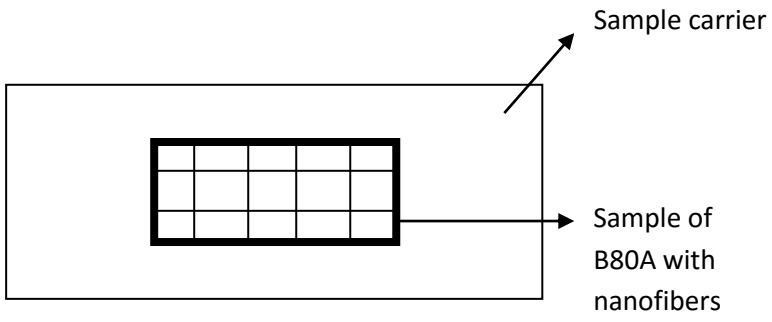

Figure 8.3: *Regions distribution for the optical microscopy characterization of B80A polyurethane samples covered with electrospun collagen nanofibers*

8.2.4.4. Surface contact angle measurament

The hydrophilic/hydrophobic character of the different polyurethane films before and after covering with a nanolayer of electrospun collagen fibers was determined by water contact angle measurements. A water drop was deposited onto the surface of the material disposed completely horizontal and the contact angle was measured from a high-definition picture captured using a Canon EOS 40D digital camera. The photographs were analyzed by an image software (Photoshop CS5) in order to obtain the accurate contact angle in each case (Figure 8.4).

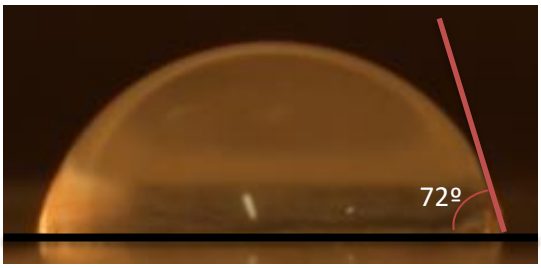

Figure 8.4. *Example of contact angle measurement from water drop photograph (polyurethane sample coated with electrospun crosslinked fibers).*

8.3. Result and discussion

8.3.1. Optimization of operational parameters to obtain electrospun collagen nanofibers

With the aim to produce a stable nanofibers jet, the operational conditions were optimized. So, a solution of 8% w/v collagen in HIPF solvent was electrospun onto the surface of polyurethane B80A. Starting from a fixed values of voltage (15kV), flow rate (0.5 ml/h) and distance between needle and collector (12 cm), slight modifications were carried to achieve an optimal range of electrospinnability. **Table 8.1** shows the operational parameters that result in a stable jet of nanofibers. Once the jet was stabilized, the nanofibers were projected over the surface of the B80A polyurethane samples and their morphology was analyzed by SEM. Particularly at 15 kV, 0.75 ml/h and 15 cm of gap distance between the syringe and the collector, both an stable jet and a smooth nanofiber surface with an average diameter size of 1150 nm ± 190 nm were obtained (Figure 8.5) which agrees with the results shown in previous researches [8.41-8.44].

***Table 8.1**: Effect of operational parameters on the stability of the jet of nanofibers from solution of collagen (8% w/v) in HIPF at room temperature*

Sample	Distance (cm)	Voltage (kV)	Rate (ml/h)	Electrospinnability
1	12	15	0.5	Unstable
2	12	10	0.5	Unstable
3	12	12.5	0.5	Unstable
4	12	11.2	0.5	Unstable
5	15	11.1	0.5	Beads
6	15	15	1	Intermittent
7	15	13	1	Intermittent
8	15	17	1	Intermittent
9	15	12	0.75	Stable
10	15	15	0.75	Stable
11	15	18	0.75	Stable

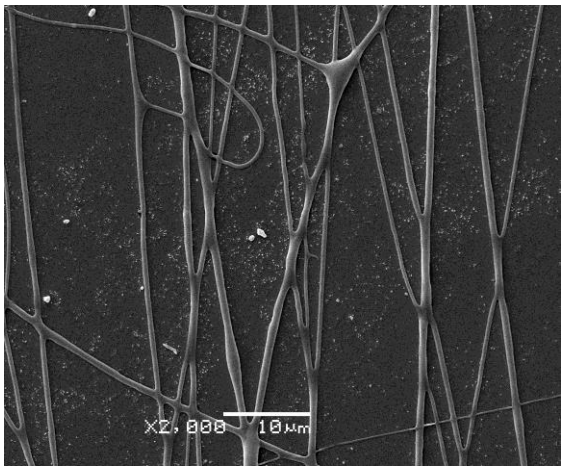

Figure 8.5: SEM image of electrospun collagen nanofibers *arranged onto B80A polyurethane.8% w/v collagen in HIPF solution was electrospun at 15 kV, 0.75 ml/h and 15 cm of gap distance between the syringe and the collector.*

8.3.2. Nanofiber distribution on polyurethane films

Surface distribution of the nanofibers onto the non-conductive polyurethane samples was found to be dependent of the arrangement of the samples in the collector. So, two types of sample arrangements were considered: i) samples located in a round conductive metal support (Figures 8.6.a), ii) samples located occupying the total surface of a small round conductive metal support turn around by a non-conductive material (Figure 8.6.b).

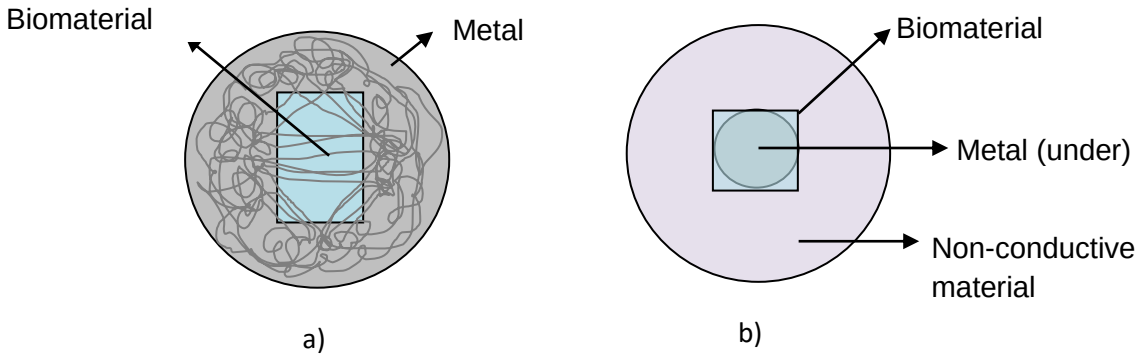

Figure 8.6: *Collector designs: a) metal based collector and b) non-conductive based collector*

For the metal based collector, the results obtained by optical microscopy (Figure 8.7) show that the collagen electrospun fibers were deposited on B80A with some preferential orientation, which can be explained by the collector design and the situation of the polyurethane on it (**Figure 8.6a**). Taking into account that the polyurethane samples are non-conductive and that they are arranged on a metal collector occupying a part of their surface, the orientation of the nanofibers occurs because the charged nanofibers fabricated are attracted by the metallic part of the collector located outside of the surface occupied by the polyurethane sample. So, nanolayers of aligned fibers can be obtained using this type of arrangement.

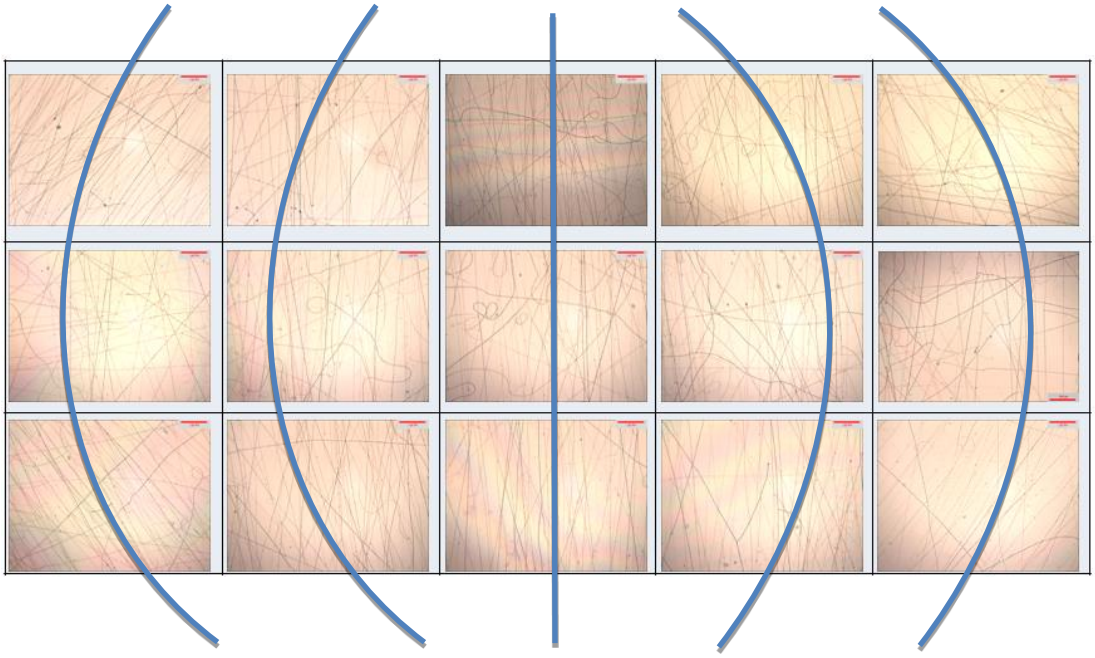

Figure 8.7 *Collage made with the microscopy photographs taken from the selected regions of the B80A scaffold covered with electrospun collagen nanofibers*

By other hand, when non-conductive based collector (**Figure 8.6b**) was used random orientation of the nanofibers was obtained (Figure 8.8) which can be useful to maximize cell proliferation [8.45].

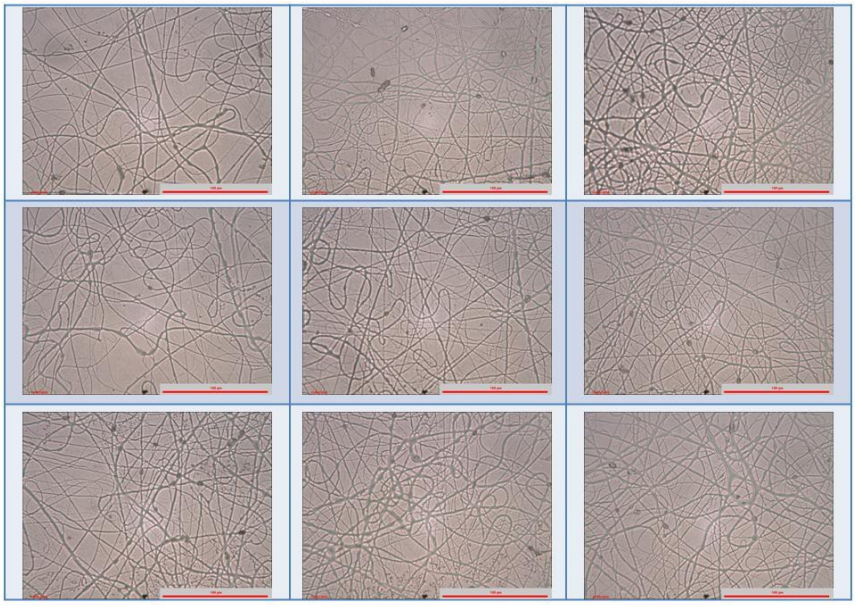

Figure 8.8. *Collage made with the microscopy photographs taken from the selected regions of the B80A polyurethane covered with electrospun collagen nanofibers using the non-conductive based collector*

8.3.3. Stability of electrospun collagen nanofibers deposited onto polyurethanes

Electrospun collagen nanofibers deposited onto polyurethane sample (Figure 8.9.a) were dissolved in contact with PBS solution (Figure 8.9.b) corroborating the lack of stability of these fibers. Taking into account that native collagen is not soluble in water it can be concluded that the resulted nanofibers did not recover the typical structure that characterize collagen fibers and therefore some denaturation process occurred during the dissolution and electrospinning processes. In order to overcome this issue a glutaraldehyde vapor-based crosslinking treatment was carried out (Figure 8.10.b). In this case the crosslinked fibers showed an adequate stability to wet treatment (Figure 8.10.c). The lfibers remain on the polyurethane surface even after its immersion in the cell culture medium (Figure 8.10.d), which allows removing the crystal salts deposited from the rising with PBS solution. Thus, the viability to obtain water-resistant electrospun collagen fibers using GA-vapor based crosslinking method was demonstrated.

a) Before rising with PBS	b) After rising with PBS
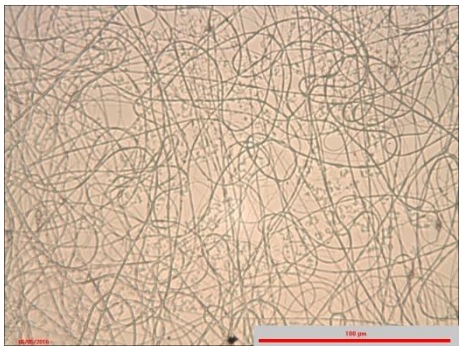	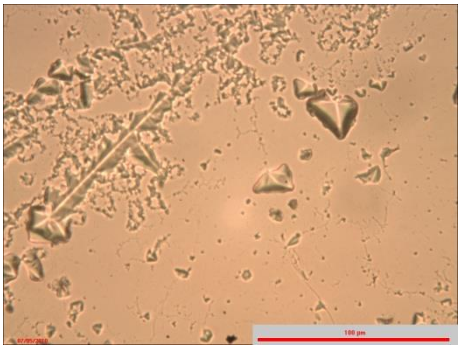

Figure 8.9. *Uncrosslinked electrospun collagen nanofibers before and after contact with PBS solution*

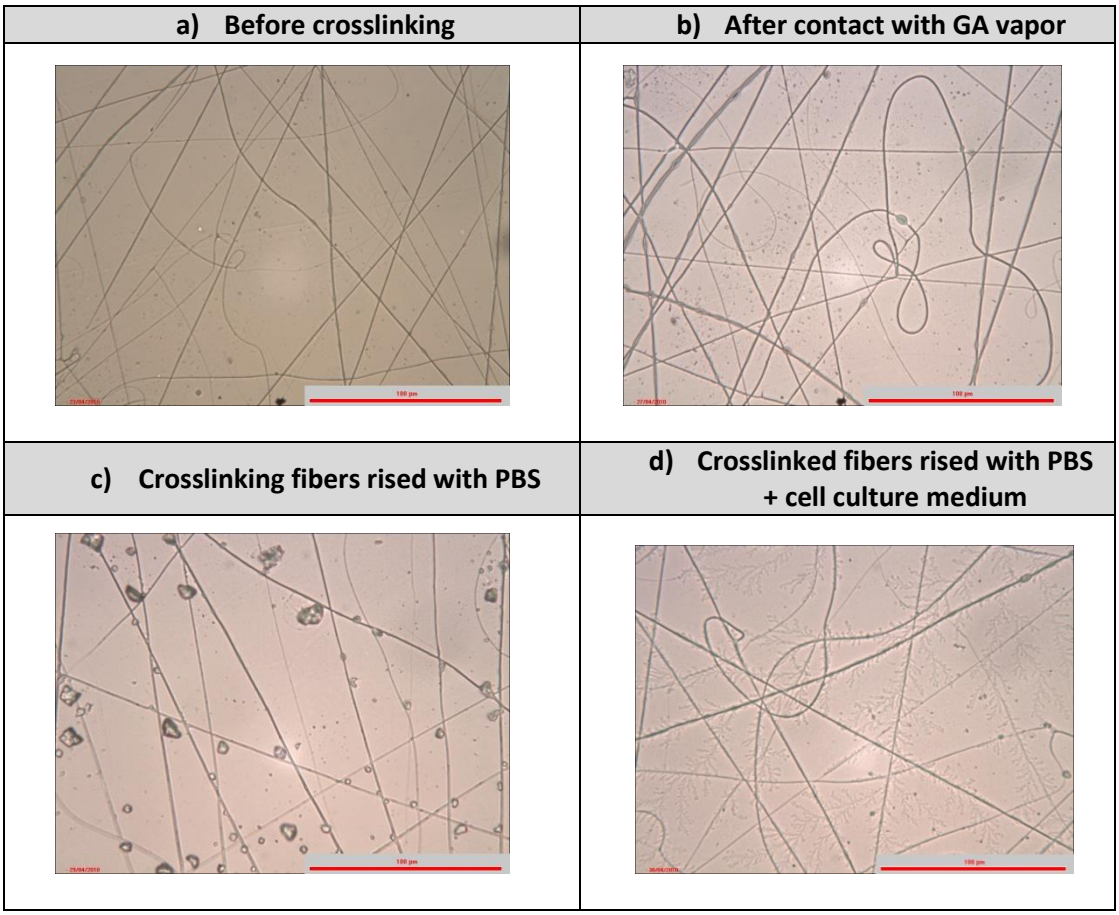

Figure 8.10. *Electrospun collagen nanofibers at different steps of the crosslinking process showing the stability of the nanofibers to PBS solution and cell culture medium*

8.3.4. Surface effects of collagen nanofibers deposited on different polyurethanes

Deposition of nanofibers onto the surface of polyurethane is expected to affect their surface properties which could have strong influence on the final biocompatibility of the biomaterial [8.46]. In this sense, three types of polyurethane (unmodified and modified with sulfonate and octadecyl end-groups) with different surface response were studied. The contact angle of each sample, before and after the deposition and crosslinking of electrospun collagen nanofibers, was measured to follow the surface changes that may be produced by the presence of this nanolayer (**Figure 8.11)**.

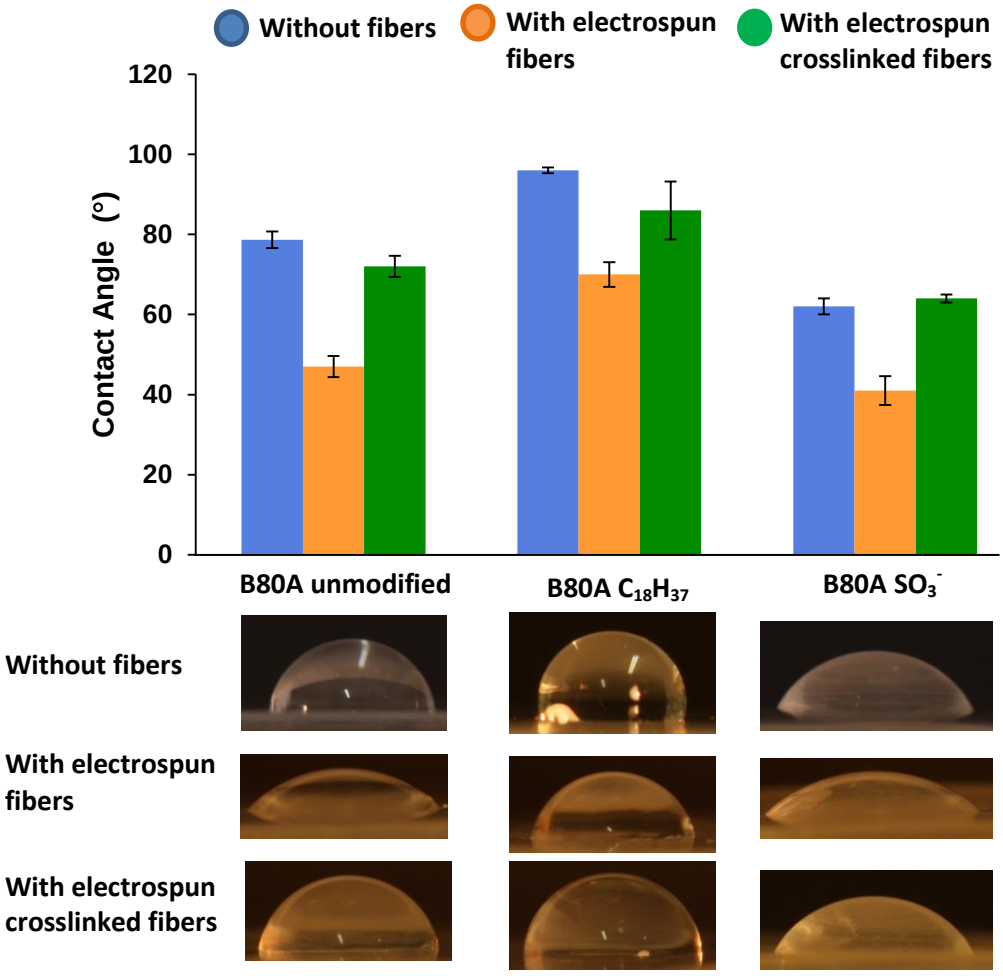

Figure 8.11. *Water contact angle values, with their respectively photographs, for the three different polyurethane used (B80A, B80A with octadecyl end-group modification ($C_{18}H_{37}$) and B80A with sulfonate end-group modification (SO_3^-)) at their original state and after being covered with a layer of collagen electrospun nanofiber before and after being crosslinked*

The results allow obtaining some conclusions. On the one hand, the contact angle of unmodified and modified polyurethanes show significant differences, being the B80 $C_{18}H_{37}$ the most hydrophobic substrate and the B80 SO_3^- the most hydrophylic. On the other hand, samples coated with electrospun fibers demonstrated lower contact angle compared to the non-coated, regardless of the polyurethane used. This behavior is probably due to an increase of hydrophylicity promoted by the non-crosslinked electrospun nanofibers. In fact, it was demonstrated that water can dissolve the non-crosslinked collagen, decreasing the contact angle. Finally, the results for polyurethanes coated with crosslinked electrospun fibers showed a similar contact angle values than the original samples, demonstrating that when the crosslinking

treatment is carried out the stable nanolayer of collagen did not significantly affect the surface energy of the polyurethane samples. Futhermore, not significant differences were found in the diameter and morphology of the nanofibers regardless the type of polyurethane used (Figure 8.12).

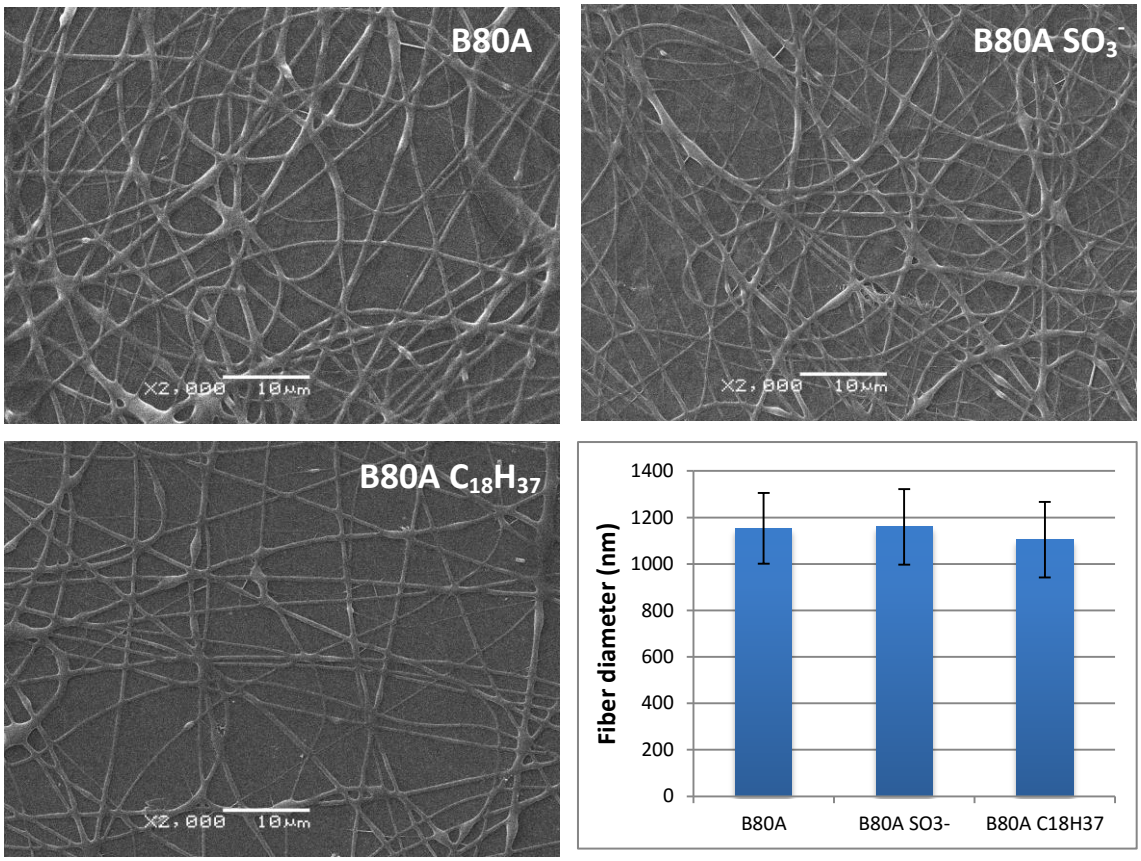

Figure 8.12: *SEM images of collagen electrospun fibers deposited onto different polyurethanes and their average fiber diameter with the standard deviation (in nm)*

8.3.5. Structural characterization of electrospun collagen nanofibers

Polyurethane coated with electrospun collagen nanofibers were analyzed by ATR to characterize their chemical structure. The results (**Figure 8.13**) determine that the surface layer of collagen electrospun fibers deposited onto polyurethane was too thin (as it was desired) and consequently the IR absorption corresponding to the collagen was not significant compared with the absorption of polyurethane. As a result, no significant differences between the spectra of polyurethane before and after the deposition of electrospun collagen fibers were detected, which doesn't means necessarily that polyurethane has not collagen fibers deposited on there.

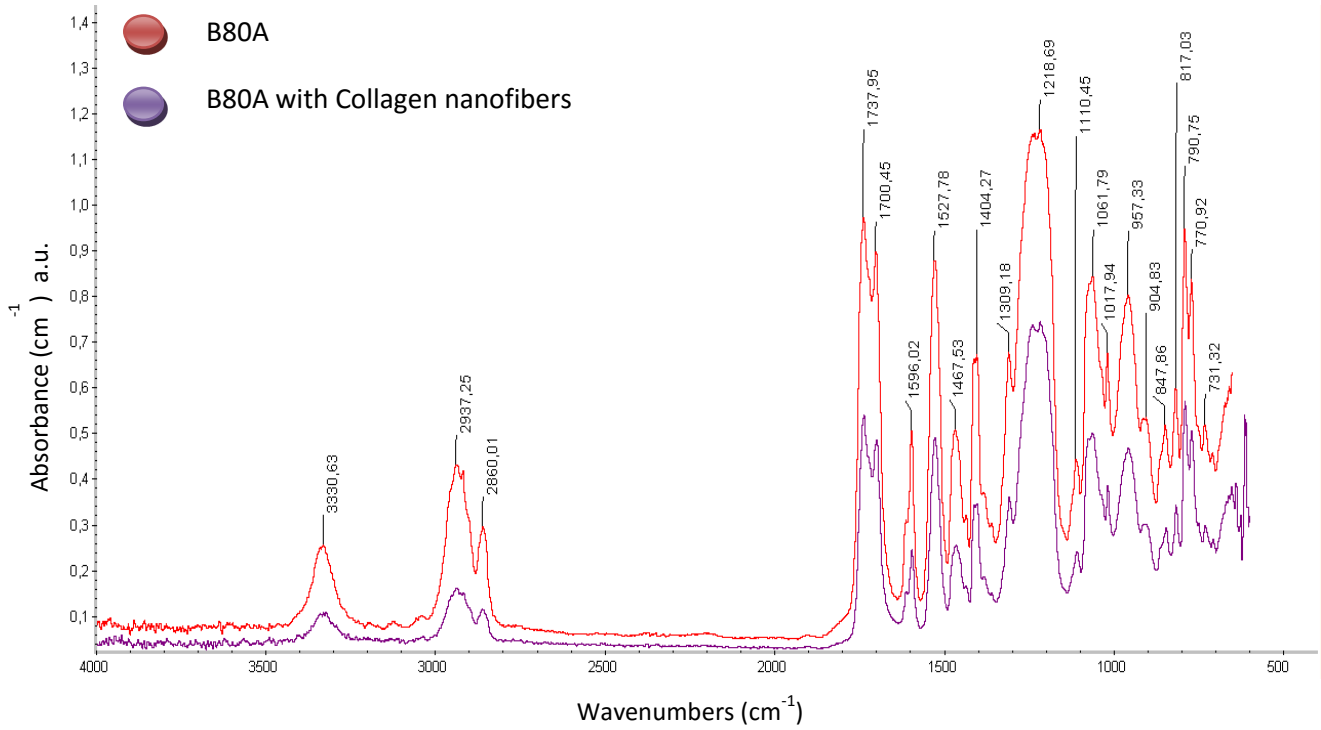

Figure 8.13: *ATR of polyurethane film (B80A) before and after the surface deposition of electrospun collagen fibers*

Alternatively to the ATR characterization, FT-IR analysis of electrospun collagen was carried out. So, electrospun collagen was collected onto a previously prepared KBr disc and the sample was analyzed by FT-IR spectroscopy. The spectra results are shown in **Figure 8.14** and were compared with the spectra obtained from a sample of pure lyophilized collagen.

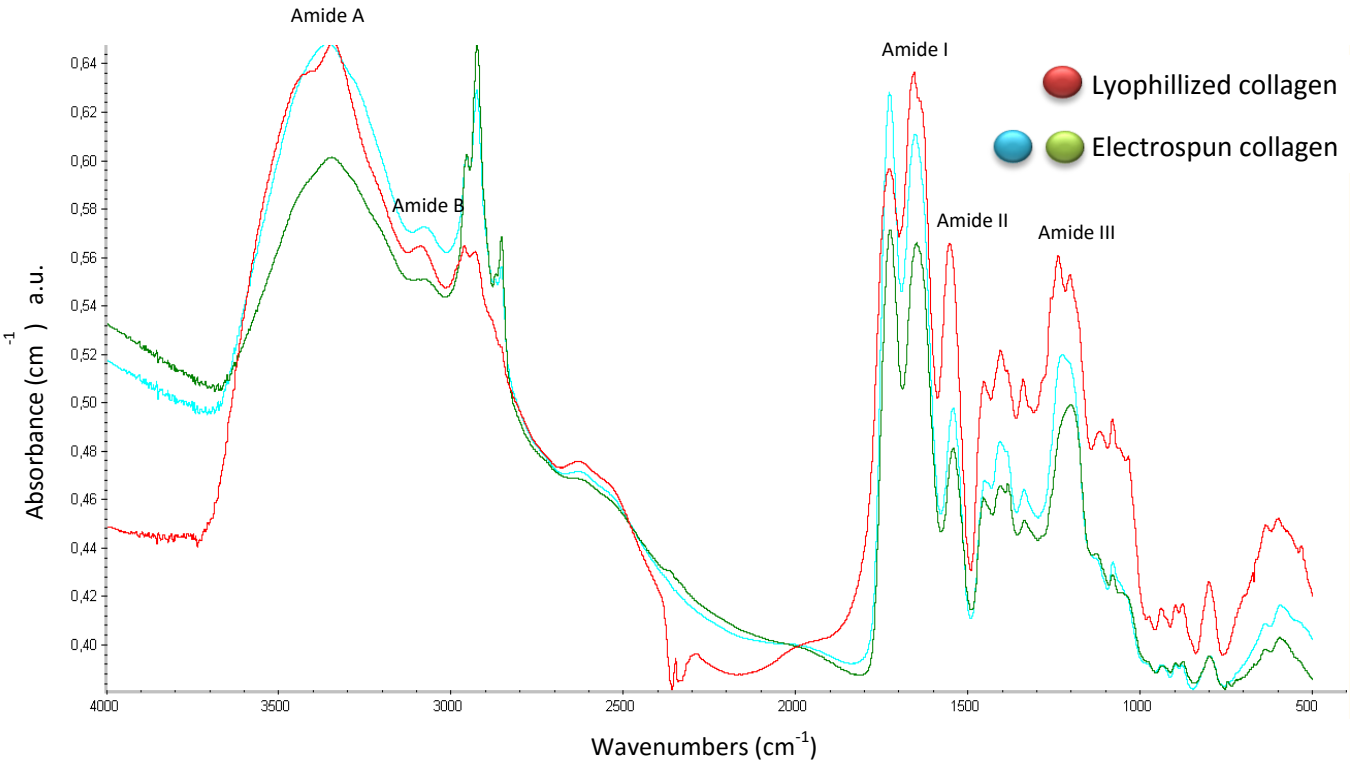

Figure 8.14. *FT-IR spectra of lyophilized collagen and electrospun collagen nanofibers collected above KBr sample*

Unlike ATR, the FTIR analysis allowed to detect the characteristics absorption peaks of collagen, previously reported in the literature [8.32, 8.47] (see Table 8.2), confirming the existence of the second structure of protein associated with the appearance of Amide I, II and III peaks. Although both lyophilized and electrospun collagen have a very similar spectra regarding the characteristics peaks, it can be note that the amide peaks, especially the amide I (1658 cm^{-1}) and amide III (1239 cm^{-1}), show a little shape differences, suggesting small changes on the structure of the native protein during the electrospinning process probably due to the denaturation of collagen, as it was reported by Zeugolis, et al. [8.21]. These differences in structure could explain the lack of stability of electrospun collagen compared with native collagen.

Table 8.2*: Characteristics absorption peaks of collagen protein*

Peaks (cm^{-1})	Groups
3333	NH involved in hydrogen bonds (**Amide A**)
3082	C-H2 asymmetrical stretch (**Amide B**)
1730	C=O stretching
1658	C=O stretching (**Amide I**)
1553	N-H bending (**Amide II**)
1239	C-H stretching (**Amide III**)

8.4. Conclusions

The electrospinning of collagen nanofibers was studied with the aim to optimize the operational parameters that allow to obtain stable nanofibers. It was found that the best conditions to perform stable jet of nanofibers from collagen solution (8% w/v in HIPF) were 15 kV of voltage, 0,5 ml/h of flow rate and 15 cm of distance between needle and collector. After that, the electrospinning technique was used to coat polyurethane biomaterials with a layer of collagen nanofibers in order to improve the biocompatibility of these biomaterials. For the coating, polyurethanes were located on the collector of the electrospinning device which was designed to obtain random (non conductive sample holder) or aligned (conductive sample holder) distribution of collagen nanofibers.

The stabilization of polyurethane scaffold covered by collagen nanofiber mats were carried out successfully by treatment with glutaraldehyde vapor atmosphere. The treated nanolayer of collagen preserves the surface properties (contact angle) of the polyurethane biomaterials. Futhermore, morphology and fiber diameter of collagen nanofibers were similar regardless the chemical end-group that characterize each polyurethane.

Finally, the FTIR analysis of a collagen electrospun mat allowed detecting the characteristics absorption peaks of collagen with slight deviation from the structure of lyophilized collagen, suggesting the possible denaturation of the protein during the dissolution and electrospinning steps involved in the process.

8.5. References

[8.1] H. Liu, X. Ding, G. Zhou, P. Li, X. Wei, Y. Fan, Electrospinning of Nanofibers for Tissue Engineering Applications, J. Nanomater. 2013 (2013) 1–11.

[8.2] P.K. Baumgarten, Electrostatic spinning of acrylic microfibers, J. Colloid Interface Sci. 36 (1971) 71–79.

[8.3] M.M. Bergshoef, G.J. Vancso, Transparent nanocomposites with ultrathin, electrospun nylon-4,6 fiber reinforcement, Adv. Mater. 11 (1999) 1362–1365.

[8.4] H.-J. Jin, S. V Fridrikh, G.C. Rutledge, D.L. Kaplan, Electrospinning Bombyx mori silk with poly(ethylene oxide)., Biomacromolecules. 3 (2002) 1233–9.

[8.5] Z.-M. Huang, Y.-Z. Zhang, M. Kotaki, S. Ramakrishna, A review on polymer nanofibers by electrospinning and their applications in nanocomposites, Compos. Sci. Technol. 63 (2003) 2223–2253.

[8.6] H. Yoshimoto, Y.M. Shin, H. Terai, J.P. Vacanti, A biodegradable nanofiber scaffold by electrospinning and its potential for bone tissue engineering, Biomaterials. 24 (2003) 2077–2082.

[8.7] C.Y. Xu, R. Inai, M. Kotaki, S. Ramakrishna, Aligned biodegradable nanofibrous structure: A potential scaffold for blood vessel engineering, Biomaterials. 25 (2004) 877–886.

[8.8] C. Xu, R. Inai, M. Kotaki, S. Ramakrishna, Electrospun nanofiber fabrication as synthetic extracellular matrix and its potential for vascular tissue engineering., Tissue Eng. 10 (2004) 1160–8.

[8.9] W.-J.W.-J. Li, R. Tuli, C. Okafor, A. Derfoul, K.G.K.G. Danielson, D.J.D.J. Hall, et al., A three-dimensional nanofibrous scaffold for cartilage tissue engineering using human mesenchymal stem cells., Biomaterials. 26 (2005) 599–609.

[8.10] W.-J. Li, C.T. Laurencin, E.J. Caterson, R.S. Tuan, F.K. Ko, Electrospun nanofibrous structure: a novel scaffold for tissue engineering, J. Biomed. Mater. Res. 60 (2002) 613–21.

[8.11] X.T. Wen, H.S. Fan, Y.F. Tan, H.D. Cao, H. Li, B. Cai, et al., Preparation of Electrospun PLA Nanofiber Scaffold and the Evaluation In Vitro, Key Eng. Mater. 288-289 (2005) 139–142.

[8.12] A. Cipitria, A. Skelton, T.R. Dargaville, P.D. Dalton, D.W. Hutmacher, Design, fabrication and characterization of PCL electrospun scaffolds-a review, J. Mater. Chem. 21 (2011) 9419–9453.

[8.13] J.H.C. Hui Wang, Xiao Hong Qin, Study on Structures of electrospinning cellulose acetate nanofibers., Adv. Mat. Res. 175-176 (2011) 242–246.

[8.14] H. Homayoni, S.A.H. Ravandi, M. Valizadeh, Electrospinning of chitosan nanofibers: Processing optimization., Carbohydr. Polym. 77 (2009) 656–661.

[8.15] S.A. Sell, M.J. McClure, K. Garg, P.S. Wolfe, G.L. Bowlin, Electrospinning of collagen/biopolymers for regenerative medicine and cardiovascular tissue engineering., Adv. Drug Deliv. Rev. 61 (2009) 1007–19.

[8.16] J.A. Matthews, G.E. Wnek, D.G. Simpson, G.L. Bowlin, Electrospinning of collagen nanofibers, Biomacromolecules. 3 (2002) 232–238.

[8.17] H. Wang, H. Shao, X. Hu, Structure of silk fibroin fibers made by an electrospinning process from a silk fibroin aqueous solution, J. Appl. Polym. Sci. 101 (2006) 961–968.

[8.18] M. Li, M.J. Mondrinos, M.R. Gandhi, F.K. Ko, A.S. Weiss, P.I. Lelkes, Electrospun protein fibers as matrices for tissue engineering, Biomaterials. 26 (2005) 5999–6008.

[8.19] A. Fiorani, C. Gualandi, S. Panseri, M. Montesi, M. Marcacci, M.L. Focarete, et al., Comparative performance of collagen nanofibers electrospun from different solvents and stabilized by different crosslinkers, J. Mater. Sci. Mater. Med. 25 (2014) 2313–2321.

[8.20] A.M. Punnoose, A. Elamparithi, S. Kuruvilla, Electrospun Type 1 Collagen Matrices Using a Novel Benign Solvent for Cardiac Tissue Engineering, J. Cell. Physiol. (2015) n/a–n/a.

[8.21] D.I. Zeugolis, S.T. Khew, E.S.Y. Yew, A.K. Ekaputra, Y.W. Tong, L.-Y.L. Yung, et al., Electro-spinning of pure collagen nano-fibres - just an expensive way to make gelatin?, Biomaterials. 29 (2008) 2293–305.

[8.22] M.R. Badrossamay, K. Balachandran, A.K. Capulli, H.M. Golecki, A. Agarwal, J.A. Goss, et al., Engineering hybrid polymer-protein super-aligned nanofibers

via rotary jet spinning, Biomaterials. 35 (2014) 3188–3197.

[8.23] M. Ahmed, T.A.D.S. Ramos, F. Damanik, B. Quang Le, P. Wieringa, M. Bennink, et al., A combinatorial approach towards the design of nanofibrous scaffolds for chondrogenesis, Sci. Rep. 5 (2015) 1–12.

[8.24] L. Yang, C.F.C. Fitié, K.O. van der Werf, M.L. Bennink, P.J. Dijkstra, J. Feijen, Mechanical properties of single electrospun collagen type I fibers., Biomaterials. 29 (2008) 955–62.

[8.25] S.Y. Chew, T.C. Hufnagel, C.T. Lim, K.W. Leong, Mechanical properties of single electrospun drug-encapsulated nanofibres, Nanotechnology. 17 (2006) 3880–3891.

[8.26] R. Inai, M. Kotaki, S. Ramakrishna, Structure and properties of electrospun PLLA single nanofibres., Nanotechnology. 16 (2005) 208–213.

[8.27] E.P.S. Tan, C.N. Goh, C.H. Sow, C.T. Lim, Tensile test of a single nanofiber using an atomic force microscope tip, Appl. Phys. Lett. 86 (2005) 1–3.

[8.28] W. Fu, Z. Liu, B. Feng, R. Hu, X. He, H. Wang, et al., Electrospun gelatin/PCL and collagen/PLCL scaffolds for vascular tissue engineering, Int. J. Nanomedicine. 9 (2014) 2335–2344.

[8.29] X. Zhang, K. Tang, X. Zheng, Electrospinning and rheological behavior of poly (vinyl alcohol)/collagen blended solutions., J. Wuhan Univ. Technol. Sci. Ed. 30 (2015) 840–846.

[8.30] J. Wang, X. Cui, Y. Zhou, Q. Xiang, Core-shell PLGA/collagen nanofibers loaded with recombinant FN/CDHs as bone tissue engineering scaffolds., Connect. Tissue Res. 55 (2014) 292–298.

[8.31] J. Zhou, C. Cao, X. Ma, J. Lin, Electrospinning of silk fibroin and collagen for vascular tissue engineering, Int. J. Biol. Macromol. 47 (2010) 514–519.

[8.32] R.L. Fischer, M.G. McCoy, S.A. Grant, Electrospinning collagen and hyaluronic acid nanofiber meshes, J. Mater. Sci. Mater. Med. 23 (2012) 1645–1654.

[8.33] C.C. Yu, J.J. Chang, Y.H. Lee, Y.C. Lin, M.H. Wu, M.C. Yang, et al., Electrospun scaffolds composing of alginate, chitosan, collagen and hydroxyapatite for applying in bone tissue engineering, Mater. Lett. 93 (2013)

133–136.

[8.34] R. Chen, C. Huang, Q. Ke, C. He, H. Wang, X. Mo, Preparation and characterization of coaxial electrospun thermoplastic polyurethane/collagen compound nanofibers for tissue engineering applications, Colloids Surfaces B Biointerfaces. 79 (2010) 315–325.

[8.35] T. Douglas, H.J. Haugen, Coating of polyurethane scaffolds with collagen: Comparison of coating and cross-linking techniques, in: J. Mater. Sci. Mater. Med., 2008: pp. 2713–2719.

[8.36] M. Erencia, F. Cano, J. a Tornero, J. Macanás, F. Carrillo, Resolving the electrospinnability zones and diameter prediction for the electrospinning of the gelatin/water/acetic Acid system., Langmuir. 30 (2014) 7198–205.

[8.37] M. Erencia, F. Cano, M.M. Tornero, Jose Antonio Fernandes, T. Tzanov, J. Macanás, F. Carrillo, Electrospinning of gelatin scaffolds with low acetic acid concentration effect of solvent composition on both diameter of nanofibers and cell viability, Summited. (2014).

[8.38] S. Zhong, W.E. Teo, X. Zhu, R.W. Beuerman, S. Ramakrishna, L. Yue, et al., An aligned nanofibrous collagen scaffold by electrospinning and its effects on in vitro fibroblast culture., J. Biomed. Mater. Res. Part A. 79A (2006) 456–463.

[8.39] W.-J. Chen, D.-J. Ying, Design and Preparation of an Electrospun Biomaterial Surgical Patch, J. Bioact. Compat. Polym. 24 (2009) 158–168.

[8.40] M. Li, M.J. Mondrinos, M.R. Gandhi, F.K. Ko, A.S. Weiss, P.I. Lelkes, Electrospun protein fibers as matrices for tissue engineering., Biomaterials. 26 (2005) 5999–6008.

[8.41] M. Erencia, F. Cano, J.A. Tornero, J. Macanás, F. Carrillo, Effect of operational and solution parameters on diameter of electrospun protein fibers., To Be Summited. (2014).

[8.42] N.S.F. Summer, U. Fellowship, S. Technologies, P. Tsing, P. Advisor, D.M. Elliott, Electrospinning natural polymers for tissue engineering applications., (n.d.) 1–15.

[8.43] M.M. Demir, I. Yilgor, E. Yilgor, B. Erman, Electrospinning of polyurethane ®

bers, 43 (2002) 3303–3309.

[8.44] a. H. Hekmati, A. Rashidi, R. Ghazisaeidi, J.-Y. Drean, Effect of needle length, electrospinning distance, and solution concentration on morphological properties of polyamide-6 electrospun nanowebs, Text. Res. J. 83 (2013) 1452–1466.

[8.45] C. Liu, C. Zhu, J. Li, P. Zhou, M. Chen, H. Yang, et al., The effect of the fibre orientation of electrospun scaffolds on the matrix production of rabbit annulus fibrosus-derived stem cells., Bone Res. 3 (2015) 15012.

[8.46] K.L. Menzies, L. Jones, The Impact of Contact Angle on the Biocompatibility of Biomaterials, 87 (2010) 387–399.

[8.47] M. Yan, B. Li, X. Zhao, G. Ren, Y. Zhuang, H. Hou, et al., Characterization of acid-soluble collagen from the skin of walleye pollock (Theragra chalcogramma), Food Chem. 107 (2008) 1581–1586.

CAPÍTULO 9:

Conclusiones generales

Conclusiones Generales

Los diferentes estudios llevados a cabo en la presente tesis doctoral han permitido alcanzar con éxito los objetivos planteados inicialmente, aportando conocimiento sobre los mecanismos físico-químicos que controlan la electrohilatura de biopolímeros de base proteica.

A continuación se exponen las conclusiones generales obtenidas a partir de un análisis global de la investigación desarrollada:

- La electrohilatura de soluciones de biopolímeros proteicos (gelatina/colágeno), se presenta como un sistema **go/no go**, en el que los parámetros de proceso (voltaje, caudal y distancia entre la aguja y el colector) **tienen sólo influencia en la capacidad para la formación de un haz estable de nanofibras pero** una vez conseguida dicha estabilidad, **no afectan significativamente al diámetro de las fibras obtenidas.**

- La conductividad del colector utilizado así como los parámetros físico-químicos de la solución tales como tipo de solvente, concentración, y tipo de polímero (peso molecular) han demostrado tener una **influencia significativa tanto en la hilabilidad como en el diámetro** de las nanofibras electrohiladas. Los distintos estudios de optimización han permitido establecer de forma clara las relaciones entre dichos parámetros y las propiedades de las fibras resultantes.

- Se ha demostrado la viabilidad de obtener nanofibras de gelatina a temperatura ambiente utilizando un solvente más benigno, alternativo a los utilizados actualmente, basado en una **solución acuosa de ácido acético**. Mediante la utilización de una solución con baja concentración de ácido acético (25 % v/v) y concentraciones de gelatina igual o superiores a 300mg/ml se ha conseguido evitar el proceso de gelificación y obtener nanofibras electrohiladas que mantienen la **estructura nativa de la gelatina, mostrando una elevada compatibilidad celular** (>90%).

- A partir de un estudio sistemático del sistema ternario gelatina-agua-acético se ha determinado el efecto de la composición de la solución en la capacidad de

electrohilar y en las propiedades (diámetro) de las nanofibras obtenidas. En concreto, este estudio ha permitido:

- Establecer un **modelo empírico** capaz de **predecir la viscosidad** de la solución a partir de la concentración de gelatina y la composición del solvente ácido-agua con una correlación del 97%.

- **Identificar las diferentes regiones de electrohilabilidad** en un diagrama ternario y **definir el rango de composiciones óptimas** para obtener nano o microfibras con diámetros comprendidos entre 200 y 3000 nm.

- Proponer un nuevo número adimensional ($B_{e,mod}$) que aplicado a las mezclas ternarias permita **establecer los dominios de electrohilabilidad** esperados, directamente relacionados con la reología de la solución. En este sentido, se ha observado el rango óptimo para la producción de nano o microfibras en este sistema: $20<B_{e,mod}<40$.

- Establecer dos modelos basados en el nuevo número adimensional $B_{e,mod}$ capaces **de predecir el diámetro de las nanofibras y microfibras obtenidas**.

- Mediante el uso de un disolvente alternativo más benigno, formado por mezclas **etanol-PBS,** ha sido posible obtener, a temperatura ambiente, nanofibras de gelatina que han mostrado una **viabilidad celular** del 90%. La optimización del proceso de electrohilatura ha permitido evaluar el efecto de los distintos parámetros de la solución en las propiedades de las nanofibras obtenidas, así como establecer un **dominio de electrohilabilidad unificado para los tres tipos de gelatinas ensayadas** basado en el desarrollo de un modelo que incorpora una adaptación del número de Berry ($Be\cdot[\eta]$).

- Las nanofibras obtenidas han sido estabilizadas mediante diferentes sistemas de reticulación basados en el uso de glutaraldehido (GA). No obstante, se ha observado una **mayor efectividad de reticulación, aunque menor estabilidad dimensional** (cambios de diámetro), para las nanofibras obtenidas a partir de **etanol-PBS**, en comparación con las obtenidas utilizando ácido acético 25%v/v, para métodos de reticulación por contacto con vapor de GA y

por inmersión en solución etanol-GA. Sin embargo, a la hora de desarrollar un método de reticulación **in-situ,** basado en la incorporación de GA en la solución de hilatura, son las nanofibras obtenidas a partir del **solvente ácido las que presentan un mejor resultado**.

- Además de nanofibras de gelatina, se han conseguido electrohilar nanofibras de colágeno, que a su vez han sido depositadas con una distribución al azar sobre soportes biomateriales funcionalizados no conductores. Para ello se han ensayado diferentes tipos de colectores fabricados ad hoc. La estabilización de la capa de nanofibras sobre el biomaterial se ha realizado mediante reticulación con vapor de glutaraldehido, confirmándose su estabilidad **frente a un proceso simulado de cultivo celular**.

CAPÍTULO 10:

Trabajo futuro

Trabajo Futuro

A partir de los resultados obtenidos en la presente tesis se plantean una serie de posibles líneas futuras de investigación relacionadas:

- Estudiar del comportamiento de los soportes de nanofibras obtenidos a partir de solventes benignos en aplicaciones de ingeniería de tejidos y comparación con soportes utilizados actualmente.

- Ampliar el estudio de viabilidad celular y biocompatibilidad de los soportes de nanofibras obtenidos.

- Estudiar sistemas naturales alternativos al gluraraldehido (genipina, transglutaminasa, etc.) para la estabilización de las nanofibras, etc.

- Profundizar en el estudio de un método de reticulación directo que permita obtener nanofibras estables que no requieran un proceso posterior de reticulación.

- Plantear la incorporación de nanopartículas o nanoestructuras (grafeno, etc.) a las nanofibras proteicas con el objetivo de mejorar y controlar las propiedades mecánicas del material compuesto obtenido.

- Ampliar el estudio a la obtención de nanofibras de otros tipos de proteínas de origen vegetal (soja, ceína, etc.), y/o mezclas con otros polímeros naturales.

- Optimizar el proceso de fabricación de nanofibras de colágeno en relación con la búsqueda de solventes alternativos más benignos que mantengan la integridad y naturaleza del polímero original. Comprobación del efecto del solvente en la estructura del colágeno y comparación con solventes comunes (HIPF, etc.).

CAPÍTULO 11:

Bibliografía general

Bibliografía General

[11.1] A. H. Hekmati, A. Rashidi, R. Ghazisaeidi, J.-Y. Drean, Effect of needle length, electrospinning distance, and solution concentration on morphological properties of polyamide-6 electrospun nanowebs, Text. Res. J. 83 (2013) 1452–1466.

[11.2] A. Bigi, G. Cojazzi, S. Panzavolta, K. Rubini, N. Roveri, Mechanical and thermal properties of gelatin films at different degrees of glutaraldehyde crosslinking, Biomaterials. 22 (2001) 3–8.

[11.3] A. Bigi, G. Cojazzi, S. Panzavolta, N. Roveri, K. Rubini, Stabilization of gelatin films by crosslinking with genipin., Biomaterials. 23 (2002) 4827–4832.

[11.4] A. Calleja, X. Granados, S. Ricart, J. Oró, J. Arbiol, N. Mestres, et al., High temperature transformation of electrospun BaZrO3 nanotubes into nanoparticle chains, CrystEngComm. 13 (2011) 7224.

[11.5] A. Cipitria, A. Skelton, T.R. Dargaville, P.D. Dalton, D.W. Hutmacher, Design, fabrication and characterization of PCL electrospun scaffolds-a review, J. Mater. Chem. 21 (2011) 9419–9453.

[11.6] A. Fiorani, C. Gualandi, S. Panseri, M. Montesi, M. Marcacci, M.L. Focarete, et al., Comparative performance of collagen nanofibers electrospun from different solvents and stabilized by different crosslinkers, J. Mater. Sci. Mater. Med. 25 (2014) 2313–2321.

[11.7] A. Formhals, Process and apparatus for preparing artificial threads., US Patent No. 1,975,504, 1934.

[11.8] A. Greiner, J.H. Wendorff, Electrospinning: a fascinating method for the preparation of ultrathin fibers, Angew. Chem. Int. Ed. Engl. 46 (2007) 5670–703.

[11.9] A. Koski, K. Yim, S. Shivkumar, Effect of molecular weight on fibrous PVA produced by electrospinning, Mater. Lett. 58 (2004) 493–497.

[11.10] A. Kundu, N. Kishore, 1,1,1,3,3,3- Hexafluoroisopropanol Induced Thermal Unfolding and Molten Globule State of Bovine □-Lactalbumin- Calorimetric and Spectroscopic Studies., Biopolymers. 73 (2004) 405–20.

[11.11] A. Saxena, K. Sachin, H.B. Bohidar, A.K. Verma, Effect of molecular weight heterogeneity on drug encapsulation efficiency of gelatin nano-particles., Colloids Surf. B. Biointerfaces. 45 (2005) 42–8.

[11.12] A. Sohrabi, P.M. Shaibani, T. Thundat, The effect of applied electric field on the diameter and size distribution of electrospun Nylon6 nanofibers., Scanning. 35 (2013) 183–8.

[11.13] A. Talebian, S.S. Kordestani, A. Rashidi, F. Dadashian, M. Montazer, The Effect of Glutaraldehyde on the Properties of Gelatin Films, 56 (2007) 537–541.

[11.14] A.G. Destaye, C.K. Lin, C.K. Lee, Glutaraldehyde vapor cross-linked nanofibrous PVA mat with in situ formed silver nanoparticles., ACS Appl. Mater. Interfaces 5 (2013) 4745–4752.

[11.15] A.G. Kanani, S.H. Bahrami, Review on Electrospun Nanofibers Scaffold and Biomedical Applications, Trends Biomater. Artif. Organs 24 (2010) 93–115.

[11.16] A.M. Jamieson, R. Simha, Newtonian viscosity of dilute, semidilute and concentrated polymer solution, in: L.A. Ultracki, A.M. Jamieson (Eds.), Polym. Phys. from Suspens. to Nanocomposites Beyond., Wiley, 2010: pp. 15–88.

[11.17] A.M. Punnoose, A. Elamparithi, S. Kuruvilla, Electrospun Type 1 Collagen Matrices Using a Novel Benign Solvent for Cardiac Tissue Engineering, J. Cell. Physiol. (2015) n/a–n/a.

[11.18] A.P.S. Immich, M.L. Arias, N. Carreras, R.L. Boemo, J.A. Tornero, Drug delivery systems using sandwich configurations of electrospun poly(lactic acid) nanofiber membranes and ibuprofen, Mater. Sci. Eng. C. Mater. Biol. Appl. 33 (2013) 4002–8.

[11.19] A.S. Nain, J.C. Wong, C.H. Amon, M. Sitti, Drawing suspended polymer micro-/nanofibers using glass micropipettes., Appl. Phys. Lett. 89 (2006).

[11.20] Acetic Acid and its Derivatives - Google Libros, (n.d.).

[11.21] B. Dhandayuthapani, Y. Yoshida, T. Maekawa, D.S. Kumar, Polymeric Scaffolds in Tissue Engineering Application: A Review, Int. J. Polym. Sci. 2011 (2011) 1–19.

[11.22] B. Dong, O. Arnoult, M.E. Smith, G.E. Wnek, Electrospinning of collagen nanofiber scaffolds from benign solvents, Macromol. Rapid Commun. 30 (2009) 539–542.

[11.23] B. Hüsing, B. Bührlen, S. Gaisser, Human Tissue Engineered Products – Today ' s Markets and Future Prospects, Karlsruhe, Germany, 2003.

[11.24] B. Mohanty, H.B. Bohidar, Systematic of alcohol-induced simple coacervation in aqueous gelatin solutions., Biomacromolecules. 4 (2003) 1080–6.

[11.25] B. Su, J. Venugopal, S. Ramakrishna, Biomimetic and bioactive nano fi brous scaffolds from electrospun composite nanofibers, 1 (2007) 623–638.

[11.26] B.D. Ulery, L.S. Nair, C.T. Laurencin, Biomedical Applications of Biodegradable Polymers., J. Polym. Sci. B. Polym. Phys. 49 (2011) 832–864.

[11.27] B.J. Papenburg, Design strategies for tissue engineering scaffolds, University of Twente, 1981.

[11.28] B.L. Hager, G.C. Berry, Moderately concentrated solutions of polystyrene. I. Viscosity as a function of concentration, temperature, and molecular weight, J. Polym. Sci. Polym. Phys. Ed. 20 (1982) 911–928.

[11.29] B.P. Chan, K.W. Leong, Scaffolding in tissue engineering: general approaches and tissue-specific considerations, Eur. Spine J. 17 (2008) 467–79.

[11.30] B.S. Jha, C.E. Ayres, J.R. Bowman, T. a. Telemeco, S. a. Sell, G.L. Bowlin, et al., Electrospun Collagen: A Tissue Engineering Scaffold with Unique Functional Properties in a Wide Variety of Applications, J. Nanomater. 2011 (2011) 1–15.

[11.31] B.S. Jha, C.E. Ayres, J.R. Bowman, T. a. Telemeco, S. a. Sell, G.L. Bowlin, et al., Electrospun Collagen: A Tissue Engineering Scaffold with Unique

Functional Properties in a Wide Variety of Applications., J. Nanomater. 2011 (2011) 1–15.

[11.32] C. Abrusci, a. Martín-González, a. Del Amo, T. Corrales, F. Catalina, Biodegradation of type-B gelatine by bacteria isolated from cinematographic films. A viscometric study, Polym. Degrad. Stab. 86 (2004) 283–291.

[11.33] C. Flor, A study of the formation of collagen nanofibers using electrospinning, Universitat Politecnica de Catalunya, 2008.

[11.34] C. Liu, C. Zhu, J. Li, P. Zhou, M. Chen, H. Yang, et al., The effect of the fibre orientation of electrospun scaffolds on the matrix production of rabbit annulus fibrosus-derived stem cells., Bone Res. 3 (2015) 15012.

[11.35] C. Xu, R. Inai, M. Kotaki, S. Ramakrishna, Electrospun nanofiber fabrication as synthetic extracellular matrix and its potential for vascular tissue engineering., Tissue Eng. 10 (2004) 1160–8.

[11.36] C. Yang, X. Wu, Y. Zhao, L. Xu, S. Wei, Nanofibrous scaffold prepared by electrospinning of poly(vinyl alcohol)/gelatin aqueous solutions., J. Appl. Polym. Sci. 121 (2011) 3047–3055.

[11.37] C. Zhang, X. Yuan, L. Wu, Y. Han, J. Sheng, Study on morphology of electrospun poly(vinyl alcohol) mats, Eur. Polym. J. 41 (2005) 423–432.

[11.38] C.C. Yu, J.J. Chang, Y.H. Lee, Y.C. Lin, M.H. Wu, M.C. Yang, et al., Electrospun scaffolds composing of alginate, chitosan, collagen and hydroxyapatite for applying in bone tissue engineering, Mater. Lett. 93 (2013) 133–136.

[11.39] C.E. Ayres, B.S. Jha, S.A. Sell, G.L. Bowlin, D.G. Simpson, Nanotechnology in the design of soft tissue scaffolds: innovations in structure and function, Wiley Interdiscip Rev Nanomed Nanobiotechnol. 2 (2010) 20–34.

[11.40] C.J. Angammana, S. Member, S.H. Jayaram, Analysis of the Effects of Solution Conductivity on Electrospinning Process and Fiber Morphology., IEEE Trans. Ind. Appl. 47 (2011) 1109–1117.

[11.41] C.J. Thompson, G.G. Chase, A. L. Yarin, D.H. Reneker, Effects of parameters on nanofiber diameter determined from electrospinning model, Polymer (Guildf). 48 (2007) 6913–6922.

[11.42] C.L. Casper, J.S. Stephens, N.G. Tassi, D.B. Chase, J.F. Rabolt, Controlling surface morphology of electrospun polystyrene fibers: Effect of humidity and molecular weight in the electrospinning process. Macromolecules. 37 (2004) 573–578.

[11.43] C.-M. Hsu, S. Shivkumar, Nano-sized beads and porous fiber constructs of Poly(ε-caprolactone) produced by electrospinning, J. Mater. Sci. 39 (2004) 3003–3013.

[11.44] C.P. Barnes, C.W. Pemble, D.D. Brand, D.G. Simpson, G.L. Bowlin, Cross-linking electrospun type II collagen tissue engineering scaffolds with carbodiimide in ethanol., Tissue Eng. 13 (2007) 1593–605.

[11.45] C.S. Ki, D.H. Baek, K.D. Gang, K.H. Lee, I.C. Um, Y.H. Park, Characterization of gelatin nanofiber prepared from gelatin–formic acid solution., Polymer (Guildf). 46 (2005) 5094–5102.

[11.46] C.Y. Xu, R. Inai, M. Kotaki, S. Ramakrishna, Aligned biodegradable nanofibrous structure: A potential scaffold for blood vessel engineering, Biomaterials. 25 (2004) 877–886.

[11.47] D. Hong, M. Hoshino, R. Kuboi, Y. Goto, Clustering of Fluorine-Substituted Alcohols as a Factor Responsible for Their Marked Effects on Proteins and Peptides., J. Am. Chem. Soc. 121 (1999) 8427–8433.

[11.48] D. Klumpp, M. Rudisle, R.I. Kühnle, A. Hess, A. Arkudas, O. Bleiziffer, et al., Three-dimensional vascularization of electrospun PCL/collagen-blend nanofibrous scaffolds in vivo., J Biomed Mater Res A. 100 (2012) 2302–2311.

[11.49] D. Lew, P.H. Liu, D.P. Orgill, Optimization of UV Cross-Linking Density for Durable and Nontoxic Collagen GAG Dermal Substitute, J Biomed Mater Res B Appl Biomater. 82 (2007) 51–56.

[11.50] D. Meyer, J.-P. Blaauwhoed, Handbook of Hydrocolloids, CRC Press, 2009.

[11.51] D. Yang, Y. Li, J. Nie, Preparation of gelatin/PVA nanofibers and their potential application in controlled release of drugs, Carbohydr. Polym. 69 (2007) 538–543.

[11.52] D.. G.E.. Wnek, Polymer biomaterial constructs for regenerative medicine and functional biological systems., Case Western Reserve University, 2012.

[11.53] D.I. Zeugolis, S.T. Khew, E.S.Y. Yew, A.K. Ekaputra, Y.W. Tong, L.-Y.L. Yung, et al., Electro-spinning of pure collagen nano-fibres - just an expensive way to make gelatin?, Biomaterials. 29 (2008) 2293–305.

[11.54] D.M. Correia, J. Padrão, L.R. Rodrigues, F. Dourado, S. Lanceros-Méndez, V. Sencadas, Thermal and hydrolytic degradation of electrospun fish gelatin membranes., Polym. Test. 32 (2013) 995–1000.

[11.55] D.W. Hutmacher, Scaffolds in tissue engineering bone and cartilage, Biomaterials. 21 (2000) 2529–43.

[11.56] E. Boland, J. Matthews, K. Pawlowski, D. Simpson, G. Wnek, G. Bowlin, Electrospinning collagen and elastin: preliminary vascular tissue engineering., Front Biosci. 1 (2004) 10.

[11.57] E. Doi, Gels and gelling of globular proteins, Trends Food Sci. Technol. 4 (1993) 1–5.

[11.58] E. Sachlos, J.T. Czemuszka, Making tissue engineering scaffolds work. Review on the application of solid freeform fabrication technology to the production of tissue engineering scaffolds. Eur Cell Mater. 30 (2003) 29–39.

[11.59] E.K. Brenner, J.D. Schiffman, E.A. Thompson, L.J. Toth, C.L. Schauer, Electrospinning of hyaluronic acid nanofibers from aqueous ammonium solutions., Carbohydr. Polym. 87 (2012) 926–929.

[11.60] E.P.S. Tan, C.N. Goh, C.H. Sow, C.T. Lim, Tensile test of a single nanofiber using an atomic force microscope tip, Appl. Phys. Lett. 86 (2005) 1–3.

[11.61] E.S. Place, N.D. Evans, M.M. Stevens, Complexity in biomaterials for tissue engineering, Nat. Mater. 8 (2009) 457–70.

[11.62] F. Carfì, S. Rigogliuso, V. La, G. Anotnio, G. Ghersi, V. Brucato, Poly Lactic Acid Based Scaffolds for Vascular Tissue Engineering, Chem. Eng. Trans. 27 (2012) 409–414.

[11.63] F. Cengiz, I. Krucińska, E. Gliścińska, Comparative Analysis of Various Electrospinning Methods of Nanofibre Formation, 17 (2009) 13–19.

[11.64] F. Cengiz, T.A. Dao, O. Jirsak, Influence of solution properties on the roller electrospinning of poly(vinyl alcohol), Polym. Eng. Sci. 50 (2010) 936–943.

[11.65] F.J. O'Brien, Biomaterials & scaffolds for tissue engineering, Mater. Today. 14 (2011) 88–95.

[11.66] F.K. Ko, Nanofiber Technology in Gogotsi Nanomaterials Handbook, in: Nanomater. Handb., 2006: pp. 553–564.

[11.67] G. Bolat, G. Lisa, I.M. Popa, Experimental dynamic viscosities of binary mixtures: acetic acid + water, benzene, toluene, n-hexane, n-heptane AT 296.15, 302.15, 308.15, 314.15 and 319.15 K, Sci. Study Res. VI (2005) 181–190.

[11.68] G. Karp, Cell and Molecular Biology: Concepts and Experiments, Wiley, 2009.

[11.69] G. Taylor, Disintegration of Water Drops in an Electric Field, Proc. R. Soc. A Math. Phys. Eng. Sci. 280 (1964) 383–397.

[11.70] GMIA, Gelatin Handbook, (2012) 26.

[11.71] H. Hajiali, S. Shahgasempour, M.R. Naimi-Jamal, H. Peirovi, Electrospun PGA/gelatin nanofibrous scaffolds and their potential application in vascular tissue engineering., Int. J. Nanomedicine. 6 (2011) 2133–2141.

[11.72] H. Hermawan, D. Ramdan, J.R.P. Djuansjah, Metals for Biomedical Applications, in: R. Frazel (Ed.), Biomed. Eng. From Theory to Appl., InTech, 2009: pp. 411–430.

[11.73] H. Homayoni, S.A.H. Ravandi, M. Valizadeh, Electrospinning of chitosan nanofibers: Processing optimization., Carbohydr. Polym. 77 (2009) 656–661.

[11.74] H. Jiang, D. Fang, B.S. Hsiao, B. Chu, W. Chen, Optimization and characterization of dextran membranes prepared by electrospinning., Biomacromolecules. 5 (2004) 326–33.

[11.75] H. Lee, S. Ahn, H. Choi, D. Cho, G. Kim, Fabrication, characterization, and in vitro biological activities of melt-electrospun PLA micro/nanofibers for bone tissue regeneration, J. Mater. Chem. B. 1 (2013) 3670.

[11.76] H. Liang, W. Chang, H. Liang, M. Lee, H. Sung, Crosslinking Structures of Gelatin Hydrogels Crosslinked with Genipin or a Water-Soluble Carbodiimide, (2003).

[11.77] H. Liu, X. Ding, G. Zhou, P. Li, X. Wei, Y. Fan, Electrospinning of Nanofibers for Tissue Engineering Applications, J. Nanomater. 2013 (2013) 1–11.

[11.78] H. Sung, I. Liang, C. Chen, R. Huang, H. Liang, Stability of a biological tissue fixed with a naturally occurring crosslinking agent (genipin), J Biomed Mater Res. 55 (2001) 538–546.

[11.79] H. Tai, M.L. Mather, D. Howard, W. Wang, L.J. White, J.A. Crowe, et al., Control of pore size and structure of tissue engineering scaffolds produced by supercritical fluid processing., Eur Cell Mater. 17 (2007) 64–77.

[11.80] H. Wang, H. Shao, X. Hu, Structure of silk fibroin fibers made by an electrospinning process from a silk fibroin aqueous solution, J. Appl. Polym. Sci. 101 (2006) 961–968.

[11.81] H. Yoshikawa, N. Tamai, T. Murase, A. Myoui, Interconnected porous hydroxyapatite ceramics for bone tissue engineering., J. R. Soc. Interface. 6 (2009) 341–348.

[11.82] H. Yoshimoto, Y.M. Shin, H. Terai, J.P. Vacanti, A biodegradable nanofiber scaffold by electrospinning and its potential for bone tissue engineering, Biomaterials. 24 (2003) 2077–2082.

[11.83] H. Zhang, Effects of electrospinning parameters on morphology and diameter of electrospun PLGA/MWNTs fibers and cytocompatibility in vitro., J. Bioact. Compat. Polym. 26 (2011) 590–606.

[11.84] H.-C. Chen, W.-C. Jao, M.-C. Yang, Characterization of gelatin nanofibers electrospun using ethanol/formic acid/water as a solvent., Polym. Adv. Technol. 20 (2009) 98–103.

[11.85] H.-J. Jin, S. V Fridrikh, G.C. Rutledge, D.L. Kaplan, Electrospinning Bombyx mori silk with poly(ethylene oxide)., Biomacromolecules. 3 (2002) 1233–9.

[11.86] H.M. Powell, S.T. Boyce, Engineered human skin fabricated using electrospun collagen-PCL blends: morphogenesis and mechanical properties., Tissue Eng. Part A. 15 (2009) 2177–2187.

[11.87] H.R. Pant, K.-T. Nam, H.-J. Oh, G. Panthi, H.-D. Kim, B. Kim, et al., Effect of polymer molecular weight on the fiber morphology of electrospun mats., J. Colloid Interface Sci. 364 (2011) 107–11.

[11.88] H.S. Kim, K. Kim, H.J. Jin, I.-J. Chin, Morphological Characterization of Electrospun Nano-Fibrous Membranes of Biodegradable Poly(L-lactide) and Poly(lactide-co-glycolide)., Macromol. Symp. 224 (2005) 145–154.

[11.89] H.-W. Kim, J.-H. Song, H.-E. Kim, Nanofiber Generation of Gelatin-Hydroxyapatite Biomimetics for Guided Tissue Regeneration, Adv. Funct. Mater. 15 (2005) 1988–1994.

[11.90] I. Migneault, C. Dartiguenave, M.J. Bertrand, K.C. Waldron, Glutaraldehyde : behavior in aqueous solution , reaction with proteins , and application to enzyme crosslinking, 37 (2004).

[11.91] I. Rault, V. Frei, D. Herbage, N. Abdul-Malak, A. Huc, Evaluation of different chemical methods for cross-linking collagen gel, films and sponges., J. Mater. Sci. Mater. Med. 7 (1996) 215–221.

[11.92] J. Bart, R. Tiggelaar, M. Yang, S. Schlautmann, H. Zuilhof, H. Gardeniers, Room-temperature intermediate layer bonding for microfluidic devices., Lab Chip. 9 (2009) 3481–8.

[11.93] J. Di, Y. Zhao, J. Yu, Fabrication of molecular sieve fibers by electrospinning, J. Mater. Chem. 21 (2011) 8511.

[11.94] J. Garcia, M.-F. Hsieh, B. Doma, D. Peruelo, I.-H. Chen, H.-M. Lee, Synthesis of Gelatin-γ-Polyglutamic Acid-Based Hydrogel for the In Vitro

Controlled Release of Epigallocatechin Gallate (EGCG) from Camellia sinensis, Polymers (Basel). 6 (2013) 39–58.

[11.95] J. Han, P. Lazarovici, C. Pomerantz, X. Chen, Y. Wei, P.I. Lelkes, Co-electrospun blends of PLGA, gelatin, and elastin as potential nonthrombogenic scaffolds for vascular tissue engineering., Biomacromolecules. 12 (2011) 399–408.

[11.96] J. He, Y.-Q. Wan, J.-Y. Yu, Effect of Concentration on Electrospun Polyacrylonitrile (PAN) Nanofibers., Fibers Polym. 9 (2008) 140–142.

[11.97] J. Jeun, Y. Kim, Y. Lim, J. Choi, C. Jung, P. Kang, Electrospinning of Poly (L-lactide- co -D , L-lactide), J. Ind. Eng. Chem. 13 (2007) 592–596.

[11.98] J. Lannutti, D. Reneker, T. Ma, D. Tomasko, D. Farson, Electrospinning for tissue engineering scaffolds, Mater. Sci. Eng. C. 27 (2007) 504–509.

[11.99] J. Lin, X. Qin, Effect of solution concentration on jet stretching of electrospinning PVA nanofiber., Int. J. Fluid Mech. Res. 38 (2011) 479–488.

[11.100] J. Tao, S. Shivkumar, Molecular weight dependent structural regimes during the electrospinning of PVA, Mater. Lett. 61 (2007) 2325–2328.

[11.101] J. Wang, X. Cui, Y. Zhou, Q. Xiang, Core-shell PLGA/collagen nanofibers loaded with recombinant FN/CDHs as bone tissue engineering scaffolds., Connect. Tissue Res. 55 (2014) 292–298.

[11.102] J. Zhang, L. Wu, D. Jing, J. Ding, A comparative study of porous scaffolds with cubic and spherical macropores., Polymer (Guildf). 46 (2005) 4979–4985.

[11.103] J. Zhao, W. Han, H. Chen, M. Tu, R. Zeng, Y. Shi, et al., Preparation, structure and crystallinity of chitosan nano-fibers by a solid–liquid phase separation technique, Carbohydr. Polym. 83 (2011) 1541–1546.

[11.104] J. Zhou, C. Cao, X. Ma, J. Lin, Electrospinning of silk fibroin and collagen for vascular tissue engineering, Int. J. Biol. Macromol. 47 (2010) 514–519.

[11.105] J.. Deitzel, J. Kleinmeyer, D. Harris, N.. Beck Tan, The effect of processing variables on the morphology of electrospun nanofibers and textiles, Polymer (Guildf). 42 (2001) 261–272.

[11.106] J.A. Kierman, Formaldehyde, formalin, paraformaldehyde and glutaraldehyde: what they are and what they do., Micros. Today. 00-1 (2000) 8–12.

[11.107] J.A. Matthews, G.E. Wnek, D.G. Simpson, G.L. Bowlin, Electrospinning of collagen nanofibers, Biomacromolecules. 3 (2002) 232–238.

[11.108] J.D. Schiffman, C.L. Schauer, Cross-linking chitosan nanofibers, Biomacromolecules. 8 (2007) 594–601.

[11.109] J.-H. Song, H.-E. Kim, H.-W. Kim, Production of electrospun gelatin nanofiber by water-based co-solvent approach., J. Mater. Sci. Mater. Med. 19 (2008) 95–102.

[11.110] J.H.C. Hui Wang, Xiao Hong Qin, Study on Structures of electrospinning cellulose acetate nanofibers., Adv. Mat. Res. 175-176 (2011) 242–246.

[11.111] J.H.S. George, Engineering of Fibrous Scaffolds for use in Regenerative Medicine Department of Materials, Imperial College, London, 2009.

[11.112] J.J. Doyle, S. Choudhari, S. Ramakrishna, R.P. Babu, Electrospun Nanomaterials : Biotechnology , Food , Water , Environment , and Energy., Conf. Pap. Mater. Sci. 2013 (2013) 1–14.

[11.113] J.-J. Max, C. Chapados, Infrared Spectroscopy of Aqueous Carboxylic Acids: Comparison between Different Acids and Their Salts, J. Phys. Chem. A. 108 (2004) 3324–3337.

[11.114] J.R. Sharpe, K.L. Harris, K. Jubin, N.J. Bainbridge, N.R. Jordan, The effect of pH in modulating skin cell behaviour, Br. J. Dermatol. 161 (2009) 671–3.

[11.115] K. Gast, A. Siemer, D. Zirwer, G. Damaschun, Fluoroalcohol-induced structural changes of proteins: some aspects of cosolvent-protein interactions., Eur. Biophys. J. 30 (2001) 273–283.

[11.116] K. Nasouri, a. M. Shoushtari, a. Kaflou, Investigation of polyacrylonitrile electrospun nanofibres morphology as a function of polymer concentration, viscosity and Berry number, Micro Nano Lett. 7 (2012) 423.

[11.117] K. Ramaesh, F. a Billson, M.C. Madigan, Effect of bile acids on fibroblast proliferation and viability, Eye (Lond). 12 (Pt 4) (1998) 717–22.

[11.118] K. Scoffin, Scaling the Scaffolds : Control of Pore Size in Tissue Engineering Scaffolds, Am. Lab. (2011) 5.

[11.119] K. Sisson, C. Zhang, M.C. Farach-Carson, D.B. Chase, J.F. Rabolt, Evaluation of cross-linking methods for electrospun gelatin on cell growth and viability., Biomacromolecules. 10 (2009) 1675–80.

[11.120] K. Sollman, E. Marschall, W. Mi, Viscosity of selected binary, ternary, and quaternary liquid mixtures, J Chem Eng. 35 (1990) 375–381.

[11.121] K. Yasuda, J. Ping Gong, Y. Katsuyama, A. Nakayama, Y. Tanabe, E. Kondo, et al., Biomechanical properties of high-toughness double network hydrogels., Biomaterials. 26 (2005) 4468–75.

[11.122] K.E. Kadler, D.F. Holmes, J.A. Trotter, J.A. Chapman, Collagen fibril formation., Biochem J. 11 (1996) 1–11.

[11.123] K.L. Menzies, L. Jones, The Impact of Contact Angle on the Biocompatibility of Biomaterials, 87 (2010) 387–399.

[11.124] K.M. Woo, J.-H. Jun, V.J. Chen, J. Seo, J.-H. Baek, H.-M. Ryoo, et al., Nano-fibrous scaffolding promotes osteoblast differentiation and biomineralization., Biomaterials. 28 (2007) 335–43.

[11.125] K.S. Rho, L. Jeong, G. Lee, B.-M. Seo, Y.J. Park, S.-D. Hong, et al., Electrospinning of collagen nanofibers: effects on the behavior of normal human keratinocytes and early-stage wound healing., Biomaterials. 27 (2006) 1452–61.

[11.126] K.Y. Lee, J. Shim, H.G. Lee, Mechanical properties of gellan and gelatin composite films, Carbohydr. Polym. 56 (2004) 251–254.

[11.127] L. a Smith, P.X. Ma, Nano-fibrous scaffolds for tissue engineering., Colloids Surf. B. Biointerfaces. 39 (2004) 125–31.

[11.128] L. Huang, K. Nagapudi, R.P. Apkarian, E.L. Chaikof, Engineered collagen–PEO nanoŽ bers and fabrics, J Biomater Sci Polym Ed. 12 (2001) 979–993.

[11.129] L. Jeong, W.H. Park, Preparation and characterization of gelatin nanofibers containing silver nanoparticles., Int. J. Mol. Sci. 15 (2014) 6857–79.

[11.130] L. Meng, O. Arnoult, M. Smith, G.E. Wnek, Electrospinning of in situ crosslinked collagen nanofibers., J. Mater. Chem. 22 (2012) 19412.

[11.131] L. Ren, J. Wang, F.-Y. Yang, L. Wang, D. Wang, T.-X. Wang, et al., Fabrication of gelatin–siloxane fibrous mats via sol–gel and electrospinning procedure and its application for bone tissue engineering, Mater. Sci. Eng. C. 30 (2010) 437–444.

[11.132] L. Solorio, C. Zwolinski, A.W. Lund, M.J. Farrell, J.P. Stegemann, Gelatin microspheres crosslinked with genipin for local delivery of growth factors., J. Tissue Eng. Regen. Med. 4 (2010) 514–23.

[11.133] L. Yang, C.F.C. Fitié, K.O. van der Werf, M.L. Bennink, P.J. Dijkstra, J. Feijen, Mechanical properties of single electrospun collagen type I fibers., Biomaterials. 29 (2008) 955–62.

[11.134] L.H.H.O. Damink, P.J. Dijkstra, M.J.A. Van Luyn, P.B. Van Wachem, P. Nieuwenhuis, J. Feijen, Glutaraldehyde as a crosslinking agent for collagen-based biomaterials, J. Mater. Sci. Mater. Med. 6 (1995) 460–472.

[11.135] L.T.H. Nguyen, S. Chen, N.K. Elumalai, M.P. Prabhakaran, Y. Zong, C. Vijila, et al., Biological, Chemical, and Electronic Applications of Nanofibers, Macromol. Mater. Eng. 298 (2013) 822–867.

[11.136] L.Y. Lee, S.H. Ranganath, Y. Fu, J.L. Zheng, H.S. Lee, C.-H. Wang, et al., Paclitaxel release from micro-porous PLGA disks., Chem. Eng. Sci. 64 (2009) 4341–4349.

[11.137] M. Ago, K. Okajima, J.E. Jakes, S. Park, O.J. Rojas, Lignin-based electrospun nanofibers reinforced with cellulose nanocrystals., Biomacromolecules. 13 (2012) 918–26.

[11.138] M. Ahmed, T.A.D.S. Ramos, F. Damanik, B. Quang Le, P. Wieringa, M. Bennink, et al., A combinatorial approach towards the design of nanofibrous scaffolds for chondrogenesis, Sci. Rep. 5 (2015) 1–12.

[11.139] M. Angarano, S. Schulz, M. Fabritius, R. Vogt, T. Steinberg, P. Tomakidi, et al., Layered Gradient Nonwovens of In Situ Crosslinked Electrospun Collagenous Nanofibers Used as Modular Scaffold Systems for Soft Tissue Regeneration, Adv. Funct. Mater. 23 (2013) 3277–3285.

[11.140] M. Chowdhury, G. Stylios, Effect of Experimental Parameters on the Morphology of Electrospun Nylon 6 fibres, Int. J. Basic Appl. Sci. 10 (2010) 70–78.

[11.141] M. Djabourov, J. Leblond, P. Papon, Gelation of aqueous gelatin solutions . II . Rheology of the sol-gel transition To cite this version : Gelation of aqueous transition Rheology of the sol-gel, (1988).

[11.142] M. Djabourov, J. Leblond, P. Papon, Gelation of aqueous gelatin solutions. I. Structural Investigation., J. Phys. Fr. 49 (1988) 319–332.

[11.143] M. Erencia Millan, Propuesta de tesis: Preparación de soportes biomateriales con estructuras fibrilares obtenidas mediante electro-hilatura., Universitat Politecnica de Catalunya, 2013.

[11.144] M. Erencia, F. Cano, J. a Tornero, J. Macanás, F. Carrillo, Preparation of electrospun nanofibers from solutions of different gelatin types using a benign solvent mixture composed of water/salt/ethanol., To Be Summited. (2014).

[11.145] M. Erencia, F. Cano, J. a Tornero, J. Macanás, F. Carrillo, Resolving the electrospinnability zones and diameter prediction for the electrospinning of the gelatin/water/acetic Acid system., Langmuir. 30 (2014) 7198–205.

[11.146] M. Erencia, F. Cano, J.A. Tornero, J. Macanás, F. Carrillo, Effect of operational and solution parameters on diameter of electrospun protein fibers., To Be Summited. (2014).

[11.147] M. Erencia, F. Cano, M.M. Tornero, Jose Antonio Fernandes, T. Tzanov, J. Macanás, F. Carrillo, Electrospinning of gelatin scaffolds with low acetic acid

concentration effect of solvent composition on both diameter of nanofibers and cell viability, Summited. (2014).

[11.148] M. Gulfam, J.M. Lee, J.-E. Kim, D.W. Lim, E.K. Lee, B.G. Chung, Highly porous core-shell polymeric fiber network., Langmuir. 27 (2011) 10993–10999.

[11.149] M. Li, M.J. Mondrinos, M.R. Gandhi, F.K. Ko, A.S. Weiss, P.I. Lelkes, Electrospun protein fibers as matrices for tissue engineering, Biomaterials. 26 (2005) 5999–6008.

[11.150] M. Li, M.J. Mondrinos, M.R. Gandhi, F.K. Ko, A.S. Weiss, P.I. Lelkes, Electrospun protein fibers as matrices for tissue engineering., Biomaterials. 26 (2005) 5999–6008.

[11.151] M. Ngiam, S. Liao, A.J. Patil, Z. Cheng, C.K. Chan, S. Ramakrishna, The fabrication of nano-hydroxyapatite on PLGA and PLGA/collagen nanofibrous composite scaffolds and their effects in osteoblastic behavior for bone tissue engineering, Bone. 45 (2009) 4–16.

[11.152] M. PX, Biomimetic materials for tissue engineering, Adv Drug Deliv. Rev. 60 (2008) 184–198.

[11.153] M. Rolandi, R. Rolandi, Self-assembled chitin nanofibers and applications., Adv. Colloid Interface Sci. 207 (2014) 216–22.

[11.154] M. Skotak, S. Noriega, G. Larsen, A. Subramanian, Electrospun cross-linked gelatin fibers with controlled diameter: the effect of matrix stiffness on proliferative and biosynthetic activity of chondrocytes cultured in vitro., J. Biomed. Mater. Res. A. 95 (2010) 828–36.

[11.155] M. Yan, B. Li, X. Zhao, G. Ren, Y. Zhuang, H. Hou, et al., Characterization of acid-soluble collagen from the skin of walleye pollock (Theragra chalcogramma), Food Chem. 107 (2008) 1581–1586.

[11.156] M. Zandi, Studies on the gelation of gelatin solutions and on the use of resulting gels for medical scaffolds., Universitat Duisburg-Essen, 2008.

[11.157] M.A. Masuelli, M.G. Sansone, D.F. Aplicada, Hydrodynamic Properties of Gelatin – Studies from Intrinsic Viscosity Measurements, in: Prod. Appl. Biopolym., 2012: pp. 85–116.

[11.158] M.A. Oraby, A.I. Waley, A.I. El-dewany, E.A. Saad, B.M.A. El-hady, E.T. Al, Electrospinning of Gelatin Functionalized with Silver Nanoparticles for Nanofiber Fabrication, 2013 (2013) 95–105.

[11.159] M.A. Oraby, A.I. Waley, A.I. El-dewany, E.A. Saad, M.A. El-hady, Electrospun Gelatin Nanofibers : Effect of Gelatin Concentration on Morphology and Fiber Diameters., Polym. J. 9 (2013) 534.

[11.160] M.B. Fisher, R.L. Mauck, Tissue engineering and regenerative medicine: recent innovations and the transition to translation., Tissue Eng. Part B. 19 (2013) 1–13.

[11.161] M.G. Haugh, M.J. Jaasma, F.J. O'Brien, The effect of dehydrothermal treatment on the mechanical and structural properties of collagen-GAG scaffolds., J. Biomed. Mater. Res. A. 89 (2009) 363–9.

[11.162] M.L. Focarete, C. Gualandi, M. Scandola, M. Govoni, E. Giordano, L. Foroni, et al., Electrospun scaffolds of a polyhydroxyalkanoate consisting of omega-hydroxylpentadecanoate repeat units: fabrication and in vitro biocompatibility studies., J. Biomater. Sci. Polym. Ed. 21 (2010) 1283–1296.

[11.163] M.L. Ottone, M.B. Peirotti, J.A. Deiber, Rheokinetic model to characterize the maturation process of gelatin solutions under shear flow, Food Hydrocoll. 23 (2009) 1342–1350.

[11.164] M.M. Bergshoef, G.J. Vancso, Transparent nanocomposites with ultrathin, electrospun nylon-4,6 fiber reinforcement, Adv. Mater. 11 (1999) 1362–1365.

[11.165] M.M. Demir, I. Yilgor, E. Yilgor, B. Erman, Electrospinning of polyurethane ® bers, 43 (2002) 3303–3309.

[11.166] M.M. Hohman, M. Shin, G. Rutledge, M.P. Brenner, Electrospinning and electrically forced jets. II. Applications, Phys. Fluids. 13 (2001) 2221.

[11.167] M.M. Stevens, J.H. George, Exploring and engineering the cell surface interface., Science. 310 (2005) 1135–8.

[11.168] M.P. Lutolf, J. a Hubbell, Synthetic biomaterials as instructive extracellular microenvironments for morphogenesis in tissue engineering, Nat. Biotechnol. 23 (2005) 47–55.

[11.169] M.R. Badrossamay, K. Balachandran, A.K. Capulli, H.M. Golecki, A. Agarwal, J.A. Goss, et al., Engineering hybrid polymer-protein super-aligned nanofibers via rotary jet spinning, Biomaterials. 35 (2014) 3188–3197.

[11.170] M.-R. Fatehi, S. Raeissi, D. Mowla, Estimation of viscosity of binary mixtures of ionic liquids and solvents using an artificial neural network based on the structure groups of the ionic liquid, Fluid Phase Equilib. 364 (2014) 88–94.

[11.171] M.R. Ladd, T.K. Hill, J.J. Yoo, S.J. Lee, Electrospun Nanofibers in Tissue Engineering, (2008).

[11.172] N. Ashammakhi, a. Ndreu, Y. Yang, H. Ylikauppila, L. Nikkola, Nanofiber-based scaffolds for tissue engineering, Eur. J. Plast. Surg. 35 (2008) 135–149.

[11.173] N. Bhardwaj, S.C. Kundu, Electrospinning: a fascinating fiber fabrication technique., Biotechnol. Adv. 28 (2010) 325–47.

[11.174] N. Choktaweesap, K. Arayanarakul, D. Aht-ong, C. Meechaisue, P. Supaphol, Electrospun Gelatin Fibers: Effect of Solvent System on Morphology and Fiber Diameters., Polym. J. 39 (2007) 622–631.

[11.175] N.M. Neves, Patterning of polymer nano fi ber meshes by electrospinning for biomedical applications, 2 (2007) 433–448.

[11.176] N.S.F. Summer, U. Fellowship, S. Technologies, P. Tsing, P. Advisor, D.M. Elliott, Electrospinning natural polymers for tissue engineering applications., (n.d.) 1–15.

[11.177] N.T.B. Linh, B.-T. Lee, Electrospinning of polyvinyl alcohol/gelatin nanofiber composites and cross-linking for bone tissue engineering application, J. Biomater. Appl. 27 (2012) 255–266.

[11.178] O. Hartman, C. Zhang, E.L. Adams, M.C. Farach-Carson, N.J. Petrelli, B.D. Chase, et al., Microfabricated electrospun collagen membranes for 3-D

cancer models and drug screening applications., Biomacromolecules. 10 (2009) 2019–32.

[11.179] O.T. Bloom, Machine for testing jelly strength of glues, gelatines and the like., 1540979, 1925.

[11.180] P. Buijtenhuijs, L. Buttafoco, A.A. Poot, W.F. Daamen, T.H. Van Kuppevelt, P.J. Dijkstra, et al., Tissue engineering of blood vessels : characterization of smooth-muscle cells for culturing on collagen-and-elastin- based scaffolds., Biotechnol Appl Biochem. 149 (2004) 141–149.

[11.181] P. Gupta, C. Elkins, T.E. Long, G.L. Wilkes, Electrospinning of linear homopolymers of poly(methyl methacrylate): exploring relationships between fiber formation, viscosity, molecular weight and concentration in a good solvent, Polymer (Guildf). 46 (2005) 4799–4810.

[11.182] P. Kumar, Effect of collector on electrospinning to fabricate aligned nanofiber, 2012.

[11.183] P. Songchotikunpan, J. Tattiyakul, P. Supaphol, Extraction and electrospinning of gelatin from fish skin., Int. J. Biol. Macromol. 42 (2008) 247–255.

[11.184] P. Supaphol, C. Mit-Uppatham, M. Nithitanakul, Ultrafine electrospun polyamide-6 fibers: Effect of emitting electrode polarity on morphology and average fiber diameter, J. Polym. Sci. Part B Polym. Phys. 43 (2005) 3699–3712.

[11.185] P. Wu, M. Imai, Novel Biopolymer Composite Membrane Involved with Selective Mass Transfer and Excellent Water Permeability., in: R. Y.Ning (Ed.), Adv. Desalin., 2012.

[11.186] P.B. Davis, H.C. Jones, The viscosities of binary mixtures of the associated liquids, water, formic acid and acetic acid, J. Am. Chem. Soc. 37 (1915) 1194–1198.

[11.187] P.F. De Almeida, B. Farias, FTIR Characterization of Gelatin from Chicken Feet, J. Chem. Chem. Eng. 6 (2012) 1029–1032.

[11.188] P.G. De Gennes, Dynamics of Entangled Polymer Solutions. II. Inclusion of Hydrodynamic Interactions, Macromolecules. 9 (1976) 594–598.

[11.189] P.J. Flory, Principles of Polymer Chemistry, Cornell University Press, New York, 1953.

[11.190] P.K. Baumgarten, Electrostatic spinning of acrylic microfibers, J. Colloid Interface Sci. 36 (1971) 71–79.

[11.191] P.N. Magee, E. Farber, Citrate-Promoted Helix Formation in Gelatin, (1962) 124–129.

[11.192] Q. Jiang, N. Reddy, S. Zhang, N. Roscioli, Y. Yang, Water-stable electrospun collagen fibers from a non-toxic solvent and crosslinking system., J. Biomed. Mater. Res. A. 101 (2013) 1237–47.

[11.193] Q. Wu, X. Zhang, B. Wu, W. Huang, Effects of microwave sintering on the properties of porous hydroxyapatite scaffolds., Ceram. Int. 39 (2013) 2389–2395.

[11.194] Q. Yang, Z. Li, Y. Hong, Y. Zhao, S. Qiu, C. Wang, et al., Influence of solvents on the formation of ultrathin uniform poly(vinyl pyrrolidone) nanofibers with electrospinning, J. Polym. Sci. Part B Polym. Phys. 42 (2004) 3721–3726.

[11.195] Q.P. Pham, U. Sharma, A.G. Mikos, Electrospinning of polymeric nanofibers for tissue engineering applications: a review, Tissue Eng. 12 (2006) 1197–211.

[11.196] R. Chen, C. Huang, Q. Ke, C. He, H. Wang, X. Mo, Preparation and characterization of coaxial electrospun thermoplastic polyurethane/collagen compound nanofibers for tissue engineering applications, Colloids Surfaces B Biointerfaces. 79 (2010) 315–325.

[11.197] R. Inai, M. Kotaki, S. Ramakrishna, Structure and properties of electrospun PLLA single nanofibres., Nanotechnology. 16 (2005) 208–213.

[11.198] R. Jalili, S.A. Hosseini, M. Morshed, The Effects of Operating Parameters on the morphology of electrospun polyacrilonitrile nanofibres., Iran. Polym. J. 14 (2005) 1074–1081.

[11.199] R. Langer, Tissue engineering., Mol. Ther. 1 (2000) 12–5.

[11.200] R. Nayak, R. Padhye, I.L. Kyratzis, Y.B. Truong, L. Arnold, Effect of viscosity and electrical conductivity on the morphology and fiber diameter in melt electrospinning of polypropylene., Text. Res. J. 83 (2012) 606–617.

[11.201] R. Schrieber, H. Gareis, Gelatin handbook- Theory and Insutrial Practice, Wiley, 2007.

[11.202] R. Vasita, D.S. Katti, Nanofibers and their applications in tissue engineering., Int. J. Nanomedicine. 1 (2006) 15–30.

[11.203] R. Zeeman, Cross-linking of collagen-based materials, University of Twente, 1970.

[11.204] R.. Colby, M. Rubinstein, Two-Parameter scaling for polymers in theta solvents, Macromolecules. 23 (1990) 2753–2757.

[11.205] R.. de Carvalho, C.R.. Grosso, Characterization of gelatin based films modified with transglutaminase, glyoxal and formaldehyde., Food Hydrocoll. 18 (2004) 717–726.

[11.206] R.B. K.C., K.W. Kim, S.R. Bhattarai, H.Y. Kim, D.R. Lee, Effect of collector temperature and conductivity on the chain conformation of nylon 6 electrospun nanofibers., Fibers Polym. 8 (2007) 186–191.

[11.207] R.L. Fischer, M.G. McCoy, S.A. Grant, Electrospinning collagen and hyaluronic acid nanofiber meshes, J. Mater. Sci. Mater. Med. 23 (2012) 1645–1654.

[11.208] R.M. Hafidz, Chemical and functional properties of bovine and porcine skin gelatin, Int. Food Res. J. 817 (2011) 813–817.

[11.209] S. a. Sell, P.S. Wolfe, K. Garg, J.M. McCool, I. a. Rodriguez, G.L. Bowlin, The Use of Natural Polymers in Tissue Engineering: A Focus on Electrospun Extracellular Matrix Analogues, Polymers (Basel). 2 (2010) 522–553.

[11.210] S. Agarwal, J.H. Wendorff, A. Greiner, Use of electrospinning technique for biomedical applications, Polymer (Guildf). 49 (2008) 5603–5621.

[11.211] S. Baiguera, C. Del Gaudio, E. Lucatelli, E. Kuevda, M. Boieri, B. Mazzanti, et al., Electrospun gelatin scaffolds incorporating rat decellularized brain extracellular matrix for neural tissue engineering., Biomaterials. 35 (2014) 1205–14.

[11.212] S. Cai, H. Xu, Q. Jiang, Y. Yang, Novel 3D electrospun scaffolds with fibers oriented randomly and evenly in three dimensions to closely mimic the unique architectures of extracellular matrices in soft tissues: fabrication and mechanism study., Langmuir. 29 (2013) 2311–8.

[11.213] S. Farris, J. Song, Q. Huang, Alternative reaction mechanism for the cross-linking of gelatin with glutaraldehyde., J. Agric. Food Chem. 58 (2010) 998–1003.

[11.214] S. Gautam, A.K. Dinda, N.C. Mishra, Fabrication and characterization of PCL/gelatin composite nanofibrous scaffold for tissue engineering applications by electrospinning method., Mater. Sci. Eng. C. Mater. Biol. Appl. 33 (2013) 1228–35.

[11.215] S. Hermanto, L.O. Sumarlin, W. Fatimah, Differentiation of Bovine and Porcine Gelatin Based on Spectroscopic and Electrophoretic Analysis, 1 (2013) 68–73.

[11.216] S. Kara, ed., A roadmap of biomedical engineers and milestones., InTech, 2012.

[11.217] S. Matsuoka, M.K. Cowman, Equation of state for polymer solution, Polymer (Guildf). 43 (2002) 3447–3453.

[11.218] S. Moon, R.J. Farris, Electrospinning of Heated Gelatin-Sodium Alginate-Water Solutions, Polym. Eng. Sci. 49 (2009) 1616–1620.

[11.219] S. Panzavolta, M. Gioffrè, M.L. Focarete, C. Gualandi, L. Foroni, A. Bigi, Electrospun gelatin nanofibers: optimization of genipin cross-linking to preserve fiber morphology after exposure to water, Acta Biomater. 7 (2011) 1702–9.

[11.220] S. Rafiei, S. Maghsoodloo, B. Noroozi, V. Mottaghitalab, A.K. Haghi, Mathematical modeling in electrospinning process of nanofibers: a detailed review, Cellul. Chem. Technol. 47 (2013) 323–338.

[11.221] S. Ramakrishna, K. Fujihara, W.-E. Teo, T.-C. Lim, Z. Ma, An introduction to electrospinning and nanofibers., 2005.

[11.222] S. Sukigara, M. Gandhi, J. Ayutsede, M. Micklus, F. Ko, Regeneration of Bombyx mori silk by electrospinning—part 1: processing parameters and geometric properties., Polymer (Guildf). 44 (2003) 5721–5727.

[11.223] S. Torres-Giner, J. V Gimeno-Alcañiz, M.J. Ocio, J.M. Lagaron, Comparative performance of electrospun collagen nanofibers cross-linked by means of different methods., ACS Appl. Mater. Interfaces. 1 (2009) 218–23.

[11.224] S. V Fridrikh, J.H. Yu, M.P. Brenner, G.C. Rutledge, Controlling the fiber diameter during electrospinning., Phys. Rev. Lett. 90 (2003) 144502.

[11.225] S. V Madihally, H.W.T. Matthew, Porous chitosan scaffolds for tissue engineering., Biomaterials. 20 (1999) 1133–1142.

[11.226] S. Zargham, S. Bazgir, A. Tavakoli, A.S. Rashidi, R. Damerchely, The Effect of Flow Rate on Morphology and Deposition Area of Electrospun Nylon 6 Nanofiber., J. Eng. Fiber. Fabr. 7 (2012) 42–49.

[11.227] S. Zhang, Y. Huang, X. Yang, F. Mei, Q. Ma, G. Chen, et al., Gelatin nanofibrous membrane fabricated by electrospinning of aqueous gelatin solution for guided tissue regeneration., J. Biomed. Mater. Res. A. 90 (2009) 671–9.

[11.228] S. Zhong, W.E. Teo, X. Zhu, R. Beuerman, S. Ramakrishna, L. Yue, et al., Formation of Collagen - Glycosaminoglycan Blended Nanofibrous Scaffolds and Their Biological Properties., Biomacromolecules. 6 (2005) 2998–3004.

[11.229] S. Zhong, W.E. Teo, X. Zhu, R.W. Beuerman, S. Ramakrishna, L. Yue, et al., An aligned nanofibrous collagen scaffold by electrospinning and its effects on in vitro fibroblast culture., J. Biomed. Mater. Res. Part A. 79A (2006) 456–463.

[11.230] S.A. Sell, M.J. McClure, K. Garg, P.S. Wolfe, G.L. Bowlin, Electrospinning of collagen/biopolymers for regenerative medicine and cardiovascular tissue engineering., Adv. Drug Deliv. Rev. 61 (2009) 1007–19.

[11.231] S.-C. Wu, W.-H. Chang, G.-C. Dong, K.-Y. Chen, Y.-S. Chen, C.-H. Yao, Cell adhesion and proliferation enhancement by gelatin nanofiber scaffolds., J. Bioact. Compat. Polym. 26 (2011) 565–577.

[11.232] S.E. Kim, D.N. Heo, J.B. Lee, J.R. Kim, S.H. Park, S.H. Jeon, et al., Electrospun gelatin/polyurethane blended nanofibers for wound healing., Biomed. Mater. 4 (2009) 044106.

[11.233] S.J. Kew, J.H. Gwynne, D. Enea, M. Abu-Rub, a Pandit, D. Zeugolis, et al., Regeneration and repair of tendon and ligament tissue using collagen fibre biomaterials., Acta Biomater. 7 (2011) 3237–47.

[11.234] S.K. Tiwari, S.S. Venkatraman, Importance of viscosity parameters in electrospinning: Of monolithic and core–shell fibers, Mater. Sci. Eng. C. 32 (2012) 1037–1042.

[11.235] S.L. Tao, T.A. Desai, Aligned Arrays of Biodegradable Poly(ε-caprolactone) Nanowires and Nanofibers by Template Synthesis., Nano Lett. 7 (2007) 1463–1468.

[11.236] S.-M. Lien, W.-T. Li, T.-J. Huang, Genipin-crosslinked gelatin scaffolds for articular cartilage tissue engineering with a novel crosslinking method, Mater. Sci. Eng. C. 28 (2008) 36–43.

[11.237] S.N. Rampersad, Multiple applications of Alamar Blue as an indicator of metabolic function and cellular health in cell viability bioassays., Sensors (Basel). 12 (2012) 12347–60.

[11.238] S.-P. Rwei, C.-C. Huang, Electrospinning PVA solution-rheology and morphology analyses, Fibers Polym. 13 (2012) 44–50.

[11.239] S.S. Ojha, M. Afshari, R. Kotek, R.E. Gorga, Morphology of electrospun nylon-6 nanofibers as a function of molecular weight and processing parameters., J. Appl. Polym. Sci. 108 (2008) 308–319.

[11.240] S.-W. Choi, Y. Zhang, Y. Xia, Three-dimensional scaffolds for tissue engineering: the importance of uniformity in pore size and structure., Langmuir. 26 (2010) 19001–6.

[11.241] S.Y. Chew, T.C. Hufnagel, C.T. Lim, K.W. Leong, Mechanical properties of single electrospun drug-encapsulated nanofibres, Nanotechnology. 17 (2006) 3880–3891.

[11.242] S.-Y. Gu, Z.-M. Wang, J. Ren, C.-Y. Zhang, Electrospinning of gelatin and gelatin/poly(l-lactide) blend and its characteristics for wound dressing., Mater. Sci. Eng. C. 29 (2009) 1822–1828.

[11.243] Sudha Gangal, Principles and Practice of Animal Tissue Culture, Second Edi, Orient Black Swan, London, 2010.

[11.244] T. Douglas, H.J. Haugen, Coating of polyurethane scaffolds with collagen: Comparison of coating and cross-linking techniques, in: J. Mater. Sci. Mater. Med., 2008: pp. 2713–2719.

[11.245] T. Garg, O. Singh, S. Arora, R.S.R. Murthy, Scaffold: A Novel Carrier for Cell and Drug Delivery, Crit. Rev. Ther. Drug Carr. Syst. 29 (2012) 1–63.

[11.246] T. Lin, X.G. Wang, Controlling the morphologies of electrospun nanofibers., in: Nanofibers Nanotechnol. Text., 2007: pp. 90–110.

[11.247] T. Subbiah, G.S. Bhat, R.W. Tock, S. Parameswaran, S.S. Ramkumar, Electrospinning of nanofibers, J. Appl. Polym. Sci. 96 (2005) 557–569.

[11.248] T. V Thamaraiselvi, S. Rajeswari, Biological Evaluation of Bioceramic Materials - A Review, Trends Biomater. Artif. Organs. 18 (2004) 9–17.

[11.249] T.A. Telemeco, C. Ayres, G.L. Bowlin, G.E. Wnek, E.D. Boland, N. Cohen, et al., Regulation of cellular infiltration into tissue engineering scaffolds composed of submicron diameter fibrils produced by electrospinning., Acta Biomater. 1 (2005) 377–85.

[11.250] T.-H. Nguyen, Fabrication and characterization of cross-linked gelatin electro-spun nano-fibers., J. Biomed. Sci. Eng. 03 (2010) 1117–1124.

[11.251] T.R. Keenan, Gelatin, in: Kirk-Othmer Encycl. Chem. Technol., 2003.

[11.252] V. Beachley, X. Wen, Effect of electrospinning parameters on the nanofiber diameter and length, Mater Sci Eng C Mater Biol Appl. 29 (2009) 663–668.

[11.253] V. Chaurey, F. Block, Y.H. Su, P.C. Chiang, E. Botchwey, C.F. Chou, et al., Nanofiber size-dependent sensitivity of fibroblast directionality to the methodology for scaffold alignment, Acta Biomater. (2012).

[11.254] V. Pillay, C. Dott, Y.E. Choonara, C. Tyagi, L. Tomar, P. Kumar, et al., A Review of the Effect of Processing Variables on the Fabrication of Electrospun Nanofibers for Drug Delivery Applications., J. Nanomater. 2013 (2013) 1–22.

[11.255] W. Fu, Z. Liu, B. Feng, R. Hu, X. He, H. Wang, et al., Electrospun gelatin/PCL and collagen/PLCL scaffolds for vascular tissue engineering, Int. J. Nanomedicine. 9 (2014) 2335–2344.

[11.256] W. He, T. Yong, W.E. Teo, Z. Ma, S. Ramakrishna, Fabrication and endothelialization of collagen-blended biodegradable polymer nanofibers: potential vascular graft for blood vessel tissue engineering., Tissue Eng. 11 (2005) 1574–88.

[11.257] W. Ritcharoen, Y. Thaiying, Y. Saejeng, I. Jangchud, R. Rangkupan, C. Meechaisue, et al., Electrospun dextran fibrous membranes., Cellulose. 15 (2008) 435–444.

[11.258] W. Xue, X. Liu, X. Zheng, C. Ding, In vivo evaluation of plasma-sprayed titanium coating after alkali modification., Biomaterials. 26 (2005) 3029–37.

[11.259] W.-H. Lin, W.-B. Tsai, In situ UV-crosslinking gelatin electrospun fibers for tissue engineering applications., Biofabrication. 5 (2013) 035008.

[11.260] W.-J. Chen, D.-J. Ying, Design and Preparation of an Electrospun Biomaterial Surgical Patch, J. Bioact. Compat. Polym. 24 (2009) 158–168.

[11.261] W.-J. Li, C.T. Laurencin, E.J. Caterson, R.S. Tuan, F.K. Ko, Electrospun nanofibrous structure: a novel scaffold for tissue engineering, J. Biomed. Mater. Res. 60 (2002) 613–21.

[11.262] W.-J. Li, J. a Cooper, R.L. Mauck, R.S. Tuan, Fabrication and characterization of six electrospun poly(alpha-hydroxy ester)-based fibrous scaffolds for tissue engineering applications., Acta Biomater. 2 (2006) 377–85.

[11.263] W.-J.W.-J. Li, R. Tuli, C. Okafor, A. Derfoul, K.G.K.G. Danielson, D.J.D.J. Hall, et al., A three-dimensional nanofibrous scaffold for cartilage tissue engineering using human mesenchymal stem cells., Biomaterials. 26 (2005) 599–609.

[11.264] W.K. Son, J.H. Youk, T.S. Lee, W.H. Park, The effects of solution properties and polyelectrolyte on electrospinning of ultrafine poly(ethylene oxide) fibers, Polymer (Guildf). 45 (2004) 2959–2966.

[11.265] X. Fang, D.H. Reneker, DNA fibers by electrospinning, J. Macromol. Sci. Part B. 36 (1997) 169–173.

[11.266] X. Geng, O.-H. Kwon, J. Jang, Electrospinning of chitosan dissolved in concentrated acetic acid solution, Biomaterials. 26 (2005) 5427–32.

[11.267] X. Yang, H. Wang, Electrospun Functional Nanofibrous Scaffolds for Tissue Engineering, in: Tissue Eng., InTech, 2010: pp. 159–178.

[11.268] X. Zhang, K. Tang, X. Zheng, Electrospinning and rheological behavior of poly (vinyl alcohol)/collagen blended solutions., J. Wuhan Univ. Technol. Sci. Ed. 30 (2015) 840–846.

[11.269] X.D.Z. Xian Tao Wen, Hong Song Fan, Yan Fei Tan, H.D. Cao, H. Li, B. Cai, Preparation of electrospun PLA nanofiber scaffold and the evaluation in vitro., Key Eng. Mater. 288-289 (2005) 139–142.

[11.270] X.T. Wen, H.S. Fan, Y.F. Tan, H.D. Cao, H. Li, B. Cai, et al., Preparation of Electrospun PLA Nanofiber Scaffold and the Evaluation In Vitro, Key Eng. Mater. 288-289 (2005) 139–142.

[11.271] Y. Ge, J. Wang, Z. Shi, J. Yin, Gelatin-assisted fabrication of water-dispersible graphene and its inorganic analogues., J. Mater. Chem. 22 (2012) 17619.

[11.272] Y. Ji, K. Ghosh, X.Z. Shu, B. Li, J.C. Sokolov, G.D. Prestwich, et al., Electrospun three-dimensional hyaluronic acid nanofibrous scaffolds., Biomaterials. 27 (2006) 3782–92.

[11.273] Y. Tabata, Biomaterial technology for tissue engineering applications., J. R. Soc. Interface. 6 (2009) 311–324.

[11.274] Y. Yang, Z. Jia, J. Liu, Q. Li, L. Hou, L. Wang, et al., Effect of electric field distribution uniformity on electrospinning., J. Appl. Phys. 103 (2008) 104307.

[11.275] Y. Zhang, H. Ouyang, C.T. Lim, S. Ramakrishna, Z.-M. Huang, Electrospinning of gelatin fibers and gelatin/PCL composite fibrous scaffolds., J. Biomed. Mater. Res. B. Appl. Biomater. 72 (2005) 156–65.

[11.276] Y.-F. Qian, K.-H. Zhang, F. Chen, Q.-F. Ke, X.-M. Mo, Cross-linking of gelatin and chitosan complex nanofibers for tissue-engineering scaffolds., J. Biomater. Sci. Polym. Ed. 22 (2011) 1099–1113.

[11.277] Y.-R. V Shih, C.-N. Chen, S.-W. Tsai, Y.J. Wang, O.K. Lee, Growth of mesenchymal stem cells on electrospun type I collagen nanofibers., Stem Cells. 24 (2006) 2391–7.

[11.278] Y.Z. Zhang, J. Venugopal, Z.-M. Huang, C.T. Lim, S. Ramakrishna, Characterization of the surface biocompatibility of the electrospun PCL-collagen nanofibers using fibroblasts., Biomacromolecules. 6 (2005) 2583–9.

[11.279] Y.Z. Zhang, J. Venugopal, Z.-M. Huang, C.T. Lim, S. Ramakrishna, Crosslinking of the electrospun gelatin nanofibers., Polymer (Guildf). 47 (2006) 2911–2917.

[11.280] Z. Li, C. Wang, Effects of Working Parameters on Electrospinning, in: One-Dimensional Nanostructures, Springer Berlin Heidelberg, Berlin, Heidelberg, 2013: pp. 15–29.

[11.281] Z. Zha, W. Teng, V. Markle, Z. Dai, X. Wu, Fabrication of gelatin nanofibrous scaffolds using ethanol/phosphate buffer saline as a benign solvent., Biopolymers. 97 (2012) 1026–1036.

[11.282] Z. Zhang, G. Li, B.I. Shi, Physicochemical properties of collagen, gelatin and collagen hydrosylate derived from bovine limed split wastes, J. Soc. Leather Technol. Chem. 90 (2006) 23.

[11.283] Z.-C. Xing, S.-J. Han, Y.-S. Shin, I.-K. Kang, Fabrication of Biodegradable Polyester Nanocomposites by Electrospinning for Tissue Engineering., J. Nanomater. 2011 (2011) 1–18.

[11.284] Z.-M. Huang, Y. Zhang, S. Ramakrishna, C.. Lim, Electrospinning and mechanical characterization of gelatin nanofibers, Polymer (Guildf). 45 (2004) 5361–5368.

[11.285] Z.-M. Huang, Y.-Z. Zhang, M. Kotaki, S. Ramakrishna, A review on polymer nanofibers by electrospinning and their applications in nanocomposites, Compos. Sci. Technol. 63 (2003) 2223–2253.

ANEXO:

Artículos publicados y participaciones en congresos

ARTÍCULOS PUBLICADOS

Autor/es: Erencia, M.; Cano, F.; Tornero, J.; Macanás, J.; Carrillo, F.	
Grupos de Investigación vinculados: POLQUITEX - Materials Polimérics i Química Téxtil; TECTEX - Grup de Recerca en Tecnologia Tèxtil	
Título: Preparation of electrospun nanofibers from solutions of different gelatin types using a benign solvent mixture composed of water/PBS/ethanol	
Revista (título, volumen, página inicial-final): Polymers for advanced technologies, vol. 27, núm. 3, pàgs. 382-392	
ISSN: 1042-7147	**Año:** 2016
Agencia de Impacto: JCR-Science Edition (2014)	**Cuartil:** Q2
Índice de Impacto: 1.757	**Número de citas:** 0
URL del texto: http://onlinelibrary.wiley.com/doi/10.1002/pat.3678/full	

Autor/es: Erencia, M.; Cano, F.; Tornero, J.; Macedo, M.M.; Tzanov, T.; Macanás, J.; Carrillo, F.	
Grupos de Investigación vinculados: GBMI - Grup de Biotecnologia Molecular i Industrial; POLQUITEX - Materials Polimérics i Química Téxtil; TECTEX - Grup de Recerca en Tecnologia Tèxtil	
Título: Electrospinning of gelatin fibers using solutions with low acetic acid concentration: effect of solvent composition on both diameter of electrospun fibers and cytotoxicity	
Revista (título, volumen, página inicial-final): Journal of applied polymer science, vol. 132, núm. 25, pàgs. 42115 (1/11)-42115 (11(11)	
ISSN: 0021-8995	**Año:** 2015
Agencia de Impacto: JCR-Science Edition (2014)	**Cuartil:** Q2
Índice de Impacto: 1.768	**Número de citas:** 4
URL del texto: http://onlinelibrary.wiley.com/doi/10.1002/app.42115/abstract	

Autor/es: Erencia, M.; Cano, F.; Tornero, J.; Macanás, J.; Carrillo, F.	
Grupos de Investigación vinculados: POLQUITEX - Materials Polimérics i Química Téxtil; TECTEX - Grup de Recerca en Tecnologia Tèxtil	
Título: Resolving the electrospinnability zones and diameter prediction for the electrospinning of the gelatin/water/acetic acid system	
Revista (título, volumen, página inicial-final): Langmuir, vol. 30, núm. 24, pàgs. 7198-7205	
ISSN: 0743-7463	**Año:** 2014
Agencia de Impacto: JCR-Science Edition (2014)	**Cuartil:** Q1
Índice de Impacto: 4.457	**Número de citas:** 4
URL del texto: http://hdl.handle.net/2117/23323	

PARTICIPACIÓN EN CONGRESOS

Autor/es: Erencia, M.; Macanás, J.; Carrillo, F.	
Título: Electrospinnability zones for the gelatin/water/acetic acid system: effect of acid content on the scaffolds cytotoxicity	
Congreso: 13th Mediterranean Congress of Chemical Engineering	
Ámbito del congreso: Nacional	
Tipo de participación: Póster	
Ciudad: Barcelona	**Año:** 2014

Autor/es: Erencia, M.; Cano, F.; Tornero, J.; Macedo, M.M.; Tzanov, T.; Macanás, J.; Carrillo, F.	
Título: Soportes biomateriales de nanofibras de gelatina obtenidos por electrohilatura de disoluciones gelatina/acético/agua: efecto de la composición en la viabilidad celular	
Congreso: XIII Congreso Nacional de Materiales	
Ámbito del congreso: Nacional	
Tipo de participación: Ponencia	
Ciudad: Barcelona	**Año:** 2014

Autor/es: Erencia, M.; Carrillo, F.; Tornero J.; Cano, F.	
Título: Deposición y reticulación de nanofibras de colágeno sobre un soporte biomaterial mediante la técnica de electrohilatura	
Congreso: I Jornada de la recerca i la innovació tecnológica	
Ámbito del congreso: Campus UPC Terrassa	
Tipo de participación: Póster	
Ciudad: Terrassa	**Año:** 2013

Autor/es: Carrillo, F.; Lee, S.; Tornero, J.; Cano, F.; Erencia, M.; Curtin, S.; Ho, S.	
Título: Programmable surface sensitive stimuli on polyurethane for controlled cell response.	
Congreso: IADR 88th General Session and Exhibition	
Ámbito del congreso: Internacional	
Tipo de participación: Ponencia	
Ciudad: Barcelona	**Año:** 2010